



저작자표시-비영리-변경금지 2.0 대한민국

이용자는 아래의 조건을 따르는 경우에 한하여 자유롭게

- 이 저작물을 복제, 배포, 전송, 전시, 공연 및 방송할 수 있습니다.

다음과 같은 조건을 따라야 합니다:



저작자표시. 귀하는 원저작자를 표시하여야 합니다.



비영리. 귀하는 이 저작물을 영리 목적으로 이용할 수 없습니다.



변경금지. 귀하는 이 저작물을 개작, 변형 또는 가공할 수 없습니다.

- 귀하는, 이 저작물의 재이용이나 배포의 경우, 이 저작물에 적용된 이용허락조건을 명확하게 나타내어야 합니다.
- 저작권자로부터 별도의 허가를 받으면 이러한 조건들은 적용되지 않습니다.

저작권법에 따른 이용자의 권리는 위의 내용에 의하여 영향을 받지 않습니다.

이것은 [이용허락규약\(Legal Code\)](#)을 이해하기 쉽게 요약한 것입니다.

[Disclaimer](#)

공학박사 학위논문

**Analysis of Microbial Communities in  
Membrane Bioreactors with and without  
Quorum Quenching**

하폐수 처리용 분리막 생물반응기에서 정족수  
감지 억제 유무에 따른 미생물 군집 분석

2016 년 8 월

서울대학교 대학원

화학생물공학부

조 성 준



## **Abstract**

# **Analysis of Microbial Communities in Membrane Bioreactors with and without Quorum Quenching**

Sung Jun Jo

School of Chemical and Biological Engineering

The Graduate School, Seoul National University

Membrane bioreactors (MBRs) are hampered particularly by membrane biofouling, resulting from microbial growth on the membrane surface and microbial production of membrane foulants in activated sludge. To mitigate biofouling, quorum quenching (QQ) has been stand out as an innovative technique in MBRs. Although the biological understanding of the effect of QQ and biofouling mechanism is crucial for the development of biofouling control strategies, the information of the microbial ecology is not sufficient in both QQ-MBR and full-scale MBRs. Therefore the investigation of microbial community in QQ-MBR and full-scale MBRs are required for the successful biofouling control in real MBRs.

Firstly, the microbial communities were investigated in relation to the QQ effect on biofilm in an anoxic/oxic (A/O) MBR. Two laboratory-scale MBRs with

and without QQ-beads (QQ-bacteria encapsulated in bead) were operated in parallel. TMP (transmembrane pressure) rise-up in QQ-MBR was delayed by approximately 100~110% compared with those in conventional-and vacant (bead without QQ-bacteria)-MBRs. The principal coordinate analysis based on weighted UniFrac distance matrix revealed that QQ had effect on microbial community in biofilm. The results of correspondence analysis revealed that QQ had effect on both bacterial composition and the change rate of bacterial composition in biofilm.

Secondly, the microbial communities of activated sludge were investigated in relation to the effect of QQ on A/O MBR for 91 days. The system performance (e.g., COD, TN removal efficiency) was stable over the period regardless of the presence of QQ beads. However, the average floc size in the QQ-MBR was substantially lower than that in the control-MBR ( $p < 0.05$ ). QQ affected the bacterial compositions of activated sludge. The network analysis revealed that QQ had effects on the microbial interactions of activated sludge.

Lastly, the microbial communities of biofilm and activated sludge were scrutinized from 10 full-scale MBR plants. Overall, *Flavobacterium*, *Dechloromonas* and *Nitrospira* were abundant in order of abundance in biofilm, whereas *Dechloromonas*, *Flavobacterium* and *Haliscomenobacter* in activated sludge. The proportions of known quorum sensing bacterial genera ranged 1.39 to 11.57% in biofilm and 3.19 to 12.14% in activated sludge. Effects of ten environmental factors on community change were investigated using Spearman correlation. MLSS, HRT, F/M ratio and  $SAD_m$  explained the variation of microbial composition in the biofilm, whereas only MLSS did in the activated sludge.

Microbial networks were constructed with the 10 environmental factors. The network results revealed that there were different topological characteristics between the biofilm and activated sludge networks. These results indicated that the different microbial associations were responsible for the variation of community composition between the biofilm and activated sludge.

The information of microbial communities in QQ-MBR and full-scale MBRs could provide new insights to develop biofouling control strategies in real MBRs.

**Keywords**

Membrane bioreactor (MBR), Quorum sensing, Quorum quenching, Biofilm, Activated sludge, Biofouling control, Microbial community

*Student Number:* 2011-30988



# Table of Contents

<b>Abstract.....</b>	<b>i</b>
<b>List of Figures.....</b>	<b>x</b>
<b>List of Tables.....</b>	<b>xv</b>
<b>I. Introduction.....</b>	<b>1</b>
<b>I.1. Backgrounds.....</b>	<b>3</b>
<b>I.2. Objectives.....</b>	<b>5</b>
<b>II. Literature Review.....</b>	<b>7</b>
<b>II.1. Biological wastewater treatment.....</b>	<b>9</b>
II.1.1. History of biological wastewater treatment.....	9
II.1.2. Biological nitrogen removal process.....	11
<b>II.2. Membrane bioreactor (MBR).....</b>	<b>16</b>
II.2.1. MBR for advanced wastewater treatment.....	16
II.2.2. History of MBR.....	21
II.2.3. MBR trends.....	26
II.2.4. Membrane fouling in MBR.....	28
II.2.5. Biofilm in MBR.....	34
II.2.6. Fouling control in MBRs.....	36
<b>II.3. Quorum sensing (QS).....</b>	<b>41</b>
II.3.1. Definition and mechanism.....	41

<b>II.4. Quorum quenching (QQ)</b> .....	<b>63</b>
II.4.1. The strategy of QQ.....	63
II.4.2. Application of QQ to the control of biofouling in MBRs.....	84
<b>II.5. Genomic analysis of microbial community</b> .....	<b>95</b>
II.5.1. What is microbial ecology?.....	95
II.5.2. Metagenomics.....	96
II.5.3. Sequencing technologies for the microbial identification .....	100
II.5.4. Software for analyzing molecular sequences and statistical analysis for understanding microbial community.....	108
II.5.5 The main reference resources for metagenomics.....	114
II.5.6. Microbial network analysis.....	117
II.5.7. Prediction of metabolic pathway from microbial community.....	124

### **III. QQ Effect on the Microbial Community of Biofilm in an Anoxic-Oxic MBR.....125**

<b>III.1. Introduction</b> .....	<b>127</b>
<b>III.2. Materials and methods</b> .....	<b>129</b>
III.2.1. Materials.....	129
III.2.2. MBR systems.....	129
III.2.3. Preparation of the QQ-beads.....	134

III.2.4. Bioassay of AHL-degrading activity.....	134
III.2.5. Analytical methods.....	135
III.2.6. Sampling for analysis of microbial community in biofilm.....	137
III.2.7. DNA extraction, PCR amplification and Miseq platform sequencing.....	138
III.2.8. Data analysis for bacterial community.....	139
III.2.9. Statistical analysis.....	140
<b>III.3. Results and discussion.....</b>	<b>141</b>
III.3.1. QQ activity of the QQ-beads and effect of QQ on MBR biofouling.....	141
III.3.2. Principal coordinate analysis based on UniFrac distance matric .....	145
III.3.3. Correspondence analysis.....	147
III.3.4. Microbial composition in biofilm.....	152
<b>III.4. Conclusions.....</b>	<b>159</b>

## **IV. QQ Effect on the Microbial Community of Activated Sludge in an Anoxic-Oxic MBR.....161**

<b>IV.1. Introduction.....</b>	<b>163</b>
<b>IV.2. Materials and methods .....</b>	<b>165</b>
IV.2.1. Analytical methods.....	165
IV.2.2. Sampling for analysis of microbial community in	

activated sludge.....	165
IV.2.3. DNA extraction, PCR amplification and Miseq platform sequencing.....	165
IV.2.4. Data analysis for bacterial community.....	166
IV.2.5. Network analysis.....	167
IV.2.6. Prediction of metabolic pathway.....	168
IV.2.7. Statistical analysis.....	170
<b>IV.3. Results and discussion.....</b>	<b>171</b>
IV.3.1. Performance of the A/O MBR with QQ.....	171
IV.3.2. Microbial composition in the A/O MBR with QQ.....	179
IV.3.3. Microbial network in the A/O MBR with QQ.....	186
IV.3.4. Prediction of metabolic pathway in activated sludge...	197
<b>IV.4. Conclusions.....</b>	<b>200</b>

## **V. Survey of Microbial Community in Full-Scale MBRs for Wastewater Treatment.....201**

<b>V.1. Introduction.....</b>	<b>203</b>
<b>V.2. Materials and methods .....</b>	<b>205</b>
V.2.1. Sampling sites and methods.....	205
V.2.2. DNA extraction, PCR amplification and Miseq platform sequencing.....	206
V.2.3. Data analysis for bacterial community.....	206
V.2.4. Network analysis.....	209

V.2.5. Statistical analysis.....	210
V.2.6. Calculation of the relative proportion of quorum sensing related bacteria.....	211
<b>V.3. Results and discussion.....</b>	<b>214</b>
V.3.1. Community diversity.....	214
V.3.2. Microbial community composition in 10 MBRs.....	219
V.3.3 Microbial Network.....	237
<b>V.4. Conclusions.....</b>	<b>254</b>
<b>VI. Conclusions.....</b>	<b>257</b>
<b>VII. 국문초록.....</b>	<b>261</b>
<b>References.....</b>	<b>264</b>

## List of Figures

Figure II-1. The nitrogen cycle.....	12
Figure II-2. (a) Conventional activated sludge process with clarifiers for solid-liquid separation, (b) membrane bioreactor process with membrane filtration for solid-liquid separation.....	17
Figure II-3. Membrane component operation.....	18
Figure II-4. (a) Global market value of MBR (b) Global daily flow of MBR.....	27
Figure II-5. Membrane fouling mechanisms: cake fouling.....	29
Figure II-6. Membrane fouling mechanisms: pore blocking.....	30
Figure II-7. Schematic illustration of the occurrence of TMP jump.....	32
Figure II-8. MBR fouling mechanism map—the three stages of fouling.....	33
Figure II-9. Schematic illustration of the formation and removal of removable and irremovable fouling in MBRs.....	38
Figure II-10. The principle of quorum sensing is depicted.....	42
Figure II-11. Diagram of the <i>P. aeruginosa</i> biofilm-maturation pathway unattached cells that approach a surface may attach.....	43
Figure II-12. Four simplified models of the described quorum sensing mechanisms.....	45
Figure II-13. Representative bacterial autoinducers.....	46
Figure II-14. AHL signaling in (a) <i>Vibrio fischeri</i> and (b) <i>Pseudomonas aeruginosa</i> .....	49
Figure II-15. Gram-positive two-component-type quorum-sensing system. Blue octagons denote processed/modified peptide autoinducers.....	54

Figure II-16. The biosynthetic pathway of AI-2 <i>in vivo</i> .....	58
Figure II-17. AI-2 quorum sensing in <i>V. harveyi</i> .....	61
Figure II-18. The strategy of quorum quenching in gram-negative bacteria.....	64
Figure II-19. Reactions catalyzed by quorum-quenching enzymes.....	66
Figure II-20. Schematic of LsrK-mediated quorum quenching.....	74
Figure II-21. Cinnamaldehyde and cinnamaldehyde derivatives and effect of cinnamaldehyde and cinnamaldehyde derivatives on AI-2 based QS.....	83
Figure II-22. A magnetic enzyme carrier by immobilizing a quorum quenching enzyme.....	85
Figure II-23. Quorum quenching enzyme was immobilized onto the nano filtration membrane surface.....	86
Figure II-24. Methods for immobilization of viable.....	87
Figure II-25. Photograph and enlarged diagram of a microbial-vessel.....	88
Figure II-26. Schematic diagram of quorum quenching bacteria entrapping beads.....	90
Figure II-27. Schematic diagram of the ceramic microbial vessel under the inner flow feeding mode.....	91
Figure II-28. Schematic diagram of the rotating microbial carrier frame (RMCF), (b) location and rotation of a RMCF in the MBR.....	93
Figure II-29. Pilot scale QQ-MBR configurations.....	94
Figure II-30. The new field of metagenomics resides at the interface of microbiology, genomics and ecology.....	98
Figure II-31. Metagenomics involves constructing a DNA library from an	

environment's microbial population and then analyzing the functions and sequences in the library.....	99
Figure II-32. Pyrosequencing chemistry: biochemical reactions and enzymes involved in the generation of light signals by DNA pyrosequencing.....	103
Figure II-33. Illumina Genome Analyzer sequencing.....	106
Figure II-34. Principle of similarity- and regression- based network inference...	118
Figure III-1. Schematic diagram of the A/O MBR.....	132
Figure III-2. Variation of the relative QQ activity of the QQ-beads during the operation of A/O MBRs.....	142
Figure III-3. TMP profile of each run.....	143
Figure III-4. Bacterial community comparison by principal coordinate plots, based on weighted UniFrac distance metric.....	146
Figure III-5. Bacterial community comparison by correspondence analysis (CA), based on OTU composition.....	148
Figure III-6. Linear relationship between variations and scores on the first ordination axis 1 of CA plots in Run 1 and Run 2.....	150
Figure III-7. Linear relationship between variations and scores on the first ordination axis 1 of CA plots in Run 3 and Run 4.....	151
Figure IV-1. The data set for the LEfSe.....	169
Figure IV-2. Time profiles of total COD removal efficiency (a) and total nitrogen removal efficiency (b).....	174
Figure IV-3. Time profiles of MLSS in oxictank (a) and MLSS in anoxic tank (b).....	175

Figure IV-4. Time profiles of floc size in oxic tank (a) and floc size in anoxic tank (b).....	176
Figure IV-5. Comparison of total COD removal efficiency (a), total nitrogen removal efficiency (b), MLSS in membrane tank (c) and anoxic tank (d), and floc size in membrane tank (e) and anoxic tank (f).....	177
Figure IV-6. Pearson correlation coefficient between relative composition of OTU 1 ( <i>Thiothrix</i> ) and approximate floc size.....	185
Figure IV-7. Microbial networks of activated sludge of control-MBR (a) and QQ-MBR (b) in oxic tank.....	188
Figure IV-8. Microbial networks of activated sludge of control-MBR (a) and QQ-MBR (b) in anoxic tank.....	192
Figure IV-9. The LDA score of metabolic pathway in activated sludge .....	199
Figure V-1. Microbial community of biofilm and activated sludge richness (a), diversity (b), and evenness (c).....	216
Figure V-2. Cluster analysis of biofilm and activated sludge from MBRs.....	220
Figure V-3. The principal coordinate analysis of biofilm and activated sludge...	221
Figure V-4. The principal coordinate analysis of biofilm (a) and activated sludge (b).....	224
Figure V-5. Average relative abundances (%) of quorum sensing related bacteria by bacterial phylotypes in the MBR.....	231
Figure V-6. Average relative abundances (%) of bacterial phylotypes in biofilm (a) and activated sludge (b).....	233
Figure V-7. Microbial networks of biofilm (a) and activated sludge (b).....	238

Figure V-8. The hub node networks of biofilm (a) and activated sludge (b).....248

Figure V-9. The sub-network conducted to identify the microbe-environment associations in biofilm (a) and activated sludge (b).....251

## List of Tables

Table II-1. Characteristic of ammonia and nitrite oxidizing bacteria.....	13
Table II-2. Biological nitrogen removal process comparison.....	15
Table II-3. The 20 largest MBRs in the World.....	23
Table II-4. List of MBR process developed in Korea.....	24
Table II-5. Some examples of AHL-dependent quorum sensing systems in Gram-negative bacteria.....	50
Table II-6. Functions regulated by AI-2 signal.....	59
Table II-7. Enzymatic AI-1 quorum quenching.....	67
Table II-8. Quorum sensing inhibitor.....	79
Table II-9. List of NGS sequencing platforms and their expected throughputs, error types and error rates.....	102
Table II-10. Major functions of seven pipelines.....	110
Table II-11. Summary of multivariate analyses in microbial ecology.....	112
Table II-12. Characteristics of the main reference resources for metagenomics focused on the 16S ribosomal RNA gene.....	116
Table II-13. The network analysis index in this study.....	121
Table III-1. Operation conditions of Anoxic/Oxic MBR.....	133
Table III-2. The hydrodynamic resistance of the membrane ( $R_m$ ) of each run.....	136
Table III-3. Average relative composition (%) of dominant bacteria in biofilm...	156
Table III-4. Relative composition (%) of dominant bacteria in biofilm.....	157
Table IV-1. The detection of <i>Rhodococcus</i> sp BH4 in QQ-bead and activated sludge in the oxic tank during QQ-MBR operation.....	172

Table IV-2. Average bacterial compositions at the species level.....	180
Table IV-3. Bacterial compositions at the species level in oxic tank.....	181
Table IV-4. Bacterial compositions at the species level in anoxic tank.....	182
Table IV-5. Characteristics of network of activated sludge without environmental factors.....	190
Table V-1. Characteristics of 10 different membrane bioreactors.....	207
Table V-2. List of quorum sensing related bacteria.....	212
Table V-3. Statistical analysis of community diversity using completely randomized block design.....	217
Table V-4. Spearman correlation coefficient ( $\rho$ ) between community diversity and MBR operation factors.....	218
Table V-5. Statistical analysis of the bacterial composition using completely randomized block design.....	222
Table V-6. Spearman correlation coefficient ( $\rho$ ) between PCoA axis 1 in Fig. V-4 and environmental factors.....	225
Table V-7. The relative abundances (%) of the bacterial phylotypes of filamentous bacteria and the Spearman correlation coefficient ( $\rho$ ) between the relative abundance (%) of filamentous bacteria and the HRT in the membrane tank (hr).....	227
Table V-8. Statistical analysis of the effect of membrane materials on the bacterial composition of biofilm using the Tukey-Kramer test.....	229
Table V-9. Average relative abundances (%) of the bacterial phylotypes in the biofilm.....	234

Table V-10. Average relative abundances (%) of the bacterial phylotypes in the activated sludge.....	235
Table V-11. Characteristics of the microbial association network without environmental factors in biofilm and activated sludge.....	242
Table V-12. Average relative abundances (%) of bacteria in the biofilm.....	244
Table V-13. Average relative abundances (%) of bacteria in the activated sludge.....	245



# Chapter I

## Introduction



## **I.1. Backgrounds**

Membrane bioreactors (MBRs), combining membrane separation with biochemical conversion, have led to a range of innovative environmental biotechnology applications for wastewater treatment and reuse (Hai et al. 2013). It provides high removal efficiency of organic pollutants, and water reclamation by allowing high concentration of mixed liquor suspended solids (MLSS) and low production of excess sludge compare to conventional activated sludge systems (Meng et al. 2009). In addition, Santos et al. (2011) reported that the market growth of MBR technology has been accelerated by rapid increase in implementation of water reuse technologies. These technologies are necessitated by the combination of elevated water scarcity and increasingly stringent legislation. However, MBRs are hampered particularly by membrane biofouling, resulting from microbial growth on the membrane surface and microbial production of membrane foulants in activated sludge (Hwang et al. 2008; Malaeb et al. 2013) because it results in decreased plant productivity/permeate yield, membrane lifespan and energy efficiency (Drews 2010).

Recently, biological approaches (e.g., quorum quenching, nitric oxide-induced biofilm dispersal and enzymatic disruption of extracellular polysaccharides and protein) have been applied to mitigate biofouling in MBRs (Xiong and Liu 2010). Particularly, Yeon et al. (2008) revealed that quorum sensing (QS) is strongly related with biofilm formation on the membrane surface in a lab-scale

MBR. Furthermore, they demonstrated that biofilm formation (biofouling) could be substantially mitigated by the quorum quenching (QQ) using an enzyme (i.e., acylase) (Yeon et al. 2009; Kim et al. 2011). However, enzymatic QQ has the issues of cost and stability. These problems necessitate more effective QQ methods. Oh et al. (2012) proposed new QQ strategy using isolation of the indigenous QQ-bacteria producing the QQ enzyme from activated sludge and developed a carrier encapsulating the QQ bacteria. This new QQ strategy is an attractive approach to control biofouling in MBR because it gives rise to less declining of treatment efficiency and less consumption of additional energy. Recently, they isolated new QQ-bacteria and developed various type of carrier to increase QQ activity (Cheong et al. 2013; Kim et al. 2013b; Cheong et al. 2014; Köse-Mutlu et al. 2015; Kim et al. 2015a) and this approach has been fully investigated in a larger pilot scale MBR using real wastewater (Lee et al. 2016).

From these results, QS control has been stand out as innovative technique to mitigate biofouling in MBR. However, although the biological understanding of the effect of QQ and biofouling mechanism is crucial for the development of new biofouling control strategies, the information of the microbial ecology is not sufficient in both QQ-MBR and full-scale MBRs. In the QQ-MBR, only a few studies reported that the enzymatic QQ had effect on the development of microbial composition in biofilm. The information of microbial community of biofilm has not been fully elucidated to date in full-scale MBRs. Therefore the investigations of microbial community in both QQ-MBR and full-scale MBRs are required for the successful biofouling control in real MBRs.

## **I.2. Objectives**

The objective of this study was to investigate the microbial community in QQ-MBR and to determine the effect of QQ on microbial community of both biofilm and activated sludge. Furthermore, the microbial communities of biofilm and activated sludge were elucidated and the effects of environmental factors on microbial communities were determined using high-throughput sequencing (an Illumina MiSeq platform) in 10 full-scale MBRs. The specific objectives of this study are as follows:

### **(1) Effect of QQ on the Microbial Community of Biofilm in an Anoxic-Oxic MBR**

Based on the transmembrane pressure (TMP) and time (d), the microbial communities of biofilm were investigated. Multivariate statistical techniques (e.g., principal component analysis and correspondence analysis) were used to reveal how TMP and time affected microbial community composition. The effects of bacterial QQ on the microbial community of the biofilm were determined.

### **(2) Effect of QQ on the Microbial Community of Activated Sludge in an Anoxic-Oxic MBR**

The effects of QQ on the function and microbial community of activated sludge were determined. Microbial network analysis based on co-occurrence

and correlation patterns has been applied to examine the complex microbial community of QQ-MBR.

### **(3) Survey of Microbial Community in Full-Scale MBRs for Wastewater Treatment**

The microbial communities were surveyed to determine which microbes play key roles in 10 full-scale MBRs with different membrane materials, nutrient removal processes and operational factors. The microbial communities of biofilm and activated sludge were elucidated and the effects of environmental factors on microbial communities determined in 10 full-scale MBRs. Microbial network analysis has been applied for a better understanding of the complex microbial community within full-scale MBRs.

# Chapter II

## Literature Review



## **II.1. Biological wastewater treatment**

### **II.1.1. History of biological wastewater treatment**

The history of modern public health and wastewater treatment was encouraged by the rapid industrialization and urbanization of mid-19th century England. This resulted in the contamination of potable water and problems with diseases and stink. So, these problems led to developments biological wastewater treatment process. Attempts to improve treatment techniques ultimately led to the invention of the activated sludge (AS) process in 1914 in UK (Jenkins 2014).

After development of the AS process, early wastewater treatments were designed to remove organic matter and to oxidize ammonia to nitrate, and this is still the goal of the biological wastewater treatment being built today. However, industrialization and population growth continued, another problem was recognized in the second half of the 20th century – eutrophication, which is the accelerated aging of lakes, bays, and so on due to excessive plant and algal growth. This is the results of the release of nutrients such as nitrogen and phosphorus. In the 1960s it became clear that the nitrogen and phosphate also need to be removed from the wastewater to limit eutrophication. To remove the nutrients, fields of bacteriology and bioenergetics were applied to wastewater treatment during 1960s. From these biological fields, biological process was developed to a very advanced level by McCarty (1964), it was realized that the nitrate produced by nitrification could be used by some heterotrophic bacteria instead of oxygen and converted into nitrogen gas. This insight led to the nitrification-denitrification AS systems, in which parts of the reactor were not aerated to induce denitrification. The post-

denitrification system, in which the non-aerated (anoxic) reactor follows the aerobic reactor, was developed by Wurhmann (1964) in Switzerland. The pre-denitrification system developed by Ludzack and Ettinger (1962) formed logical next step. In South Africa, 1972, Barnard combined the post- and pre-denitrification reactors and introduced recycle flows to control the nitrate entering the pre-denitrification reactor in the 4 stage Bardenpho system Phosphorus, mainly in the form of orthophosphate from detergents and human waste, also needed to be removed because in many ecosystems phosphorus proved to be the main limiting elements for eutrophication. There are two main methods to remove phosphorus in wastewater. Chemical method removed phosphorus using precipitation followed by tertiary filtration appeared during the 1970s. Biological method removed phosphorus using phosphate accumulated organisms. Srinath et al. (1959) observed that sludge from a certain treatment plant exhibited excessive phosphate uptake was when aerated. Later, this called enhanced biological phosphate removal (EBPR) was noticed in other wastewater treatment plants (Henze 2008; Grady Jr et al. 2011).

At this time, the demands on the biological wastewater treatments are continuously increasing, with an increased attention on micro-pollutants and energy problems.

## II.1.2. Biological nitrogen removal process

Nitrogen is a major element of the atmosphere and an essential component of many biomolecules (protein or DNA). Conventionally, the nitrogen cycle is described by nitrification, denitrification, and N<sub>2</sub> fixation (Figure II-1).

Nitrification is the biological oxidation of ammonia to nitrate, via hydroxylamine and nitrite. In the Table II-1, Ammonia Oxidation Bacteria (AOB) can combine hydroxylamine with nitrite to give dinitrogen-oxide gas. Nitrite Oxidation Bacteria (NOB) can combine nitrite with oxygen to give nitrate. This process was referred to as aerobic de-ammonification. Under anoxic conditions in the presence of NO<sub>2</sub> the organisms can convert ammonium with NO<sub>2</sub> to NO gas. Both conversions lead to the removal of ammonium from the water phase, but are clearly not desired since the end products are either toxic or a strong greenhouse gas.

Denitrifying microbes are present in almost all environments. The ability to utilize nitrate or nitrite as terminal electron acceptor when oxygen becomes limited is widespread among the prokaryotes, although not all denitrifiers possess the entire pathway. Denitrifying bacteria are found among the  $\alpha$ -,  $\beta$ -, and  $\gamma$ -groups of *Proteobacteria*, but also within the group of Gram-positive bacteria with high GC contents (Baumann 1997). Moreover, completely new microbial group has been discovered. It is the anaerobic ammonium oxidizers or Anammox bacteria. They oxidize ammonia to N<sub>2</sub> gas with nitrite as electron acceptor under anaerobic conditions.

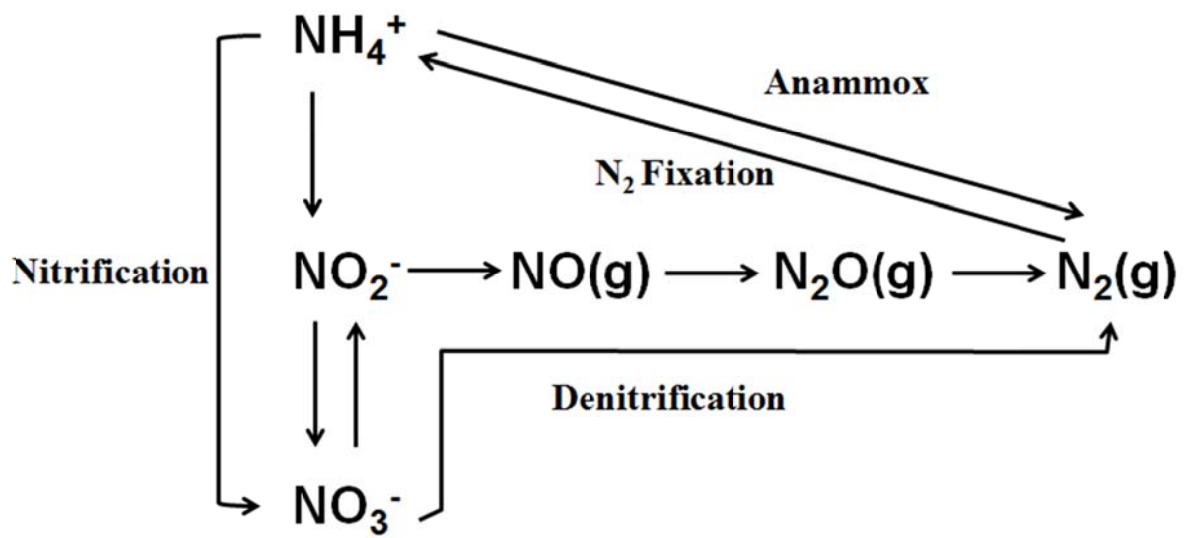


Figure II-1. The nitrogen cycle.

**Table II-1. Characteristic of ammonia and nitrite oxidizing bacteria (Gerardi 2003; Slonczewski and Foster 2009).**

Nitrifying bacteria that oxidize ammonia		
Phylogenetic group	Genus	Characteristics
Beta	<i>Nitrosomonas</i>	Gram-negative short to long rods, motile (polar flagella) or nonmotile, peripheral membrane systems
Gamma	<i>Nitrosococcus</i>	Large cocci, motile, vesicular or peripheral membranes
Beta	<i>Nitrospira</i>	Spirals, motile (peritrichous flagella), no obvious membrane system
Nitrifying bacteria that oxidize nitrite		
Alpha	<i>Nitrobacter</i>	Short rods, reproduce by budding, occasionally motile (single subterminal flagella) or non-motile; membrane system arranged as a polar cap
Delta	<i>Nitrospina</i>	Long, slender rods, nonmotile, no obvious membrane system
Gamma	<i>Nitrococcus</i>	Large Cocci, motile (one or two subterminal flagellum) membrane system randomly arranged in tubes
Nitrospirae	<i>Nitrospira</i>	Helical to vibroid-shaped cells, nonmotile, no internal membranes

The biological nitrogen removal processes were developed using these mechanisms. The characteristics of biological nitrogen removal process were organized in the Table II-2 (Grady Jr et al. 2011). The modified Ludzak-Ettinger (MLE) process offers good nitrogen removal, moderate bioreactor volume requirements, alkalinity recovery, good sludge settleability, reduced oxygen requirements compared to conventional systems, and simple control. However, a high level of nitrogen removal cannot generally be achieved. Practical recirculation flow rate limit N removal to between 60 and 85%.

Bardenpho process includes a second anoxic zone. Performance data from full scale wastewater treatment plants demonstrate this difference. Processes with one anoxic zone typically produce effluents with total nitrogen concentrations ranging between 5 and 10 mg/L as N, while processes with two anoxic zones typically produce effluents with concentration ranging between 1.5 and 4 mg/L as N. However, this improved performance is at the expense of a larger bioreactor volume.

Denitrification also reduces the oxygen requirement in the aerobic zone because nitrate-N serves as the electron acceptor during oxidation of some of the biodegradable organic matter, thereby removing the need for oxygen to do so.

Significant nitrogen removal can also occur in separate stage suspended growth denitrification. It received nitrified effluent and removed nitrogen through anoxic and aerobic stage in series. It has not mixed liquor recirculation.

**Table II-2. Biological nitrogen removal process comparison (Grady Jr et al. 2011).**

Process	Defining Characteristics	Benefits	Drawbacks
Modified Ludzack-Ettinger (MLE)	<ul style="list-style-type: none"> <li>• anoxic(ANX) and aeration(AER) in series</li> <li>• Recirculation from AER to ANX</li> </ul>	<ul style="list-style-type: none"> <li>• Good nitrogen removal</li> <li>• Moderate reactor volume</li> <li>• Alkalinity recovery</li> <li>• Good solids settleability</li> <li>• Reduced oxygen requirement</li> <li>• Simple control</li> </ul>	<ul style="list-style-type: none"> <li>• High level of nitrogen removal not generally possible</li> </ul>
Four-stage Bardenpho	<ul style="list-style-type: none"> <li>• ANX and AER like MLE</li> <li>• Downstream ANX for denitrification</li> <li>• Downstream AER for nitrogen gas stripping</li> </ul>	<ul style="list-style-type: none"> <li>• Excellent nitrogen removal</li> <li>• Alkalinity recovery</li> <li>• Good solids settleability</li> <li>• Reduced oxygen requirement</li> <li>• Simple control</li> </ul>	<ul style="list-style-type: none"> <li>• Large reactor volume</li> </ul>
Denitrification in aerobic reactor	<ul style="list-style-type: none"> <li>• SRT significantly longer than minimum SRT to nitrify</li> <li>• Low DO zones so that denitrification can occur</li> </ul>	<ul style="list-style-type: none"> <li>• Alkalinity recovery</li> <li>• Reduced energy requirement</li> <li>• Easily applied to some existing facilities</li> </ul>	<ul style="list-style-type: none"> <li>• Large reactor volume</li> <li>• Complex control</li> <li>• May result in poor sludge settleability</li> </ul>
Separate stage suspended growth denitrification	<ul style="list-style-type: none"> <li>• Receive nitrified effluent</li> <li>• ANX and AER in series</li> <li>• No mixed liquor recirculation</li> </ul>	<ul style="list-style-type: none"> <li>• Excellent nitrogen removal</li> <li>• Minimum reactor volume</li> </ul>	<ul style="list-style-type: none"> <li>• Requires upstream nitrification</li> <li>• Supplemental electron donor required</li> <li>• High energy requirement</li> </ul>

## **II.2. Membrane bioreactor (MBR)**

### **II.2.1. MBR for advanced wastewater treatment**

MBR is a combination technology of activated sludge process and membrane filtration process for the critical solids-liquid separation and biological treatment. In an activated sludge processes, the biomass (microorganisms) aggregate into flocs and these flocs are suspended in the wastewater to remove contaminants. Once the wastewater is treated, the flocculated biomass must be separated from the clean water. Conventionally, a clarifier is used for solid-liquid separation, as shown in Figure II-2 (a). Conventional activated sludge (CAS) process relies on the development of flocs that settle well. MBR simply replaces the clarifier with a membrane for separation, as illustrated in Figure II-2 (b). These early designs of MBRs were made up of external membrane (Figure II-3, External MBR schematic). However, most MBRs are now designed with the membrane submerged within the bioreactor component of the system (Figure II-3, Immersed MBR schematic). In this design, the activated sludge is located at the outside of the fibers and membrane are operated under suction and permeate is flowing from the outside of the membrane to the inside of the membrane. Coarse-bubble aeration is provided to promote shear at the outside of the membrane surfaces for mitigation of membrane fouling. This design is used for hollow fiber and flat sheet membrane types.

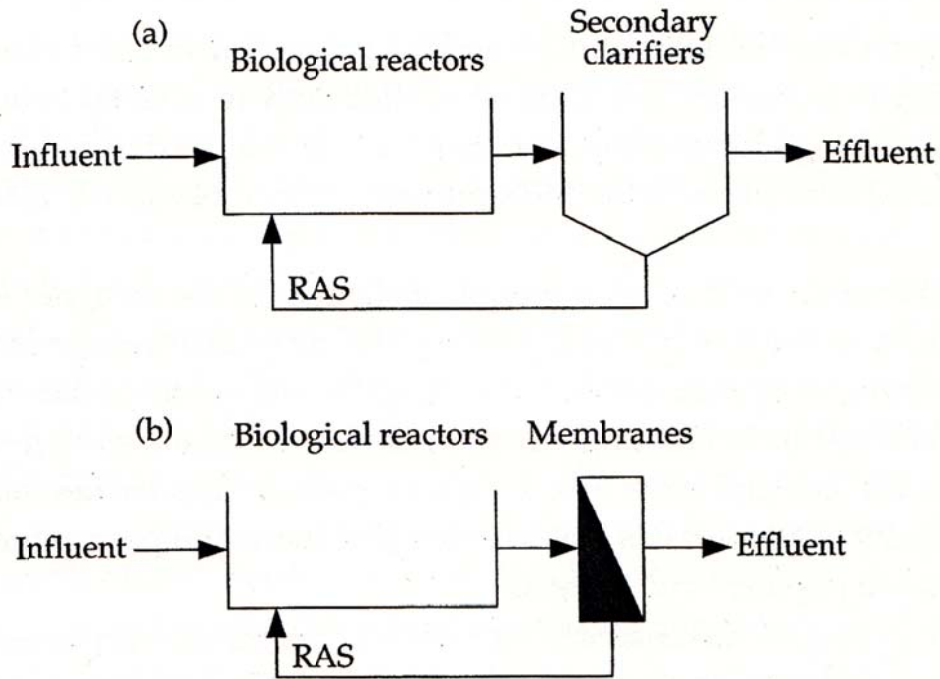
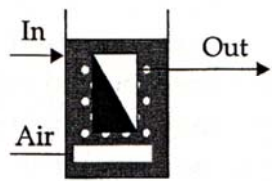
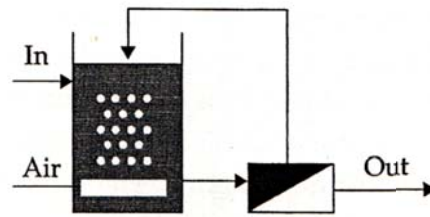


**Figure II-2. (a) Conventional activated sludge (CAS) process with clarifiers for solid-liquid separation, (b) membrane bioreactor process with membrane filtration for solid-liquid separation (WEF press et al. 2011).**



Immersed MBR schematic



External MBR schematic

**Figure II-3. Membrane component operation (WEF press et al. 2011).**

### **II.2.1.1. Advantages and disadvantages of MBR**

The advantages were offered by MBR over CAS process are widely recognized in wastewater treatment (Judd 2008).

- (i) Production of high quality, clarified and largely disinfected permeate product in a single stage; the membrane has an effective pore size  $<0.1$  mm – significantly smaller than the pathogenic bacteria viruses in the sludge.
- (ii) Independent control of solids and hydraulic retention time (SRT and HRT, respectively). In a CAS separation of solid is achieved by sedimentation, which then relies on growth of the mixed liquor solid particles to sufficient size (50  $\mu$ m) to allow their removal by settlement. This then demands an appropriately long HRT for growth. In an MBR the particles need only be larger than the membrane pore sizes
- (iii) Operation at higher mixed liquor suspended solids (MLSS) concentration, which reduces the required the reactor size and promotes the development of specific nitrifying bacteria, thereby enhancing ammonia removal.
- (iv) Reduced sludge production, which results from operation at long SRTs because the longer the solids are retained in the biological tank the lower the sludge production.

Although MBR processes have these advantages, compared with conventional biological treatment process, MBRs are to some extent constrained primarily by:

- (i) Greater process complexity; membrane separation demands additional operation protocols relating to the maintenance of membrane cleanliness.
- (ii) Higher capital equipment and operating costs; the membrane component of the MBR incurs a significant capital cost over and above that of an CAS and maintaining membrane cleanliness demands further capital equipment and operating costs. This is only partly offset by the small size of the plant.

## **II.2.2. History of MBR**

The application of membrane technology in the wastewater treatment was implemented by Dorr-Oliver, Inc. (Milford, Connecticut, USA) in the early 1960s for the separation of fine particulate from wastewater. In 1974, Dorr-Oliver engineers entered into a licensing agreement with Sanki Engineering Company (Tokyo, Japan). The Japanese government had mandated that wastewater is reclaimed and reused to reduce the need for potable water as well as the amount of wastewater being discharged to wastewater treatment. Sanki installed approximately 20 membrane wastewater reclamation systems similar to the one used in the Pikes Peak visitor's center. These facilities incorporated modules that held cartridges of flat-sheet membranes installed in a horizontal plane and referred to as the membrane wastewater treatment system (Bemberis 1971).

Other bench-scale membrane separation process linked with a CAS was reported at around the same time (Bailey et al. 1971). These processes were all based on what have come to known as side stream configuration.

The major breakthrough, which allowed the MBR to grow much faster, was the development in Japan. From 1980s to early 1990s, the Japanese government instigated water recycling program which promoted pioneering work by Yamamoto, Hiasa, Mahmood and Matsuo (Yamamoto et al. 1989). To develop an immersed hollow fiber – ultra filtration (UF) MBR process, as well as the development of an flat sheet-microfiltration (MF) submerged MBR by the agricultural machinery company, Kubota. By the end of 1996, there were already 60 Kuboda plants installed in Japan for domestic wastewater treatment. At the

same time, the USA Thetford Systems were developing their *Cycle-Let*® process, another sidestream process. Zenon Environmental, a company formed in 1980 and who subsequently acquired Thetford System were developing MBR system. By the early 1990s, the ZenoGem® immersed hollow fiber-MF MBR process had been patented and introduced to the market in 1993.

In 1997, the first Kubota municipal wastewater treatment works installed outside of the Japan was Porlack in the United Kingdom (UK). And the first Zenon membrane based plant of similar size installed outside of the USA was the Veolia *Biosep*® plant at Perthes en Gatinais in France in 1999. Both these plants have a peak flow capacity just below 2 mega liter per day (MLD), and represent landmark plants development and implementation of immersed MBR technology. At this time, there were either existing or planned MBR installations of more than 10 MLD capacities (Table II-3). In Korea, there are many membrane makers (Kolon, Econity, Philos, Pure envitec etc). These membrane makers joined with domestic engineering & construction (E&C) companies were developing various types of MBR systems (Table II-4) ([http://www.hwenc.com/Hceng/engRnd/major\\_01.jsp](http://www.hwenc.com/Hceng/engRnd/major_01.jsp) (accessed May 29, 2015); [http://www.dwconst.re.kr/skill/skill02\\_2.asp#s02\\_2](http://www.dwconst.re.kr/skill/skill02_2.asp#s02_2) (accessed May 29, 2015); <https://eng.hec.co.kr/rd/research/hant.asp> (accessed May 29, 2015); <http://kolonmbr.co.kr/eng/processes/processesKIMAS.do> (accessed May 29, 2015); <http://kolonmbr.co.kr/eng/processes/processesI3System.do> (accessed May 29, 2015)).

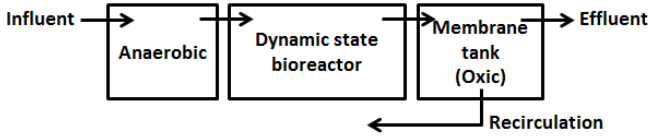
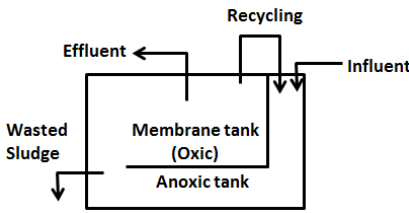
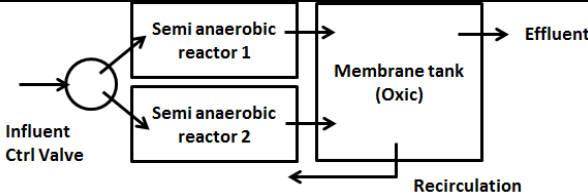
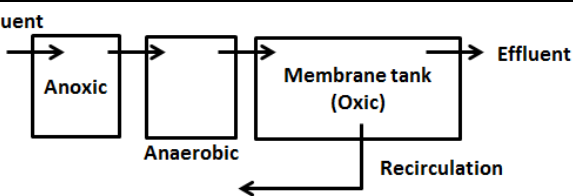
**Table II-3. The 20 largest MBRs in the World**

(<http://www.thembrsite.com/about-mbrs/largest-mbr-plants/>, accessed April 19, 2016).

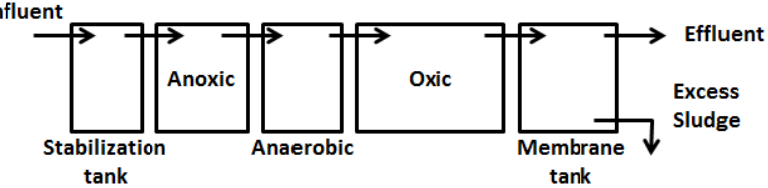
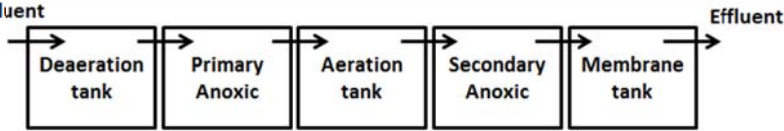
Installations	Location	Technology Provider	(Expected) date of commissioning	PDF (MLD)	ADF (MLD)
Henriksdal	nr Stockholm, Sweden	GEWPT	2016-2019	864	536
Seine Aval	Acheres, France	GEWPT	2016	357	224
Canton WWTP	Ohio, USA	Ovivo USA/Kubota	2015-2017	333	159
Water Affairs Integrative EPC	Xingyi, Guizhou, China	OW		307	
Euclid	Ohio, USA	GEWPT	2018	250	83
9 <sup>th</sup> and 10 <sup>th</sup> WWTP	Kunming, Yunnan, China	OW	2013	250	
Shunyi	Beijing, China	GEWPT	2016	234	180
Macau	Macau Special Administrative Region, China	GEWPT	2017	210	210
Wuhan Sanjintang WWTP	Hubei Province, China	OW	2015	200	
Jilin WWTP (Phase 1, upgrade)	Jilin Province, China	OW	2015	200	
Caotan WWTP PPP project	Xian, Shaanxi, China	OW	2015	200	
Brussels Sud	Brussels, Belgium	GEWPT	2017	190	86
Macau	China	GEWPT	2014	189	137
Riverside	California, USA	GEWPT	2014	186	124
Brightwater	Washington, USA	GEWPT	2011	175	122
Visalia	California, USA	GEWPT	2014	171	85
Qinghe WRP (Phase 2)	Beijing, China	OW	2011	150	
Nanjing East WWTP (Phase 3)	Jiangsu Province, China	OW	2014	150	
Yantai Taozi Wan WWTP	Shandong Province, China	OW	2014	150	
Jilin WWPT (Phase 2)	Jilin Province, China	OW	2014	150	

PDF: Peak daily flow, Mega liters per day, ADF: Average daily flow, Mega liters per day, GEWPT: GE Water and Process Technologies, OW: (Beijing) Origin Water, MRC: Mitsubishi Rayon Corporation

**Table II-4. List of MBR process developed in Korea.**

Process	Process scheme & Characteristics
<p>KS(K water Ssangyong)-MBR</p> <p>Company : Econity, SSangyoung E&amp;C, K water</p>	 <ul style="list-style-type: none"> <li>• The dynamic state bioreactors are aerated intermittently with at any one time, one reactor operating continuously under anoxic conditions and the other operating in batch mod with anoxic/oxic/anoxic conditions- three shifts over a 1hr cycles. This achieved simultaneous nitrification and denitrification.</li> </ul>
<p>D(Daewoo)MBR</p> <p>Company : Daewoo E&amp;C</p>	 <ul style="list-style-type: none"> <li>• Unlike the existing anoxic reactor and aerobic reactor which are arranged horizontally, this system is arranged vertically to save the space.</li> </ul>
<p>DF(Dynamic Flow)-MBR</p> <p>Company : Hanwha E&amp;C</p>	 <ul style="list-style-type: none"> <li>• DF-MBR consists of two semi-anaerobic reactors and aerobic reactor.</li> <li>• The semi-anaerobic reactors turn anoxic into anaerobic conditions periodically by controlling the inflow and it maximizes N, P removal efficiency. The excess sludge is solubilized by bio-chemical process and is treated with influent.</li> </ul>
<p>HANT(Hyundai Advanced Nutrients Treatment)-MBR</p> <p>Company : Hyundai Engineering</p>	 <ul style="list-style-type: none"> <li>• Locating anoxic tank in the front place of biological treatment process</li> <li>• Continual supply of Scrubbing air at a constant rate per projected unit area and Intermittent Operation (Suction pump on/off in a certain time)</li> </ul>

**Table II-4. (continued).**

Process	Process scheme & Characteristics
KIMAS  Company : Kolon	 <p> <ul style="list-style-type: none"> <li>Enhancing carbon source usage</li> <li>Optimizing DO control for denitrification</li> </ul> </p>
I <sup>3</sup> system  Company : Kolon, POSCO E&C, Daewoo E&C	 <p> <ul style="list-style-type: none"> <li>The technology composed of Deaeration Tank, 1<sup>st</sup> Anoxic Tank, Aerobic Tank, 2<sup>nd</sup> Anoxic Tank and Membrane Tank which uses submersed Membrane by Suction filtration. The 2 Stage-Anoxic gives it great capability of loading fluctuation.</li> </ul> </p>

### **II.2.3. MBR trends**

Since first been developed at 1960s, the MBR has been widely used in water reuse systems in building, industry, sanitary treatment and municipal wastewater treatment. In commercial use for little more than a decade, MBR is beginning to realize its market potential in wastewater treatment and water recycling for industrial, municipal, in-building and marine use.

The global market expenditure on MBR was estimated to \$547 million in 2008 and is rising at a compound annual growth rate (CAGR) of 20.2% (Figure II-4). So, the company name of Frost and Sullivan was forecast to \$3,441 million in 2018. In addition, the global daily flow of MBR was estimated to 11,436,000 m<sup>3</sup> in 2018 and is rising at a CAGR of 28.2 % (Research and Market 2012).



(a)



(b)

Figure II-4. (a) Global market value of MBR (Frost and Sullivan, 2013), (b) Global daily flow of MBR (Research and Market 2012).

## II.2.4. Membrane fouling in MBR

Membrane fouling is a major obstacle for wide application of MBRs in wastewater treatment. Generally, membrane fouling was divided into reversible fouling and irreversible fouling. The irreversible fouling should be defined as the fouling that cannot be removed by any methods including chemical cleaning. The reversible (removable) fouling can be easily eliminated by implementation of physical cleaning such as backwashing (Meng et al. 2009). Membrane fouling occurs through a variety of mechanisms. Cake fouling refers to the physical accumulation of colloidal and suspended material on the membrane surface. This material is larger in size than the membrane pores and forms a cake layer on the surface, which offers an additional resistance for filtration. Cake fouling is physically reversible, and is graphically resented in Figure II-5. Pore blocking is graphically explained in Figure II-6. It occurs when colloids, solutes, and microbial cells precipitate inside the membrane pores, and may include the precipitation of inorganic compounds. Pore blocking is typically chemically reversible, but, in some instances, may be irreversible, particularly for certain types of inorganic fouling (WEF press et al. 2011).

Generally, a three stage fouling history might be proposed (Cho and Fane 2002):

- (i) Stage 1: an initial short term rise in TMP due to ‘conditioning’;
- (ii) Stage 2: long-term rise in TMP, either linear or weakly exponential;
- (iii) Stage 3: a sudden rise in TMP, with a sharp increase in  $dTMP/dt$ , also known as the TMP jump

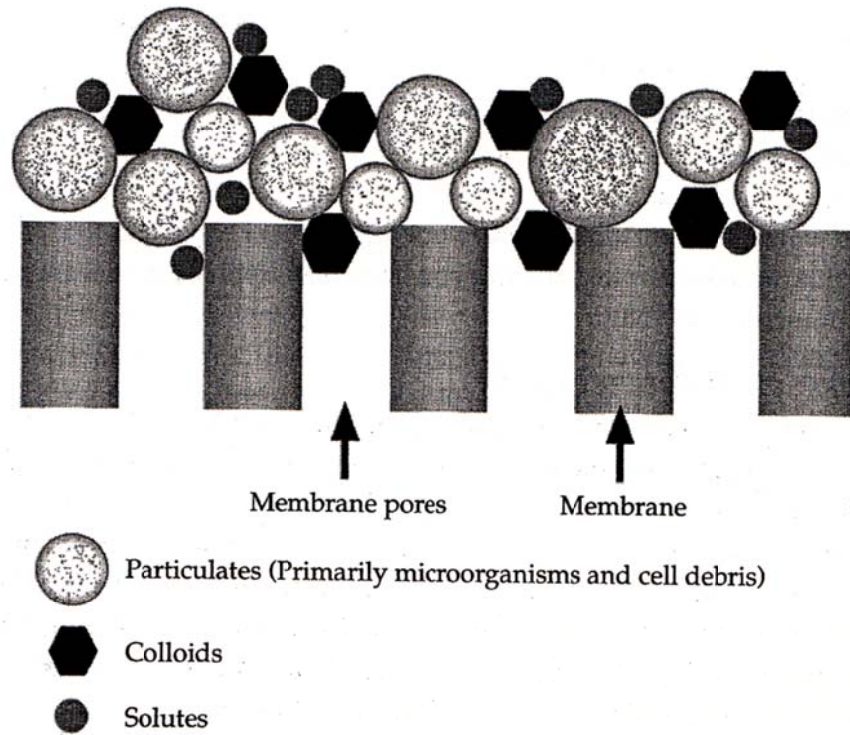


Figure II-5. Membrane fouling mechanisms: cake fouling (WEF press et al. 2011).

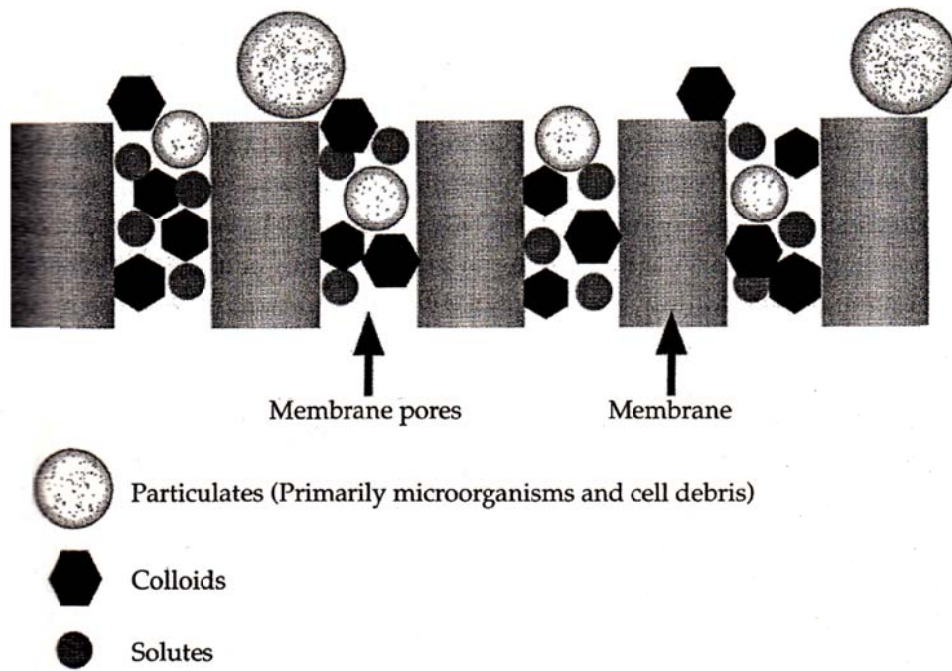


Figure II-6. Membrane fouling mechanisms: pore blocking (WEF press et al. 2011).

Figure II-7 shows the schematic illustration of the occurrence of TMP jump. The TMP jump is believed to be the consequence of severe membrane fouling (Meng et al. 2009). Zhang et al. (2006) summarized a three stage history for membrane fouling in MBRs (Figure II-8).

From the viewpoint of fouling components, the fouling in MBRs can be classified into three major categories: biofouling, organic fouling, and inorganic fouling. Among all types of fouling, biofouling is a dynamic, complex and relatively slow process that involves interactions not yet thoroughly understood. While it is possible to conduct controlled experiments on other foulants, the enormous diversity of bacterial communities and their close association with excreted extracellular polymers (EPS) and soluble microbial products (SMP) complicate experimental approaches that would help explicate this challenging phenomenon. Microbial production of membrane foulants in the activated sludge as well as microbial colonization on membrane surfaces are the main causal agents for biofouling (Malaeb et al. 2013).

Recently, as the control of membrane biofouling (particularly biofouling) in MBR has been recognized as a key factor for reducing the operating and maintenance costs through energy saving, numerous methods of fouling control have been studied reported and implemented in pilot and/or industrial scale MBRs (Hai et al. 2013).

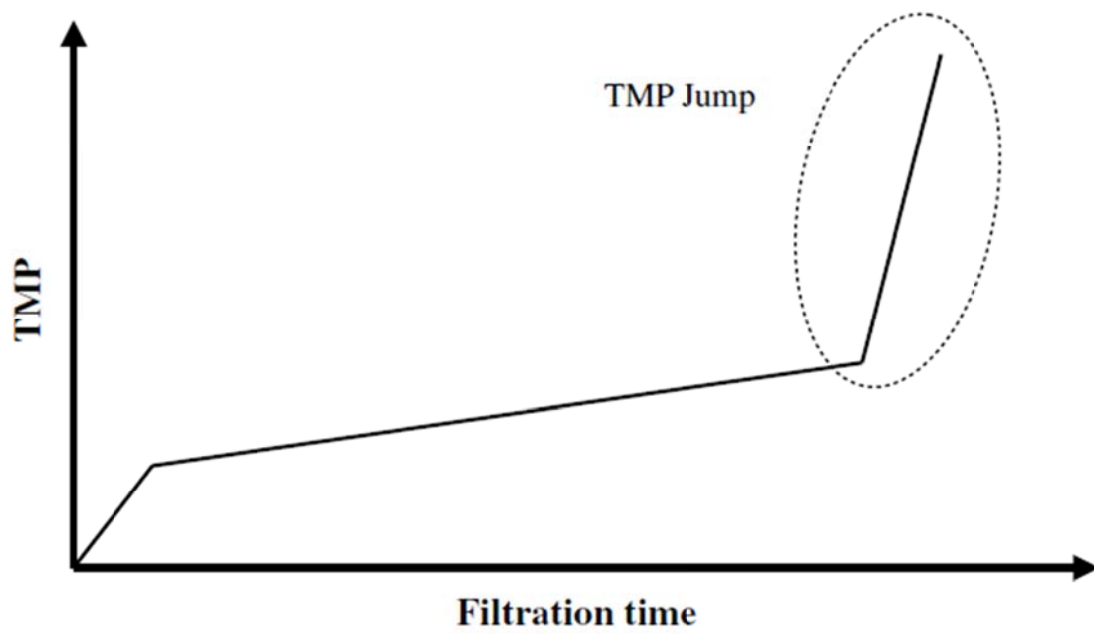


Figure II-7. Schematic illustration of the occurrence of TMP jump.

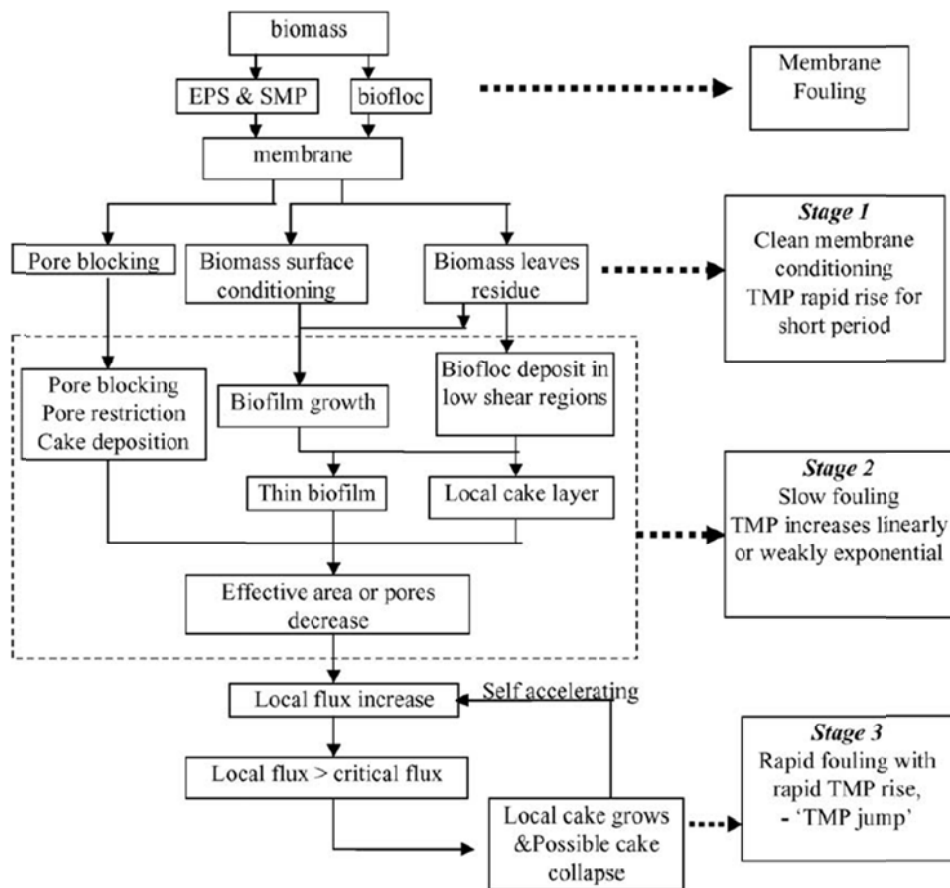


Figure II-8. MBR fouling mechanism map—the three stages of fouling.

### **II.2.5. Biofilm in MBR**

Recently, biofilms started to be introduced to understand the biofouling in the MBR and become the main research stream in MBRs for wastewater treatment. Lewandowski and Beyenal (2005) tried to identify biofouling mechanisms for better membrane design, better membrane modules, and better membrane cleaning procedures. Lee et al. (2008) discussed biofilms in an MBR particularly focusing on the architecture of biofilms (e.g., porosity, thickness and live/dead ratio) formed under various operating conditions such as variations of TMP and position on membrane. Hwang et al. (2008) reported that they observed the typical two-stage TMP increase under subcritical conditions. When a constant flux augmented and reached the supercritical conditions, however, the dual TMP change gradually transformed into a steeper, one-stage TMP increase. They found that the second stage TMP increase under the subcritical flux was closely related to the sudden increase in the concentration of extra-cellular polymeric substances (EPSs) at the bottom layer of the bio-cake. Lee et al (2009) revealed that the local bio-cake porosity was determined experimentally and correlated with the local flux measured by a newly developed experimental method. This result made it possible to suggest the optimum position of an aerator in the reactor to obtain minimal membrane biofouling by analyzing the spatial distribution of biocake porosity on the hollow fiber membrane immersed in MBR system.

Quorum sensing is to control group behaviors of microorganisms, for instance, bioluminescence, antibiotic production, virulence, biofilm formation and sporulation, in response to fluctuations in population density using signal

molecules (Miller and Bassler 2001). Yeon et al. (2008) revealed that quorum sensing is involved with the biofilm formation on MBR membrane surface. They revealed that signal molecules such as *N*-acyl homoserine lactone (AHL) were produced in the MBR using bioassay with *Agrobacterium tumefaciens* reporter strain. Furthermore, they suggested that the biocake showed strong AHL activity simultaneously with abrupt increase in the transmembrane pressure. It implies that QS is in close association with membrane biofouling.

## **II.2.6. Fouling control in MBRs**

As mentioned in the previous section, fouling on the membrane surface is a major obstacle of MBRs in wastewater treatment. Thus, many researchers have been carried out over 20 years for fouling control.

### **II.2.6.1. Physical approach**

Physical approach is normally achieved either by backflushing or relaxation, while continuing to scour the membrane with air bubbles. Air can also be enhanced the effect of backflushing or membrane relaxation (Judd 2010). Aeration is an essential operating factor in MBR to provide the oxygen required for the microbial growth, air bubble scour and disturb the deposition of solids on membrane surface (Meng et al. 2009). However, although aeration rate invariably increase the performance of MBR, it is normally prohibitively expensive.

### **II.2.6.2. Chemical approach**

#### **[1] Chemical cleaning**

Physical cleaning is supplemented with chemical cleaning to remove residual and irreversible fouling (Figure II-9), with this type of cleaning tending to comprise some combination of:

- (i) Maintenance cleaning at moderate chemical concentrations on a twice weekly to monthly basis, designed to remove residual fouling
- (ii) Recovery chemical cleaning once or twice a year, used to remove the irreversible fouling.

## **[2] Chemical additives**

The chemical additives are based on the remove the major foulants (small colloid or biopolymer). Lee et al. (2001) reported that small biological colloids from 0.1 to 2  $\mu\text{m}$  have been observed to coagulate and form lager aggregate when alum is added to MBR. With the addition of natural zeolite, membrane permeability was greatly enhanced by the formation of rigid floc that had lower specific resistance than that of the control activated sludge floc.

A membrane fouling reducer (MFR), a type of cationic polymer, was developed to control membrane fouling in MBR. For instances, Nalco company developed the cationic polymers called MPE (Membrane Performance Enhancer). It was reported that MPE reduced the level of polysaccharide and it was successfully applied in pilot- and full-scale MBRs (Yoon et al. 2005; Yoon and Collins 2006).

Hwang et al. (2007) reported that the soluble EPS concentration in the MFR reactor was lower, but the bound EPS concentration was higher than in the control reactor. During the flocculation of microbial flocs by the added MFR, a portion of the soluble EPS in the bulk phase was entrapped and become incorporated into the coagulated microbial flocs, which led to greater cake porosity.

Lee et al. (2010) reported that the addition of absorbents (Powdered Activated Carbon, PAC) into MBR substantial increased in membrane permeability. The addition of PAC led to a reduction in EPS, which act as glue-like materials, which in turn weakened the cohesion strength of the microorganisms.

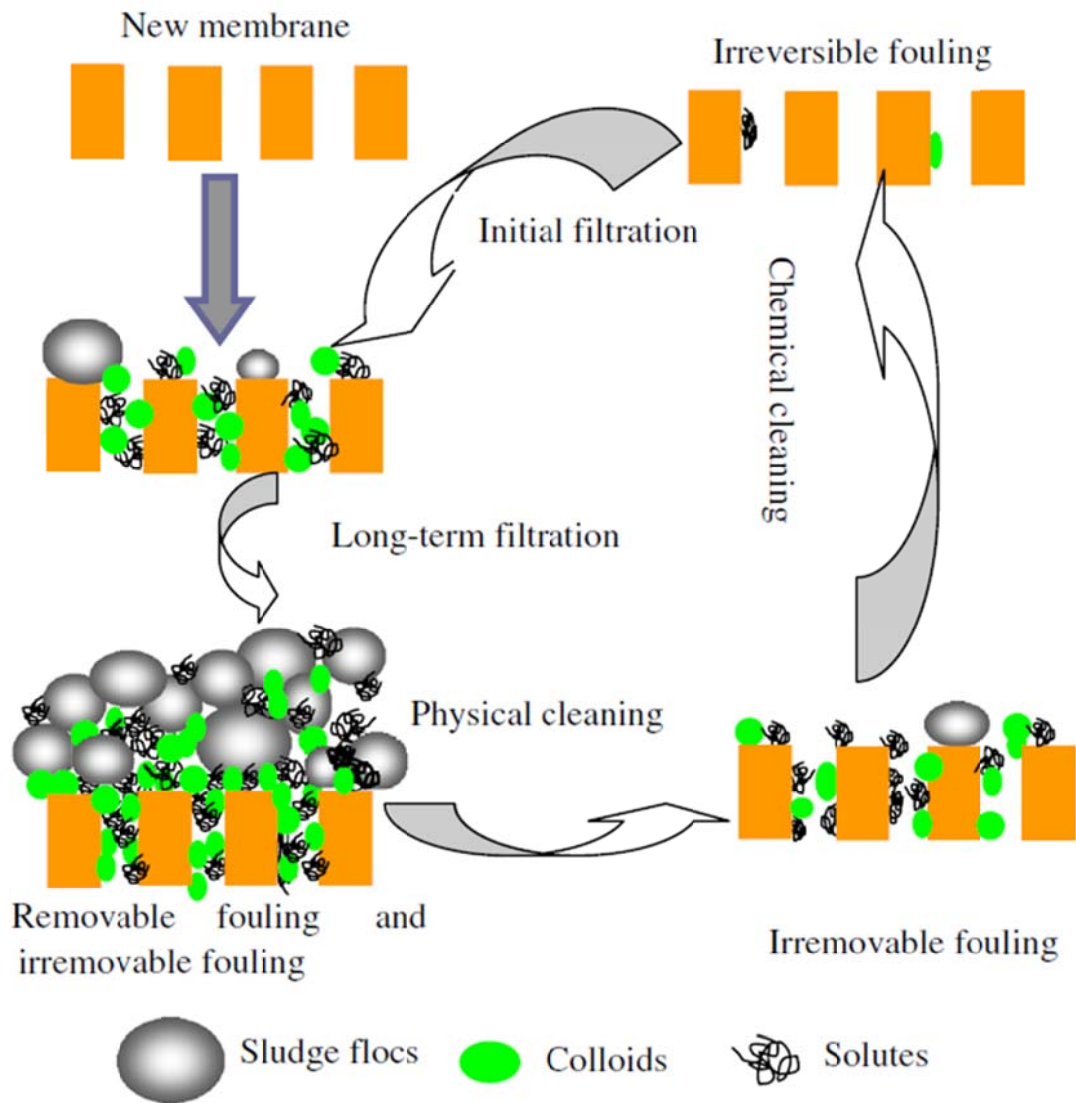


Figure II-9. Schematic illustration of the formation and removal of removable and irremovable fouling in MBRs (Meng et al. 2009).

### **II.2.6.3. Material approach**

Membrane fouling is an interfacial phenomenon between solid membrane surface and mixed liquor containing various organic pollutants and microbes. Thus, increasing intrinsic fouling resistance of membrane surface can be a one of fouling control methods.

Futamura et al. (1994) reported that the transmembrane pressure (TMP) increase rate of hydrophobic membranes was higher than that of hydrophilic ones. This result suggested that fouling resistance of the membrane surface can be enhanced by regulating the hydrophilicity of the surface. Sainbayar et al. (2001) modified the surface of polypropylene membrane by ozone treatment followed by graft polymerization with 2-hydroxyl-ethyl methacrylate and they revealed this method enhanced the water permeability in the anaerobic MBR. Tan and Obendorf (2007) suggested that an antimicrobial property to microporous polyurethane membrane surface by grafting N-halamine precursor and subsequent chlorine bleaching enhanced efficiency of fouling control in the MBR systems. Recently, Lee et al. (2013) reported that membrane including graphene oxide nanoplatelets has better anti-biofouling capability and the rise-up of TMP was delayed in MBR test using this membrane.

### **II.2.6.4. Biological approach**

Recently, biological approaches have been suggested to mitigate biofouling in MBRs, including i) inhibition of QS (i.e., quorum quenching), ii) Nitric oxide (NO) regulated biofilm dispersal, iii) enzymatic disruption of

extracellular polysaccharides (EPS), iv) mitigation of biofouling by cell wall hydrolases (e.g., lysozyme) (Biological control of microbial attachment: a promising alternative for mitigating membrane biofouling) (Xiong and Liu 2010). Although these methods do not yet arrive at puberty, they would provide new insight to develop the biofouling control strategy. It is because they have great potentials in mitigating membrane biofouling.

## II.3. Quorum sensing (QS)

### II.3.1. Definition and mechanism

Quorum sensing is the regulation of gene expression in response to fluctuations in cell-population density. For this purpose, small chemical signal molecules are synthesized and secreted into the environment. By using specific detection systems to sense the concentration of these signal molecules, the surrounding bacteria are aware of the bacterial cell density. The gene expression and, as a result, the group behavior is changed when the signal molecule concentration reaches a critical threshold (Figure II-10) (Miller and Bassler 2001; Boyen et al. 2009).

Particularly, some bacterial species engage in the formation of surface-associated communities known as biofilms. Irie and Parsek (2008) reported that one can predict different ways in which QS might influence biofilm formation. For instance, QS-regulated functions might serve to initiate biofilm formation. Inducing concentrations of QS signals might precede starvation and other types of stress associated with crowded planktonic bacterial populations. To protect themselves from such types of stress, bacteria may form biofilms, a lifestyle that is characteristically more stress-resistant. Most biofilm systems have demonstrated enhanced resistance to external insults such as antibiotics, shear force, and the host immune system. Parsek and Greenberg (2000) explained the development of biofilm in *P. aeruginosa* (Figure II-11). Unattached cells that approach a surface may attach. Attachment involves specific functions. Attached cells will proliferate on a surface and use specific functions to actively move into micro colonies.

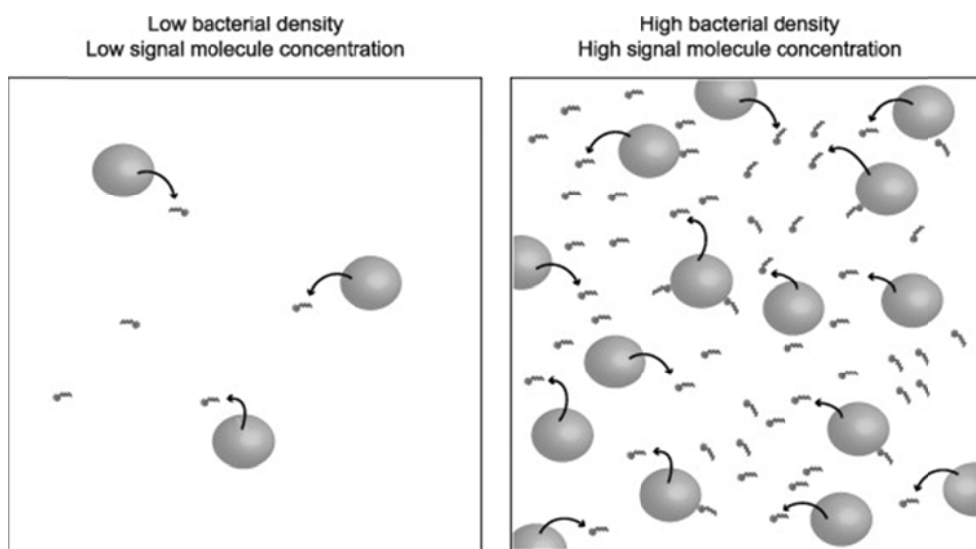


**Figure II-10. The principle of quorum sensing is depicted (Boyen et al. 2009).**

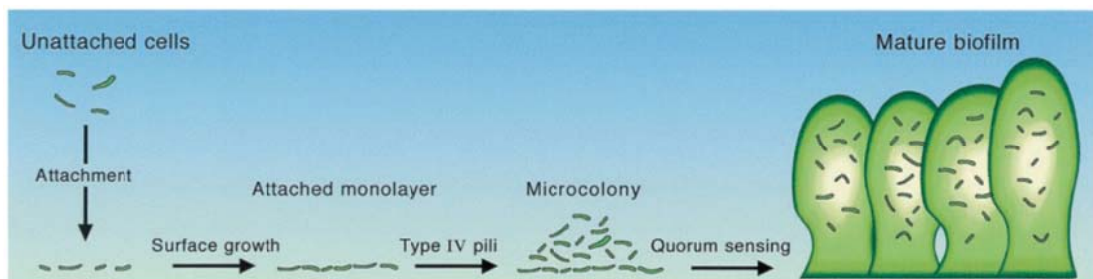


**Figure II-11. Diagram of the *P. aeruginosa* biofilm-maturation pathway** unattached cells that approach a surface may attach. Attachment involves specific functions. Attached cells will proliferate on a surface and use specific functions to actively move into microcolonies. The high-density microcolonies differentiate into mature biofilms by a 3OC12-HSL-dependent mechanism (Parsek and Greenberg 2000).

The high-density micro colonies differentiate into mature biofilms by a 3OC12-HSL-dependent mechanism. QS system can be divided into four general classes based on the type of autoinducer signal (Figure II-12 and II-13) and apparatus used for its detection

- (1) Quorum sensing in Gram-negative bacteria: N-acylhomoserine lactones
- (2) Quorum sensing in Gram-positive bacteria: auto-inducing polypeptides
- (3) Quorum sensing in both Gram-positive and Gram-negative bacteria:  
autoinducer 2
- (4) Quorum sensing beyond bacterial borders: autoinducer 3

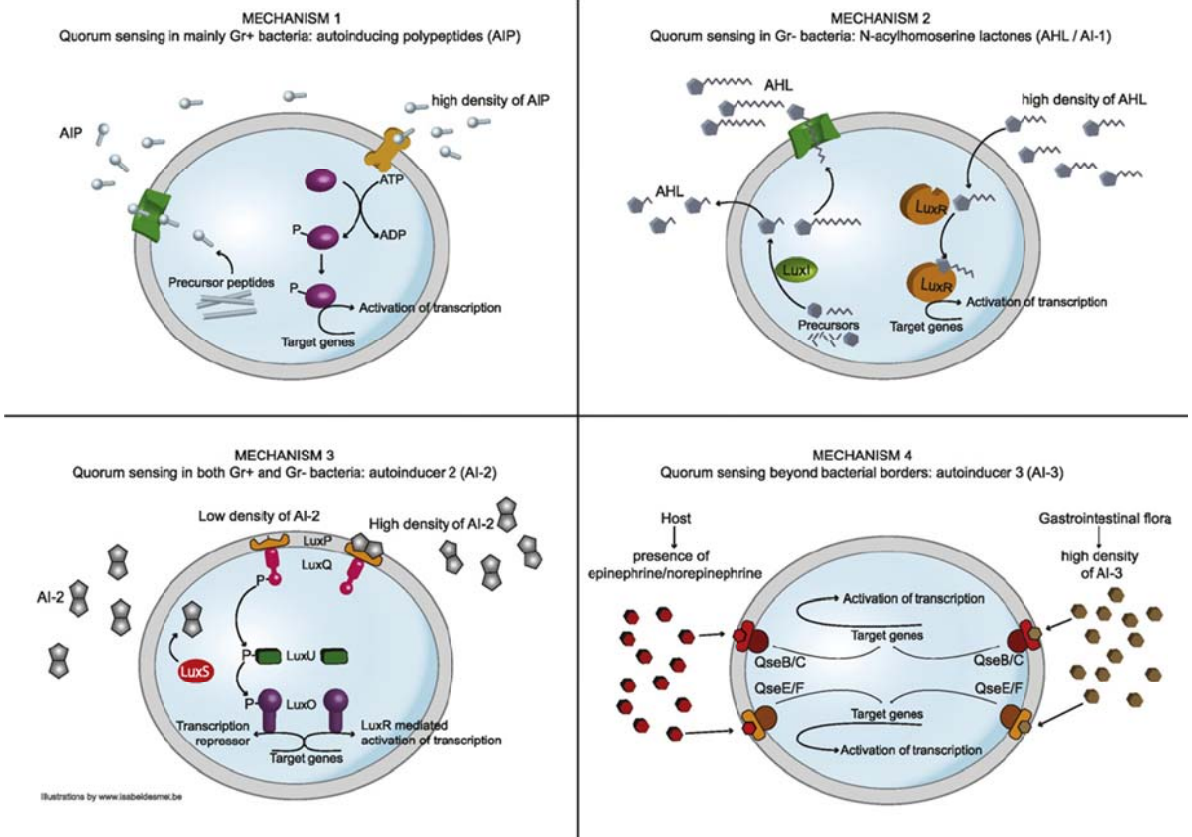
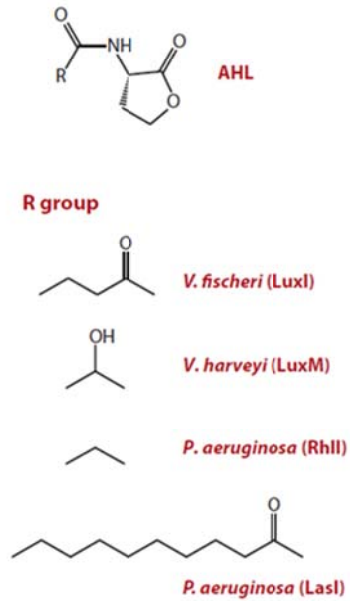
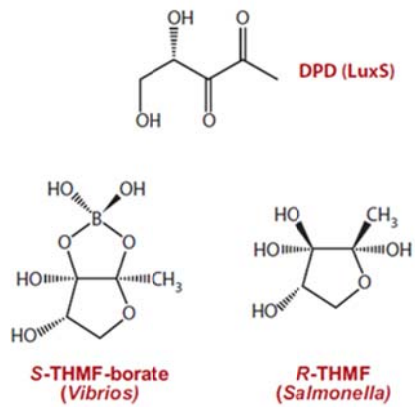


Figure II-12. Four simplified models of the described quorum sensing mechanisms (Boyen et al. 2009).

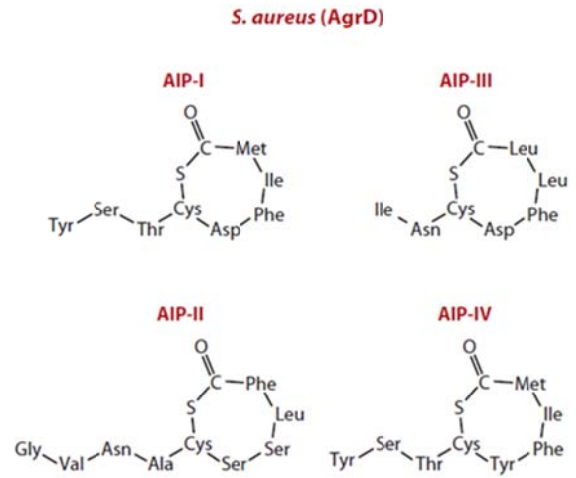
- N-acyl homoserine lactone (AHL) for gram-negative bacteria



- Autoinducer-2 (AI-2) for interspecies communication



- Oligopeptide for gram-positive bacteria



- Others

-Autoinducer-3 (AI-3)  
EHEC O157:H3

-*Pseudomonas* quinoline signal (PQS)

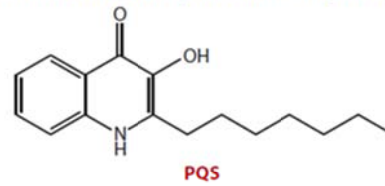


Figure II-13. Representative bacterial autoinducers (Waters and Bassler 2005; Ng and Bassler 2009).

### **II.3.1.1. Quorum sensing in Gram-negative bacteria:**

#### ***N*-acylhomoserine lactones**

In this type of QS system, *N*-acyl homoserine lactone (AHLs) which consist of a homoserine lactone ring joined to a fatty acid side that can vary in the number of carbons and modifications on the third carbon is used as an autoinducer, as shown in Figure II-13. Acyl-HSL signals are generated by the activity of a single enzyme that uses as substrates *S*-adenosylmethionine (SAM) and an intermediate of fatty acid biosynthesis, acyl-acyl carrier protein (acy-ACP). The enzyme is generally a member of the LuxI family of acyl-HSL synthases. Different LuxI homologs generate different acyl-HSLs. Thus *Pseudomonas aeruginosa* RhII primarily catalyzes the synthesis of *N*-butyryl-HSL (C4-HSL), and *P. aeruginosa* LasI directs the synthesis of *N*-(3-oxododecanoyl)-HSL (3OC12-HSL). The acyl side-chain length and the substitutions on the side chain provide signal specificity. Acyl side chains of these signals can be fully saturated, they can have hydroxyls or carbonyls on the third carbon, and they can have lengths of 4 to 16 carbons. Short-chain signals such as C4-HSL diffuse freely through the cell membrane, and 3OC12-HSL partitions into cells, presumably in the membrane. The 3OC12-HSL signal can diffuse into the surrounding environment but export is enhanced by the *mexAB-oprM*, and perhaps other, efflux pumps. Regardless, the cellular concentration of an acyl-HSL is defined by the environmental concentration, and environmental concentrations can rise only when there is a sufficient population of the signal-producing bacterium. The specific receptors for acyl-HSL signals are members of the LuxR family of transcriptional regulators. LuxR family members

have been proposed to consist of two domains, a C-terminal DNA-binding domain, and an N-terminal acyl-HSL-binding domain. A simple model depicting an acyl-HSL quorum-sensing circuit is shown in Fig. II-14. Quite often the two regulatory genes (the R and I genes) are linked, but not always. The orientation of the two genes with respect to each other is variable (Parsek and Greenberg 2000).

AHL signals are made by members of the LuxI family of signal synthases and specifically interact with LuxR family transcription factors. At high cell density, AHLs accumulate and interact with LuxR homologs. AHL binding controls activity of LuxR family members. (a) In *V. fischeri*, LuxI and LuxR produce and respond to 3OC6-HSL, respectively. (b) In *P. aeruginosa*, the LasIR system produces and responds to 3OC12-HSL, and the RhlR system produces and responds to C4-HSL. QscR is an orphan LuxR receptor that is not linked to a luxI synthase gene. QscR responds to 3OC12-HSL produced by LasI. Each quorum-sensing regulon is shown as a distinct entity, but in reality there is overlapping regulation among the controlled genes. Abbreviations: AHL, acyl-homoserine lactone; 3OC6-HSL, 3-oxo-hexanoyl-homoserine lactone; 3OC12-HSL, 3-oxo-dodecanoyl-homoserine lactone; C4-HSL, butanoyl-homoserine lactone (Schuster et al. 2013). There are more than 25 species of bacteria that mediate QS by AHL signal molecules Table II-5.

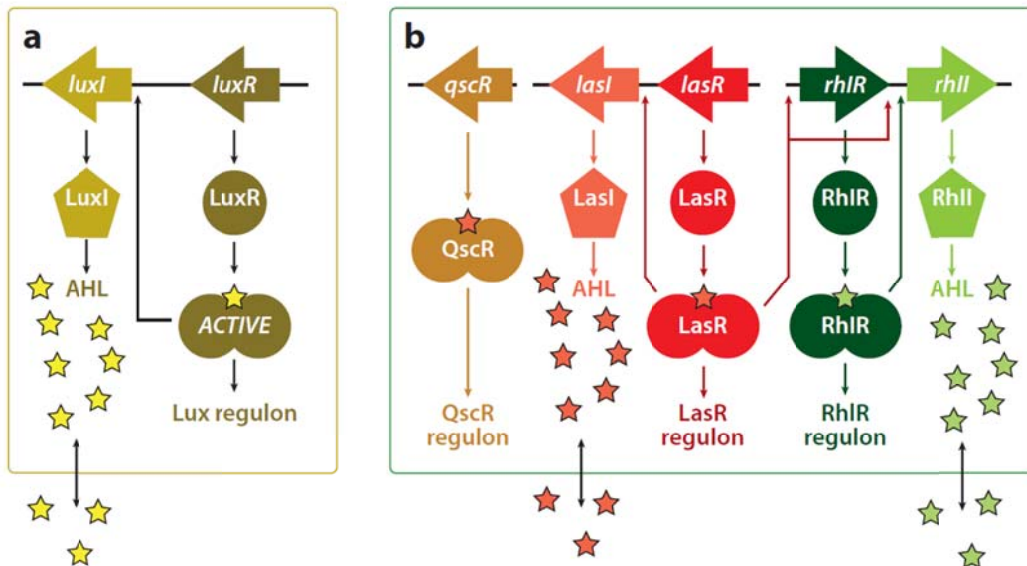


Figure II-14. AHL signaling in (a) *Vibrio fischeri* and (b) *Pseudomonas aeruginosa*. AHL signals are made by members of the LuxI family of signal synthases and specifically interact with LuxR family transcription factors. At high cell density, AHLs accumulate and interact with LuxR homologs. AHL binding controls activity of LuxR family members. (a) In *V. fischeri*, LuxI and LuxR produce and respond to 3OC6-HSL, respectively. (b) In *P. aeruginosa*, the LasIR system produces and responds to 3OC12-HSL, and the RhIR system produces and responds to C4-HSL. QscR is an orphan LuxR receptor that is not linked to a luxI synthase gene. QscR responds to 3OC12-HSL produced by LasI. Each quorum-sensing regulon is shown as a distinct entity, but in reality there is overlapping regulation among the controlled genes. Abbreviations: AHL, acyl-homoserine lactone; 3OC6-HSL, 3-oxo-hexanoyl-homoserine lactone; 3OC12-HSL, 3-oxo-dodecanoyl-homoserine lactone; C4-HSL, butanoyl-homoserine lactone (Schuster et al. 2013).

**Table II-5. Some examples of AHL-dependent quorum sensing systems in Gram-negative bacteria (Matthew TG Holden 2007).**

Organism	Phenotype	Major AHLs
<i>Aeromonas hydrophila</i>	Biofilms, exoproteases, virulence	C4-HSL, C6-HSL
<i>Aeromonas salmonicida</i>	Exoproteases	C4-HSL, C6-HSL
<i>Agrobacterium tumefaciens</i>	Plasmid conjugation	3-oxo-C8-HSL
<i>Agrobacterium vitiae</i>	Virulence	C14:1-HSL, 3-oxo-C16:1-HSL
<i>Burkholderia cenocepacia</i>	Exoenzymes, biofilm formation, swarming motility, siderophore, virulence	C6-HSL, C8-HSL
<i>Burkholderia pseudomallei</i>	Virulence, exoproteases	C8-HSL, C10-HSL, 3-hydroxy-C8-HSL, 3-hydroxy-C10-HSL, 3-hydroxy-C14-HSL
<i>Burkholderia mallei</i>	Virulence	C8-HSL, C10-HSL
<i>Chromobacterium violaceum</i>	Exoenzymes, cyanide, pigment	C6-HSL
<i>Erwinia carotovora</i>	Carbapenem, exoenzymes, virulence	3-oxo-C6-HSL
<i>Pantoea (Erwinia) stewartii</i>	Exopolysaccharide	3-oxo-C6-HSL
<i>Pseudomonas aeruginosa</i>	Exoenzymes, exotoxins, protein secretion, biofilms, swarming motility, secondary metabolites, 4-quinolone signalling, virulence	C4-HSL, C6-HSL, 3-oxo-C12-HSL
<i>Pseudomonas aureofaciens</i>	Phenazines, protease, colony morphology, aggregation, root colonization	C6-HSL
<i>Pseudomonas chlororaphis</i>	Phenazine-1-carboxamide	C6-HSL
<i>Pseudomonas putida</i>	Biofilm formation	3-oxo-C10-HSL, 3-oxo-C12-HSL
<i>Pseudomonas syringae</i>	Exopolysaccharide, swimming motility, virulence	3-oxo-C6-HSL
<i>Rhizobium leguminosarum</i>	bv. viciae Root nodulation/symbiosis, plasmid transfer, growth inhibition, stationary phase adaptation	C14:1-HSL, C6-HSL, C7-HSL, C8-HSL, 3-oxo-C8-HSL, 3-hydroxy-C8-HSL

**Table II-5. (Continued).**

Organism	Phenotype	Major AHLs
<i>Rhodobacter sphaeroides</i>	Aggregation	7-cis-C14-HSL
<i>Serratia</i> spp. ATCC 39006	Antibiotic, pigment, exoenzymes	C4-HSL, C6-HSL
<i>Serratia liquefaciens</i> MG1	Swarming motility, exoprotease, biofilm development, biosurfactant	C4-HSL, C6-HSL
<i>Serratia marcescens</i> SS-1	Sliding motility, biosurfactant, pigment, nuclease, transposition frequency	C6-HSL, 3-oxo-C6-HSL, C7-HSL, C8-HSL
<i>Serratia proteamaculans</i> B5a	Exoenzymes	3-oxo-C6-HSL
<i>Sinorhizobium meliloti</i>	Nodulation efficiency, symbiosis, exopolysaccharide	C8-HSL, C12-HSL, 3-oxo-C14-HSL, 3-oxo-C16:1-HSL, C16:1-HSL, C18-HSL
<i>Vibrio fischeri</i>	Bioluminescence	3-oxo-C6-HSL
<i>Yersinia enterocolitica</i>	Swimming and swarming motility	C6-HSL, 3-oxo-C6-HSL, 3-oxo-C10-HSL, 3-oxo-C12-HSL, 3-oxo-C14-HSL
<i>Yersinia pseudotuberculosis</i>	Motility, aggregation	C6-HSL, 3-oxo-C6-HSL, C8-HSL

### **II.3.1.2. Quorum sensing in Gram-positive bacteria: auto-inducing polypeptides**

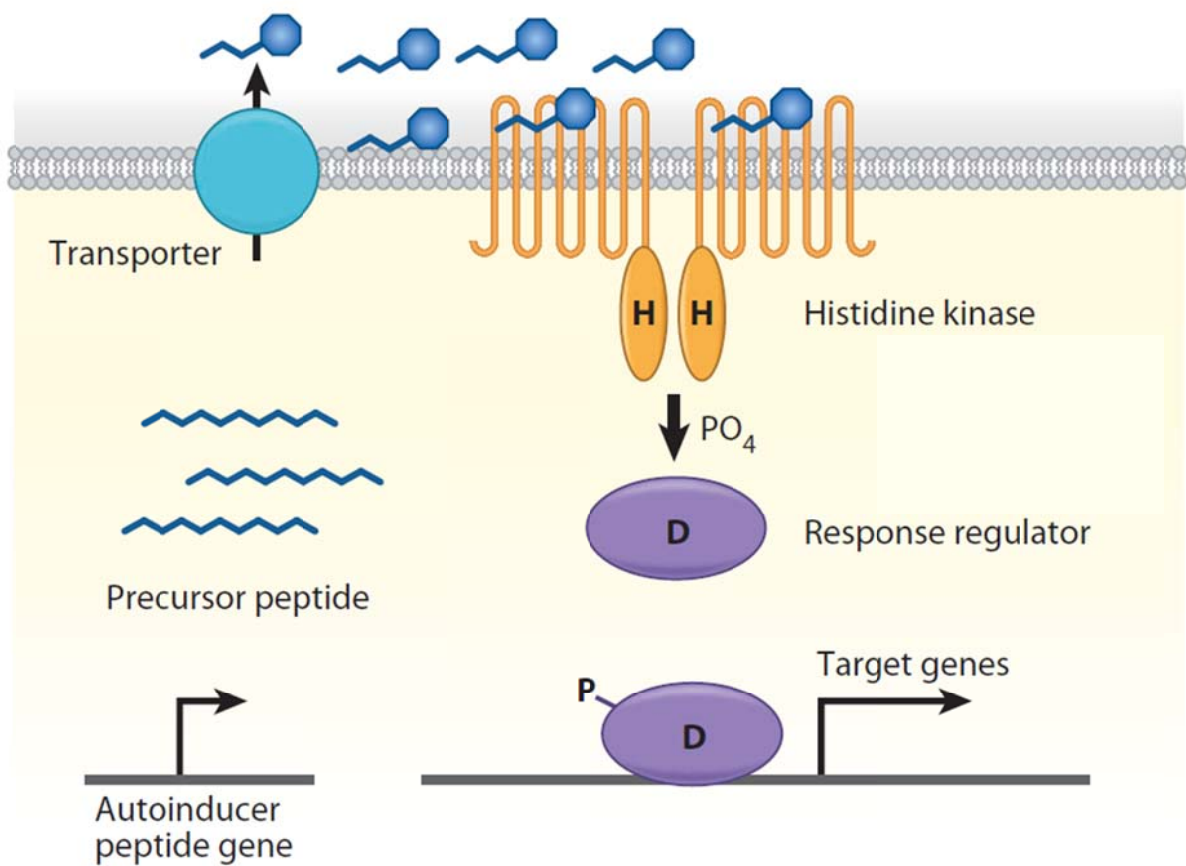
In the gram-positive bacteria, several processes are known that are also regulated in a cell-density-cell-dependent manner. Examples of such quorum-sensing modes in Gram-positive bacteria are the development of genetic competence in *Bacillus subtilis* and *Streptococcus pneumoniae*, the virulence response in *Staphylococcus aureus*, and the production of antimicrobial peptides by several species of Gram-positive bacteria including lactic acid bacteria (Kleerebezem et al. 1997).

Figure II-13 showed that gram-positive bacteria primarily use modified oligopeptides as autoinducers in quorumsensing controlled gene expression systems. One major difference between LuxIR-based and oligopeptide-based quorum-sensing systems is the location of the cognate receptors; whereas the LuxR-type receptors are cytoplasmic, the sensors for oligopeptide autoinducers in Gram-positive bacteria are membrane-bound receptors (two-component systems). A typical two-component system consists of a membrane-bound histidine kinase receptor and a cognate cytoplasmic response regulator, which functions as a transcriptional regulator. The model for oligopeptide mediated quorum sensing is depicted in Figure II-15. As in AHL quorum-sensing systems, the concentration of secreted oligopeptide autoinducer increases as the cell density increases. Peptide binding to the membrane-bound histidine kinase receptor stimulates its intrinsic autophosphorylation activity, resulting in ATP driven phosphorylation of a conserved histidine residue (H) in the cytoplasm. The phosphate group is

subsequently transferred to the conserved aspartate residue (D) of a cognate response regulator. Phosphorylated response regulators are active and they function as DNA binding transcription factors to modulate expression of target genes (Ng and Bassler 2009).

Role of the agr QS System reported that the formation and regulation of staphylococcal biofilms is a complex and multifaceted affair, depending on the organism's genotype as well as on experimental conditions. As with many other species, QS has an important role in staphylococcal biofilm formation (Novick and Geisinger 2008).

Recently, other researcher reported that a QS signal, termed competence stimulating peptide (CSP), involved in the development of competence for natural transformation in the gram-positive bacterium *Streptococcus intermedius*, also favors biofilm formation. The addition of synthetic CSP not only induced competence when cells were exposed to a transformable plasmid but it also significantly enhanced biofilm formation (Suntharalingam and Cvitkovitch 2005).



**Figure II-15. Gram-positive two-component-type quorum-sensing system. Blue octagons denote processed/modified peptide autoinducers (Ng and Bassler 2009).**

### **II.3.1.3. Quorum sensing in both Gram-positive and Gram-negative bacteria: autoinducer 2**

Together with all the recognized autoinducers, AI-2, which tendered to be concerned in interspecies communication, is brought up by diverse species of Gram-negative and -positive bacteria. A essential compound in the AI-2-mediated quorum sensing pathway is 4,5-dihydroxy-2,3-pentanedione (DPD), which can present in a couple of forms that are collectively designated as “AI-2”. LuxS is a mandatory enzyme in the biosynthesis of DPD and subsist in more than 70 categories of bacteria, which enclose both Gram-positive and Gram-negative bacteria. It should be highlighted that these species amalgamate a growing pool of bacteria that regulate pathogenic procedures, such as virulence factor production, cell motility and bacterial conjugation in an AI-2 dependent demeanour. Biosynthesis of AI-2 is found in approximately half of bacterial species as indicated in Figure II-16. It begins with *S*-adenosyl-L-homocysteine (SAH), the product of *S*-adenosylmethionine dependent transmethylation. SAH is hydrolyzed to *S*-ribosyl- L-homocysteine (SRH) and adenine by SAH/5'- methylthioadenosine nucleosidase (SAHN or MTAN). The enzyme LuxS (*S*-ribosylhomocysteine lyase) then cleaves SRH to yield L-homocysteine (Hcy) and 4,5-dihydroxy-2,3-pentanedione (DPD); the latter is the precursor of AI-2. Subsequently, DPD cyclizes to generate a couple of AI-2 forms, for example, DPD will be converted into a hydrated form S-DHMF, consequently be incorporated with boric acid to obtain AI-2 signal molecule, *S*-THMF-borate, in *V. harveyi*. However, the hydration of DPD can as well lead to AI-2 signal, *R*-THMF in *Salmonella*

*typhimurium*. One thing should be noted that the chemical synthesis of DPD is quite complicated because it is unstable at high concentrations and therefore gives rise to oligomerization. Manikandan Kadirvel reported a novel synthesis of (*S*)-DPD via (2*S*)-2,3-O-isopropylidene-glyceraldehyde and its unnatural enantiomer (*R*)-DPD via (2*R*)-2,3-O-isopropylidene-glyceraldehyde. The authors disclosed (*S*)-DPD has higher activity when compared with (*R*)-DPD in *Vibrio harveyi*. The precursor molecule, DPD, undergoes various rearrangements and additional reactions to form distinct biologically active AI-2 signal molecules. The *V. harveyi* AI-2 (*S*-THMF-borate) is produced by Route 1, in the meanwhile the *S. typhimurium* AI-2 (*R*-THMF) is originated by Route 2. Therefore, strategies for inhibiting the AI-2 quorum sensing pathway may include inhibiting the biosynthesis of DPD, finding receptor antagonists to prevent signal reception, as well as converting and trapping DPD in an inactive form. (Zhu and Li 2012).

A clear role in quorum sensing has been demonstrated for AI-2 in certain bacterial species (Table II-6). In the Figure II-17, (a) at low cell density, phosphate fluxes from the membrane receptors, LuxN, LuxPQ and CqsS, to LuxU and then LuxO. Accumulation of phosphorylated LuxO activates the transcription of five regulatory sRNAs, Qrr1-5, which in turn destabilize the luxR mRNA and inhibit expression of this high cell density master regulator. Conversely, Qrr1-5 supports expression of AphA, the low cell density regulator, which leads to changes in the regulation of more than 100 genes. (b) At high cell density, the autoinducers CAI-1, AI-2 and 3OH4CHSL accumulate in the surrounding media and bind to their corresponding receptors, CqsS, LuxPQ, and LuxN, respectively. Ligand binding

promotes the phosphatase activity of these proteins, such that phosphate flow through the pathway is reversed. The resulting unphosphorylated LuxO does not induce the transcription of Qrr1-5; LuxR is produced which regulates the quorum sensing regulon of *V. harveyi*, whilst inhibiting the expression of AphA, such that a high cell density phenotype is induced. *Vibrio cholerae* has a similar circuit, although it does not have the 3OHC4HSL-LuxN circuit, contains four Qrrs and not five, and LuxR is called HapR. Note that the *V. harveyi* LuxR is not homologous to the LuxR in canonical LuxI/LuxR-type circuits (Pereira et al. 2013).

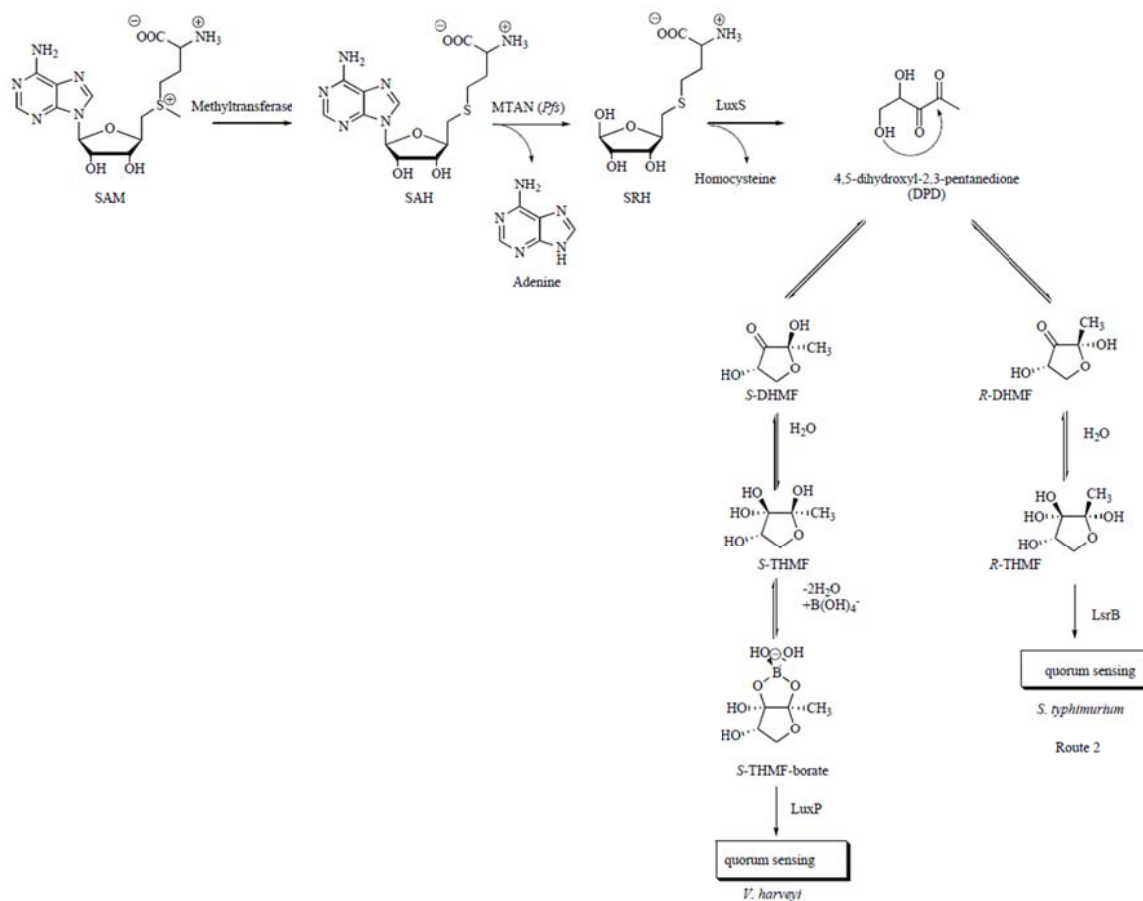


Figure II-16. The biosynthetic pathway of AI-2 *in vivo* (Zhu and Li 2012).

**Table II-6. Functions regulated by AI-2 signal (Pereira et al. 2013).**

Species	Functions regulated by AI-2	AI-2 receptor
<i>Actinobacillus pleuropneumoniae</i>	Biofilm formation, adherence to host cells and growth in iron-limited medium	Unknown
<i>Actinomyces naeslundii</i> and <i>Streptococcus oralis</i>	Mutualistic biofilm formation	Unknown
<i>Aggregatibacter actinomycetemcomitans</i>	Biofilm formation	LsrB and RbsB
<i>Bacillus cereus</i>	Biofilm formation	LsrB
<i>Borrelia burgdorferi</i>	Increased expression of the outer surface lipoprotein VlsE	Unknown
<i>E. coli</i> EHEC	Chemotaxis towards AI-2, Motility and HeLa cell attachment	LsrB
<i>E. coli</i> K12	Biofilm formation and motility AI-2 incorporation and chemotaxis towards	LsrB
<i>Haemophilus influenzae</i> strain 86-028NP	AI-2 incorporation and biofilm formation	RbsB
<i>Helicobacter pylori</i>	Motility	Unknown
<i>Moraxella catarrhalis</i>	Biofilm formation and antibiotic resistance	Unknown
<i>Mycobacterium avium</i>	Biofilm formation	Unknown
<i>Pseudomonas aeruginosa</i>	Virulence factor production	Unknown
<i>Salmonella enterica</i> ssp. <i>enterica</i> serovar	Pathogenicity island 1 gene expression and invasion into eukaryotic cells	LsrB
<i>Typhimurium</i>	AI-2 incorporation	LsrB
<i>Sinorhizobium meliloti</i>	AI-2 incorporation	LsrB
<i>Staphylococcus aureus</i>	Capsular polysaccharide gene expression and survival rate in human blood and macrophages	Unknown
<i>Staphylococcus epidermidis</i>	Expression of phenol-soluble modulins, acetoin dehydrogenase, gluconokinase, bacterial apoptosis protein LrgB, nitrite extrusion protein and fructose PTS system subunit	Unknown
<i>Streptococcus anginosus</i>	Susceptibility to antibiotics	Unknown
<i>Streptococcus intermedius</i>	Haemolytic activity, biofilm formation and susceptibility to antibiotics	Unknown
<i>Streptococcus gordonii</i>	Biofilm formation	Unknown
<i>Streptococcus gordonii</i> and <i>Streptococcus oralis</i>	Mutualistic biofilm formation	Unknown

**Table II-6. (Continued).**

Species	Functions regulated by AI-2	AI-2 receptor
<i>Streptococcus pneumoniae</i>	Biofilm formation	Unknown
<i>Vibrio cholerae</i>	Biofilms, protease and virulence factor production, and competence	LuxP
<i>Vibrio harveyi</i>	Bioluminescence, colony morphology, siderophore production, biofilm formation, type III secretion and metalloprotease production	LuxP

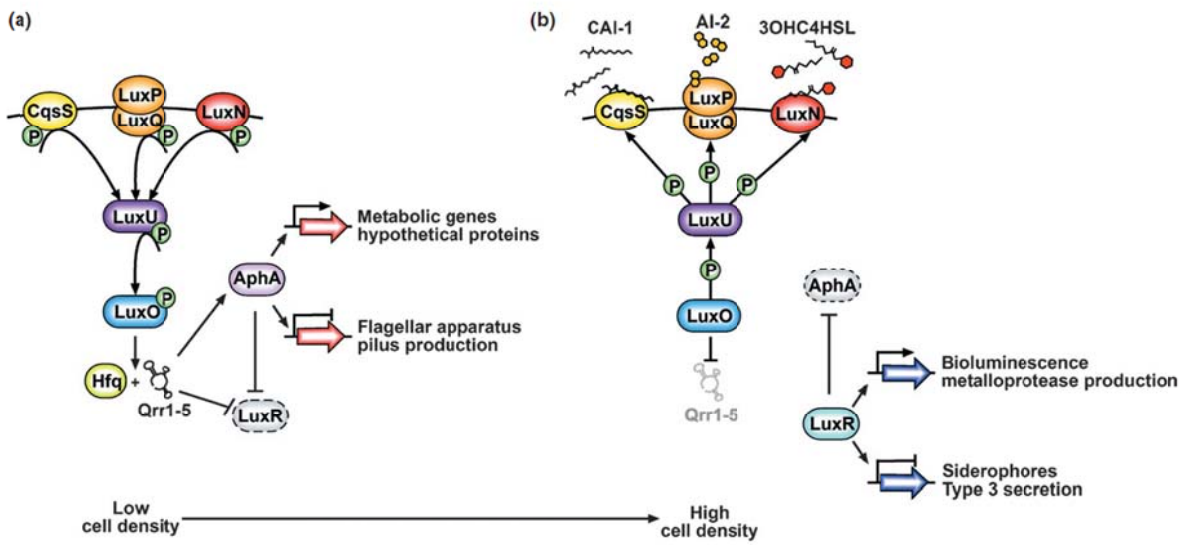


Figure II-17. AI-2 quorum sensing in *V. harveyi* (Pereira et al. 2013).

#### II.3.1.4. Quorum sensing beyond bacterial borders: auto-inducer 3

*Enterohaemorrhagic Eschericia coli* (EHEC) is the cause of various food-borne outbreaks of severe intestinal disease and the causative agent of serious disease in humans. EHEC motility, attaching and effacing virulence genes are regulated by a QS mechanism that involves the poorly characterized auto inducer 3 (AI-3), which is produced by several bacteria. AI-3 probably is structurally similar to epinephrine/norepinephrine because epinephrine/norepinephrine can induce the same virulence gene expression in EHEC and the effects of AI-3 can be inhibited by adrenergic receptor inhibitor (Boyen et al. 2009).

*P. aeruginosa* also produces a third autoinducer, 2-heptyl-3-hydroxy-4-quinolone, designated the *Pseudomonas* quinolone signal (PQS) (Figure II-13). Production of PQS is influenced both positively and negatively by the LasIR and RhIR systems, respectively (Ng and Bassler 2009). A major induction of *rhlI'-lacZ* was caused by PQS. PQS had less effect on the transcription of *lasR'-lacZ* and *rhlR'-lacZ*. PQS was not produced maximally until the late stationary phase of growth. PQS acts as a link between the *las* and *rhl* quorum sensing systems and this signal is not involved in cell density (McKnight et al. 2000).

## **II.4. Quorum quenching (QQ)**

### **II.4.1. The strategy of QQ**

There are three strategies to control the AHL type QS system of gram negative bacteria (Figure II-18). Strategies and focal points for controlling the QS system are listed below;

- (1) Blockage of AHL synthesis (Blockage of LuxI homologue)
- (2) Interference with signal receptor (Interference of LuxR homologue)
- (3) Inactivation of AHL molecules  
(Degradation or modification of AHL molecules)

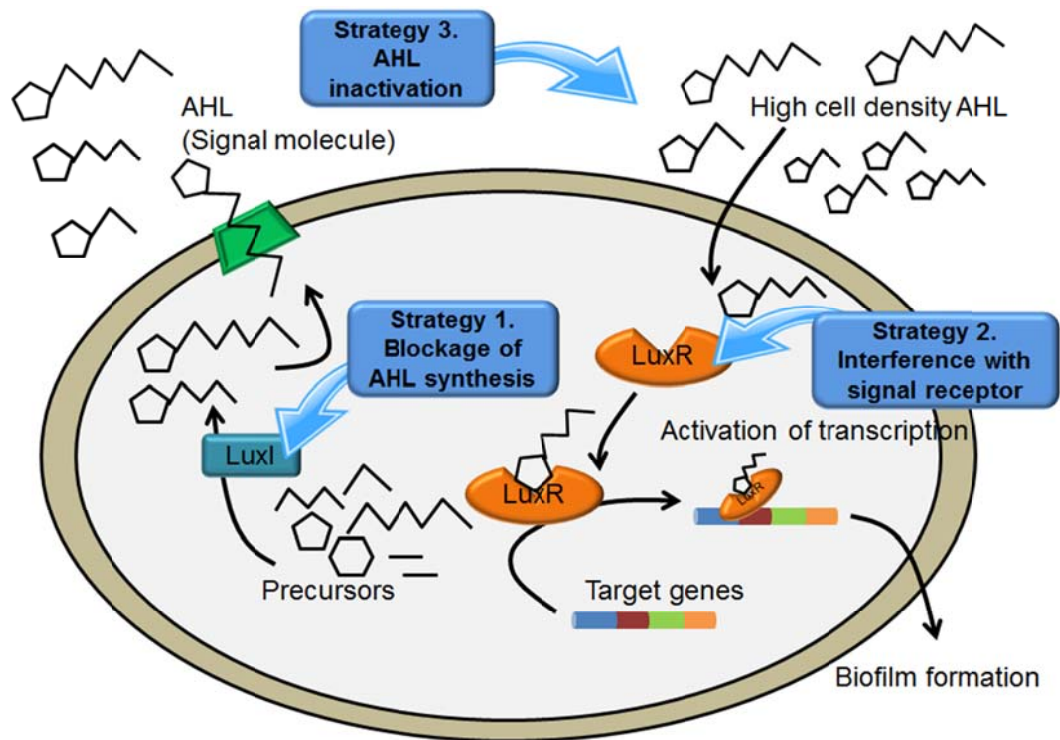


**Figure II-18. The strategy of quorum quenching in gram-negative bacteria.**

### II.4.1.1. Enzymatic QQ

#### [1] AHL-lactonases

Dong et al. (2000) reported that a gene encoding autoinducer inactivation (aiiA) has been cloned from the gram-positive bacterium *Bacillus* sp. 240B1. They revealed that the gene AiiA, is an AHL-lactonase that hydrolyses the ester bond of the homoserine lactone ring of AHLs (Figure II-19) (Dong et al. 2001). This is the first QQ lactonase, belongs to the metallo  $\beta$ -lactamase superfamily; others are similar to phosphotriesterases or are members of the paraoxonase family. The AHL lactonase have been found in a wide variety of organisms and among different protein families (Table II-7). For several AHL lactonases, it was shown that heterologous expression of the respective gene in the plant pathogen *Pectobacterium carotovorum* (formerly, *Erwinia carotovora*) reduced the AHL levels, decreased the levels of extracellular pectolytic enzymes and attenuated the virulence of this pathogen in tobacco, potato, or other plants (Fetzner 2015).

In the MBRs, Oh et al. (2012) suggested that new anti-biofouling strategy using indigenous quorum quenching bacteria (*Rhodococcus* sp. BH4). They revealed that the enzyme from *Rhodococcus* sp. BH4 hydrolyzes the lactone bond of AHL and the *N*-acyl homoserine lactone hydrolase (AHL-lactonase) gene of strain BH4 showed a high degree of identity to *qsda* in *Rhodococcus erythropolis* W2.

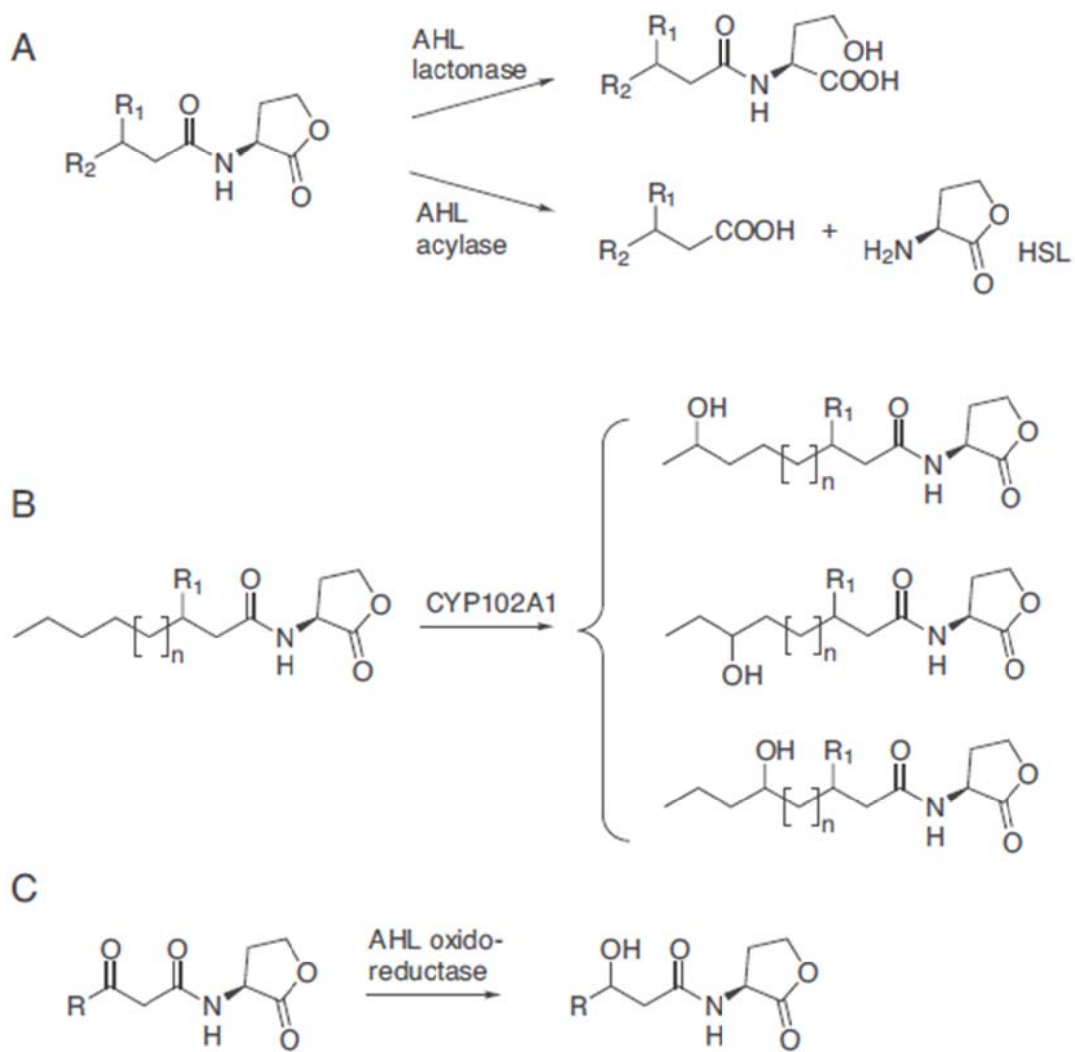


**Figure II-19. Reactions catalyzed by quorum-quenching enzymes. (A) Hydrolytic cleavage of AHLs by AHL lactonases and AHL acylases. (B) Hydroxylation of AHLs by the cytochromeP450 monooxygenase CYP102A ( $n = 5-9$ ). (C) Reduction of 3-oxo-substituted AHLs by AHL oxidoreductases (R, C5 to C11 n-alkyl).**

**Table II-7. Enzymatic AI-1 quorum quenching (Fetzner 2015).**

Protein	Source	Protein family	Localization/ signal peptide	Substrates
AHL lactonase				
AiiA	<i>Bacillus</i> spp. ( <i>B. cereus</i> group)	Metallo- $\beta$ -lactamase superfamily	Cytoplasmic	C4-, C6-, C8-, C10-HSL; 3OC4-, 3OC6-, 3OC8-, 3OC12-HSL; 3-OH-C4-HSL
AhIS	<i>Solibacillus silvestris</i> StLB046	Metallo- $\beta$ -lactamase superfamily	No SP	C10-HSL
AhID	<i>Arthrobacter</i> sp. IBN110	Metallo- $\beta$ -lactamase superfamily	No SP	C6-, C8-, C10-HSL, 3OC6-, 3OC12-HSL
AttM (AiiB)	<i>Agrobacterium tumefaciens</i> C58, M103	Metallo- $\beta$ -lactamase superfamily	No SP	C4-, C6-, C7-, C8-, C10-HSL; 3OC6-, 3OC8-HSL
QsdR1	<i>Rhizobium</i> sp. NGR234	Metallo- $\beta$ -lactamase superfamily	No SP	3OC8-HSL
AhIK	<i>Klebsiella pneumonia</i> KCTC2241	Metallo- $\beta$ -lactamase superfamily	No SP	C6-HSL, 3OC6-HSL
AidC	<i>Chryseobacterium</i> sp. StRB126	Metallo- $\beta$ -lactamase superfamily	SP	C6-, C8-, C10-, C12-HSL; 3OC6-, 3OC8-, 3OC10-, 3OC12-HSL
QlcA	Soil metagenome (acidobacterial origin)	Metallo- $\beta$ -lactamase superfamily	No SP	C6-HSL
PPH, identical to Php of strain H37Rv	<i>Mycobacterium tuberculosis</i>	Phosphotriesterase/kinase (PLL); amidohydrolase superfamily	No SP	C4-, C10-HSL; 3OC8-HSL
MCP (MAP366 8c)	<i>M. avium</i> ssp. <i>paratuberculosis</i> K-10	PLL	No SP	C6-, C7-, C8-, C10-, C12-HSL; 3-oxo-C8-HSL
QsdA (AhlA)	<i>Rhodococcus erythropolis</i> W2, SQ1, Mic1, MP50, CECT3008; <i>Rhodococcus</i> sp. BH4	PLL	No SP; cell-associated	C4-HSL, C6- to C14-HSLs, with or without substitution at C3'
SsoPox	<i>Sulfolobus solfataricus</i> P2 (ATCC 35092)	PLL	n.d.	C4-, C6-, 8-, C12-HSL; 3OC6-, 3OC8-, 3OC10-, 3OC12-HSL

**Table II-7. (Continued).**

Protein	Source	Protein family	Localization/ signal peptide	Substrates
SisLac	<i>Sulfolobus islandicus</i> M.16.4	PLL	n.d.	C4-, C8-, C12-HSL; 3OC8-,3OC10-, 3OC12-HSL
PON1	Mammalian liver, serum	Paraoxonase (PON) family	Secreted protein, associated with high-density lipoprotein (HDL) in serum	C7-, C12-, C14-HSL 3OC6-,3OC10-, 3OC12-HSL
PON2	All mammalian tissues	PON family	Nonsecreted transmembrane protein, extracellular active site	C7-, C12-, C14-HSL; 3OC6-,3OC10-, 3OC12-HSL
PON3	Mammalian liver (and kidney), serum	PON family	Secreted protein, associated with HDL in serum	C7-, C12-, C14-HSL 3OC12-HSL
Bacterial PON	<i>Oceanicaulis alexandrii</i> HTCC2633	PON family	Membrane- associated	C12-HSL, 3OC10-, 3OC12-HSL
AiiM	<i>Microbacterium testaceum</i> StLB037	$\alpha/\beta$ Hydrolase superfamily	No SP	C6-, C8-, C10, C12- HSL; 3OC6-, 3OC8-, 3OC10, 3OC12-HSL
AidH	<i>Ochrobactrum</i> sp. T63	$\alpha/\beta$ Hydrolase superfamily	No SP	C4-, C6-, C10-HSL; 3OCC6-, 3OC8-HSL; 3-OH-C6-HSL
DlhR	<i>Rhizobium</i> sp. NGR234	Dienelactone hydrolase	SP	3OC8-HSL
BpiB07	Soil metagenome	Dienelactone hydrolase	No SP	3OC8-HSL
QsdH	<i>Pseudoalteromo nas byunsanensis</i> 1A01261	GDSL (SGNH) hydrolase family (N-terminal domain)	GDSL hydrolase domain facing the periplasm , RND-type efflux transporter transmembrane domain	C4-, C6-, C8-, C10-, C12-, C14-HSLs; 3OC6-, 3OC8-HSL
BpiB04	Soil metagenome	Glycosyl hydrolase	No SP	3OC8-HSL
BpiB01	Soil metagenome	Hypothetical	No SP	3OC8-HSL
BpiB05	Soil metagenome	Hypothetical	No SP	3OC6-, 3OC8-, 3OC12-HSL

**Table II-7. (Continued).**

Protein	Source	Protein family	Localization/ signal peptide	Substrates
AHL acylases				
n.i.	<i>Variovorax paradoxus</i> VAI-C	n.i.	n.i.	C4-, C6-, C8-, C10-, C12-, C14-HSL; 3OC6-HSL
AhlM	<i>Streptomyces</i> sp. M664	N-terminal nucleophile (Ntn) hydrolase family	Extracellular	C6-, C8-, C10-HSL; 3OC6-, 3OC8-, 3OC12-HSL
AibP	<i>Brucella melitensis</i> 16M (ATCC 23456)	Ntn hydrolase	No SP	C12-HSL; 3OC12-HSL
AiiD	<i>Ralstonia</i> sp. XJ12B	Ntn hydrolase	SP	3OC6-, 3OC8-, 3OC10-, 3OC12-HSL,
Aac	<i>Ralstonia solanacearum</i> GMI1000	Ntn hydrolase	Cell-associated;SP	C7-, C8-, C10-HSL; 3OC8-HSL
PvdQ (PA2385)	<i>P. aeruginosa</i> PAO1	Ntn hydrolase	SP	C7-, C8-, C10-, C11-, C12-, C14-HSL; 3OC10-, 3OC12-, 3OC14-HSL; 3OH-C12-, 3OH-C14-HSL
QuiP (PA1032)	<i>P. aeruginosa</i> PAO1	Ntn hydrolase	SP	C7-, C8-, C10-, C12-, C14-HSL; 3OC12-HSL
HacB (PA0305)	<i>P. aeruginosa</i> PAO1	Ntn hydrolase	SP	C14-HSL; 3OC10-, 3OC12-, 3OC14-HSL
HacB (Psyn 4858)	<i>P. syringae</i> B728a	Ntn hydrolase	Cell-associated	C4-, C6-, C8-, C10-, C12-HSL; 3OC6-, 3OC8-HSL
HacA (Psyn 1971)	<i>P. syringae</i> B728a	Ntn hydrolase	Extracellular	C8-, C10-, C12-HSL; 3OC8-HSL
Aac	<i>Shewanella</i> sp. MIB015	Ntn hydrolase	SP	C8-, C12-, C12-HSL
AiiC	<i>Anabaena</i> sp. PCC7120	Ntn hydrolase	Cell-associated; SP	C4-, C6-, C8-, C10-, C12-, C14-HSL; 3OC4-, 3OC6-, 3OC8-, 3OC10-, 3OC12-, 3OC14-HSL and corresponding 3OH-Cx-HSLs
AiiO	<i>Ochrobactrum</i> sp. A44	$\alpha/\beta$ Hydrolase superfamily	Cytoplasmic	C4-, C6-, C10-, C12-, C14-HSL; 3OC4, 3OC6, 3OC8-, 3OC10-, 3OC12-, 3OC14-HSL and corresponding 3OH-Cx-HSLs

**Table II-7. (Continued).**

Protein	Source	Protein family	Localization/ signal peptide	Substrates
QsdB	Soil metagenome	Amidase signature (AS) family	No SP	C6HSL; 3OC8-HSL
n.i.	<i>Rhodococcus erythropolis</i> W2	n.i.	Cell-associated	3OC6-, 3OC10-HSL; 3-OH-C10HSL
n.i.	<i>Comamonas</i> sp. D1	n.i.	Cell-associated	C6-, C12-, C16-HSL; 3OC6-, 3OC8-, 3OC10-, 3OC12-, 3OC14-HSL; 3OH-C12-HSL to C16 AHLs, with or without substitution at C3'
n.i.	<i>Tenacibaculum maritimum</i> NCIMB2154	n.i.	Cell-associated	C10-HSL
Oxidoreductases active toward AHLs				
CYP102A1 (P450BM-3)	<i>Bacillus megaterium</i>	Cytochrome P450 monooxygenase	Cytoplasmic	C12- to C16-HSL; 3OC12-HSL ( $\omega$ -1, $\omega$ -2, $\omega$ -3-hydroxylation)
n.i.	<i>Rhodococcus erythropolis</i> W2	n.i.	Cell-associated	3OC8-, 3OC10-, 3OC12-, 3OC14-HSL (reduction to 3OH-HSL)
n.i.	<i>Burkholderia</i> sp. GG4	n.i.	n.i.	3OC4-, 3OC6-, 3OC8-HSL (reduction to 3OH-HSL)
BpiB09	Soil metagenome	Short-chain dehydrogenase/reductase (SDR) family	Cytoplasmic	3OC12-HSL (NADPH-dependent reduction to 3OH-C12-HSL)
Enzymes acting on AQs				
2-Alkyl-3-hydroxy-4(1H)-quinolone 2,4-dioxygenase (Hod)	<i>Arthrobacter</i> sp. Rue61a	$\alpha/\beta$ Hydrolase superfamily	Cytoplasmic	C1- to C9-n-alkyl-3-hydroxy- 4(1H)-quinolones
Enzymes acting on AI-2				
AI-2 kinase (LsrK)	<i>E. coli</i> , other enteric bacteria	FGGY family of carbohydrate kinases	Cytoplasmic	Linear form of AI-2 (4,5- dihydroxy-2,3-pentanedione)

SP: predicted signal peptide; No SP: no signal peptide predicted from amino acid

sequence (SignalP/LipoP Server).n.d., not determined,.n.i., not identified.

## [2] AHL-acylase

Leadbetter and Greenberg (2000) reported that *Variovorax paradoxus* is able to utilize AHLs as source of energy and nitrogen. They suggested that the first step in the metabolism of acyl-HSLs involves a carboxypeptidase or aminoacylase that releases the fatty acid from HSL (Fig. 3A). AHL acylases were later also identified in *P. aeruginosa*, *Ralstonia* strains, *Comamonas* sp., *P. syringae*, *Shewanella* sp., *Ochrobactrum* sp., the cyanobacterium *Anabaena* sp. PCC7120 and the actinobacteria *R. erythropolis* W2 and *Streptomyces* sp. M664 (Table II-7) (Fetzner 2015).

In the membrane system, Yeon et al. (2009) reported the mitigation of biofouling using a magnetic enzyme carrier (MEC) was prepared by immobilizing the AHL-acylase from porcine kidney in MBR. Kim et al. (2011) prepared the acylase-immobilized nanofiltration membrane. They revealed that quorum quenching activity of acylase-immobilized nanofiltration membrane has a great antibiofouling feature by suppressing EPS secretion and thus biofilm maturation.

In additions, Cheong et al. (2013) isolated QQ bacteria (strain 1A1) from MBR and it belongs to *Pseudomonas* using 16S rRNA gene sequences. They revealed that this strain produced extracellular QQ enzymes and enzyme of *Pseudomonas* sp. 1A1 was highly likely to be an AHL-acylase using the comparison with AHL-acylase homologue genes and analysis of molecular weight.

### **[3] AHL-oxidoreductases**

Oxidoreductases had ability to oxidize long chain fatty acyl homoserine lactones. CYP102A1, a widely studied cytochrome P450 from *Bacillus megaterium*, is capable of very efficient oxidation of AHLs and their lactonolysis products acyl homoserines (Chowdhary et al. 2007). Uroz et al. (2005) reported that *R. erythropolis* W2 has an oxidoreductase. Oxidoreductase from *R. erythropolis* W2 catalyzes the reduction of 3-oxo-C(8-14)-HSLs to the corresponding 3-hydroxy-HSLs, thereby inactivating the signal molecules (Figure II-19 C). However, Chowdhary et al. (2007) reported that the AHL oxidation products still act as QS autoinducers. Thus, it was speculated that there are few applications of oxidoreductases to mitigate biofouling in membrane system because the QQ activity is less than other enzymes.

### **[4] Enzymatic AI-2 quorum quenching**

Recently, the QS system based on the interspecies signaling molecule autoinducer-2 (AI-2) is targeted because of its prevalence among prokaryotes (it functions in over 80 bacterial species). Roy et al. (2010) reported that the *Escherichia coli* AI-2 kinase, LsrK, can phosphorylate AI-2 in vitro, and when LsrK-treated AI-2 is added ex vivo to *E.coli* populations, the native AI-2 QS response was significantly reduced (Figure II-20). LsrK mediated degradation of AI-2 attenuates the QS response among *Salmonella typhimurium* and *Vibrio harveyi*, although, the AI-2 signal transduction mechanisms and the phenotypic responses are species-specific. Their analogous results were obtained from a

synthetic ecosystem where three species of bacteria (enteric and marine) were co-cultured and the addition of LsrK and ATP to growing co-cultures of *E. coli* and *S. typhimurium* exhibited significantly reduced the interspecies signaling that ordinarily existed among and between species in an ecosystem.

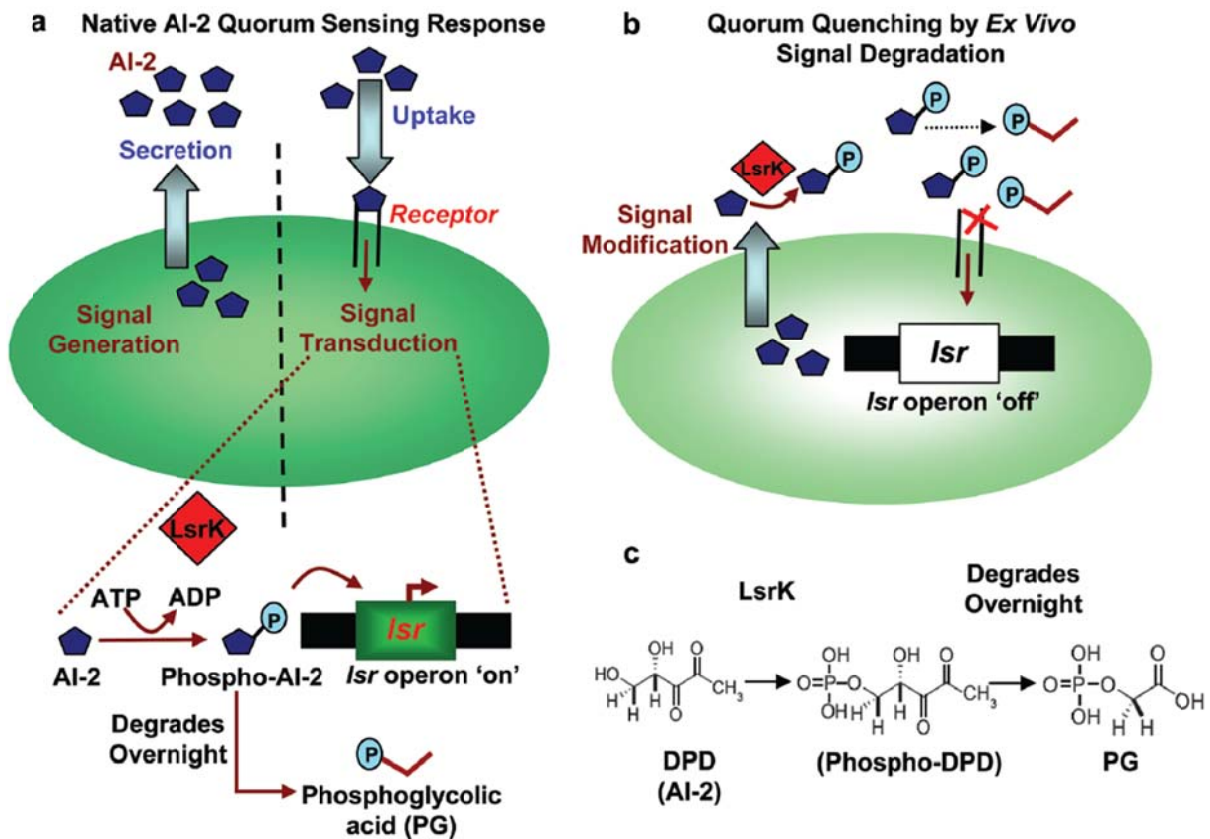


Figure II-20. Schematic of LsrK-mediated quorum quenching. a) Native quorum sensing is mediated by the generation, secretion, and uptake of autoinducer-2 (AI-2) followed by signal transduction indicated by *lsr* gene expression; phospho-AI-2 degrades overnight to 2-phosphoglycolic acid (PG). b) LsrK and ATP delivered outside the cell phosphorylate AI-2; phospho-AI-2 is presumably prevented from being transported into the cells and is degraded to PG. In this scenario, the quorum sensing response is quenched. c) LsrK phosphorylates DPD (AI-2 precursor); phospho-DPD degrades to PG overnight *in vitro*.

#### II.4.1.2. AI-1 quorum quenching bacteria

The four various AHL-degrading enzymatic activities have been described in *Rhodococcus* sp. (Uroze et al. 2003; Uroze et al. 2005; Park et al. 2006, Uroz et al. 2008; Oh et al. 2012). Uroz et al. (2005) observed an AHL-degrading activity of *R. erythropolis* strain W2 with a preference for 3-oxo-substituted AHLs. The following studies have revealed that 3-oxo-AHLs are converted into their 3-hydroxy-derivatives by means of an oxidoreductase activity. The oxidoreductase activity is not specific solely to AHLs with a 3-oxo-substituent. This enzyme is also able to reduce AHL derivative such as *N*-(3-oxo-6-phenylhexanoyl) homoserine lactone (which contains an aromatic acyl chain substituent) or 3-oxododecanamide (which lacks the homoserine lactone ring) Further investigation of AHL degradation by *R. erythropolis* W2 has resulted in the discovery of another type of enzymatic activity-AHL acylase. Park et al. reported a third enzymatic activity involved in AHL decomposition by *Rhodococcus* strains an AHL lactonase. Two *Rhodococcus* isolates strain LS31 and PI 33- were able to utilize AHLs, but with different AHL degrading spectra. Uroz revealed the genetic background of the AHL lactonase activity in this genus the *qsda* gene, first described for *R. erythropolis* W2 encodes a novel class of wide spectrum substrate AHL lactonase. The QsdA lactonase belong to the phosphotriesterase (PTE) family of zinc-dependent metalloproteins. It is not related to any known Zn-dependent AHL lactonase from the glyoxylase family, or to any known AHL acylase from the beta-lactamase family. The *qsda* gene was found in almost all tested strains from the *Rhodococcus* genus but not in *R. erythropolis* DCL 14, although this strain is still able to degrade

AHLs. The PTE lactonase is exclusively found in the *Rhodococcus* genus, in strain capable of hydrolyze AHLs. Recently, Oh et al. (2012) isolated an indigenous quorum quenching bacterium (*Rhodococcus* sp. BH4) from a real MBR plant. The 16S rRNA gene sequence of the strain BH4 showed 99 % identity with that of *R. erythropolis* W2. The AHL–lactonase gene of strain BH4 was compared with the known AHL–lactonase gene (*qsda*) of *R. erythropolis* W2. The nucleotide sequence of the cloned gene shows 98.6 % sequence identity with that of *qsda* from *R. erythropolis* W2. They confirmed that the kind of enzyme that strain BH4 produces degraded the C8-HSL by opening its lactone ring using HPLC and ESI-MS. In additions, Cheong et al. (2013) reported the isolation of new QQ bacteria (*Pseudomonas* sp. 1A1) from MBR and they revealed that this strain produced extracellular AHL-acylase.

#### **II.4.1.3. Quorum sensing inhibitor**

Many natural compounds of plant origin are well known for inhibit quorum sensing while not affecting bacterial growth. Several compounds of natural origin were reported that they can interfere with bacterial quorum sensing system and inhibit biofilm formation have been identified as secondary metabolites produced by algae, fungi, bacteria and higher plants. A major advantage of natural compounds is that it solves the problem of bacterial resistance to conventional antibiotics, as it specifically interferes with expression of specific behaviors. The natural compounds are structurally similar to those of quorum sensing signal molecules and thus antagonize them and also have ability to inhibit LuxR/LasR

signal receptors. A summary of the known natural quorum sensing inhibitory compounds derived from plant, fungi, algae and bacteria is provided in Table II-8 (Lade et al. 2014).

Recently, natural quorum sensing inhibitory compounds was used to mitigate biofouling in membrane system. Natural products such as furanone and vanillin have a potential to prevent biofouling of reverse osmosis (RO) membrane (Kappachery et al. 2010; Ponnusamy et al. 2010). Nam et al. (2015) reported that 250 mg/L of vanillin in feed solutions showed great potential as an anti-biofouling agent for MBRs without any interference on microbial activity for wastewater treatment. Yu et al. (2012) investigated the impact of D-tyrosine on cell attachment and biofilm formation of *P. aeruginosa* in continuous flow nanofiltration system. Lade and Kweon (2015) revealed the combined effect of curcumin with epigallocatechin gallate on the enhanced inhibition of AHL-mediated biofilm formation in bacteria from activated sludge. Siddiqui et al. (2012) observed that Piper betle extract has mitigated membrane fouling by inhibition of AHL production in MBR.

In additions, cinnamaldehyde (CA) was reported to inhibit biofilm formation. Niu et al. (2006) showed that low concentration of CA were effective at inhibiting both AHL mediated QS and autoinducer-2 (AI-2) mediated QS. Furthermore, Brackman et al. (2008) reported that CA and CA derivatives interfere with AI-2 based QS in various *Vibrio* spp. by decreasing the DNA-binding ability of LuxR (Figure II-21). To apply CA in membrane process, Zodrow et al. (2012) fabricated poly(lactic-co-glycolic acid) (PLGA) film with CA. They observed that

*E. coli*, *P. aeruginosa* and *S. aureus* biofilms were significantly reduced by CA and they suggested that the controlled-release platform can be used to encapsulate CA to slow membrane biofouling using *E. coli*. (Zodrow et al. 2012; Zodrow et al. 2014). Thus, it was speculated that CA will be another quorum sensing inhibitory compound to mitigate biofouling in membrane system.

**Table II-8. Quorum sensing inhibitor (Lade et al. 2014).**

Natural compound(s)	Source	QS activity
Furanone/ 2(5H)-Furanone/	Macroalga ( <i>Delisea pulchra</i> )	Mimics AHL signal by occupying the binding site on putative regulatory protein which results in the disruption of QS-mediated gene regulation. Inhibit biofilm formation in <i>Aer. Hydrophila</i> . Repress LuxR protein dependent expression of P(luxI)-gfp(ASV) reporter fusion. Inhibit virulence factor in <i>E. coli</i> XL-1.
(5Z)-4-bromo-5-(bromomethylene)-3-butyl-2(5 H)-furanone.	Macroalga ( <i>Delisea pulchra</i> )	Disrupts QS-regulated bioluminescence in <i>V. harveyi</i> by interacting with Hfq protein. Inhibit swarming motility and biofilm formation in <i>E. coli</i>
Ajoene (1-Allyldisulfanyl-3-(prop-2-ene-1-sulfinyl)-propene)	Garlic extract ( <i>Allium sativum</i> )	Blocks the QS-regulated productions of rhamnolipid resulting in phagocytosis of biofilm. Targets Gac/RSM part of QS and lowers the expression of regulatory RNAs in <i>P. aeruginosa</i> PAO1
Iberin (1-Isothiocyanato-3-(methylsulfinyl)propane)	Horseradish extract ( <i>Armoracia rusticana</i> )	Inhibit expression of QS-regulated <i>lasB-gfp</i> and <i>rhlA-gfp</i> genes responsible for virulence factor in <i>P. aeruginosa</i>
Sulforaphane (1-Isothiocyanato-4-(methylsulfinyl)butane)	Boroccoli	Reduce the expression of <i>lasI-luxCDABE</i> reporter in <i>P. aeruginosa</i>
Erucin (4-methylthiobutyl isothiocyanate)	Boroccoli	Reduce the expression of <i>lasI-luxCDABE</i> reporter in <i>P. aeruginosa</i>
Naringin (4'5-diOH-Flavone-7-rhgluc)	Citrus extract	Decrease the QS mediated biofilm formation and swimming motility in <i>Y. enterocolitica</i>
Naringenin (4',5,7-Trihydroxyflavanone)	Malagasy bark extract ( <i>Combretum albiflorum</i> )	Reduces production of pyocyanin and elastase in <i>P. aeruginosa</i> PAO1. Also inhibit 3-oxo-C12-HSL and C4-HSL synthesis driven by <i>lasI</i> and <i>rhlI</i> genes

**Table II-8. (Continued).**

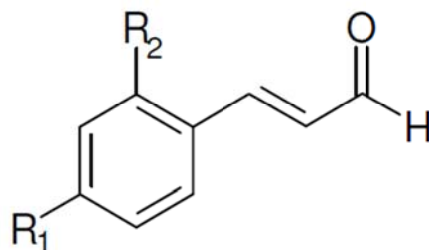
Natural compound(s)	Source	QS activity
Taxifolin/ Distylin (dihydroquercetin)	Malagasy plant extract ( <i>Combretum albiflorum</i> )	Reduces production of pyocyanin and elastase in <i>P. aeruginosa</i> PAO1
Morin (2',3,4',5,7-Pentahydroxyflavone)	Grapefruit ( <i>Artocarpus heterophyllus</i> )	Inhibit LasR and RhIR dependent protease, elastase and hemolysin in <i>P. aeruginosa</i> PAO1
Patulin/ Clavacin (4-Hydroxy-4 <i>H</i> -furo[3,2- <i>c</i> ]pyran-2(6 <i>H</i> )-one)	<i>Penicillium</i> sp.	Targets the RhIR and LasR proteins. Down-regulates QS genes for biofilm formation and virulence in <i>P. aeruginosa</i>
Penicillic acid (3-Methoxy-5-methyl-4-oxo-2,5-hexadienoic acid)	<i>Penicillium</i> sp.	Down-regulates QS genes for biofilm formation in <i>P. aeruginosa</i>
Vanillin (4-Hydroxy-3-methoxybenzaldehyde)	Vanilla beans extract ( <i>Vanilla planifolia</i> Andrews)	Interfere with AHL receptors. Inhibit C4-HSL, C6-HSL, C8-HSL, 3-oxo-C8-HSL. Inhibit biofilm formation in <i>Aer. hydrophila</i>
Agrocinopine B ([ (3 <i>S</i> ,4 <i>R</i> ,5 <i>R</i> )-3,4,5,6-tetrahydroxy-2-oxohexyl] [(2 <i>R</i> ,3 <i>S</i> ,4 <i>S</i> )-3,4,5-trihydroxy-1-oxopentan-2-yl] hydrogen phosphate)	Crown gall cells	Control conjugation of pTiC58 by regulating expression of the arc operon in <i>A. tumefaciens</i>
L-canavanine (L- $\alpha$ -Amino- $\gamma$ -(guanidinoxy)- <i>n</i> -butyric acid)	Seed exudates ( <i>Medicago sativa</i> )	Inhibit the expression of QS-regulated phenotype exopolysaccharide II production in <i>Si. meliloti</i>
Gamma-aminobutyric acid (GABA) (4-Aminobutanoic acid)	Plants ( <i>Arabidopsis</i> sp.)	Induce the expression of attKLM operon to stimulate inactivate 3-oxo-C8-HSL by <i>A. tumefaciens</i> lactonase AttM
Rosmarinic acid (R-O-(3,4-Dihydroxycinnamoyl)-3-(3,4-dihydroxyphenyl) lactic acid)	Sweet basil ( <i>Ocimum basilicum</i> )	Inhibit protease, elastase, hemolysin production, biofilm formation and virulence factor in <i>P. aeruginosa</i>

**Table II-8. (Continued).**

Natural compound(s)	Source	QS activity
Salicylic acid (2-Methyl-5-tert-butylsalicylic acid)	Plant phenolic secondary	Metabolite Inhibit the expression of vir regulon in <i>A. tumefaciens</i> . Also stimulates AHL-lactonase expression which degrades AHLs.
Chlorogenic acid (3-Caffeoylquinic acid)	Plant extract ( <i>Moringa oleifera</i> )	Inhibit QS-regulated violacein production in <i>C. violaceum</i> 12472
Allin (2-Amino-3-[prop-2-ene-1-sulfinyl]-propionic acid)	Garlic extract ( <i>Allium sativum</i> )	Inhibit QS-regulated gene expression by interacting with receptors in <i>P. aeruginosa</i> and make biofilm sensitive to antibiotics.
Ursolic acid (3beta-Hydroxyurs-12-en-28-oic acid)	Plant extract ( <i>Sambucus chinensis</i> )	Inhibit biofilm formation by suppressing cysteine synthesis in <i>E. coli</i>
Ellagic acid (Benzoic acid)	Fruit extract of <i>Terminalia chebula Retz.</i>	Down-regulate the expression of virulence gene in <i>P. aeruginosa</i> PAO1. Reduces biofilm formation and swarming motility in <i>B. cepacia</i>
$\alpha$ -Hydroxybutyric acid (2-hydroxy-butanoic acid)	<i>Arabidopsis exudates</i>	Induce the expression of attKLM-lacZ fusion in <i>A. tumefaciens</i>
Epigallocatechin gallate (Epigallocatechol)	Green tea ( <i>Camellia sinensis</i> L.)	This compound has gallic acid moiety and specifically block AHL-mediated biofilm formation in <i>Sta. aureus</i> and <i>B. cepacia</i> . Inhibit transfer of conjugative R plasmid in <i>E. coli</i>
Pyrogallol (1,2,3-Trihydroxybenzene)	Plant extract ( <i>Punica granatum</i> )	Inhibit AI-2 mediated bioluminescence in <i>V. harveyi</i> Inhibit AI-2 mediated bioluminescence in <i>V. harveyi</i>
Cinnamon oil/ Cynnamaldehyde ( trans-Cinnamaldehyde)	<i>Cinnamomum zeylanicum</i>	Interfere with AI-2 based QS and decreases the DNA-binding ability of LuxR protein to reduce virulence in <i>V. spp.</i> Reduces LuxR-mediated transcription from the PluxI promoter which influences biofilm formation in <i>P. aeruginosa</i>

**Table II-8.(Continued).**

Natural compound(s)	Source	QS activity
Furocoumarin/ Psoralen (7H- Furo[3,2- g][1]benzopyran-7- one)	Grapefruit juice and extract ( <i>Psoralea corylifolia</i> L.)	The structural resemblance of furan moiety results in QS- mediated inhibition of biofilm formation in <i>E. coli</i> . Inhibit QS- mediated swarming motility in <i>P. aeruginosa</i> PAO1
Urolithin (3,8- Dihydroxy- benzo[c]chromen-6- one)	Ellagitannin-rich extract from Pomegranate	Inhibit C6-HSL and 3-oxo-C6- HSL associated biofilm formation in <i>Y. enterocolitica</i> . Inhibit QS- mediated swarming motility in <i>E. coli</i>
Curcumin (E,E)-1,7- bis(4-Hydroxy-3- methoxyphenyl)-1,6- heptadiene-3,5-dione	From <i>Curcuma longa</i>	Down-regulates virulence factors and biofilm initiation genes in <i>P. aeruginosa</i> PAO1 and inhibit its phenotype expression. Attenuate QS-dependent EPS production, swarming motility and biofilm formation in uropathogenic <i>E. coli</i> , <i>P. aeruginosa</i> , <i>Pr. Mirabilis</i> and <i>S. marcescens</i> .
$\alpha$ -D-galactopyranosyl- (1→2)-glycerol (floridoside) (N), Betonicine (O), and Isethionic acid	Red alga ( <i>Ahnfeltiopsis flabelliformis</i> )	Inhibit C8-HSL mediated QS in <i>A. tumefaciens</i> NTL4
Musaceae	Musaceae extract ( <i>Musa paradisiaca</i> )	Inhibit QS-mediated elastase production and biofilm formation in <i>P. aeruginosa</i> PAO1
Garlic	Garlic extract	Interferes with expression of QS- controlled virulence genes in <i>P. aeruginosa</i>
<i>Piper betle</i>	<i>Piper betle</i> extract	Inhibit QS-mediated biofilm formation in <i>P. aeruginosa</i>
<i>Cuminum cyminum</i>	<i>Cuminum cyminum</i> extract	Reduce LuxR dependent biofilm formation and swarming motility of <i>P. aeruginosa</i>



Compound	abbreviation	R1	R2	MW (g/mol)
Cinnamaldehyde	CA	H	H	132.16
4-methoxy-cinnamaldehyde	4-MeO-CA	OMe-	H	162.19
2-methoxy-cinnamaldehyde	2-MeO-CA	H	OMe-	162.19
4-nitro-cinnamaldehyde	4-NO <sub>2</sub> -CA	NO <sub>2</sub> -	H	177.16
2-nitro-cinnamaldehyde	2-NO <sub>2</sub> -CA	H	NO <sub>2</sub> -	177.16
4-dimethyl-amino-cinnamaldehyde	4-Me <sub>2</sub> N-CA	Me <sub>2</sub> N-	H	175.23

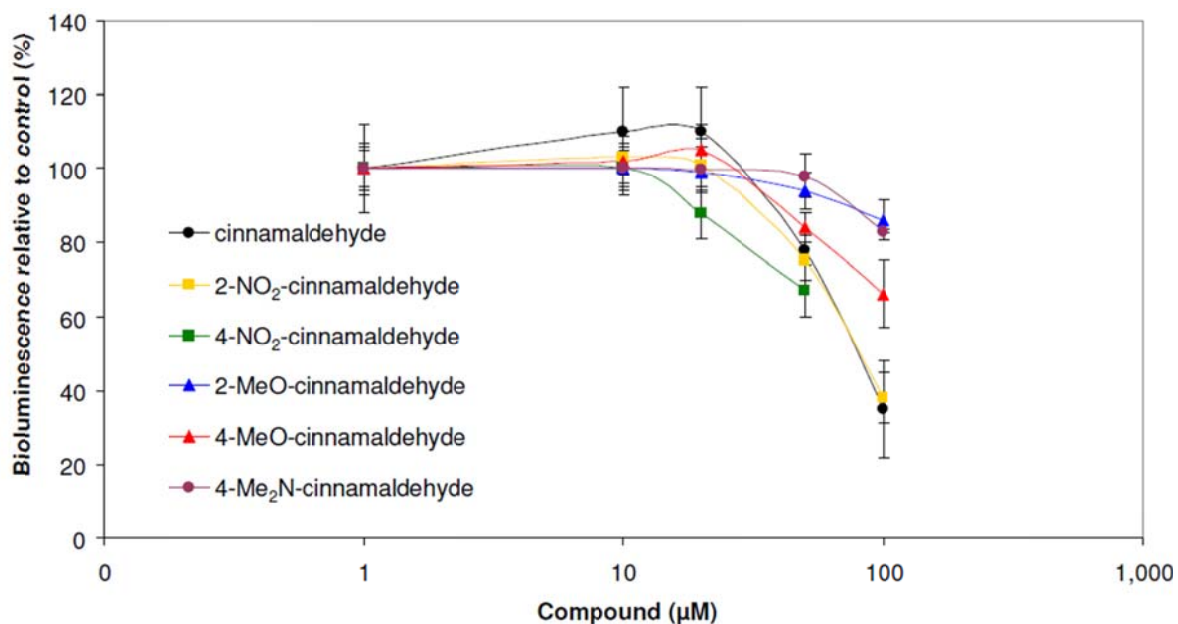


**Figure II-21. Cinnamaldehyde and cinnamaldehyde derivatives and Effect of cinnamaldehyde and cinnamaldehyde derivatives on AI-2 based QS (Brackman et al. 2008).**

## **II.4.2. Application of QQ to the control of biofouling in MBRs**

Yeon et al. (2009) prepared a magnetic enzyme carrier by immobilizing a quorum quenching enzyme, acylase, onto magnetic particles and demonstrated its potential as a novel approach to control biofouling in MBR (Figure II-22). Kim et al. (2011) immobilized acylase onto the membrane surface and showed mitigation of membrane biofouling in nano filtration system (Figure II-23).

However, the enzyme immobilization methods have drawbacks, such as the high cost of enzyme extraction and purification as well as enzyme instability. As an alternative to enzymatic quorum quenching, Oh et al. (2012) isolated bacteria (*Rhodococcus* sp. BH4) that produce quorum quenching enzymes and designed cell immobilization method to apply MBRs. Immobilization is a general term that describes many different forms of cell attachment or entrapment. These different forms include flocculation, adsorption on surfaces, covalent bonding to carriers, cross-linking of cells and encapsulation in a polymer-gel and entrapment in a matrix (Figure II-24). Thus, they developed a microbial vessel in which quorum quenching bacteria were encapsulated using hollow fiber membrane (Figure II-25). They observed that an internal submerged MBR equipped with the micro vessel has a much lower biofouling tendency compared with a conventional MBR. Daniel et al. (2012) revealed that the optimum position of the microbial-vessel in an external submerged MBR in which a bioreactor and a membrane tank are separated from each other.

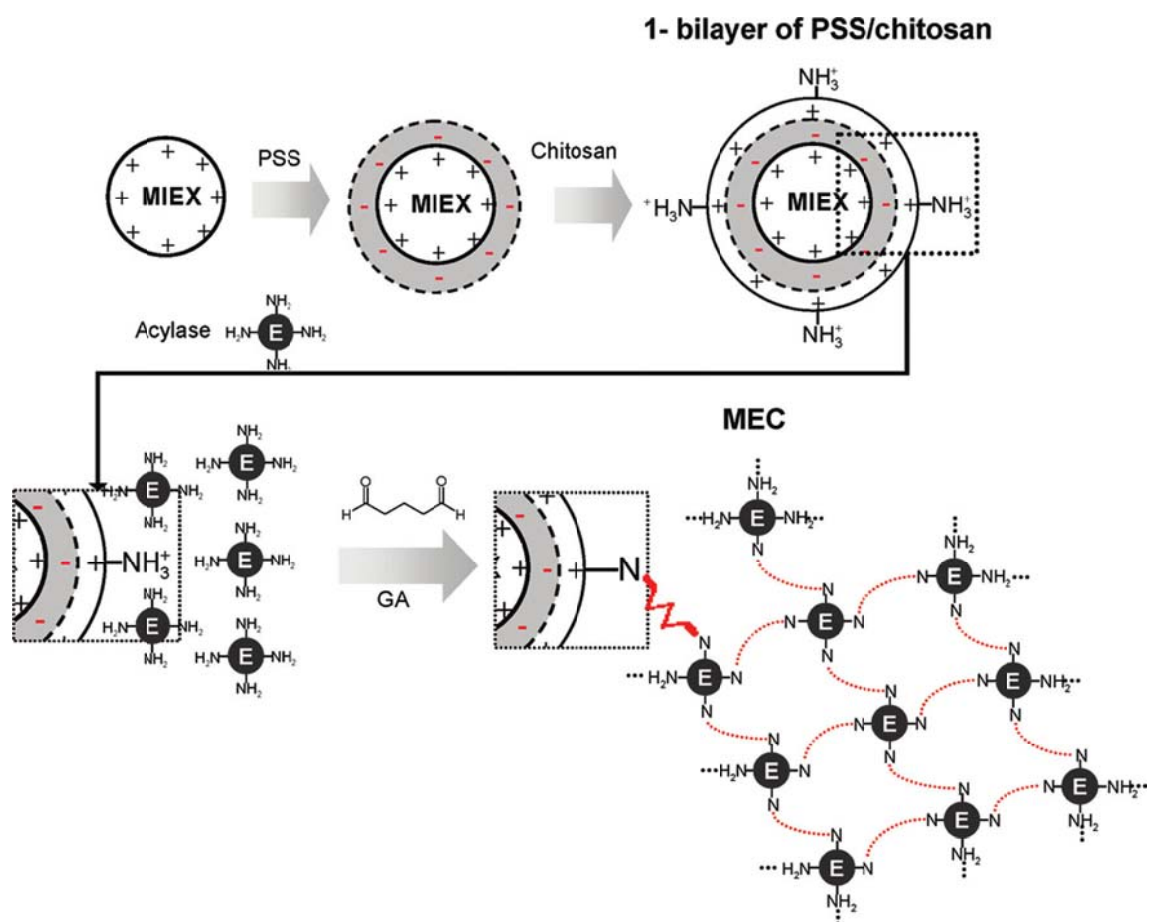


Figure II-22. A magnetic enzyme carrier by immobilizing a quorum quenching enzyme (acylase).

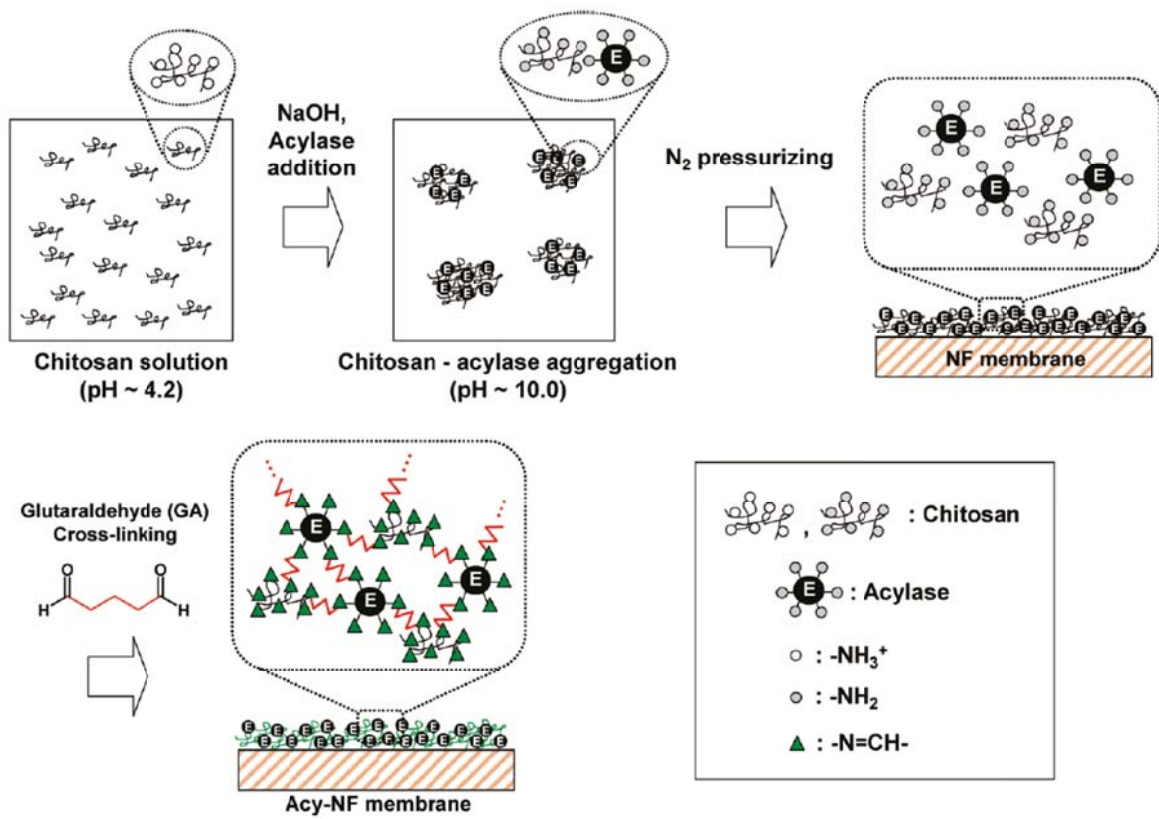
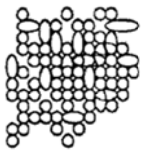
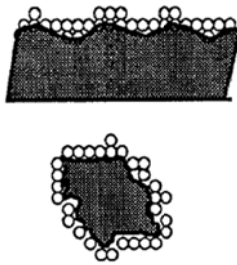


Figure II-23. Quorum quenching enzyme (acylase) was immobilized onto the nano filtration membrane surface.

1. Flocculation



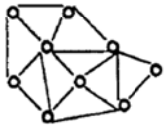
2. Adsorption to surfaces



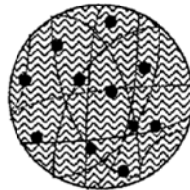
3. Covalent bonding to carrier



4. Cross-linking of cells



5. Encapsulation in polymer-gel



6. Entrapment in matrix



Figure II-24. Methods for immobilization of viable (Cassidy et al. 1996).

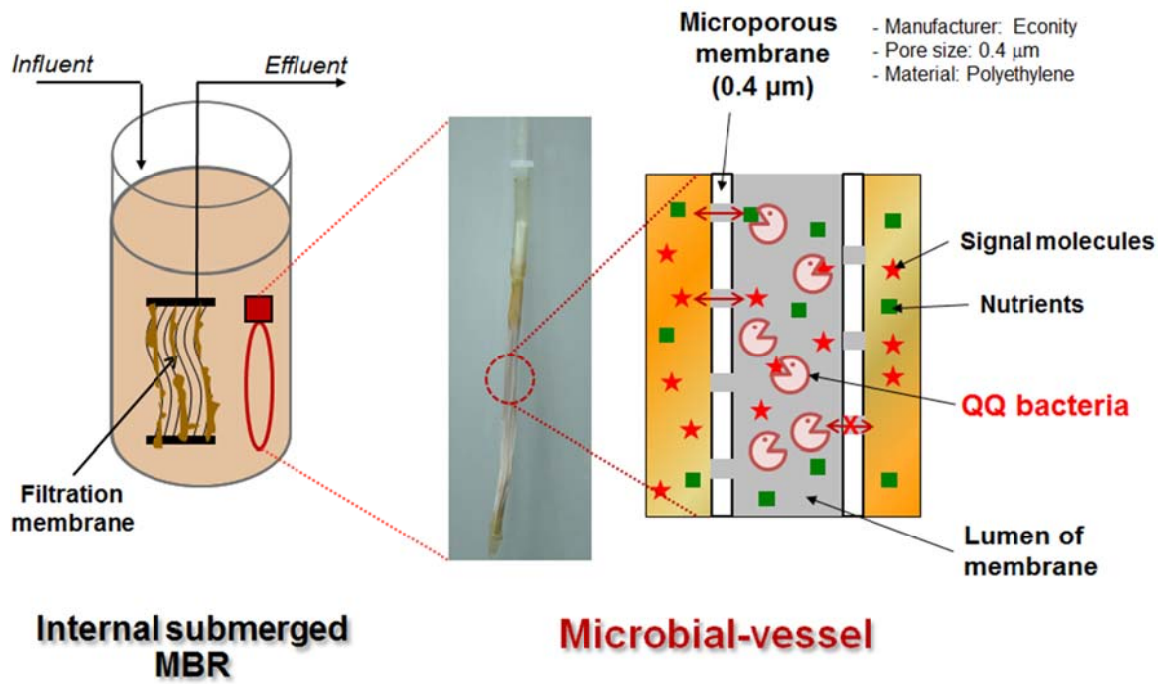


Figure II-25. Photograph and enlarged diagram of a microbial-vessel.

However, quorum quenching bacteria were confined within a small vessel that was submerged in a fixed place in the MBR so that they could degrade only soluble signal molecules that were able to diffuse into the vessel. As such, the mass transfer of signal molecules from the mixed liquor to the inside of the microbial vessel was limited. Thus, Kim et al. (2013b) suggested that *Rhodococcus* sp. BH4 was entrapped in alginate bead as an alternative to micro vessel (Figure II-26). They observed that the time to reach a transmembrane pressure (TMP) of 70 kPa was 10 times longer than without these beads in MBRs. They revealed that physical (friction) and biological (quorum quenching) effects of this methods contributed to the mitigation of biofouling because microbial cells in the biofilm produced fewer extracellular polymeric substances by the effect of quorum quenching.

Cheong et al. (2014) suggested that a ceramic microbial vessel (CMV) was designed to overcome the extremely low F/M ratio inside a microbial vessel (II-27). They reported that the inner flow feeding mode facilitated nutrient transport to QQ bacteria in the CMV and thus enabled relatively long-term maintenance of cell viability. The quorum quenching effect of the CMV on controlling membrane biofouling in the MBR was more pronounced with the inner flow feeding mode, which was identified by the slower increase in the transmembrane pressure as well as by the visual observation of a biocake that formed on the used membrane surface.

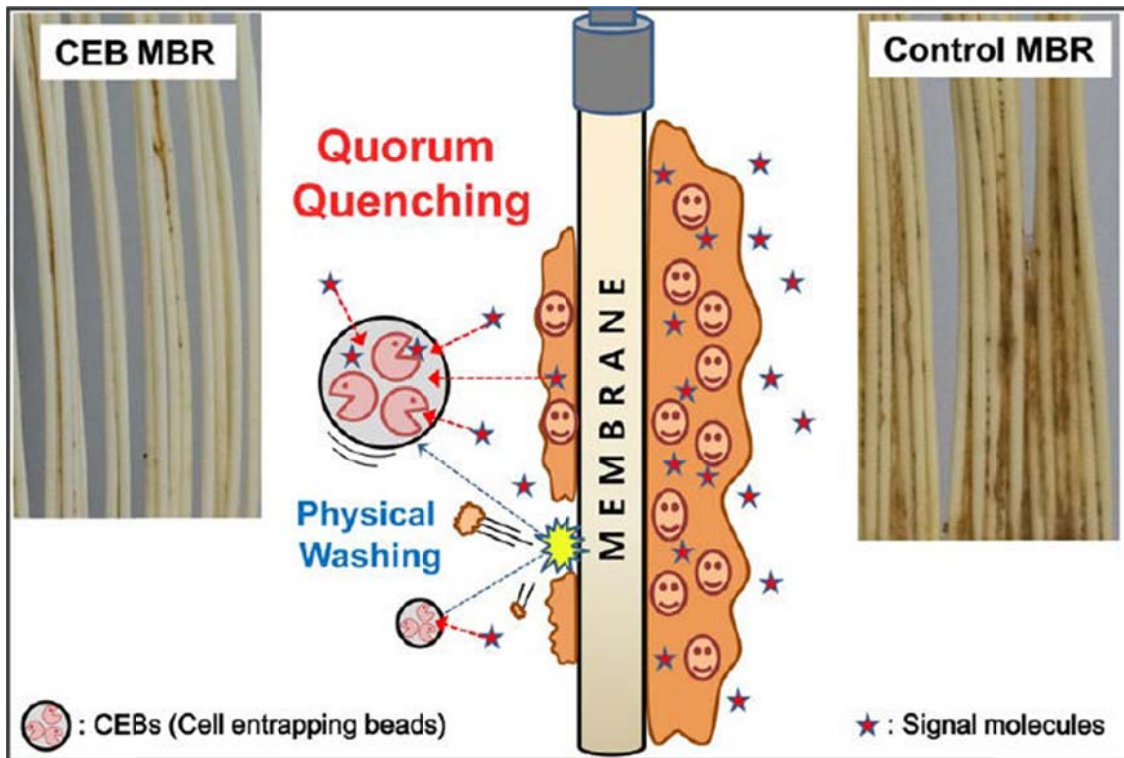


Figure II-26. Schematic diagram of quorum quenching bacteria entrapping beads.

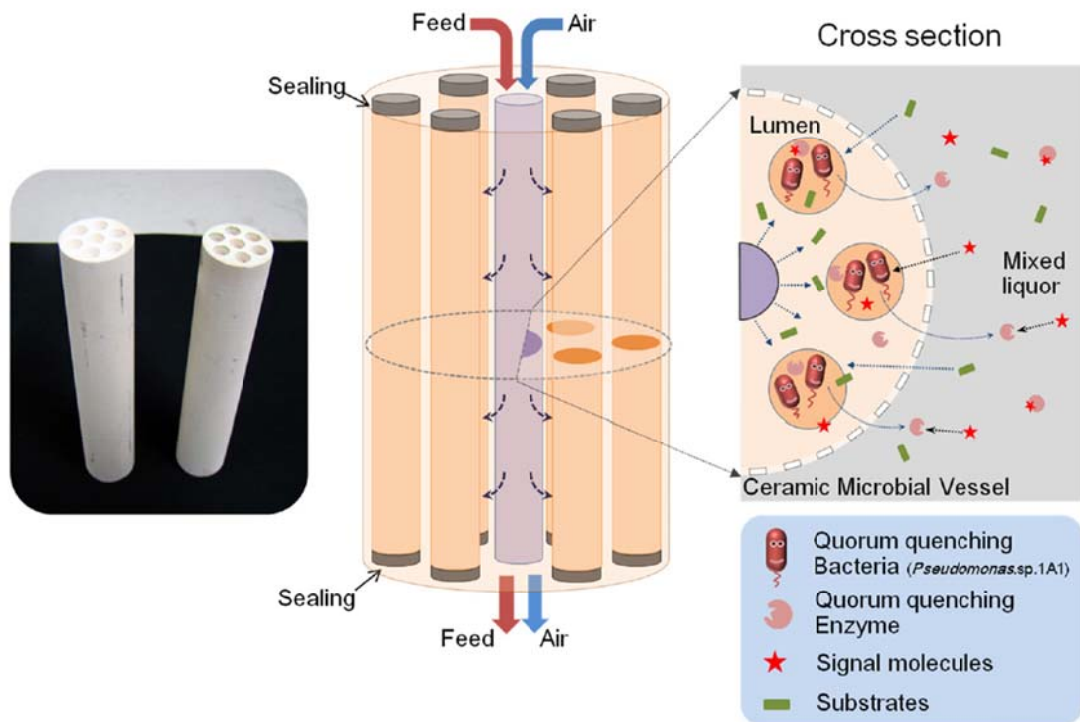


Figure II-27. Schematic diagram of the ceramic microbial vessel under the inner flow feeding mode.

Köse-Mutlu et al. (2015) developed new QQ carrier. They suggested that rotating microbial carrier frame (RMCF) is more feasible for pilot- and real-scale MBR plants when the manufacturing costs of QQ products are taken into consideration (Figure II-28).

Lee et al. (2016) attempted to bring QQ-MBR closer to potential practical application. They installed two types of pilot-scale QQ-MBRs (Figure II-29) with QQ bacteria entrapping beads (QQ-beads) and run at a wastewater treatment plant, feeding real municipal wastewater to test the systems' effectiveness for membrane fouling control and thus the amount of energy savings, even under harsh environmental conditions. They confirmed that the rate of transmembrane pressure (TMP) build-up was significantly mitigated in QQ-MBR compared to that in a conventional-MBR.

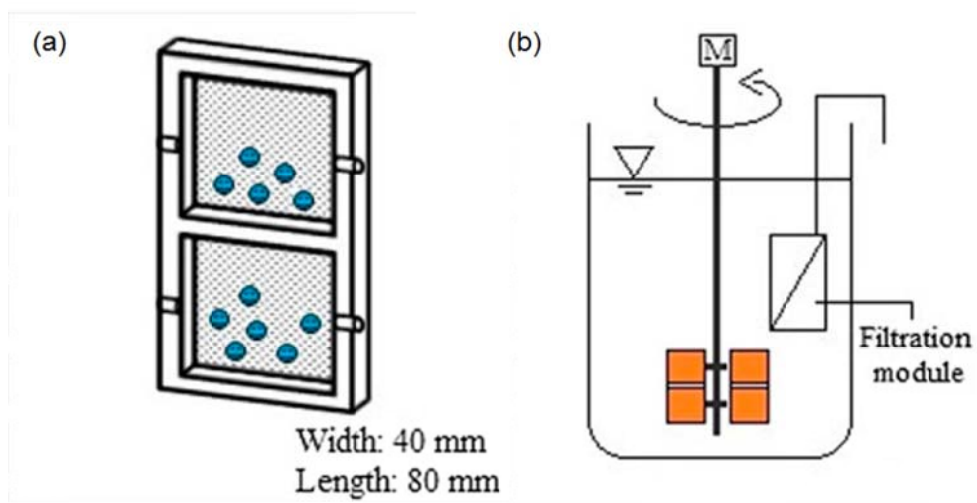
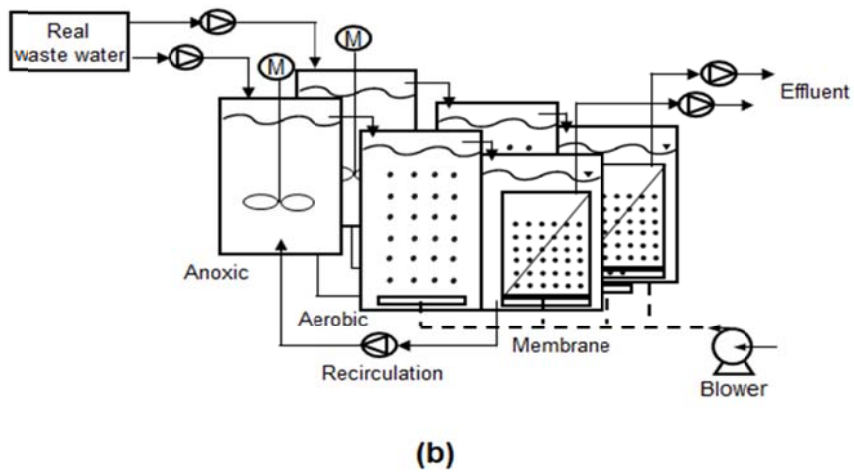
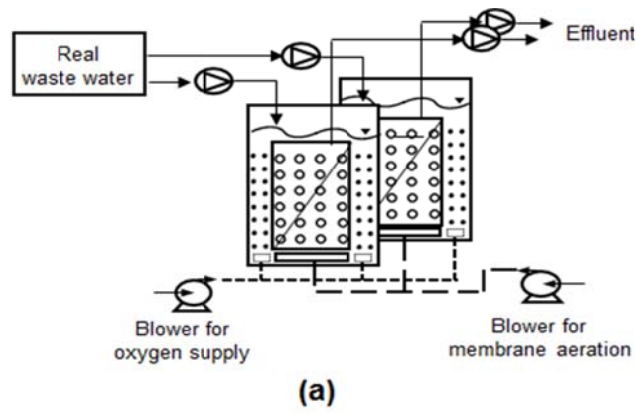


Figure II-28. Schematic diagram of the rotating microbial carrier frame (RMCF), (b) location and rotation of a RMCF in the MBR.



**Figure II-29. Pilot scale QQ-MBR configurations. (a) Two one-stage MBRs in parallel, each of which consists of only a membrane tank where two types of aerations are equipped: one for oxygen supply to activated sludge, and the other for membrane scouring. (b) Two three-stage MBRs in parallel, each of which consists of an anoxic, an aerobic and a membrane tank.**

## **II.5. Genomic analysis of microbial community**

### **II.5.1. What is microbial ecology?**

Microorganisms in the environment are commonly organized into several levels of hierarchical organizations, from simple to complex: individuals, populations, guilds (metabolically related populations), communities (sets of interacting guilds), and ecosystems. Microbial ecology examines the diversity of microorganisms and how microbes interact with each other and with their environment to generate and to maintain such diversities. Consequently, microbial ecologists have traditionally focused on two areas of study (Xu 2006):

- (i) Microbial diversity, including the isolation, identification and quantification of micro-organisms in various habitats;
- (ii) Microbial activity, that is, what microorganisms are doing in their habitats and how their activities contribute to the observed microbial diversity and biogeochemical cycling.

## **II.5.2. Metagenomics**

Metagenomics refers to culture-independent studies of the collective set of genomes of mixed microbial communities and applies to explorations of all microbial genomes in consortia that reside in environmental niches, in plants, or in animal hosts (Petrosino et al. 2009). Many environments have been the focus of metagenomics, including soil, the oral cavity, feces, and aquatic habitats, as well as the hospital metagenome, a term intended to encompass the genetic potential of organisms in hospitals that contribute to public health concerns such as antibiotic resistance and nosocomial infections (Riesenfeld et al. 2004). Metagenomics, the study “beyond genomics” or the study of the “genome of all combined genomes,” represents the interface between microbiology, ecology and genomics (Figure II-30) (Li 2011).

The origins of molecular evolutionary study lie in the 1960s when Zuckerkandl and Pauling (1965) used amino acid sequence differences in hemoglobin from different organisms to look at evolution. These researchers postulated that amino acid sequence differences can be used as a direct measure of evolutionary distance and coined the term “molecular clock.” However, since hemoglobin is not universally present in all organisms, this approach is not universally applicable. In the 1970s Carl Woese looked at another molecule, the 16S rRNA. The 16S rRNA (or 18S rRNA) molecule is a much better candidate since it is a structural component of the protein synthesis machinery and thus universally present in all organisms. It shows a high amount of conservation in all living organisms due to its sequence constraints as a structural component of the

ribosome. In the 1970s Pace began using 16S rRNA sequence difference as a means for classifying bacteria. By that time sequencing technology had made great leaps forward (Sanger sequence), so 16S rRNA gene sequence analysis became the most important tool to study microbial diversity (Li 2011)

Metagenomics aim to characterize the microbial diversity, genetic complexity and metabolic potential of a community in a particular environment by analyzing the community nucleic acid composition. Community diversity can and has been assessed using 16S rRNA DNA PCR amplicons generated from environmental DNA samples. These studies are aimed at answering the question, “Who is there?” Metagenomics has taken this approach one step further It is aimed at the answering the question, “What are they doing?” Community DNA obtained from an environmental sample is cloned as a small or large insert clone library and subjected to nucleotide sequence analysis, or it is directly sequenced with a shotgun approach using novel next generation sequencing. (Figure II-31) This system biology approach of analyzing/sequencing community DNA directly from a particular environment and analyzing the metagenome without the need to cultivate the individual members of the communities facilitates surveys of genomic and metabolic potentials in diverse environments and has already led to may new and important discoveries.

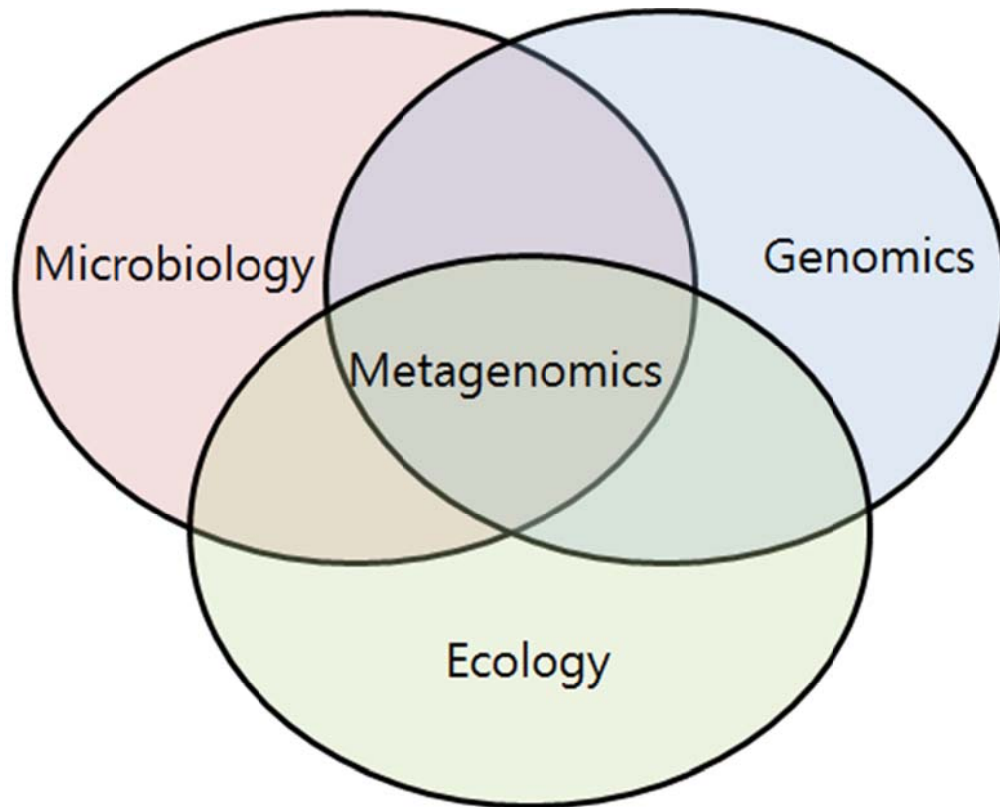


**Figure II-30. The new field of metagenomics resides at the interface of microbiology, genomics and ecology (Li 2011).**

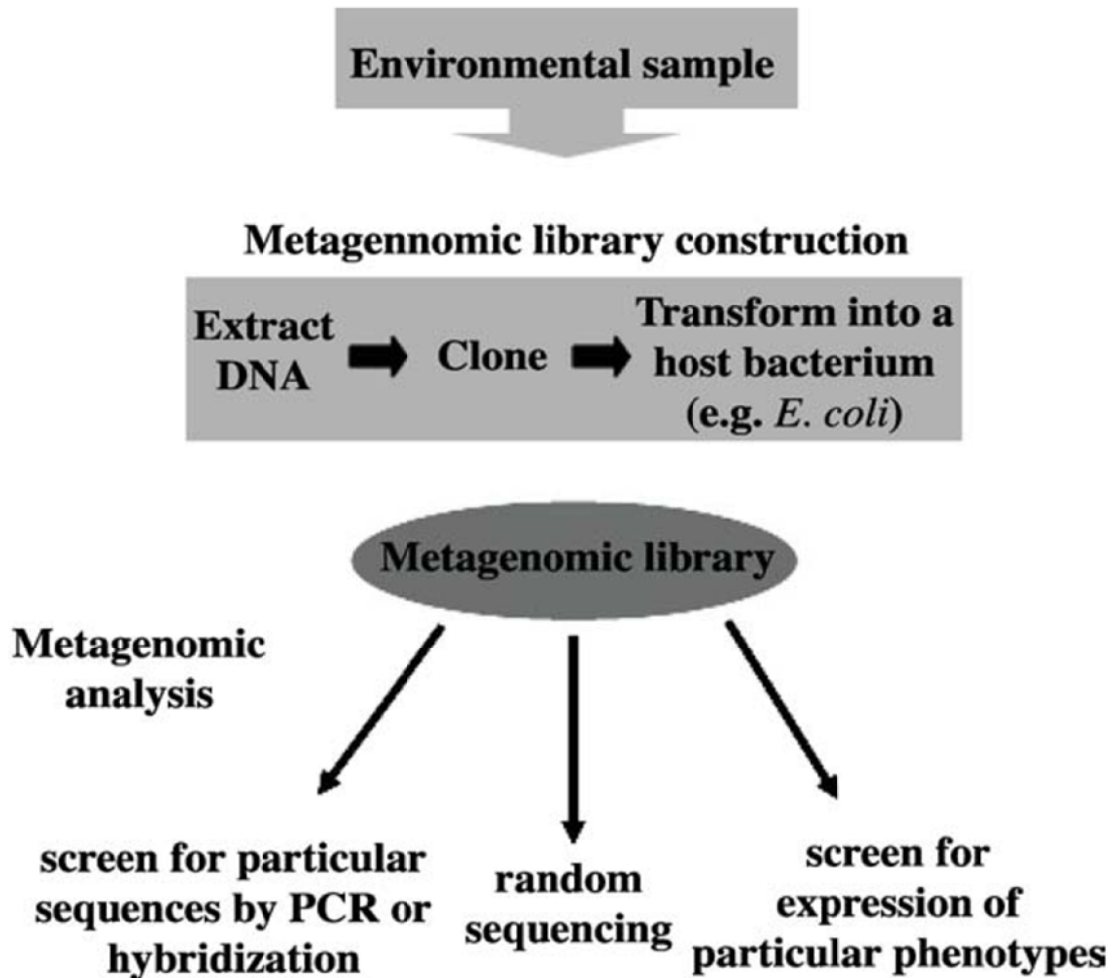


Figure II-31. Metagenomics involves constructing a DNA library from an environment's microbial population and then analyzing the functions and sequences in the library (Riesenfeld et al. 2004).

### **II.5.3. Sequencing technologies for the microbial identification**

The initial studies of microbial identification were based on Sanger-sequencing strategies that included targeted sequencing of 16S rRNA genes (approximately 1.5 kb of target sequence). Such “long read” approaches enabled investigators to identify many individual genera and species that could not be identified with biochemical methods. Sequence-based identification could be established with a reasonable amount of confidence from relatively long reads and with the aid of sequence classifier algorithms that included most of the 16S rDNA coding sequence; however, less than half of the coding sequence (approximately 500 bp), including several hypervariable regions, may be sufficient for genus- and species-level pathogen identification via Sanger sequencing (Petrosino et al. 2009)

For the past 15 years, Sanger sequencing and fluorescence based electrophoresis technologies have been extensively used in somatic and germline genetic studies. Improvements in instrumentation coupled with the development of high performance computing and bioinformatics have reduced the cost of sequencing. However, increases in the throughput of Sanger DNA sequencing are achieved by the use of additional sequencers in parallel, owing to the requirement of gel electrophoresis or additional wells for the capillary sequencing of each reaction. Using different approaches, Next-generation sequencing (NGS, massively parallel sequencing methods) overcome the limited scalability of traditional Sanger sequencing by either creating micro-reactors and/or attaching the DNA molecules to be sequenced to solid surfaces or beads, allowing for millions of sequencing

reactions to happen in parallel. Recently, as new NGS technologies continue to emerge, the field of metagenomics has adapted to the new types of sequencing data (Table II-9) (Reis-Filho 2009; Scholz et al. 2012).

DNA pyrosequencing, or sequencing by synthesis, was developed in the mid 1990s as a fundamentally different approach to DNA sequencing. Sequencing by synthesis occurs by a DNA polymerase driven generation of inorganic pyrophosphate, with the formation of ATP and ATP-dependent conversion of luciferin to oxyluciferin (Figure II-32). The generation of oxyluciferin causes the emission of light pulses, and the amplitude of each signal is directly related to the presence of one or more nucleosides. One important limitation of pyrosequencing is its relative inability to sequence longer stretches of DNA (sequences rarely exceed 100–200 bases with first- and second-generation pyrosequencing chemistries). The term 454 sequencing refers to high-throughput sequencing platforms (e.g., Roche/454 Life Sciences) for metagenomics that are based on pyrosequencing chemistry. DNA pyrosequencing has been successfully applied in a variety of applications, including genotyping, single-nucleotide polymorphism detection, and microorganism identification. The relatively short read lengths of DNA pyrosequencing have placed a premium on careful target selection and oligonucleotide primer placement. Pyrosequencing has been successfully applied to microbial identification by combining informative target selection (e.g., hypervariable regions within the 16S rRNA gene) and signature sequence matching (Petrosino et al. 2009).

**Table II-9. List of NGS sequencing platforms and their expected throughputs, error types and error rates. Each platform has distinct advantages, owing to cost, error rate, read length, and so on (Scholz et al. 2012).**

Platform	Run time (h)	Read length (bp)	Throughput per run (Mb)	Error type	Error rate (%)
<i>Roche</i>					
454 FLX+	18–20	700	900	Indel	1
454 FLX Titanium	10	400	500	Indel	1
454 GS	10	400	50	Indel	1
<i>Illumina</i>					
GAIIx.	14	2 x 150	900,000	Substitution	>0.1
HiSeq 2000	8	2 x 100	400,000	Substitution	>0.1
HiSeq 2000 V3	10	2 x 150	<600,000	Substitution	>0.1
MiSeq	1	2 x 150	1000	Substitution	>0.1
<i>Life technologies</i>					
SOLiD 4	12	50 x 35	71,000	A-T Bias	>0.06
SOLiD 5500xl	8	75 x 35 PE 60 x 60 MP	155,000	A-T Bias	>0.01
<i>Ion torrent</i>					
PGM 314 Chip	3	100	10	Indel	1
PGM 316 Chip	3	100+	100	Indel	1
PGM 318 Chip	3	200	1000	Indel	1
<i>Pacific biosciences</i>					
RS	14/8 Smart Cells	1500	45/SC	Insertions	15

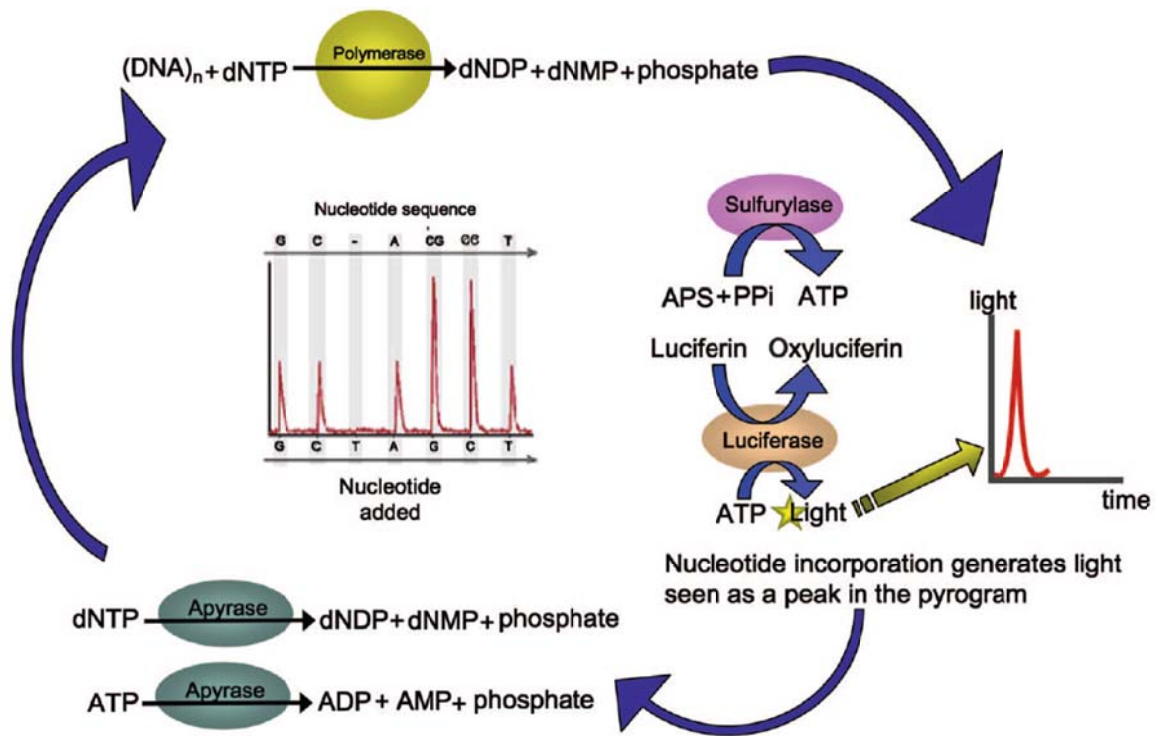
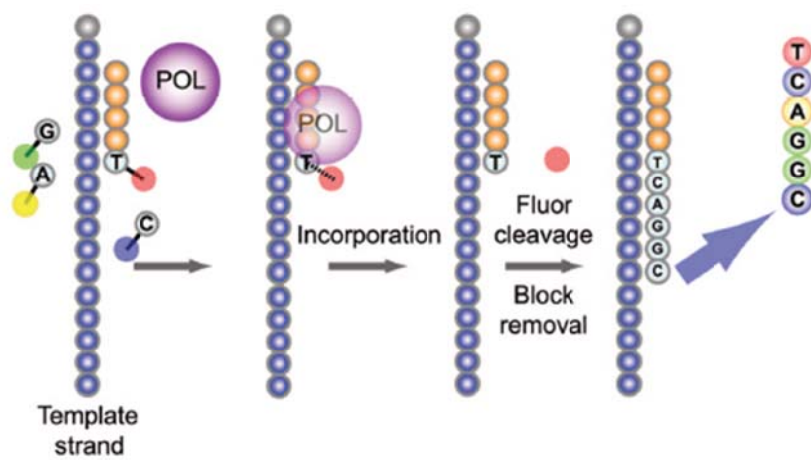
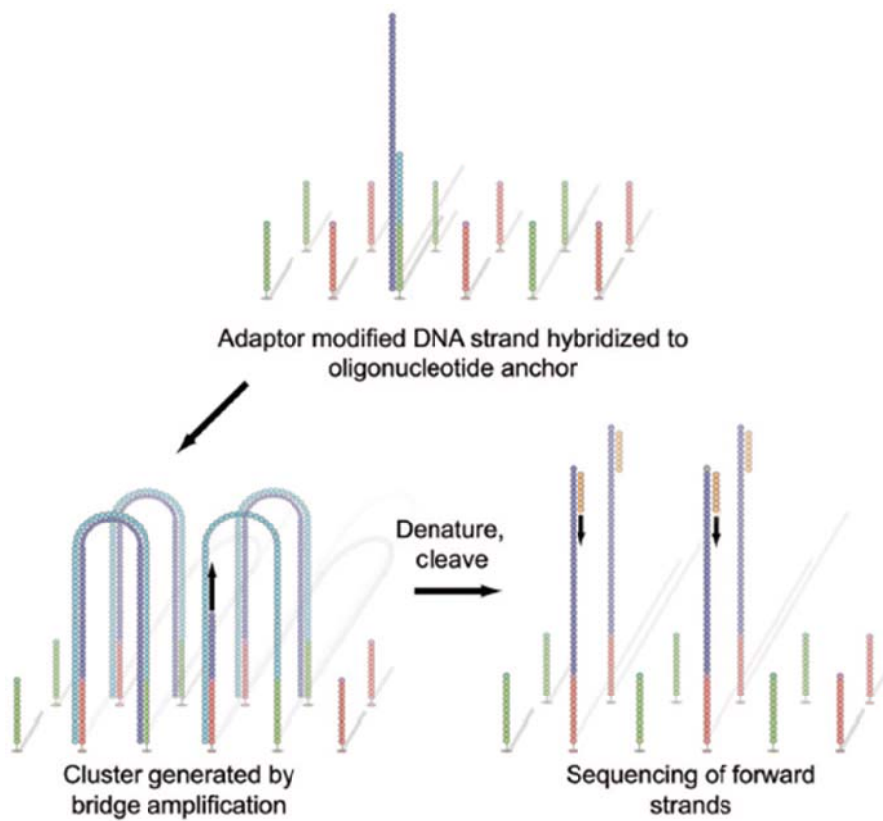


Figure II-32. Pyrosequencing chemistry: biochemical reactions and enzymes involved in the generation of light signals by DNA pyrosequencing.

### **II.5.3.1. Illumina MiSeq**

In 1997, British chemists Shankar Balasubramanian and David Klenerman conceptualized an approach for sequencing single DNA molecules attached to microspheres. They founded Solexa in 1998, and their goal during early development of sequencing single DNA molecules was not achieved, requiring a shift toward sequencing clonally amplified templates. By 2006, the Solexa Genome Analyzer, the first “short read” sequencing platform, was commercially launched. Acquired by Illumina (<http://www.Illumina.com>) in 2006, the Genome Analyzer uses a flow cell consisting of an optically transparent slide with 8 individual lanes on the surfaces of which are bound oligonucleotide anchors (Voelkerding et al. 2009). It support massively parallel sequencing using a proprietary method that detects single bases as they are incorporated into growing DNA strands. This sequencing relies on chain termination to determine sequences of DNA fragments. Adaptors are attached to DNA fragments, the adaptors hybridise with a flow cell which has a forest of adaptors. A flow cell consists of an optically transparent slide with 8 individual lanes on the surfaces of which are bound oligonucleotide anchors. The fragments bend over to attach to adaptors and bridge amplification takes place to generate multiple copies of the fragments (cluster growth). This technology uses chemical modification of the nucleotides with fluorescent molecules of different colors to read the base. Laser detection is incorporated to detect read ref. (Figure II-33). A fluorescently labeled reversible terminator is imaged as each dNTP is added, and then cleaved to allow incorporation of the next base. Since all 4 reversible terminator-bound dNTPs are present during each sequencing cycle, natural

competition minimizes incorporation bias. The end result is true base-by-base sequencing that enables the industry's most accurate data for a broad range of applications. The method virtually eliminates errors and missed calls associated with strings of repeated nucleotides (homopolymers). Illumina sequencing supports both single-read and paired-end libraries. It is the only platform that offers a short-insert paired-end capability for high-resolution genome sequencing, as well as long-insert paired-end reads for efficient sequence assembly, de novo sequencing, structural variation detection, and more. The combination of short inserts and longer reads increases the ability to fully characterize any genome (<http://www.illumina.com>).



Sequencing by reversible dye terminators

Figure II-33. Illumina Genome Analyzer sequencing (Voelkerding et al. 2009).

**Adapter-modified, single-stranded DNA is added to the flow cell and immobilized by hybridization. Bridge amplification generates clonally amplified clusters. Clusters are denatured and cleaved; sequencing is initiated with addition of primer, polymerase (POL) and 4 reversible dye terminators. Postincorporation fluorescence is recorded. The fluor and block are removed before the next synthesis cycle.**

## **II.5.4. Software for analyzing molecular sequences and statistical analysis for understanding microbial community**

There are many software systems to analyze the molecular sequences. The mothur project was initiated by Dr. Patrick Schloss and his software development team at the University of Michigan. This project seeks to develop a single piece of open-source, expandable software to fill the bioinformatics needs of the microbial ecology community. Mothur aims to be a comprehensive software package that allows users to use a single piece of software to analyze community sequence data. It builds upon previous tools to provide a flexible and powerful software package for analyzing sequencing data (Schloss et al. 2009).

QIIME (quantitative insights into microbial ecology) an open-source software pipe line built using the PyCogent toolkit<sup>6</sup>, to address the problem of taking sequencing data from raw sequences to interpretation and database deposition. It supports a wide range of microbial community analyses and visualizations that have been central to several recent high-profile studies, including network analysis, histograms of within- or between-sample diversity and analysis of whether ‘core’ sets of organisms are consistently represented in certain habitats (Caporaso et al. 2010).

Nilakanta et al. (2014) explained about other software systems (pipe line). WATERS was developed with the main objective to expand sequencing analysis to non-bioinformaticians. RDP pipeline was created for high-volume amplicon sequencing data. VAMPS was also designed to allow ecologists and clinicians to

easily analyze sequencing data with a “point and click” interface. Genboree likewise was created for individuals of all bioinformatic levels. Lastly, SnoWMan was designed with a straightforward analysis interface and basically operates as a pipeline of pipelines. They have compiled a listing of the capabilities of each program (Table II-10).

In additions, Multivariate analysis is based on the statistical principle of multivariate statistics, which involves observation and analysis of more than one statistical outcome variable at a time. In the microbial ecology, these techniques were used to explain the complex interactions of microbial community and evaluate the data statistically and visually. Complex data sets are mostly explored via principal component analysis (PCA), or correspondence analysis (CA), and hypothesis-driven techniques such as redundancy analysis or canonical correspondence analysis (CCA). It was summarized the advantage and disadvantage of multivariate analysis in the Table II-11 (Ramette 2007; Gonzalez and Knight 2012).

**Table II-10. Major functions of seven pipelines (Nilakanta et al. 2014).**

Capabilities		Mothur	Qiime	Waters	RD-Pipeline	VAMPS	Genboree	SnoWMAn
Documentation	Available guides	√	√	√	√	√	√	√
Installation	Shortcut option(instant download)	√	√					
	Native version: Mac OSX	√	√	√				
	Native version: Windows	√	√	√				
	Native version: Linux	√	√	√				
	Web based				√	√	√	√
Updating	Re-download entire program	√	√	√				
	Re-download updated section		√					
Interface	Command line	√	√					
	Graphic User Interface			√				
	Web from GUI				√	√	√	√
Sequencing platform	Illumina	√	√	√	√	√	√	√
	454 Pyroseq	√	√	√	√	√	√	√
Preparing sequences	Accepted file formats							
	sff	√	√		√	√	√	
	Fasta	√	√	√	√	√	√	√
	Quality score	√	√		√			√
	Flow file data	√	√					
	User defined barcodes or primers	√	√	√	√	√	√	√
	User defined metadata	√	√	√	√	√	√	√
Preparing sequences	Alignment	√	√	√	√	√	√	√
	Summary function	√	√		√			
	Trims barcodes and primers off of sequence	√	√	√	√	√	√	√
	Removes short reads	√	√	√	√	√	√	√
	Identify and remove chimeras	√	√	√	√	√	√	√

**Table II-10. (Continued).**

Capabilities		Mothur	Qiime	Waters	RD-Pipeline	VAMPS	Genboree	SnoWMA
	Remove contaminants	√	√					
Approaches to analyze files	OTU binning/clustering	√	√	√	√	√	√	√
	Phylotype binning	√	√					√
	Phylogenetic tree	√	√	√			√	
Analysis output	Alpha diversity	√	√	√	√	√	√	√
	Beta diversity	√	√	√	√	√	√	√
	Ecological indexes	√	√	√	√	√	√	√
	Unifrac	√	√	√	√	√	√	√
	Visualizataion	√	√	√	√	√	√	√

**Table II-11. Summary of multivariate analyses in microbial ecology (Ramette 2007; Gonzalez and Knight 2012).**

<b>Name</b>	<b>Advantages</b>	<b>Disadvantages</b>	<b>Example application</b>
Principal component analysis (PCA)	Allows visualization of high dimensional data using lower dimensions.	On the basis of Euclidean distances for dissimilarity comparisons, it can hide biologically relevant patterns. Non-linear growth in processing time.	Showed significant correlation between relative abundance of Bacteroidetes and metagenome functions associated with obesity.
Redundancy analysis (RDA)	This method can be considered as an extension of PCA in which the main axes are constrained to be linear combination of environmental variables.	On the basis of Euclidean distances for dissimilarity comparisons, it can hide biologically relevant patterns.	To test whether the occurrence of biocontrol bacteria with specific carbon source utilization profiles was related to their origin from different root samples.
Multidimensional scaling (MDS)/principal coordinate analysis (PCoA)	Allows visualization of high dimensional data using lower dimensions allowing the use of any dissimilarity metric.	Non-linear growth in processing time.	Showed high variability in microbial community through time while preserving differences between body sites.
Non-metric Multidimensional scaling (NMDS)	In general, preserves the high-dimensional structure with fewer axes. On the basis of numerical optimization, relaxing linear assumptions.	Can be more time-consuming than MDS.	NMDS plots showed that short-term storage conditions for soil and human related samples do not affect community composition.

**Table II-11. (Continued).**

<b>Name</b>	<b>Advantages</b>	<b>Disadvantages</b>	<b>Example application</b>
Correspondence analysis (CA)	<p>This can be visualized by plotting species abundance against the environmental parameter.</p> <p>It is recommended when species display unimodal relationships with environmental gradients.</p>	<p>The distance between the points of different sets is not defined and it does not include significance testes for effects or interactions.</p>	<p>It generally used to determine whether patterns in microbial OUT distribution could reflect differentiation in community composition as a function of seasons or habitat structure.</p>
Canonical correspondence analysis (CCA)	<p>This method can be considered as an extension of CA.</p> <p>It provides useful information about the linear correlation between species and environmental parameter.</p>	<p>Only two data sets considered</p> <p>CCA diagram would become near uninterpretable.</p>	<p>It has been used in study dealing with microbial assemblages in marine and soil ecosystems.</p>

### **II.5.5. The main reference resources for metagenomics**

The Ribosomal Database Project (RDP) provides phylogenetic classification for the prokaryotic organisms in the sequence databases. Work in the project started by two University of Illinois at Urbana-Champaign (UIUC) faculty members, Carl R. Woese and Gary J. Olsen. Woese recognized that, due to rRNA's conserved sequence, ribosomal RNA could be used to elicit phylogenetic relationships between organisms. They predicted that making a collection of rRNA sequences available would be useful to the research community and stimulate research in this area. The first release was published in 1992, where the number of 16S rRNA sequences was just 471. After some releases, the project moved to Michigan State University in 1998. RDP contains 3,224,600 sequences as bacterial sequences.

Greengenes provides phylogenetic classification for the 16S sequences. One of its goals is to incorporate suggestions and manual curations from its user community, ranging from the overriding of some fields in the database to the proposal of a new name for a taxonomic group. The Greengenes taxonomy includes 1,049,116 aligned sequences of length >1250 nucleotides.

SILVA provides comprehensive, quality checked and regularly updated datasets of aligned small (16S/18S, SSU) and large subunit (23S/28S, LSU) ribosomal RNA (rRNA) sequences for all three domains of life. SILVA provides three different alignments for 16S rRNA: SSUParc, with 4,985,791 sequences, is intended for biodiversity analyses, its quality filtering is basic and there is no guiding tree. SSU Ref, with 1,756,783 sequences, contains only high quality,

nearly full-length sequences, and it is intended for phylogenetic analysis and probe design. SSU Ref NR 99, with 597,607 sequences, contains a 99% identity criterion to remove highly identical sequences.

EzTaxon provides phylogenetic classification for the type strain 16S sequences. The EzTaxon database (Kim et al. 2012) is an extension of the original EzTaxon database, and was developed with the aim of covering uncultured species that are often found in microbial ecological studies. EzTaxon contains 60,384 sequences as bacterial sequences.

**Table II-12. Characteristics of the main reference resources for metagenomics focused on the 16S ribosomal RNA gene (Santamaria et al. 2012).**

<b>Data base</b>	<b>Chimera detection</b>	<b>Aligner</b>	<b>Tree builder</b>	<b>Alignment</b>
RDP	Pintail	Infernal	RDP Classifier	Automatic
Greengenes	UCHIME, Chimera Slayer	Infernal	FastTree	Automatic
SILVA	Pintail	SINA	ARB Parsimony	Curated
EzTaxon-e	No	SINA	ARB Parsimony	Curated

### **II.5.6. Microbial network analysis**

Recently, network analysis has been applied for better understanding of the complex microbial community within the system. Co-occurrence (the interactions between organisms and environmental effects on coexistence within biological communities) and correlation patterns found in metagenomics and 16S pyrosequencing data sets are increasingly used for the prediction of species interactions in environments (Faust and Raes 2012). It offers new insight into the structure of complex microbial communities, insight that complements and expands on the information provided by the more analytical approaches (Williams et al. 2014, Barberán et al. 2012).

The networks were all built with similarity-based techniques, mainly using either Pearson (Pearson's correlation coefficient is a measure of the strength of the association between the two variables) or Spearman correlations (This is a non-parametric measure the degree of association between two variables) for abundance data and the hypergeometric distribution for presence-absence data. Another popular similarity-based network inference methodology is local similarity analysis (LSA) (Local similarity analysis reveals unique associations among marine bacterioplankton species and environmental factors), which can detect similarity between shifted abundance profiles and is therefore frequently used to build association networks from time series data. To set thresholds on similarity scores, most authors use a permutation test. Figure II-34 described principle of similarity- and regression-based network inference.

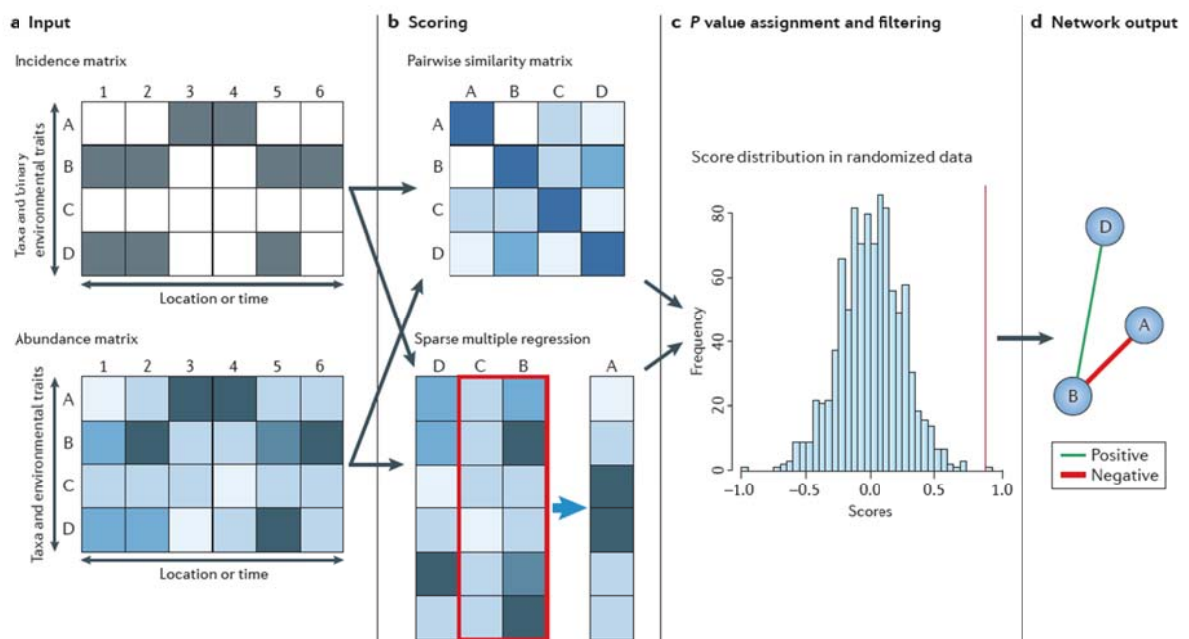


**Figure II-34. Principle of similarity- and regression- based network inference (Faust and Raes 2012).**

The goal of network inference is to identify combinations of microorganisms that show significant co-presence or mutual exclusion patterns across samples and to combine them into a network. Figure II-34 a) explained that network inference starts from an incidence or an abundance matrix, both of which store observations across different samples, locations or time points. Figure II-34 b) described that pairwise scores between taxa are then computed using a suitable similarity or distance measure. A range of such measures are used in the literature (for example, Pearson, Spearman, hypergeometric distribution and the Jaccard index). In contrast to similarity-based approaches, multiple regression can detect relationships that involve more than two taxa. To reduce over-fitting, sparse multiple regression is usually carried out that is, the source taxa subset that best predicts the target taxon's abundance is selected. In addition, the regression model is cross-validated: that is, after regression coefficients have been identified with a training data set, the model's prediction accuracy is quantified on a test data set. Figure II-34 c) explained that a random score distribution is generated by repeating the scoring step a large number of times (often 1,000 times or more). The random score distribution computes the  $P$  value (that is, the probability of obtaining a score by chance that is equal to or better than the observed score) to measure the significance of the predicted relationship. The  $P$  value is usually adjusted for multiple testing with procedures such as Bonferroni or Benjamini–Hochberg. Figure II-34 d) described that taxon pairs with  $P$  values below the threshold are visualized as a network, where nodes represent taxa and edges represent the significant relationships between them. The edge thickness can reflect the strength

of the relationship (Faust and Raes 2012).

However LSA, as originally developed, does not consider time series data with replicates, which hinders the full exploitation of available information. Thus, LSA technique was extended to time series data with replicates and termed it extended LSA, or eLSA. Simulations showed the capability of eLSA to capture subinterval and time-delayed associations (Xia et al. 2011).

Network concepts can be used as descriptive statistics for networks. While some network concepts (e.g. connectivity) have found important uses in biology and genetics, other network concepts (e.g. network centralization) appear less interesting to biologists. Before attempting to understand why some concepts are more interesting than others, it is important to understand how network concepts relate to each other in biologically interesting networks. Thus, various parameters of the networks are explained in the Table II-13 (<http://med.bioinf.mpi-inf.mpg.de/netanalyzer/help/2.6.1/> accessed Jan 12, 2016; Dong and Horvath 2007; Deng et al. 2012).

**Table II-13. The network analysis index in this study.**

Indexes	Formula	Explanation	Note
Node	-	-	a node is a connection point (i.e. species)
Edge	-	-	A edge is connection among nodes (i.e. interactions)
Clustering coefficient	$C_n = \frac{2l_n}{k_n(k_n - 1)}$ $N/M$	<p><math>k_n</math> is the number of neighbors of <math>n</math> and <math>l_n</math> is the number of connected pairs between all neighbors of <math>n</math>.</p> <p><math>N</math> is the number of edges between the neighbors of <math>n</math>, and <math>M</math> is the maximum number of edges that could possibly exist between the neighbors of <math>n</math>.</p>	<p>This index describes how well a node is connected with its neighbors. If it is fully connected to its neighbors, the clustering coefficient is 1. A value close to 0 means that there are hardly any connections with its neighbors.</p>
Connected component	-	-	Two nodes are connected if there is a path of edges between them. Within a network, all nodes that are pairwise connected form a connected component. The number of connected components indicates the connectivity of a network. (The lower number of connected components suggests a stronger connectivity.)
Network diameter	-	-	The network diameter is the largest distance between two nodes. If a network is disconnected, its diameter is the maximum of all diameters of its connected components. The diameter can also be described as the maximum node eccentricity (eccentricity is the maximum non-infinite length of a shortest path between $n$ and another node in the network. If $n$ is an isolated node, the value of this attribute is zero).

**Table II-13. (Continued).**

Indexes	Formula	Explanation	Note
Shortest paths	-	-	The length of a path is the number of edges forming it. The shortest path length, also called distance, between two nodes $n$ and $m$ is denoted by $L(n,m)$ . The shortest path length distribution gives the number of node pairs $(n,m)$ with $L(n,m) = k$ for $k = 1, 2, \dots$
Characteristic path length	$(\text{sum of shortest path length}) / n(n-1)$	$n$ is number of node	The average shortest path length, also known as the characteristic path length, gives the expected distance between two connected nodes.
Avg. number of neighbors	$S_1(k)/n$	$S_1(k)$ is sum of total connectivity, $n$ is number of node	The average number of neighbors indicates the average connectivity of a node in the network. A normalized version of this parameter is the network density.
Network density	$Density = 2S_1(k)/n(n-1)$	$S_1(k)$ is sum of total connectivity, $n$ is number of node	This index is closely related to the average connectivity. The density is a value between 0 and 1. It shows how densely the network is populated with edges (self-loops and duplicated edges are ignored). A network which contains no edges and solely isolated nodes has a density of 0. In contrast, the density of a clique is 1. A normalized version of Avg. number of neighbors is the network density.

**Table II-13. (Continued).**

Indexes	Formula	Explanation	Note
Network centralization	$Centralization = \frac{n}{n-2} \left( \frac{\max(k)}{n-1} - Density \right) \approx \frac{\max(k)}{n} - Density$	<p><math>Max(k)</math> is the maximal value of all connectivity values, <math>n</math> is number of node</p>	<p>Networks whose topologies resemble a star have a value of centralization close to 1, whereas decentralized networks are characterized by having a value of centralization close to 0. The normalized connectivity centralization (also known as degree centralization) is a simple and widely used index of the connectivity distribution. The centralization index has been used to describe structural differences of metabolic networks</p>
Network heterogeneity	$Heterogeneity = \frac{\sqrt{variance(k)}}{mean(k)}$	<p><math>Mean(k)</math> is average value of all connectivity, <math>variance(k)</math> is variance of all connectivity, <math>S_1(k)</math> is sum of total connectivity, <math>S_2(k)</math> is sum of variance of all connectivity</p>	<p>Many measures of network heterogeneity are based on the variance of the connectivity, and authors differ on how to scale the variance. Biological networks tend to be very heterogeneous: while some 'hub' nodes are highly connected, the majority of nodes tend to have very few connections. The network heterogeneity reflects the tendency of a network to contain hub nodes.</p>

### **II.5.7. Prediction of metabolic pathway from microbial community**

Profiling phylogenetic marker genes, such as the 16S rRNA gene, is a key tool for studies of microbial communities but does not provide direct evidence of a community's functional capabilities. Recently, PICRUSt (phylogenetic investigation of communities by reconstruction of unobserved states) that uses evolutionary modeling to predict metagenomes from 16S data and a reference genome database was developed (Langille et al. 2013). This technique uses an extended ancestral-state reconstruction algorithm to predict which gene families are present and then combines gene families to estimate the composite metagenome. It reported that correlations between inferred and metagenomically measured gene content approached 0.9 and averaged ~ 0.8 in the best cases. It recaptured most of the variation in gene content obtained by metagenomics sequencing using only a few hundred 16S sequences and in some cases outperformed the metagenomes measured at particularly shallow sampling depths.

## Chapter III

# QQ Effect on the Microbial Community of Biofilm in an Anoxic-Oxic MBR



### **III.1. Introduction**

As mentioned in the previous chapter, the bacterial QQ is an attractive approach to control biofouling in MBRs because it increases treatment efficiency and requires less consumption of additional energy (Oh et al. 2012). Recently, new QQ-bacteria was isolated and different types of carriers developed to increase QQ activity (Cheong et al. 2013; Kim et al. 2013b; Cheong et al. 2014; Köse-Mutlu et al. 2015; Kim et al. 2015a) and this approach has been fully investigated in a larger pilot scale MBR using real wastewater (Lee et al. 2016).

Although, the information of microbial community of biofilm is crucial for the development of QQ strategies, the available information is not sufficient in QQ-MBR. A few studies have reported that the enzymatic QQ had an effect on the development of microbial composition in biofilm in a laboratory-scale MBR (a 2.5-L reactor with a hollow fiber membrane) (Kim et al. 2013a). However, this study did not consider the QQ mechanisms in terms of microbial ecology. Although, microbial community diversity influences microbial system function (Bell et al. 2005), this study did not address the effect of QQ on the community diversity of biofilm. In addition, the microbial community shift of biofilm from a conventional-MBR has already been observed in previous studies (Miura et al. 2007b; Lim et al. 2012; Gao et al. 2014a), implying a need for more investigation of the effect of QQ on the microbial community in biofilm.

Based on transmembrane pressure (TMP) and time (d), the microbial community of biofilm was observed in the QQ-MBR. Multivariate statistical techniques (e.g., principal component analysis and correspondence analysis) were

used to reveal how TMP and time affect microbial community composition. Such techniques are often too simplistic to explain the complex interactions in microbial systems (Kim et al. 2015b). Therefore, the main objectives of this study were to elucidate the change of microbial community and to determine the effects of bacterial QQ on the microbial community in the biofilm.

## III.2. Materials and methods

### III.2.1. Materials

The components of the synthetic wastewater prepared as follows: glucose (Samyang Genex, Seoul, Korea); Difco yeast extract (BD Life Sciences); Bactopectone (Laboratoris Conda, Madrid, Spain);  $\text{KH}_2\text{PO}_4$  (Duksan Pure Chemical);  $\text{MgSO}_4 \cdot 7\text{H}_2\text{O}$ ,  $\text{FeCl}_3 \cdot 3\text{H}_2\text{O}$ , and  $\text{MnSO}_4 \cdot 5\text{H}_2\text{O}$  (Junsei chemical, Tokyo, Japan);  $(\text{NH}_4)_2\text{SO}_4$ ,  $\text{CaCl}_2 \cdot 2\text{H}_2\text{O}$  and  $\text{NaHCO}_3$  (Daejung Chemical and Materials, Siheung, Korea) (Oh et al. 2012). The C8-HSL, *N*-(decanoyl)-DLhomoserine lactone was purchased from Sigma-Aldrich (USA) for measurement of AHL-degrading activity.

### III.2.2. MBR systems

The laboratory-scale submerged anoxic/oxic (A/O) MBR consisted of interconnected anoxic (2.5 L) and oxic (5 L) tanks (Figure III-1). The synthetic wastewater was fed first into the anoxic tank equipped with an agitator. The feed COD and total nitrogen (TN) were  $539.2 \pm 19.3$  and  $39.9 \pm 2.3$  mg/L, respectively. The removal efficiency of COD was 98 ~ 100%, and that of nitrogen was 73 ~ 83%. The mixed liquor overflowed from the anoxic tank into the aerobic tank in which two membrane modules were immersed. The aerobic tank was equipped with a coarse bubble diffuser connected to a blower (2L/min aeration rate) that mixed the activated sludge and maintained the dissolved oxygen concentration at 2.5 mg/L and above. The rate of recirculation flow from the middle of the aerobic tank to the

anoxic tank was maintained at two times the feed flow rate,  $Q$ . The screener (hole size: approximately 1 mm) was placed in the oxic tank so that vacant- or QQ-beads were constantly retained in the oxic tank. The concentrations of the mixed liquor-suspended solids (MLSS) were maintained at  $6404 \pm 797$  mg/L in the anoxic tank and  $8199 \pm 854$  mg/L in the aerobic tank. The hydraulic retention time (HRT) and solid retention time (SRT) were maintained at 8 hours and 30 days, respectively. Both tanks were maintained at a temperature of  $25 \pm 3$  °C and a pH of 6.4-7.8. The two identical membrane modules were mounted vertically within the aerobic tank. One was used to maintain the MBR operation. Another was used for biofilm sampling. The effective area of the hollow fiber membrane module was  $370$  cm<sup>2</sup> for water filtration and  $155$  cm<sup>2</sup> for biofilm sampling. New membrane modules for biofilm sampling were used in each run to collect the biofilm. Each membrane module for biofilm sampling has a value of resistance similar to the membrane (Table III-2). Polyvinylidene fluoride (PVDF) hollow fiber microfiltration membranes (ZeeWeed, GE-Zenon, USA) with a membrane pore size of  $0.04$  μm were used. Two sets of MBR operation were run under the same conditions. Each reactor was operated at a filtration flux of  $28$  L/m<sup>2</sup>·h to maintain MBR operation. The permeate of the filtration module was used to maintain the water level in the MBR through level sensor and three-way valve. A membrane module for biofilm sampling was operated at a filtration flux of  $20$  L/m<sup>2</sup>·h. The permeate of the sampling module was recycled in the oxic tank. After a filtration period of 59 minutes, the membrane module for biofilm sampling was relaxed for 1 minute. TMP is an important membrane performance parameter and the extent of

membrane biofouling is quantified by monitoring changes in the TMP (Hai et al. 2013). TMP variations were monitored for four runs. In the first and second runs, TMP profiles of the conventional (without vacant beads) and QQ-MBR were compared and then the vacant beads were inserted into the conventional MBR (vacant-MBR). TMP profiles of the vacant and QQ-MBR were also compared at the third of fourth runs. QQ beads were injected in the oxic tank, and the injection volume of QQ beads was 1.2% of the total volume of the oxic tank. The other operating parameters for the A/O MBR are listed in Table III-1. The composition of the synthetic wastewater was as follows (mg/L): glucose, 400; yeast extract, 14; bactopectone, 115;  $(\text{NH}_4)_2\text{SO}_4$ , 104.75;  $\text{KH}_2\text{PO}_4$ , 21.75;  $\text{MgSO}_4 \cdot 7\text{H}_2\text{O}$ , 32;  $\text{FeCl}_3 \cdot 3\text{H}_2\text{O}$ , 0.125;  $\text{CaCl}_2 \cdot 2\text{H}_2\text{O}$ , 3.25;  $\text{MnSO}_4 \cdot 5\text{H}_2\text{O}$ , 2.875; and  $\text{NaHCO}_3$ , 255.5. The feed COD and total nitrogen (TN) were  $539.2 \pm 19.3$ , and  $39.9 \pm 2.3$  mg/L.

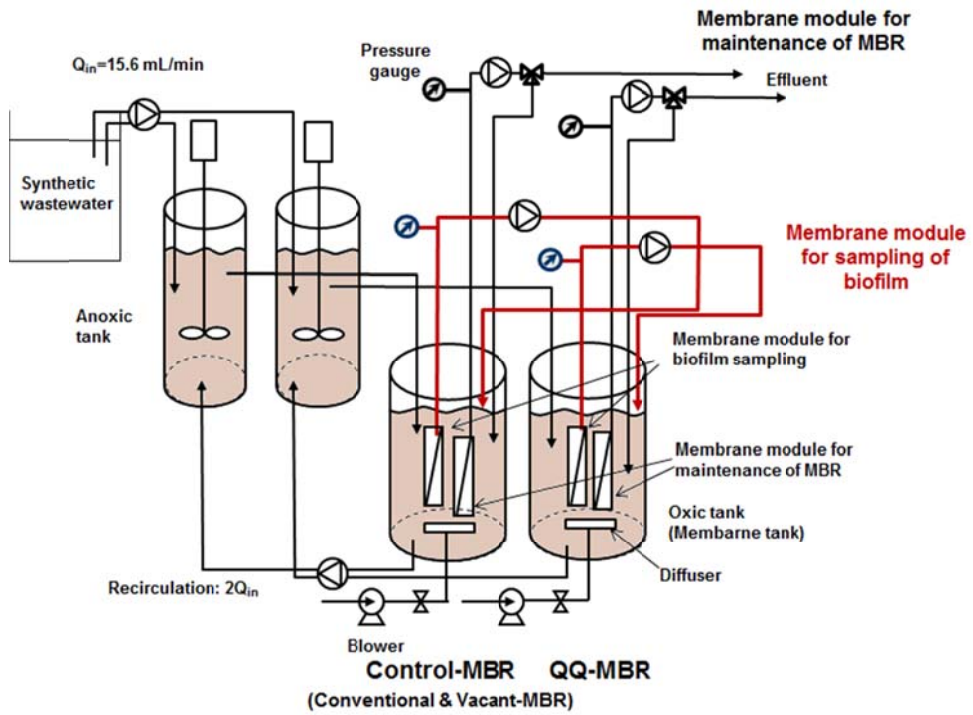


Figure III-1. Schematic diagram of the A/O MBR.

**Table III-1. Operation conditions of Anoxic/Oxic MBR.**

Total working volume (L, anoxic tank / oxic tank)	7.5 (2.5 /5.0)
Total HRT (h)	8
SRT (day)	30
Membrane type (materials)	hollow fiber (PVDF, GE-Zeeweed)
pore size ( $\mu\text{m}$ )	0.04
Membrane area ( $\text{cm}^2$ ) for water filtration	370
Flux ( $\text{L}/\text{m}^2\cdot\text{hr}$ ) for water filtration	28
Membrane area ( $\text{cm}^2$ ) for sampling	155
Flux ( $\text{L}/\text{m}^2\cdot\text{hr}$ ) for sampling	20
Operation mode of membrane module for sampling (Filtration/Relaxation)	59 min/ 1 min
pH (anoxic/oxic)	6.8 - 7.8 / 6.4 - 7.8
Aeration in oxic tank ( L/min )	2.0
Average of COD in synthetic wastewater (mg/L)	$539.2 \pm 19.3$
Average of total nitrogen in synthetic wastewater (mg/L)	$39.9 \pm 2.3$
Reactor temperature ( $^{\circ}\text{C}$ )	$25 \pm 3$
Dissolved oxygen (mg/L) (anoxic tank / membrane tank)	below 0.5 / 2.5 and over
Seeding sludge	Sihwa
Concentration of beads (% v(beads) / v(membrane tank))	1.2%

### **III.2.3. Preparation of the QQ-beads**

The quorum quenching (QQ) bacteria used in this study is *Rhodococcus* sp. BH4 (Oh et al. 2012). *Rhodococcus* sp. BH4 was incubated in LB broth for 1 day (30 °C, 200 rpm) for the preparation of the QQ-beads. The QQ-beads were prepared using the dripping method, and the material and solidification method were modified to reinforce the stability of the QQ-beads, which are made of an alginate matrix that decomposes in real wastewater. (Lee et al. 2016). The concentration of dried *Rhodococcus* sp. BH4 in beads was approximately 3.5 ~ 3.8 mg per g of beads. The average size and density of QQ-beads were approximately 4.3 ~ 4.6 mm and 1.0 ~ 1.1 g/mL, respectively.

### **III.2.4. Bioassay of AHL-degrading activity**

To determine the AHL-degrading activity of QQ-beads, the 50 QQ-beads were incubated in 20 ml of C8-HSL (*N*-(decanoyl)-DLhomoserine lactone, Sigma-Aldrich, USA) in a Tris-HCl buffer (50 mM, pH 7.0) for 2 hr (30 °C, 200 rpm). The concentration of C8-HSL was 200nM. Every 30 min the supernatants were sampled to measure AHL-degrading activity. The concentrations of C8-HSL molecules were measured via luminescence method (Oh et al. 2013) using the reporter strain of *Agrobacterium tumefaciens* A136 (Fuqua and Winans 1996). First, the 95 µl of reporter strain (OD600 0.1) and the 5 µl of sample included C8-HSL standard were mixed and loaded on the microwell plate (Greiner bio-one, Austria). The microwell plate was placed on the incubator

to keep the temperature at 30 °C for 1.5 h, and then the 30 µl of Beta-Glo® Assay solution (Promega, USA) was added to the solution for the luminescent reaction with β-galactosidase produced by the reporter strain. After 40 min, the luminescence was measured by a luminometer (Synergy 2, Biotek®, USA). The amounts of AHLs were calculated using the calibration curve derived from standard samples of C8-HSL.

### III.2.5. Analytical methods

The concentration of MLSS, floc size, soluble COD, total nitrogen (TN), DO and pH in activated sludge were measured at 1, 5, 12, 19, 26, 33, 40, 47, 54, 61, 68, 75, 82, 89 and 91 days. To measure soluble COD and TN concentration, All of samples were filtered using 0.45 µm hydrophilic polypropylene (PP) membrane filter (Pall corp., USA). Filtered samples were measured for COD and TN in duplicate using the Hach digestion vials and DR 4000U spectrophotometer (Hach Co., Denver, Co, U.S.A). Dissolved oxygen concentration was measured by the DO meter (YSI, Model DO200, U.S.A). The pH in activated sludge was determined using pH meter (iSTEK, Model pH-20N, Korea). To determine the hydrodynamic resistance of the membrane ( $R_m$ ), the new membrane module was inserted in 5 L of distilled water and operated at a filtration flux of 20 L/m<sup>2</sup>·h. The  $R_m$  was calculated using the measurement of TMP and resistance of the membrane equation ( $R_m = \frac{\Delta P}{\eta \cdot J}$ ) (Mulder 2012) the water viscosity was assumed to be 0.00089 Pa.s (at 25°C) (Table III-2).

**Table III-2. The hydrodynamic resistance of the membrane ( $R_m$ ) of each run.**

<b>Run</b>	<b>MBR</b>	<b><math>R_m</math> (<math>\times 10^{11}</math>)</b>	
		<b>Minimum</b>	<b>Maximum</b>
1	Conventional-MBR	7.08	7.69
	QQ-MBR	7.08	8.09
2	Conventional-MBR	6.88	7.89
	QQ-MBR	6.67	7.89
3	Vacant-MBR	8.29	9.10
	QQ-MBR	7.69	8.67
4	Vacant-MBR	9.71	10.52
	QQ-MBR	9.51	10.11

### **III.2.6. Sampling for analysis of microbial community in biofilm**

Biofilm was collected to analyze the microbial community. Samples of biofilm were taken from the membrane module at the TMPs of 15, 25 and 45 kPa in the first and third runs. Samples of biofilm were taken from the membrane module at the time when the TMPs of conventional- and vacant-MBR reached 15, 25 and 45 kPa in second and fourth runs. Four strings of hollow fiber membranes (47.7 cm<sup>2</sup> effective areas) with biofilm were cut from the membrane module for each sampling point. After cutting the membrane, the membrane module was sealed by EVA (ethylene-vinyl acetate copolymer). The cut membranes with biofilm were then dipped in the distilled water for 5 minutes to remove activated sludge. After soft washing, the pieces of membrane with biofilm were transferred to 50 ml conical tube. We designated samples as R1C1, R1C2.....R4Q3". R indicates experimental run and C, V and Q indicate conventional-, vacant- and QQ-MBR. The number following letter "R" indicates the order of experimental run and the number following letter "C", "V" and "Q" indicate the sampling order of biofilm. To compare biofilm and activated sludge, the 50 ml activated sludge samples were collected at the first biofilm sampling time (R1C1, R1Q1, R2C1, R2Q1, R3C1, R3Q1, R4C1 and R4Q1) of each run from the oxic tank. As soon as the sampling finished, DNA was extracted from all samples. The remaining samples were stored in a deep-freezer at -80 °C. After removing the membrane from the membrane module, the filtration rate was decreased to maintain the filtration flux at 20 L/m<sup>2</sup>·h.

### **III.2.7. DNA extraction, PCR amplification and Miseq platform sequencing**

The sample preparation for DNA extraction was as follows: Two strings of hollow fiber membrane (4 ~ 5 cm) with biofilm were cut into small pieces and the pieces of the membrane with biofilm were inserted into the bead tube for DNA extraction. A total of 1.5 ml of activated sludge was harvested by centrifugation (10,000 g, 1 min, 25 °C), the pellet was resuspended in 0.5 ml of DI water and the resuspended solution was injected into bead tube for DNA extraction. DNA was extracted from the precipitates using the NucleoSpin Soil kit (Macherey-Nagel GmbH, Düren, Germany). DNA was eluted in 100 µl of the elution buffer. DNA was quantified using the ND-1000 spectrophotometer (Nanodrop Inc., Wilmington, DE, USA).

Each sequenced sample was prepared according to the Illumina 16S Metagenomic Sequencing Library protocols. The quantification of DNA and the DNA quality were measured by PicoGreen and Nanodrop. The V3-V4 regions of 16S rRNA genes were amplified with primers 341F (5'-CCTACGGGNGGCWGCAG-3') and 785R (5'-GACTACHVGGGTATCTAATCC-3') (Klindworth et al. 2012). Input gDNA (12.5 ng) was amplified with 16S V3-V4 primers and a subsequent limited-cycle amplification step was performed to add multiplexing indices and Illumina sequencing adapters. The final products were normalized and pooled using the PicoGreen, and the sizes of libraries were verified using the LabChip GX HT DNA High Sensitivity Kit (PerkinElmer, Massachusetts, USA). Next, a sample was sequenced using the MiSeq™ platform (Illumina, San

Diego, USA) by Macrogen Incorporation (Seoul, Korea).

### **III.2.8. Data analysis for bacterial community**

Sequencing data were divided into 4 runs. Each run consisted of 2 activated sludge samples and 6 biofilm samples. Each sequencing data were trimmed and analyzed using the Mothur program version 1.35.1 (Schloss et al. 2009). Sequences were filtered by standard operating procedure for Miseq (Kozich et al. 2013). The primer sequences and low quality sequences, which had an ambiguity, and were under 300 bp and over 500 bp, were removed using the Mothur program. The average nucleotide length was 412 bp for the bacterial libraries. Chimeric sequences were removed using the Uchime function with the abundant sequences as reference. All of the sequences were classified using the SILVA reference library. The sequencing reads obtained in this study were deposited into the DNA data Bank of Japan (DDBJ) Sequence Read Archive (<http://trace.ddbj.nig.ac.jp/dra>) under accession no. DRA004065.

For community analysis, OTU (operational taxonomic unit)-based approaches were conducted using Mothur software. OTUs were determined at 3 % dissimilarity. Each read was taxonomically assigned at the genus level with bootstrap values of more than 80% resulting in taxonomic classification from phylum to genus. A total of 1,246,792 (Run1, 335,983; Run2, 361,310; Run3, 282,444; Run4, 267,055) effective sequences were obtained after the cleaning of raw reads. A principal coordinate analysis (PCoA) was conducted using Mothur software.

### **III.2.9. Statistical analysis**

The statistical analysis was carried out in the R environment ([www.r-project.org](http://www.r-project.org)). The values of community diversity (i.e., Chao 1 richness, Shannon diversity and Shannon evenness) were divided into control-(conventional- and vacant-) and QQ-MBR. The differences of community diversity between control- and QQ-MBR were analyzed using t-test. PCoA was conducted using a fast distance-based phylogenetic tree construction method and weighted UniFrac distance metric (Evans et al. 2006; Lozupone et al. 2007). OTU based correspondence analysis (CA), a multivariate statistical technique, was applied to determine the relationship among communities, using Canoco version 4.5 software (Microcomputer Power, Ithaca, USA). The sequences were randomly normalized to 27,490 sequences per sample for the correspondence analysis.

### **III.3. Results and discussion**

#### **III.3.1. QQ activity of the QQ-beads and effect of QQ on MBR biofouling**

As shown in Figure III-2, the relative activity of QQ-beads was decreased by approximately 10% after 91 days of operation. Previous researchers reported that the QQ activity of QQ-bacteria maintained its stability for at least 100 days in a laboratory-scale MBR (Jahangir et al. 2012) and that the stability of QQ-beads in terms of the QQ activity, viability and mechanical strength was maintained well for at least for 100 days in real wastewater (Lee et al. 2016).

QQ-beads were continuously applied to MBRs to test their biofouling inhibition activity of biofouling in MBRs (Figure III-3). Two laboratory-scale MBRs in continuous mode were operated in parallel under identical operating conditions except for the addition of QQ-beads to one MBR. The rise of the transmembrane pressure (TMP) profile of the conventional- and QQ-MBRs was compared to evaluate the inhibition of biofouling by QQ activity (Fig. III-3 a and b).

As shown in Figure III-3 (a), the conventional-MBR took 14.3 d for the TMP to reach 47 kPa in the first run, whereas the QQ-MBR took 28.3 d for the first run. QQ mitigated the formation of biofilm and extended the time required to reach the TMP of 45 kPa by 97%, compared with the conventional-MBR. The effect of QQ on the mitigation of biofouling was reconfirmed in the next run.

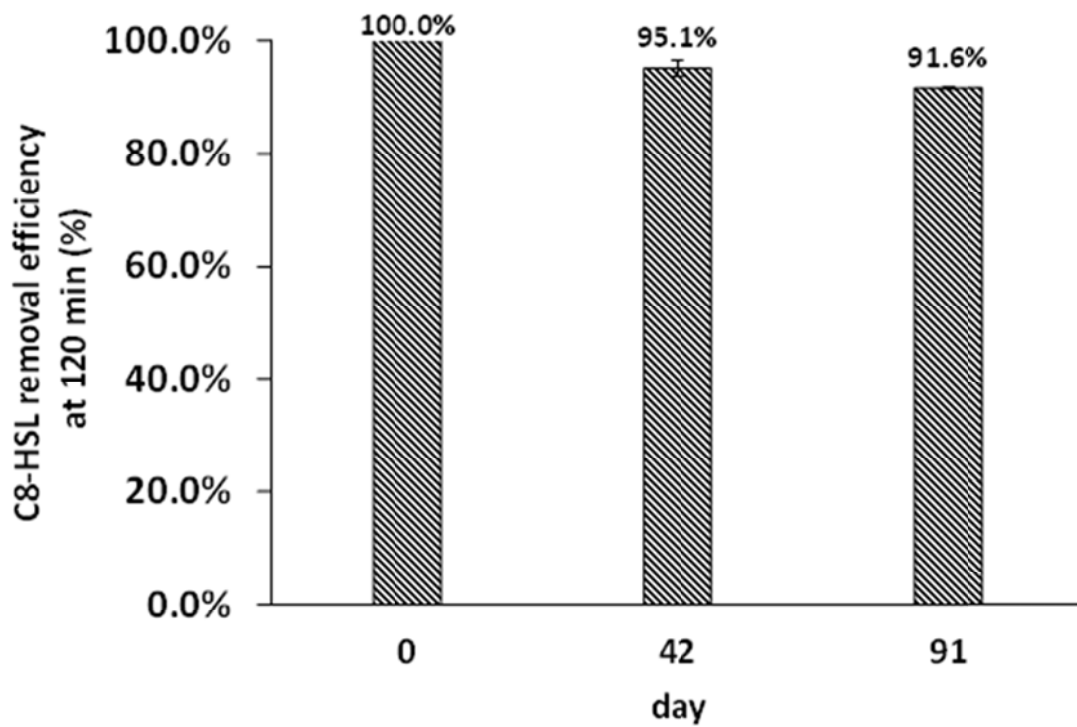


**Figure III-2. Variation of the relative QQ activity of the QQ-beads during the operation of A/O MBRs. QQ activity: degradation ratio of standard C8-HSL for 120 min in the presence of QQ-beads. Error bar: standard deviation (n = 2).**

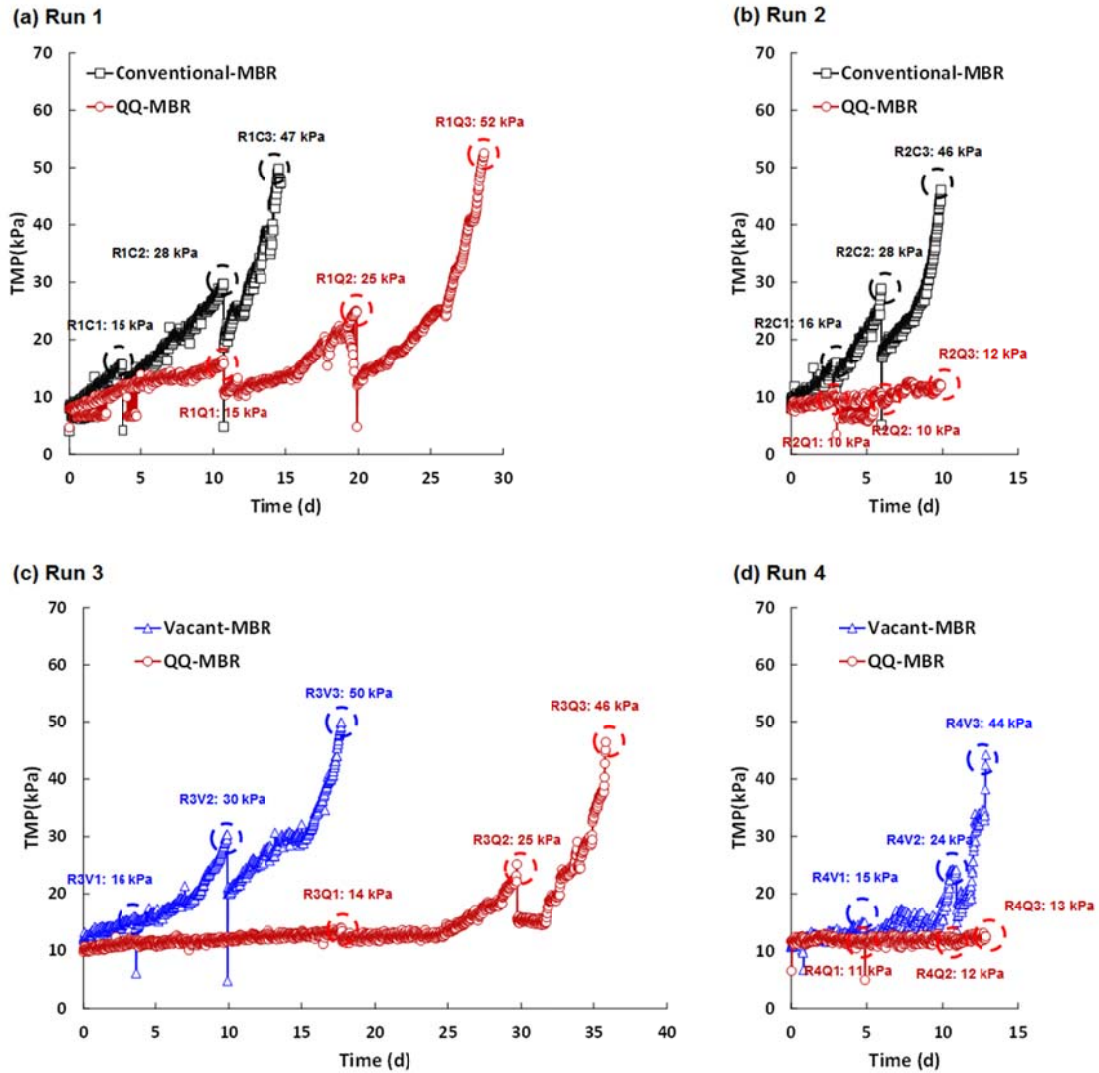
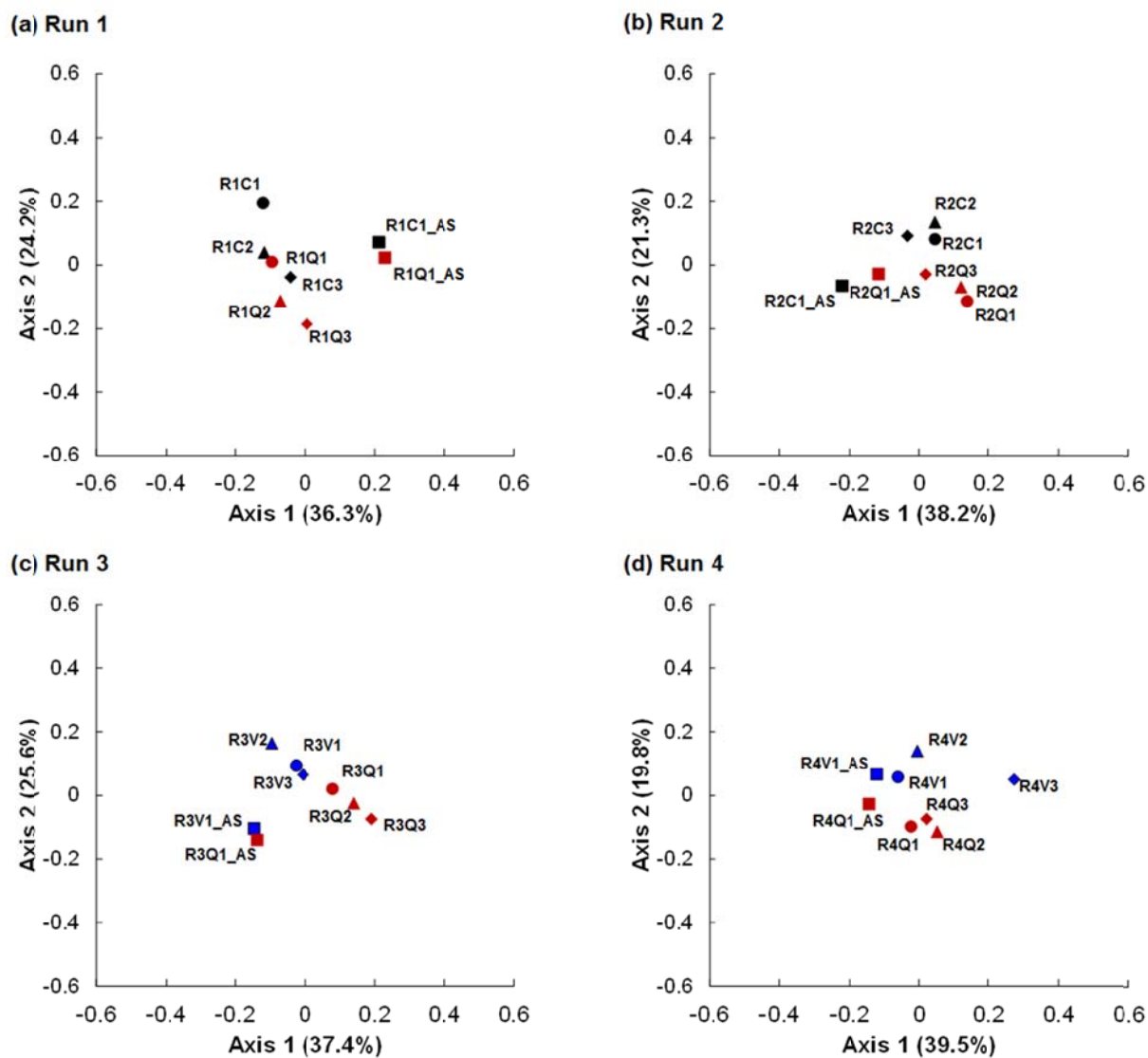


Figure III-3. TMP profile of each run. A circle indicates a sampling point of the biofilm from the membrane module.

In the second run, the rise of the TMP profiles of the conventional-MBR took 9.8 d for the TMP to reach 45 kPa, while the TMP of QQ-MBR was maintained at 10~12 kPa. In the third run, the vacant-bead without QQ-bacteria was injected into the conventional-MBR (vacant-MBR). As shown in Figure III-3 (c), the vacant-MBR took 17.4 d for the TMP to reach 45 kPa in the third run, whereas the QQ-MBR took 35.8 d for the first run. QQ mitigated the formation of biofilm and extended the time required to reach the TMP of 45 kPa by 106%, compared with the vacant-MBR. The effect of QQ on the mitigation of biofouling was reconfirmed in the next run. In the fourth run, shows that the rise of the TMP profiles of the vacant-MBR took 12.9 d for the TMP to reach 44 kPa. The TMP profile of QQ-MBR was still maintained at a low level. The effect of QQ on the membrane biofouling is similar to the result of a previous study in the three-stage (anaerobic/aerobic/ membrane tanks) MBR system (Lee et al. 2016).

### **III.3.2. Principal coordinate analysis based on UniFrac distance metric**

Principal coordinate analysis (PCoA) was applied to distinguish between the communities on the basis of weighted UniFrac distance metric (Figure III-4). The first and second axes of the PCoA plot explained 37.9% and 22.7% of the community composition variations, respectively. The PCoA plot showed the difference between the inoculum community (activated sludge) and the biofilm communities. The PCoA plot shows the difference between the inoculum community (activated sludge) and the biofilm communities. This result is similar to the results of many previous studies. Previous studies have reported differences between the activated sludge and biofilm communities in laboratory-scale MBRs (Lim et al. 2012; Piasecka et al. 2012). Microbial communities of biofilm were categorized into two distinct groups: conventional- and vacant-MBR vs. QQ-MBR. The previous study reported that QQ had an effect on the proportion of quorum sensing bacteria with AHL-like autoinducers (such as *Enterobacter*, *Pseudomonas*, and *Acinetobacter*) using the enzymatic QQ method at the genus level (Kim et al. 2013a). Thus, it was speculated that QQ had an effect on the microbial communities of biofilm.



**Figure III-4. Bacterial community comparison by principal coordinate plots, based on weighted UniFrac distance metric.**

### III.3.3. Correspondence analysis

Correspondence analysis (CA) was applied to distinguish between the communities on the basis of their OTU composition (Figure III-4). The first and second axes of the CA plot explained 34.3% and 24.1% of the community composition variations, respectively (Fig. III-5). The CA plot showed the difference between the inoculum community (activated sludge) and the biofilm communities. The CA plot shows the difference between the inoculum community (activated sludge) and the biofilm communities. This result is similar to the results of previous section. Microbial communities of biofilm were categorized into two distinct groups: conventional- and vacant-MBR vs. QQ-MBR. Microbial communities in Figure III-5 showed patterns of variation by TMP and time. The relationships between the bacterial composition and variations (TMP and time (d)) were investigated using the value of slope from the linear regression equation. Figure III-5 and Figure III-6 show the relationship between the variations (TMP and time) and scores on the first ordination axis of the CA plots in Figure III-5.

The change in bacterial composition was observed in Figure III-5 (a) by TMP. The absolute value of slope (the change rate of bacterial composition) was  $3.13 \times 10^{-2}$  and  $1.48 \times 10^{-2}$  in conventional- and QQ-MBR. The change rate of microbial composition in the conventional-MBR was 2.1-fold higher than QQ-MBR. The change of microbial composition is observed in Figure III-5 (b) by sampling time (d). The absolute value of slope was  $2.68 \times 10^{-2}$  and  $2.32 \times 10^{-2}$  in conventional- and QQ-MBR.

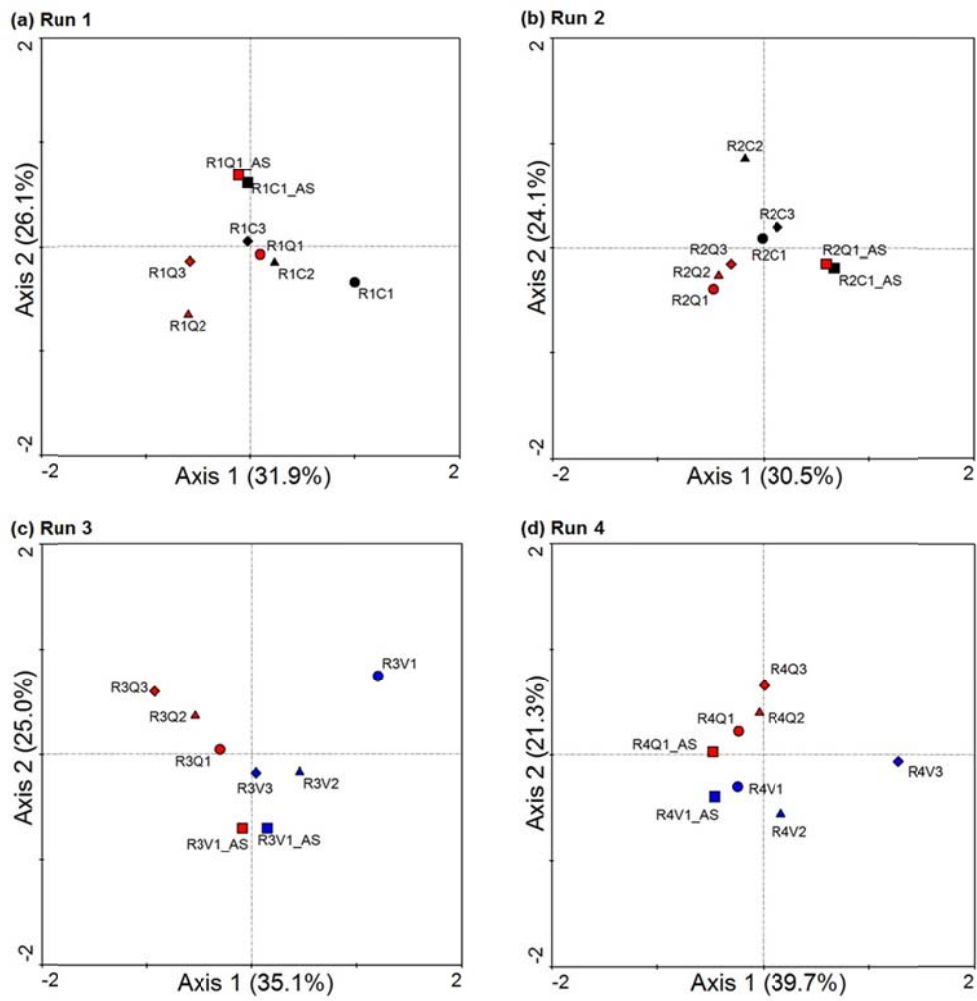


**Figure III-5. Bacterial community comparison by correspondence analysis (CA), based on OTU composition (number of sequences =27,490).**

The change rate of microbial composition in conventional-MBR was 1.1-fold higher than QQ-MBR. The TMP of conventional-MBR samples was increased from 16 to 46 kPa, whereas the TMP of QQ-MBR was maintained at 10 ~ 12 kPa.

Figure III-6 shows the difference in the change of bacterial composition between vacant- and QQ-MBR. The change in microbial composition is observed in Fig. III-6 (a) by biofouling (TMP). The absolute value of slope was  $3.90 \times 10^{-2}$  and  $2.31 \times 10^{-2}$  in the vacant- and QQ-MBR. The change rate of microbial composition in vacant-MBR was 1.7-fold higher than QQ-MBR. The change of microbial composition was observed in Figure III-6 (b) by sampling time (d).

The TMP of vacant-MBR is increased from 15 to 44 kPa, whereas the TMP of QQ-MBR was maintained at 11 ~ 13 kPa. The absolute value of slope was  $16.2 \times 10^{-2}$  and  $3.26 \times 10^{-2}$  in the vacant- and QQ-MBR. The change rate of microbial composition in vacant-MBR was 5.0-fold higher than QQ-MBR. The change rate of the microbial community in Non-QQ-MBRs (conventional-and vacant-MBRs) was higher than the QQ-MBR.

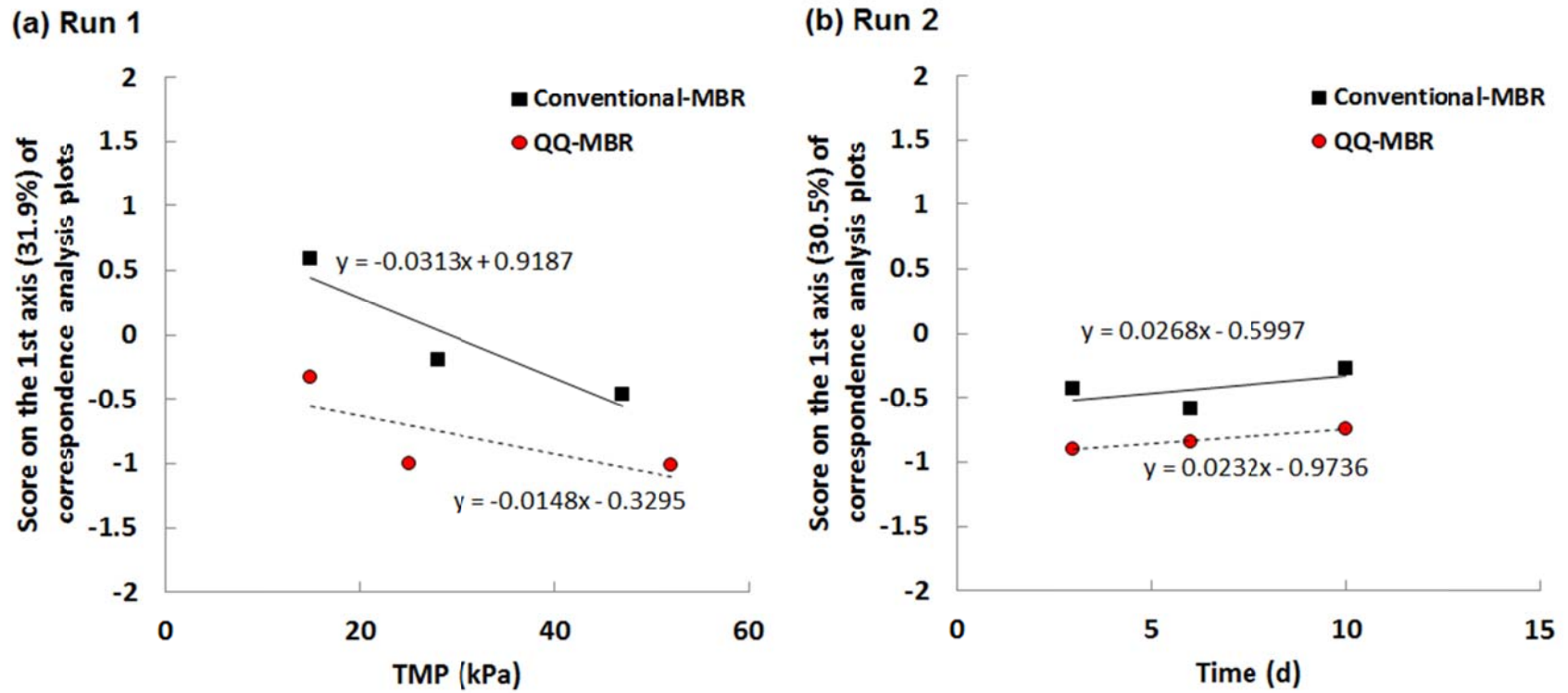
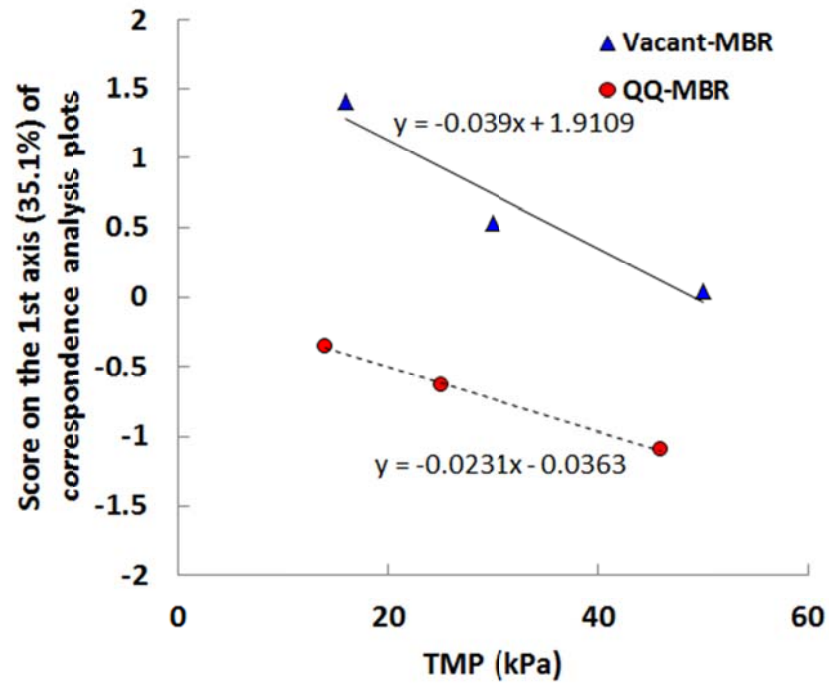


Figure III-6. Linear relationship between variations (TMP and time) and scores on the first ordination axis 1 of correspondence analysis (CA) plots in Run 1 and Run 2.

(a) Run 3



(b) Run 4

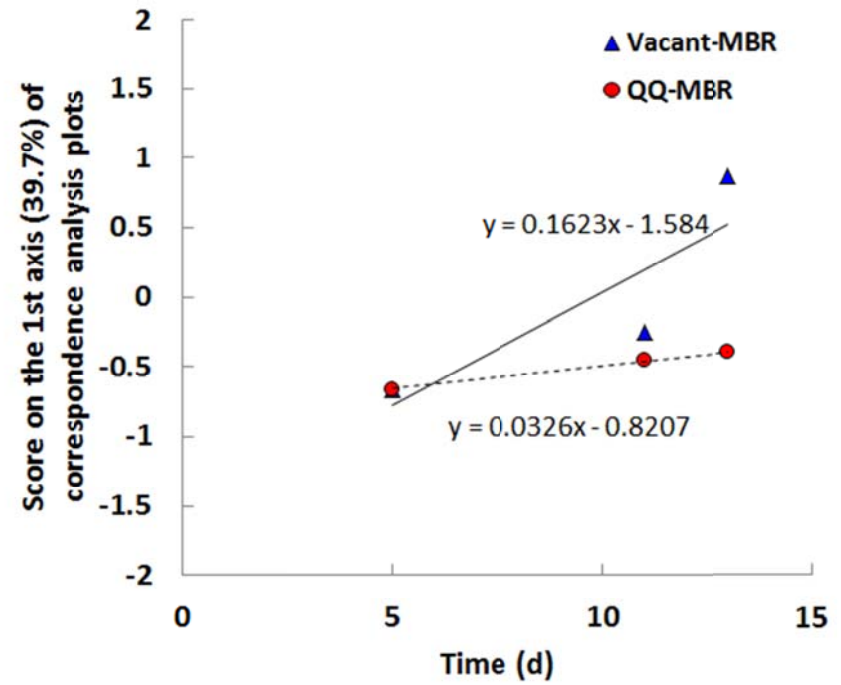


Figure III-7. Linear relationship between variations (TMP and time) and scores on the first ordination axis 1 of correspondence analysis (CA) plots in Run 3 and Run 4.

A considerable temporal change of microbial composition was observed in both control- (conventional- and vacant-MBR) and QQ-MBR as TMP increased (Figs. III-6a and Figs. III-7a). However, variation in the microbial composition was smaller in the QQ-MBR than that in the control-MBR. Variation in microbial composition in QQ-MBR was less than that of control-MBR at the same sampling time because QQ delayed the TMP rise (Figs. III-6b and Figs. III-7b). These results indicated that change of microbial composition was coincided with the development of biofilm and QQ reduced the variation in microbial composition in biofilm. QQ reduced the variation in biofilm microbial composition. Gao et al. (2014) reported that the succession of microbial communities might be the cause of membrane fouling in laboratory-scale A/O MBRs. Thus, the reduction of variation in microbial composition in QQ-MBR might affect the development of biofilm.

#### **III.3.4. Microbial composition in biofilm**

The average relative abundances of dominant bacteria species are listed in Table III-3 and more specific relative abundances of bacteria species are listed in Table III-4. These bacteria existed abundantly in the biofilm. In the first run, OTU 1 (*Thiothrix*), OTU 2 (*Rhodobacter*), OTU 3 (*unclassified*), and OTU 9 (*Gp4*) were more abundant in conventional-MBR than those in QQ-MBR, while OTU 5 (*Dokdonella*), OTU 7 (*Sphingobacteriales*) and OTU 10 (*Nannocystineae*) in conventional-MBR were less abundant than in QQ-MBR. The relative compositions of OTU 4 (*unclassified*), OTU 6 (*Chloroflexi*), and OTU 9 (*Cytophagaceae*) were similar between conventional-and QQ-MBRs in the biofilm.

In the second run, OTU 1 (*Thiothrix*), OTU 2 (*Chloroflexi*), OTU 3 (*Bacteroidetes*), OTU 7 (*unclassified*) and OTU 9 (*Chlamydiales*) were more abundant in conventional-MBR than in QQ-MBR, while OTU 4 (*Haliscomenobacter*), OTU 8 (*Lactococcus*) in conventional-MBR was less abundant than in QQ-MBR. OTU 5 (*Rhodobacter*), OTU 6 (*Cytophagaceae*) and OTU 10 (*Chloroflexi*) were similar between conventional-and QQ-MBRs in the biofilm.

In the third run, OTU 1 (*Thiothrix*), OTU 2 (*Tolomonas*) and OTU 3 (*Chloroflexi*) were more abundant in vacant-MBR than in QQ-MBR, while OTU 4 (*Haliscomenobacter*), OTU 6 (*Rhodobacter*), OTU 7 (*Pseudomonas*), OTU 8 (*Dokdonella*), OTU 9 (*Gp4*) and OTU 10 (*Nitrospira*) in vacant-MBR were less abundant than in QQ-MBR. The relative abundances of OTU 5 (*Cytophagaceae*) were similar between vacant-and QQ-MBR in the biofilm.

In the fourth run, OTU 1 (*Thiothrix*), OTU 2 (*Sphingomonadaceae*), OTU 6 (*Chloroflexi*) and OTU 10 (*Parachlamydiaceae*) were more abundant in vacant-MBR than in QQ-MBR, while OTU 3 (*Nitrospira*), OTU 4 (*Rhodobacter*), OTU 5 (*Chloroflexi*), OTU 7 (*Rhodocyclaceae*) and OTU 9 (*Ferruginibacter*) in vacant-MBR were less abundant than in QQ-MBR. The relative abundance of OTU 8 (*Geminicoccus*) was similar between vacant-and QQ-MBRs in the biofilm.

The average relative abundance of *Thiothrix* sp. in conventional- and vacant-MBRs was higher than that of the QQ-MBR in the biofilm. *Thiothrix* are filamentous, colorless and sulfur-oxidizing bacteria that may form rosettes and gonidia and deposit sulfur when grown in the presence of sulfide or thiosulphate

(Williams and Unz 1985). They were found to be principal bacterial components of aquatic biofilms causing biofouling in selected municipal water storage tanks, private wells, and drip irrigation systems (Brigmon et al. 1997). It was observed as the dominant population in biocake in the laboratory-scale A/O MBRs (Gao et al. 2014a). They reported that it could secrete the extracellular polymers in the infancy of the membrane fouling because it is a filamentous microbe. It is not clear whether *Thiothrix* sp. produces the signal molecules for the quorum sensing or not. It was reported that a member of *Thiothrix* has the *LuxR* homolog for the detection of AHLs without *LuxI* (BioProject: PRJNA51139) for the synthesis of the signal molecules. Diggle et al (2007) reported that the AHLs produced by other bacteria could have an effect on the bacteria that detect AHLs but do not produce, using a *Pseudomonas aeruginosa* mutant (PAO1 *lecA::luxΔlasI*). They showed that the addition of AHLs increased the population of the *P. aeruginosa* mutant. Thus, we speculate that *Thiothrix* populations could be affected by the QQ because its members might possess the *LuxR* homolog gene.

*Rhodobacter* has the ability to remove nitrogen (Hiraishi et al. 1995) and has been shown to control cellular aggregation based on QS (Puskas et al. 1997). They reported that the floc size was decreased by QS. However, the average relative composition of *Rhodobacter* sp. in the QQ-MBR decreased in the first and second runs, while it was increased in the third and fourth runs. The role of the QS system in *Rhodobacter* sp. is not yet fully elucidated in the biofilm, and it is not clear that the QS system controls the biofilm growth.

Previous studies reported that *Pseudomonas* spp. produce AHL signal

molecules (Fekete et al. 2010; Venturi 2006). However, *Pseudomonas* was more abundant in the QQ-MBR than in the vacant-MBR in the third run. Many signal molecules (i.e., *N*-acylhomoserine lactones (AHL or AI-1), autoinducer-2 (AI-2), autoinducer-3 (AI-3), cholerae autoinducer-1 (CAI-1), pseudomonas quinolone signal (PQS) and autoinducer peptides (AIP)) are involved in bacterial quorum sensing systems (Zhu and Li 2012) and *Pseudomonas* spp. produce AHLs as well as *Pseudomonas* Quinolone Signal (PQS). It has been reported that PQS is involved in biofilm formation (Spoering and Gilmore 2006). Thus, the abundance of *Pseudomonas* sp. in QQ-MBR suggested that there was another signal molecule (e.g., PQS) involved in the biofilm formation of *Pseudomonas*.

Some bacteria (e.g. *Haliscomenobacter* sp., *Dokdonella* sp., *Nitrospira* sp., and *Lactococcus* sp.) remained or increased in abundance in the QQ-MBR. Many kinds of signal molecules are involved in bacterial quorum sensing systems, and microbes without quorum sensing systems may exist in biofilm.

**Table III-3. Average relative composition (%) of dominant bacteria in biofilm.**

Run1				Run2		
OTU No.	Classification	Conventional-MBR	QQ-MBR	Classification	Conventional-MBR	QQ-MBR
1	<i>Thiothrix</i>	27.6±6.9	23.3±1.5	<i>Thiothrix</i>	24.8±4.5	19.7±5.9
2	<i>Rhodobacter</i>	3.2±0.6	2.3±0.5	<i>Chloroflexi*</i>	4.5±0.7	2.6±0.3
3	<i>unclassified*</i>	6.3±2.1	2.6±2.2	<i>Bacteroidetes*</i>	5.9±1.1	2.3±0.6
4	<i>unclassified*</i>	4.1±1.2	4.2±0.5	<i>Haliscomenobacter</i>	3.3±0.8	4.1±0.7
5	<i>Dokdonella</i>	2.9±1.3	4.0±0.4	<i>Rhodobacter</i>	2.1±0.6	2.2±0.4
6	<i>Chloroflexi*</i>	1.5±1.0	1.6±0.7	<i>Cytophagaceae*</i>	2.3±0.6	2.7±1.9
7	<i>Sphingobacteriales*</i>	1.6±0.7	2.7±0.5	<i>unclassified*</i>	3.0±0.6	2.1±0.9
8	<i>Gp4*</i>	1.9±0.4	1.6±0.4	<i>Lactococcus</i>	1.4±0.8	3.7±1.9
9	<i>Cytophagaceae*</i>	1.2±0.1	1.3±0.5	<i>Chlamydiales*</i>	2.6±1.7	0.5±0.3
10	<i>Nannocystineae*</i>	1.8±1.3	2.5±1.1	<i>Chloroflexi*</i>	1.5±0.1	1.3±0.1
Run3				Run4		
OTU No.	Classification	Vacant-MBR	QQ-MBR	Classification	Vacant-MBR	QQ-MBR
1	<i>Thiothrix</i>	12.1±4.2	6.9±4.2	<i>Thiothrix</i>	17.3±10.9	13.7±3.8
2	<i>Tolomonas</i>	8.6±13.0	1.1±1.4	<i>Sphingomonadaceae*</i>	19.9±13.0	6.5±2.1
3	<i>Chloroflexi*</i>	2.6±0.6	1.5±0.3	<i>Nitrospira</i>	2.0±1.2	2.4±0.3
4	<i>Haliscomenobacter</i>	1.6±1.6	3.7±0.7	<i>Rhodobacter</i>	1.7±0.9	2.0±0.1
5	<i>Cytophagaceae*</i>	2.5±1.0	2.3±1.6	<i>Chloroflexi*</i>	1.8±0.6	2.2±0.1
6	<i>Rhodobacter</i>	1.2±0.6	2.3±0.4	<i>Chloroflexi*</i>	2.4±1.9	0.9±0.4
7	<i>Pseudomonas</i>	1.9±0.5	3.8±0.8	<i>Rhodocyclaceae*</i>	1.3±0.2	2.2±0.9
8	<i>Dokdonella</i>	1.8±1.5	2.4±0.8	<i>Geminicoccus</i>	1.6±0.6	1.6±0.2
9	<i>Gp4*</i>	1.3±0.8	2.5±1.4	<i>Ferruginibacter</i>	1.2±0.6	1.7±0.5
10	<i>Nitrospira</i>	0.7±0.5	3.0±1.7	<i>Parachlamydiaceae*</i>	2.7±3.7	1.5±1.4

**OTU was classified at the genus level, and the asterisk indicates that the OTU was assigned at the taxonomic classification level.**

**Table III-4. Relative composition (%) of dominant bacteria in biofilm.**

OTU No.	Classification	Run1						Run2						
		Conventional-MBR			QQ-MBR			Classification	Conventional-MBR			QQ-MBR		
		TMP (kPa)							Time (d)					
		15	28	47	15	25	52		3	6	10	3	6	10
1	<i>Thiothrix</i>	30.6	19.6	32.4	23.1	21.9	24.8	<i>Thiothrix</i>	29.9	23.1	21.3	26.2	18.4	14.6
2	<i>Rhodobacter</i>	2.4	3.6	3.5	2.8	2.0	2.0	<i>Chloroflexi*</i>	4.0	4.3	5.2	2.7	2.3	2.7
3	<i>unclassified*</i>	7.7	7.2	3.9	5.0	2.1	0.7	<i>Bacteroidetes*</i>	6.3	6.8	4.6	1.8	2.9	2.0
4	<i>unclassified*</i>	2.7	4.7	4.9	3.8	4.2	4.7	<i>Haliscomenobacter</i>	2.5	4.1	3.3	3.4	4.8	4.0
5	<i>Dokdonella</i>	1.5	4.2	2.9	4.4	3.7	4.0	<i>Rhodobacter</i>	1.6	1.9	2.7	1.7	2.2	2.6
6	<i>Chloroflexi*</i>	0.7	1.1	2.6	1.2	1.2	2.5	<i>Cytophagaceae*</i>	1.6	2.4	2.8	1.2	2.3	4.8
7	<i>Sphingobacteriales*</i>	0.9	2.2	1.8	2.9	2.2	3.0	<i>unclassified*</i>	2.5	3.7	2.7	2.8	2.6	1.1
8	<i>Gp4*</i>	1.8	2.3	1.6	1.9	1.8	1.2	<i>Lactococcus</i>	0.9	1.0	2.3	3.3	2.1	5.9
9	<i>Cytophagaceae*</i>	1.2	1.3	1.2	1.7	1.6	0.7	<i>Chlamydiales*</i>	3.6	3.5	0.7	0.8	0.4	0.2
10	<i>Nannocystineae*</i>	0.4	2.2	2.9	1.3	2.8	3.4	<i>Chloroflexi*</i>	1.5	1.4	1.6	1.4	1.1	1.3

**OTU was classified at the genus level, and the asterisk indicates that the OTU was assigned at the taxonomic classification level.**

**Table III-4. (Continued).**

OTU No.	Classification	Run3						Run4						
		Vacant-MBR			QQ-MBR			Classification	Vacant-MBR			QQ-MBR		
		TMP (kPa)							Time (d)					
16	30	50	14	25	46	5	11		13	5	11	13		
1	<i>Thiothrix</i>	8.4	16.7	11.3	5.4	11.7	3.6	<i>Thiothrix</i>	24.9	22.1	4.8	15.9	15.8	9.3
2	<i>Tolomonas</i>	23.6	1.7	0.5	0.4	2.7	0.0	<i>Sphingomonadaceae*</i>	5.5	23.2	30.8	4.2	7.8	7.6
3	<i>Chloroflexi*</i>	1.9	2.8	3.1	1.8	1.5	1.2	<i>Nitrospira</i>	2.9	2.4	0.7	2.6	2.1	2.7
4	<i>Haliscomenobacter</i>	0.0	1.6	3.2	4.4	3.0	3.8	<i>Rhodobacter</i>	2.6	1.7	0.7	1.8	2.0	2.1
5	<i>Cytophagaceae*</i>	3.3	2.8	1.4	4.2	1.6	1.3	<i>Chloroflexi*</i>	2.3	1.9	1.1	2.3	2.1	2.2
6	<i>Rhodobacter</i>	0.5	1.4	1.7	2.1	2.0	2.7	<i>Chloroflexi*</i>	3.8	3.2	0.3	1.3	0.7	0.7
7	<i>Pseudomonas</i>	2.4	1.8	1.4	4.7	3.5	3.3	<i>Rhodocyclaceae*</i>	1.4	1.0	1.4	3.2	2.1	1.3
8	<i>Dokdonella</i>	0.4	1.7	3.4	3.3	1.9	1.9	<i>Geminicoccus</i>	1.9	2.0	0.9	1.7	1.6	1.4
9	<i>Gp4*</i>	0.5	1.3	2.1	4.0	2.1	1.4	<i>Ferruginibacter</i>	1.9	1.0	0.8	1.3	1.4	2.3
10	<i>Nitrospira</i>	0.4	0.4	1.3	1.6	2.4	4.9	<i>Parachlamydiaceae*</i>	1.1	0.1	7.0	3.0	1.4	0.2

OTU was classified at the genus level, and the asterisk indicates that the OTU was assigned at the taxonomic classification level.

### **III.4. Conclusions**

The effect of QQ on microbial community of biofilm was investigated in an A/O MBR. The following conclusions could be drawn:

- Although the relative activity of QQ-beads was decreased, biofouling was mitigated substantially by QQ-beads. The TMP rise-up in QQ-MBRs was delayed by approximately 100~110% compared with conventional-and vacant-MBR.

- The QQ had an effect on the microbial community and reduced the variation of the bacterial composition in biofilm.



## Chapter IV

# QQ Effect on the Microbial Community of Activated Sludge in an Anoxic-Oxic MBR



## IV.1. Introduction

A few studies have reported that the acylase as a QQ enzyme had effect on the development of microbial community in biofilm in a lab-scale MBR (a 2.5-L reactor with a hollow fiber membrane), but it did not affect the microbial community structure of activated sludge (Kim et al. 2013a). It is logical that QQ agents can affect microbial community structure in activated sludge processes where they are applied since they interfere with interactions among microorganisms within the microbial community. Thus, it is necessary to study the effect of QQ on activated sludge processes because it is possible that they adversely affect MBR performance and/or activated sludge microbial consortium.

Nutrient removal such as organic pollutants, nitrogen and phosphorous is an important priority for wastewater treatment (Singh and Thomas 2012), However, most of previous studies were focused on the removal of organic pollutants in an aerobic QQ-MBR (Jiang et al. 2013; Kim et al. 2013b; Maqbool et al. 2015; Weerasekara et al. 2014), but neglected the removal of nitrogen Therefore, nitrogen removal performance must be taken into account for the evaluation of QQ as a biological agent.

Network analysis based on co-occurrence and correlation patterns has been applied to examine the complex microbial community within the system (Faust and Raes 2012, Fuhrman 2009). It offers new insight into the structure of complex microbial communities, insight that complements and expands on the information provided by the more analytical approaches (Barberán et al. 2012). Faust and Raes (2012) suggested that it can predict the outcome of community

changes and the effects of perturbations, and thus, they could eventually help to engineer complex microbial communities. The main objectives of this study were to determine the effects of QQ on the microbial community in activated sludge. These results provide useful information to apply QQ strategy in full-scale MBRs.

## **IV.2. Materials and methods**

### **IV.2.1. Analytical methods**

The concentration of MLSS, floc size, soluble COD, total nitrogen (TN), DO and pH in activated sludge were measured at 1, 5, 12, 19, 26, 33, 40, 47, 54, 61, 68, 75, 82, 89 and 91 days. The concentration of MLSS was measured in duplicate by standard methods (APHA et al. 2005). The COD, TN, DO and pH were measured as described above. The mean particle size of activated sludge was measured in triplicate by MICROTRAC S3500.

### **IV.2.2. Sampling for analysis of microbial community in activated sludge**

The sampling time of activated sludge was determined according to the sampling time of biofilm in each MBR. To detect the QQ bacteria (*Rhodococcus* sp. BH4) in QQ-bead, 10 QQ-beads were collected at 0 (initial) and vigorously rinsed with D.I. water to remove debris and excess cells. As soon as finished sampling, DNA extracted from all samples. Remained samples were stored in deep-freezer at -80 °C.

### **IV.2.3. DNA extraction, PCR amplification and Miseq platform sequencing**

The sample prepared as follows for DNA extraction. 2 or 3 QQ-beads were cut into small pieces (1 mm x 1mm). The 1.5 ml of activated sludge was

harvested by centrifugation (10,000 g, 1 min, 25 °C) and the pellet was resuspended in 0.5 ml of DI water. DNA was extracted using the NucleoSpin Soil kit (Macherey-Nagel GmbH, Düren, Germany). DNA was eluted in 100 µl of the elution buffer. DNA was quantified using the ND-1000 spectrophotometer (Nanodrop Inc., Wilmington, DE, USA). Each sequenced sample is prepared as described above.

#### **IV.2.4. Data analysis for bacterial community**

Sequencing data were trimmed and analyzed as described above. The average nucleotide length was 412 bp for the bacterial libraries. Chimeric sequences were removed using the Uchime function with the abundant sequences as reference. All of sequences classified using SILVA reference library. The sequencing reads obtained in this study were deposited into DNA data Bank of Japan (DDBJ) Sequence Read Archive (<http://trace.ddbj.nig.ac.jp/dra>) under accession no. DRA004065.

For community analysis, OTUs (operational taxonomic units)-based approaches was conducted using the Mothur. OTUs were determined at 3 % dissimilarity. Each read was taxonomically assigned at the genus level with bootstrap values more than 80% resulting in taxonomic classification from phylum to genus. A total 1,623,329 effective sequences were obtained after the cleaning of raw reads. To detect the QQ bacteria in activated sludge, sequencing data of initial QQ-bead (1 sample) with activated sludge of oxic tank in QQ-MBR (12 samples) were analyzed as above. A total 410,708 effective sequences were obtained after

the cleaning of raw reads.

#### **IV.2.5. Network analysis**

Associations among the relative abundances of bacterial OTUs were calculated using extended local similarity analysis (Xia et al. 2011). Only bacterial OTUs which have the average of relative abundance  $\geq 0.15\%$  in all of activated sludge samples were chosen. The analysis was performed with a 2-time lag as a delay option. OTU was classified at the genus level, and the asterisk indicates that the OTU was assigned at the taxonomic classification level. A connection indicates a positive local similarity score if LS (local similarity score)  $> 0.75$  and negative local similarity score if LS  $< -0.75$ . Microbial associations were visualized from local similarity scores, and their  $p$  values were determined using the Cytoscape program version 3.2.1 (Shannon et al. 2003). Nonsignificant associations (edge) with  $p \geq 0.05$  were excluded. The shape of node was circle. Node size indicates the relative abundance of each OTU. The red color of the nodes indicates the number of connections to the nodes. Solid edges are positive associations, and dashed edges are negative associations. Arrow indicates time-delay direction. Network topology characteristics were examined using Network Analyzer tool (Assenov et al.2008).

## **IV.2.6. Prediction of metabolic pathway**

To predict the metabolic pathway from microbial community, the OTU table was constructed using the Mothur, and all of sequences classified using Greengenes reference library. The resulting OTU table was then fed into PICRUSt version 1.0.0 (Langille et al. 2013). The analysis of PICRUSt was processed in Qiime version 1.8.0 (Caporaso et al. 2010). Functional predictions were made according to the metagenome inference workflow described by the developers (<http://picrust.github.com/picrust/tutorials/quickstart.html#quickstartguide>).

PICRUSt results were analyzed using HUMAnN (The HMP Unified Metabolic Analysis Network) version 0.99 (Abubucker et al. 2012). HUMAnN is a pipeline for efficiently and accurately determining the presence/absence and abundance of microbial pathways in a community from metagenomic data. It takes gene abundances as inputs and produces summaries of gene and pathway as outputs. The results of HUMAnN were then fed into the linear discriminant analysis (LDA) effect size (LEfSe) (Segata et al. 2011). The analysis of LEfSe was conducted in the Galxy framework. For the LEfSe, the dataset was constructed according to the levels described in Figure IV-1. Threshold on the logarithmic LDA score for discriminative features was used at  $\log_{10} 2.0$ .

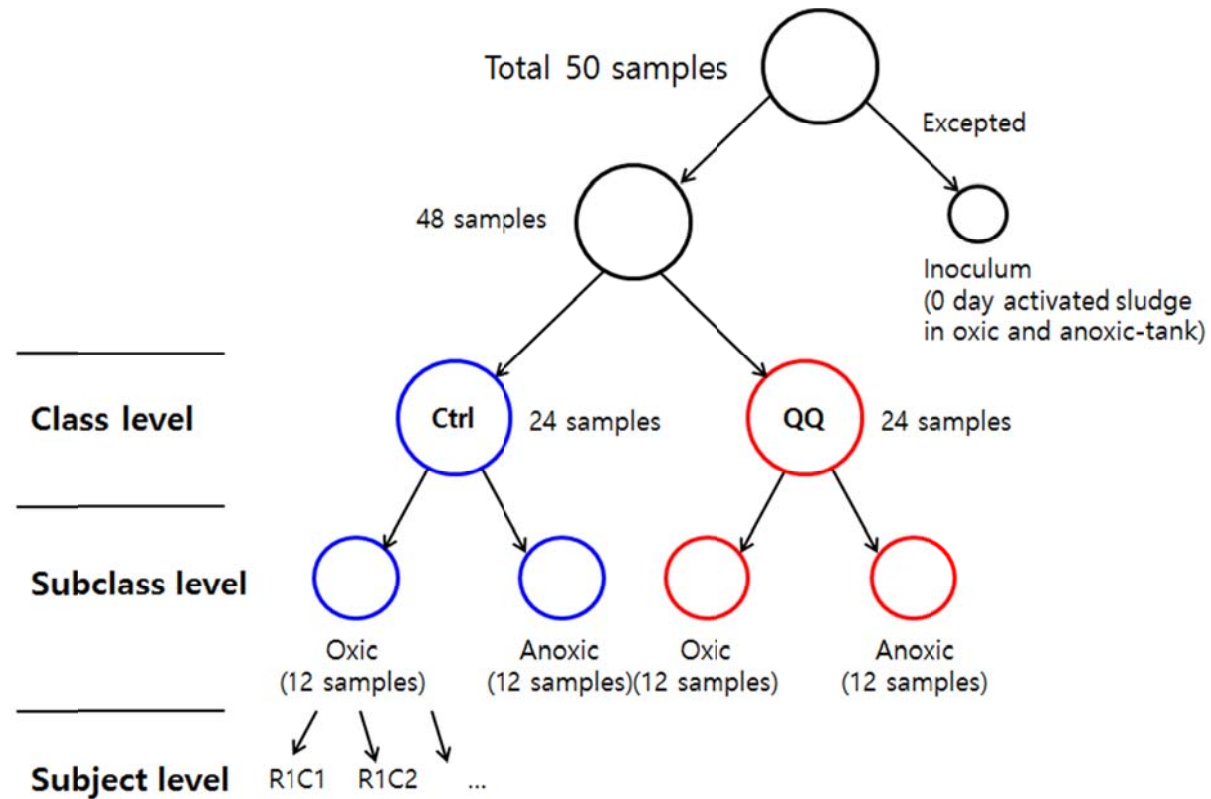


**Figure IV-1. The data set for the LEfSe. The activated samples were designated as R1C1, R1C2... in subject level. These samples were collected at the same time of biofilm sample in Chapter III.**

### IV.2.7. Statistical analysis

The statistical analysis was carried out in the R environment ([www.r-project.org](http://www.r-project.org)). The values of community diversity (i.e., Chao 1 richness, Shannon diversity and Shannon evenness) and environmental factors (i.e., COD, TN removal efficiency, floc size and concentration of MLSS) were divided into control- and QQ-MBR. The differences of community diversity and environmental factor between control- and QQ-MBR were analyzed using t-test. The Pearson correlation between the relative composition of *Thiothrix* sp. and approximate floc size was analyzed to elucidate the relation between relative composition of *Thiothrix* sp. and the floc size. The value of approximate floc size was interpolated by averaging its values of before and after the sample's sampling time because some samples did not have floc size data at the same sampling time. The absolute value of the Pearson correlation coefficient greater than 0.5 ( $p < 0.05$ ) was considered significant in this study. The statistical analysis was carried out in the R environment ([www.r-project.org](http://www.r-project.org)).

## IV.3. Results and discussion

### IV.3.1. Performance of the A/O MBR with QQ

Nutrient removal is an important priority for the pollutant degradation in wastewater treatment systems. Therefore, the microbial system of activated sludge should be elucidated to understand the process and its technological aspects better in the QQ-MBR. This study used 16 rRNA-based high-throughput sequencing and various community analysis methods, including network analysis, to investigate the response of a microbial community of activated sludge to the application of QQ in the A/O MBR.

The relative QQ-activity, defined by the degradation ratio of standard C8-HSL for 120 min in the presence of used QQ-beads from the A/O MBR, was monitored against the operating time. The viability of *Rhodococcus* sp. BH4 as a QQ bacterium was shown to be stable during MBR operation because the relative activity of QQ-beads was decreased by only 10% of their initial degree during 91 days (Figure III-2). Also, the spill of *Rhodococcus* sp. BH4 from QQ-bead was monitored by detecting its partial 16S rDNA gene in activated sludge: it was not detected in activated sludge in the QQ-MBR (Table IV-1). It was speculated that QQ-bacteria, BH4 might not adapt well in the activated sludge since BH4 strain was not detected in activated sludge of QQ-MBR during 91days. Thus, it was confirmed that the microbial community of activated sludge is less likely to be affected by the growth of BH4 in the QQ-MBR.

**Table IV-1. The detection of *Rhodococcus* sp BH4 in quorum quenching (QQ)-bead and activated sludge in the oxic tank during QQ-MBR operation. Operational taxonomic units (OTUs) were determined at 3 % dissimilarity. OTUs were classified at the genus level.**

	QQ-bead	Activated sludge of oxic tank in QQ-MBR											
	Initial (0 days)	11 days	20 days	29 days	34 days	37 days	41 days	60 days	72 days	78 days	83 days	89 days	91 days
<i>Rhodococcus</i> sp. BH4	85.4%	n.d.	n.d.	n.d.	0.0%	n.d.							

*Abbreviations:* n. d.; not detected.

The removal efficiency of total COD and nitrogen are shown in Figure IV-1 and IV-4 (a, b). The variation of removal efficiency of COD and nitrogen was observed during operation period (IV-2). The removal efficiency of COD was  $99 \pm 1\%$  and nitrogen was  $78 \pm 5\%$  (IV-5 (a, b)). The results of statistical analysis (t-test) indicated that there were no significant difference of COD and nitrogen removal between control-MBR and QQ-MBR. These performances did not differ between the control-MBR and QQ-MBR.

The concentrations of MLSS in oxic and anoxic tank are shown in Figure IV-3 and IV-5 (c, d). The variation of MLSS was observed during operation period (IV-3). The concentration of control-MBR was  $8159 \pm 882$  mg/L and that of QQ-MBR was  $8238 \pm 839$  mg/L in the oxic tank (IV-5 (c)). The concentration of control-MBR was  $6498 \pm 922$  mg/L and that of QQ-MBR was  $6311 \pm 654$  mg/L in the anoxic tank (IV-5 (d)). These results were similar to that of previous studies using QQ-beads. Kim et al. (2013b) and Maqbool et al. (2015) reported that QQ-MBR had similar effluent COD concentration to control-MBR. Lee et al. (2016) reported no significant differences of COD and nitrogen in three stages MBR (anoxic-oxic-membrane tank). They also reported that the concentration of MLSS in QQ-MBR was similar to control-MBR.

The average floc size of oxic and anoxic tank is shown in Figure IV-4 and IV-5 (e, f). The variation of floc size was observed during operation period (IV-4). The floc size between control- and QQ-MBR was significantly different in both oxic and anoxic tank ( $p < 0.05$ ). The floc size of control-MBR was  $319 \pm 40$   $\mu\text{m}$  and that of QQ-MBR was  $293 \pm 39$   $\mu\text{m}$  in the oxic tank (IV-5 (e)).

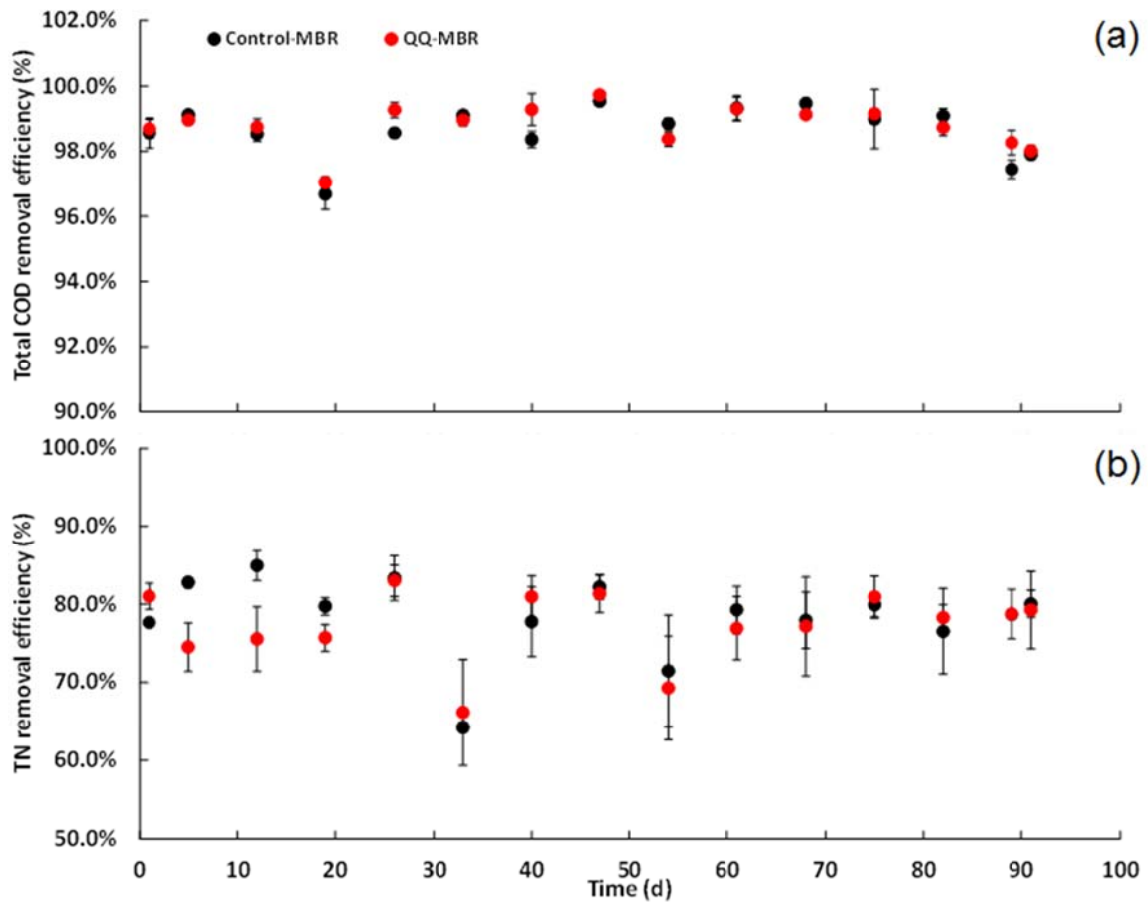


Figure IV-2. Time profiles of total COD removal efficiency (a) and total nitrogen removal efficiency (b). Error bar: standard deviation (n =2).

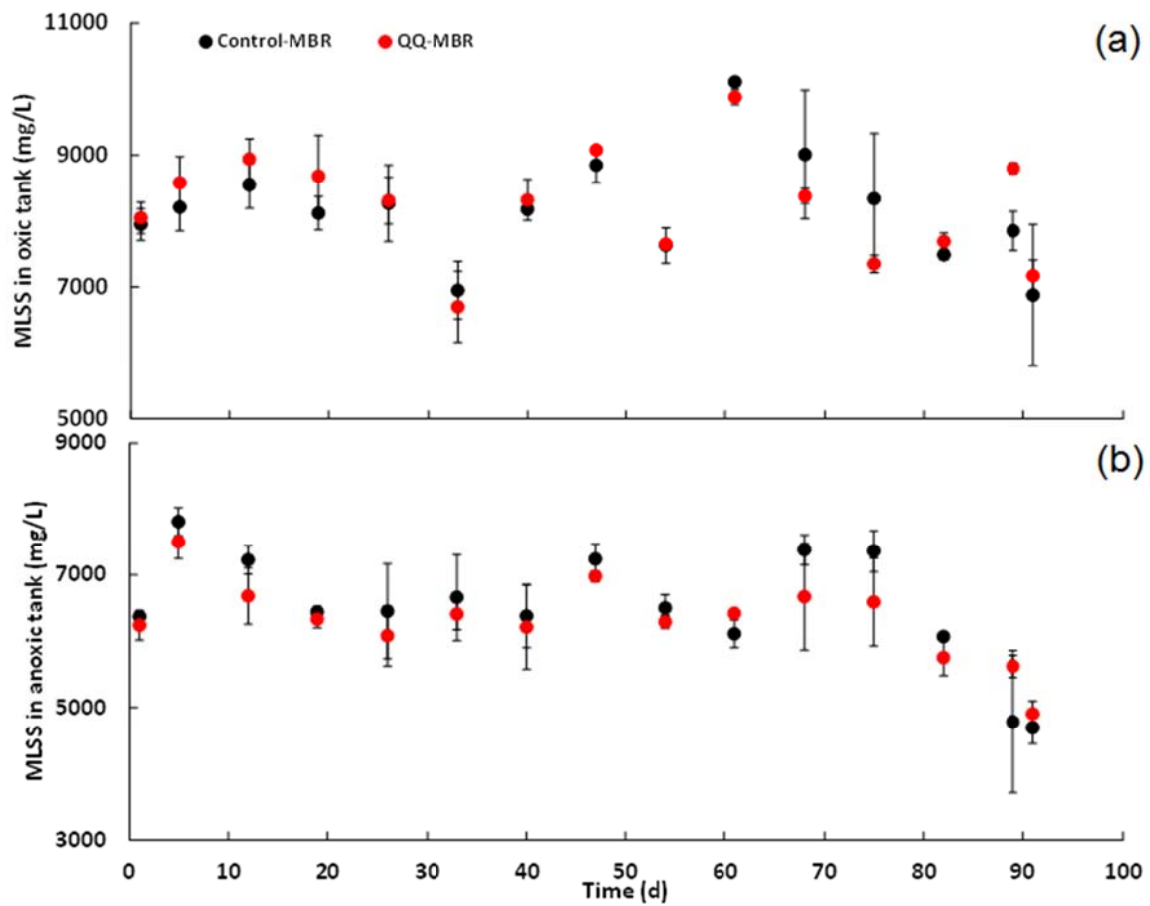


Figure IV-3. Time profiles of MLSS in oxic tank (a) and MLSS in anoxic tank (b). Error bar: standard deviation (n = 2).

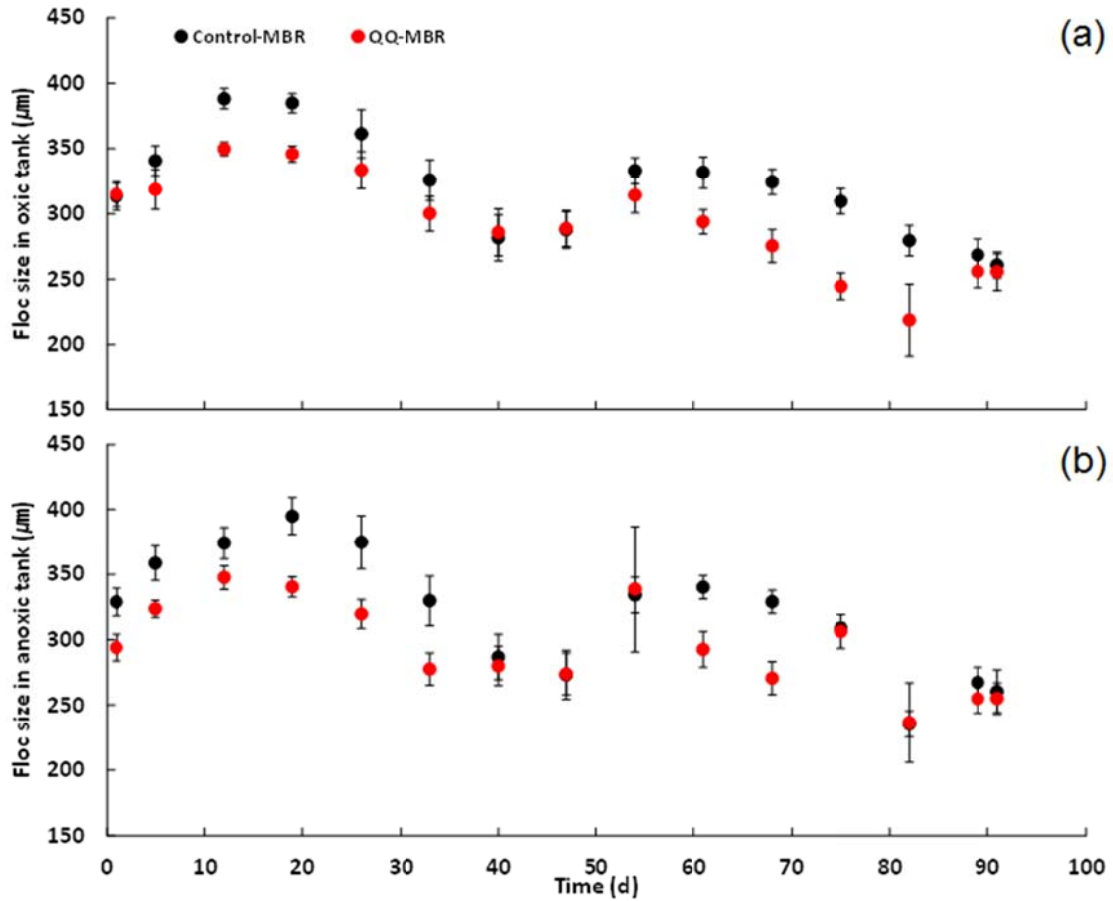


Figure IV-4. Time profiles of floc size in oxic tank (a) and floc size in anoxic tank (b). Error bar: standard deviation ( $n = 3$ ).

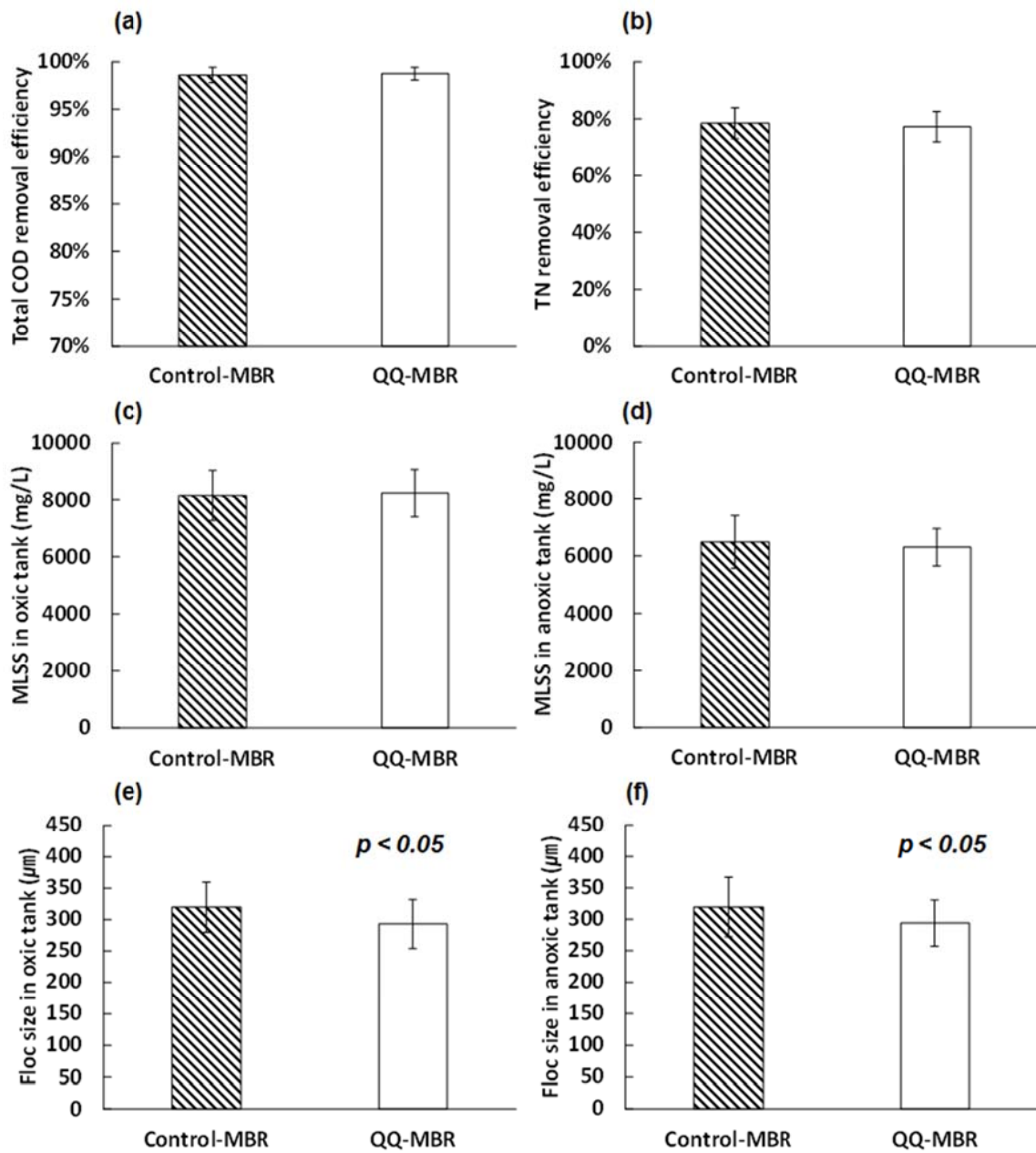


Figure IV-5. Comparison of total COD removal efficiency (a), total nitrogen removal efficiency (b), MLSS in membrane tank (c) and anoxic tank (d), and floc size in membrane tank (e) and anoxic tank (f). Error bar: standard deviation (n = 30 and n=45 for floc size).

The average floc size of control-MBR was  $320 \pm 47 \mu\text{m}$  and that of QQ-MBR was  $294 \pm 37 \mu\text{m}$  in the anoxic tank (IV-5 (f)). Thus, these results indicated that QQ had not affected the function of activated sludge for nutrient removal and biomass, while it decreased the floc size of activated sludge during the MBR operation. It was speculated that the EPS in activated sludge was decreased by the effect of QQ. Jiang et al. (2013) reported that the size of the activated sludge floc and EPS (extracellular polymeric substances) in activated sludge was decreased by enzymatic quorum quenching. However, discrepancies have been found among several different reports about the QQ effects on floc size. Lee et al. (2016) reported that no significant difference of the average floc size between QQ-MBR and non QQ-MBR was observed in the three-stage MBR (anoxic-oxic-membrane tank). They speculated that the main reason of this result was the mechanical split of activated sludge by the recirculation pumping device. However, the significant difference of floc size between control-and QQ-MBR was observed. Thus, it was speculated that usage of peristaltic pump and slow flow rate might have caused different results from the previous study.

### IV.3.2. Microbial composition in the A/O MBR with QQ

The average relative abundances of bacteria species are listed in Table IV-2 and specific relative abundances of bacteria species are listed in Table IV-3 and 4. The top 20 OTUs comprised a least 42.8% of each community. These bacteria generally existed in the control and QQ-MBR. In the inoculum of oxic and anoxic tank, OTU 1 (*Thiothrix*, 27.1 ~ 27.5%), OTU 2 (*Chloroflexi*, 4.2 ~ 4.6%), OTU 3 (*Rhodobacter*, 6.8 ~ 8.4%), OTU 4 (*Cytophagaceae*, 4.3 ~ 4.6%) and OTU 14 (*Sphingobacteriales*, 4.3 ~ 4.6%) were more abundant than other bacteria species. In the oxic tank, OTU 1 (*Thiothrix*, 21.8%), OTU 2 (*Chloroflexi*, 7.0%), OTU 3 (*Rhodobacter*, 4.9 %), OTU 4 (*Cytophagaceae*, 2.9%) and OTU 5 (*Sphingomonadaceae*, 3.8%) were relatively dominant bacteria species in the control-MBR and OTU 1 (*Thiothrix*, 17.3%), OTU 2 (*Chloroflexi*, 5.0%), OTU 3 (*Rhodobacter*, 4.7 %), OTU 4 (*Cytophagaceae*, 2.5%) and OTU 5 (*Sphingomonadaceae*, 1.8%) were relatively dominant bacteria species in the QQ-MBR. In the anoxic tank, OTU 1 (*Thiothrix*, 20.4%), OTU 2 (*Chloroflexi*, 7.0%), OTU 3 (*Rhodobacter*, 5.0 %), OTU 4 (*Cytophagaceae*, 2.8%) and OTU 5 (*Sphingomonadaceae*, 3.6%) were relatively dominant bacteria species in the control-MBR and OTU 1 (*Thiothrix*, 17.9%), OTU 2 (*Chloroflexi*, 5.1%), OTU 3 (*Rhodobacter*, 4.1%), OTU 4 (*Cytophagaceae*, 2.3%) and OTU 5 (*Sphingomonadaceae*, 1.7%) were relatively dominant bacteria species in the QQ-MBR.

**Table IV-2. Average bacterial compositions at the species level. Operational taxonomic units (OTUs) were determined at 3 % dissimilarity. OTUs were classified at the genus level.**

OTU No.	Classification	Inoculum in oxic tank	Inoculum in anoxic tank	Oxic tank		Anoxic tank	
				Control-MBR	QQ-MBR	Control-MBR	QQ-MBR
1	<i>Thiothrix</i>	27.1	27.5	21.8 ± 10.4	17.3 ± 6.4	20.4 ± 10.4	17.9 ± 7.3
2	<i>Chloroflexi</i> *	4.2	4.6	7.0 ± 2.9	5.0 ± 2.7	7.0 ± 3.0	5.1 ± 2.7
3	<i>Rhodobacter</i>	8.4	6.8	4.9 ± 1.5	4.7 ± 1.9	5.0 ± 1.9	4.1 ± 1.0
4	<i>Cytophagaceae</i> *	4.6	4.3	2.9 ± 1.7	2.5 ± 1.2	2.8 ± 1.7	2.3 ± 1.1
5	<i>Sphingomonadaceae</i> *	0.1	0.1	3.8 ± 8.2	1.8 ± 2.9	3.6 ± 7.5	1.7 ± 2.9
6	<i>Rhodocyclaceae</i> *	2.4	3.0	2.5 ± 1.4	2.1 ± 1.5	2.5 ± 1.4	2.2 ± 1.5
7	<i>Haliscomenobacter</i>	0.0	0.0	2.2 ± 2.1	2.5 ± 1.6	2.2 ± 2.1	2.3 ± 1.6
8	<i>Chloroflexi</i> *	1.5	1.5	1.8 ± 0.5	2.1 ± 0.6	1.9 ± 0.5	2.1 ± 0.6
9	<i>Nitrospira</i>	1.8	1.8	1.6 ± 1.0	1.9 ± 0.9	1.6 ± 1.0	2.0 ± 1.1
10	<i>Gp4</i> *	1.9	2.0	1.4 ± 0.6	2.0 ± 0.5	1.6 ± 0.6	1.8 ± 0.5
11	<i>Ferruginibacter</i>	1.8	1.7	1.6 ± 0.7	1.7 ± 0.5	1.5 ± 0.6	1.6 ± 0.5
12	<i>Dokdonella</i>	1.8	1.9	1.5 ± 0.4	1.5 ± 0.5	1.5 ± 0.4	1.5 ± 0.5
13	<i>Rhodocyclaceae</i> *	0.0	0.0	1.3 ± 1.0	1.5 ± 1.4	1.2 ± 1.0	1.5 ± 1.4
14	<i>Sphingobacteriales</i> *	4.6	4.3	1.1 ± 1.3	0.9 ± 1.1	1.1 ± 1.2	0.9 ± 1.0
15	<i>Zoogloea</i>	0.1	0.1	1.0 ± 1.2	1.3 ± 0.8	1.2 ± 1.2	1.4 ± 1.0
16	<i>Defluviicoccus</i>	1.1	1.2	0.7 ± 0.4	1.4 ± 0.7	0.7 ± 0.4	1.6 ± 0.7
17	<i>Chloroflexi</i> *	0.5	0.4	0.8 ± 0.3	1.4 ± 0.7	0.8 ± 0.3	1.4 ± 0.7
18	<i>Rhodocyclaceae</i> *	0.6	0.7	1.2 ± 1.0	0.9 ± 0.6	1.2 ± 0.9	0.9 ± 0.6
19	<i>Bacteroidetes</i> *	0.7	0.6	0.9 ± 0.7	1.0 ± 1.0	1.0 ± 0.9	0.9 ± 0.9
20	<i>Geminicoccus</i>	0.7	0.8	0.9 ± 0.8	1.1 ± 0.7	0.8 ± 0.7	1.2 ± 0.8

The asterisk indicates that the OTU was assigned at the taxonomic classification level such as family, order, class and phylum.

**Table IV-3. Bacterial compositions at the species level in oxic tank. Operational taxonomic units (OTUs) were determined at 3 % dissimilarity. OTUs were classified at the genus level, and the asterisk indicates that the OTU was assigned at the taxonomic classification level.**

OTU	Inoculum	C1	C2	C3	C4	C5	C6	C7	C8	C9	C10	C11	C12	Q1	Q2	Q3	Q4	Q5	Q6	Q7	Q8	Q9	Q10	Q11	Q12
OTU 1 ( <i>Thiothrix</i> )	27.1	34.5	36.1	25.4	31.9	26.4	24.8	20.9	17.1	16.9	19.4	5.6	2.4	27.2	24.7	22.8	22.0	20.4	17.9	19.3	10.0	9.3	12.9	11.8	9.2
OTU 2 ( <i>Chloroflexi</i> *)	4.2	5.7	6.7	7.6	8.5	8.5	9.4	8.7	9.6	10.4	5.6	2.0	1.1	6.9	4.4	6.8	7.5	8.4	8.2	4.9	5.1	3.3	2.0	1.4	0.7
OTU 3 ( <i>Rhodobacter</i> )	8.4	7.3	4.4	7.2	5.4	5.3	6.4	5.1	3.3	2.4	4.3	4.4	3.3	9.9	5.9	5.5	5.7	3.8	4.1	3.7	4.7	3.2	3.2	3.0	3.2
OTU 4 ( <i>Cytophagaceae</i> *)	4.6	3.9	2.9	3.3	2.3	3.2	4.1	5.3	4.6	3.8	0.8	0.2	0.0	3.6	3.3	2.9	3.2	2.7	3.8	4.0	2.4	1.6	1.3	0.8	0.3
OTU 5 ( <i>Sphingomonadaceae</i> *)	0.1	0.1	0.1	0.1	0.1	0.1	0.1	0.2	0.1	0.1	3.8	14.5	26.0	0.1	0.1	0.1	0.1	0.1	0.1	0.1	0.6	1.8	3.1	6.9	8.6
OTU 6 ( <i>Rhodocyclaceae</i> *)	2.4	2.8	3.6	3.4	3.3	3.5	2.8	4.2	2.9	2.2	0.3	0.3	0.2	3.4	4.0	3.6	2.5	3.3	2.9	3.3	1.2	0.6	0.5	0.3	0.2
OTU 7 ( <i>Haliscomenobacter</i> )	0.0	0.0	0.1	0.2	2.6	3.4	2.9	3.6	4.6	6.2	1.8	0.4	0.1	0.1	0.6	2.7	4.2	4.1	3.2	4.9	3.7	2.9	2.0	1.1	0.3
OTU 8 ( <i>Chloroflexi</i> *)	1.5	1.1	1.5	1.6	2.0	1.8	2.1	1.4	1.5	1.2	2.9	2.2	2.4	2.2	1.9	1.9	1.7	1.5	1.5	1.8	2.6	3.5	3.3	2.2	2.2
OTU 9 ( <i>Nitrospira</i> )	1.8	0.9	0.5	1.5	1.3	1.0	1.0	1.1	1.6	1.2	2.2	4.0	2.8	1.4	1.7	0.9	1.2	0.8	1.3	2.4	2.0	2.3	3.4	2.6	3.4
OTU 10 ( <i>Gp4</i> *)	1.9	2.1	2.3	2.4	0.9	1.0	1.2	1.1	1.3	1.4	1.5	0.6	0.6	2.5	1.2	2.0	1.6	1.5	1.8	1.9	2.7	2.9	2.3	1.5	1.5
OTU 11 ( <i>Ferruginibacter</i> )	1.8	1.2	1.2	1.5	0.7	0.7	0.8	1.5	1.8	2.0	2.8	2.6	1.9	1.3	1.5	1.1	1.0	1.2	1.8	1.9	1.9	1.6	1.8	2.4	2.7
OTU 12 ( <i>Dokdonella</i> )	1.8	1.9	2.0	2.3	1.9	1.8	1.4	1.2	1.0	1.4	1.2	1.3	1.2	2.2	2.4	2.2	1.5	1.9	1.8	1.3	1.2	1.0	1.0	0.8	1.1
OTU 13 ( <i>Rhodocyclaceae</i> *)	0.0	0.0	0.1	0.1	0.4	0.4	1.0	1.3	2.1	2.3	2.3	2.4	2.5	0.1	0.1	0.3	0.3	0.5	0.7	1.4	3.5	3.4	3.8	2.2	1.9
OTU 14 ( <i>Sphingobacteriales</i> *)	4.6	3.6	2.3	3.4	0.8	0.8	0.4	0.4	0.3	0.3	0.4	0.2	0.1	3.1	2.8	1.7	0.9	0.9	0.6	0.3	0.3	0.3	0.2	0.1	0.1
OTU 15 ( <i>Zoogloea</i> )	0.1	0.2	0.7	0.9	0.3	0.4	0.3	2.0	2.7	3.7	0.2	0.3	0.1	0.1	0.9	1.6	1.4	2.7	2.0	1.7	2.3	1.3	0.4	0.7	0.5
OTU 16 ( <i>Defluviicoccus</i> )	1.1	0.4	0.2	0.8	0.7	0.6	0.5	0.7	0.6	0.3	0.8	1.8	1.3	0.5	1.5	1.1	1.2	0.5	0.7	1.7	1.4	1.6	1.9	1.9	3.0
OTU 17 ( <i>Chloroflexi</i> *)	0.5	0.4	0.6	0.6	0.7	0.6	1.0	0.7	1.0	0.6	1.7	0.9	0.9	0.7	0.7	0.9	0.9	1.0	1.2	1.0	1.3	2.1	2.2	2.7	1.7
OTU 18 ( <i>Rhodocyclaceae</i> *)	0.6	0.6	0.5	0.6	1.3	1.8	1.3	2.0	2.3	3.5	0.5	0.3	0.2	0.6	0.6	1.0	1.0	1.6	1.4	2.0	1.4	0.5	0.3	0.3	0.2
OTU 19 ( <i>Bacteroidetes</i> *)	0.7	0.9	0.9	1.7	1.3	2.3	1.7	1.0	0.7	0.6	0.0	0.0	0.0	0.7	1.2	1.7	2.5	2.4	2.3	0.4	0.7	0.1	0.0	0.0	0.0
OTU 20 ( <i>Geminicoccus</i> )	0.7	0.5	0.3	0.4	0.6	0.6	0.6	0.7	0.6	0.2	2.1	2.1	2.3	0.5	1.3	0.4	0.5	0.2	0.6	1.0	1.2	1.3	2.2	2.4	1.9

**Table IV-4. Bacterial compositions at the species level in anoxic tank. Operational taxonomic units (OTUs) were determined at 3 % dissimilarity. OTUs were classified at the genus level, and the asterisk indicates that the OTU was assigned at the taxonomic classification level.**

OTU	Inoculum	C1	C2	C3	C4	C5	C6	C7	C8	C9	C10	C11	C12	Q1	Q2	Q3	Q4	Q5	Q6	Q7	Q8	Q9	Q10	Q11	Q12
OTU 1 ( <i>Thiothrix</i> )	27.5	32.3	38.0	27.3	26.8	15.7	24.9	18.7	15.4	17.9	20.6	4.3	2.4	33.4	22.6	21.1	23.7	21.2	22.0	15.1	11.2	11.0	13.5	9.9	9.6
OTU 2 ( <i>Chloroflexi</i> *)	4.6	5.3	6.2	7.3	9.4	9.0	8.4	9.2	9.5	10.5	5.6	2.2	1.2	6.4	5.0	7.2	7.2	8.0	6.6	8.6	4.9	2.9	2.0	1.4	0.8
OTU 3 ( <i>Rhodobacter</i> )	6.8	7.0	4.7	8.6	7.0	2.7	5.9	5.6	3.3	3.1	4.0	4.8	3.1	5.0	6.0	4.8	5.2	3.6	4.6	4.1	4.0	3.0	3.3	3.2	2.7
OTU 4 ( <i>Cytophagaceae</i> *)	4.3	3.8	3.0	3.5	2.8	2.3	4.4	4.2	4.8	4.1	0.7	0.2	0.0	3.1	3.2	2.6	2.9	2.9	3.5	3.7	2.0	1.5	1.1	0.7	0.3
OTU 5 ( <i>Sphingomonadaceae</i> *)	0.1	0.1	0.1	0.1	0.1	0.1	0.1	0.1	0.1	0.1	3.4	15.7	22.7	0.1	0.1	0.1	0.1	0.1	0.1	0.1	0.3	1.6	3.2	7.0	8.2
OTU 6 ( <i>Rhodocyclaceae</i> *)	3.0	2.6	3.2	3.8	2.6	3.6	3.0	4.4	3.4	1.8	0.5	0.2	0.2	3.3	3.7	4.0	3.0	3.7	2.7	3.0	1.4	0.6	0.6	0.3	0.3
OTU 7 ( <i>Haliscomenobacter</i> )	0.0	0.0	0.0	0.2	2.9	4.1	2.7	3.4	4.5	6.0	1.5	0.6	0.1	0.1	0.6	2.4	3.5	4.2	2.6	5.3	3.2	2.8	1.7	1.0	0.3
OTU 8 ( <i>Chloroflexi</i> *)	1.5	1.2	1.5	1.4	2.5	1.5	2.0	1.7	1.4	1.4	2.7	2.4	2.5	1.5	2.3	1.9	1.9	1.6	1.4	1.5	2.1	2.5	3.5	3.0	2.5
OTU 9 ( <i>Nitrospira</i> )	1.8	1.0	0.8	1.3	1.3	0.5	1.2	1.4	1.3	1.4	2.8	3.7	2.7	0.8	2.0	0.9	1.4	0.8	1.3	1.6	2.5	3.0	3.8	2.6	3.6
OTU 10 ( <i>Gp4</i> *)	2.0	2.1	2.0	2.4	1.2	0.9	1.2	1.1	1.0	1.4	1.3	0.6	0.5	2.1	1.1	1.6	1.5	1.3	1.4	2.1	2.0	2.5	2.4	1.7	1.6
OTU 11 ( <i>Ferruginibacter</i> )	1.7	1.3	1.1	1.4	0.7	0.8	0.8	1.5	1.8	1.7	2.3	2.5	2.1	1.1	1.5	1.2	1.0	1.4	1.6	1.5	1.5	1.7	1.9	2.3	2.6
OTU 12 ( <i>Dokdonella</i> )	1.9	1.8	1.8	2.2	1.6	2.0	1.5	1.0	1.2	1.1	1.3	1.0	1.1	2.0	1.9	2.5	1.6	1.9	1.6	1.3	1.1	1.2	1.1	0.9	1.1
OTU 13 ( <i>Rhodocyclaceae</i> *)	0.0	0.1	0.1	0.1	0.4	0.6	0.8	1.5	2.3	1.8	2.2	2.8	2.2	0.1	0.1	0.2	0.3	0.5	0.7	1.6	2.7	3.7	4.1	2.6	1.9
OTU 14 ( <i>Sphingobacteriales</i> *)	4.3	3.6	2.5	3.1	0.7	0.8	0.4	0.5	0.3	0.3	0.4	0.2	0.1	2.8	2.7	1.6	0.9	0.9	0.5	0.2	0.3	0.2	0.2	0.2	0.1
OTU 15 ( <i>Zoogloea</i> )	0.1	0.2	0.6	0.7	0.4	2.6	0.2	2.0	3.0	3.4	0.4	0.4	0.1	0.5	0.9	1.8	1.6	2.3	2.2	3.6	1.8	1.3	0.2	0.7	0.5
OTU 16 ( <i>Defluviicoccus</i> )	1.2	0.5	0.3	0.6	0.9	0.1	0.5	0.8	0.5	0.3	1.2	1.3	1.1	0.4	2.1	1.5	1.4	0.6	1.3	0.8	2.7	2.3	2.1	2.0	2.4
OTU 17 ( <i>Chloroflexi</i> *)	0.4	0.4	0.6	0.5	1.0	0.7	0.9	0.9	0.9	0.6	1.6	1.2	0.8	0.5	0.8	1.0	0.9	1.0	0.9	0.9	1.4	2.0	2.1	2.7	2.0
OTU 18 ( <i>Rhodocyclaceae</i> *)	0.7	0.6	0.5	0.7	1.0	1.8	1.4	2.1	2.6	2.5	0.5	0.3	0.2	0.5	0.6	1.1	1.0	1.8	1.3	1.8	1.2	0.6	0.4	0.3	0.2
OTU 19 ( <i>Bacteroidetes</i> *)	0.6	1.0	0.7	1.5	1.2	3.2	2.0	1.0	0.6	0.8	0.0	0.0	0.0	1.0	1.3	1.5	1.9	2.7	1.9	0.4	0.6	0.1	0.0	0.0	0.0
OTU 20 ( <i>Geminicoccus</i> )	0.8	0.5	0.3	0.4	0.6	0.1	0.7	0.5	0.5	0.2	2.0	2.0	1.7	0.4	1.6	0.6	0.6	0.3	0.6	0.4	2.0	1.5	2.4	1.8	2.1

OTU 1 (*Thiothrix*) was most abundant bacteria in this study. *Thiothrix* are filamentous, colorless and sulfur-oxidizing bacteria that may form rosettes and gonidia, and deposit sulfur when grown in the presence of sulfide or thiosulphate (Williams and Unz 1985). The average relative abundance of OTU 1 (*Thiothrix*) in control-MBR was more abundant than that of the QQ-MBR in the oxic tank and the anoxic tank. It was reported that a member of *Thiothrix* has the *LuxR* homolog for the detection of AHLs without *LuxI* (BioProject: PRJNA51139) for the synthesis of the signal molecules. Diggle et al. (2007) reported that the AHLs produced by other bacteria could have an effect on the bacteria that detect AHLs but do not produce, using a *Pseudomonas aeruginosa* mutant (PAO1 *lecA::luxΔlasI*). They showed that the addition of AHLs increased the population of the *P. aeruginosa* mutant. Thus, we speculate that *Thiothrix* populations could be affected by the QQ because its members might possess the *LuxR* homolog gene.

The relation between the relative proportion of OTU 1 (*Thiothrix*) and approximate floc size in activated sludge was investigated, because the overgrowth of *Thiothrix* has an effect on severe bulking problems in an industrial wastewater treatment plant (Nielsen et al. 2000). Many previous studies reported that sludge bulking was related to floc size in activated sludge. Andreadakis (1993) observed that the floc density was decreased by the increase of floc size and Jin et al. (2003) reported that sludge volume index (SVI) was positively correlated with floc size. In the Figure IV-6, relative composition of OTU 1 (*Thiothrix*) had correlation with the approximate floc size ( $p < 0.05$ ). Thus, it was speculated that the OTU 1 (*Thiothrix*) was related with floc size in activated sludge and the decrease of relative

composition of OTU 1 (*Thiothrix*) may be a one of reasons to explain the decreased floc size in the QQ-MBR.

The average relative composition of OTU 3 (*Rhodobacter*) in QQ-MBR was similar to the control-MBR and the average floc size in QQ-MBR was smaller than control-MBR in both oxic and anoxic tank. This result is contradictory to previous study because the floc size of *Rhodobacter* was deflocculated by QS (Puskas et al. 1997) in pure culture. The difference between this result and the previous study may have been caused by the mixed culture system.

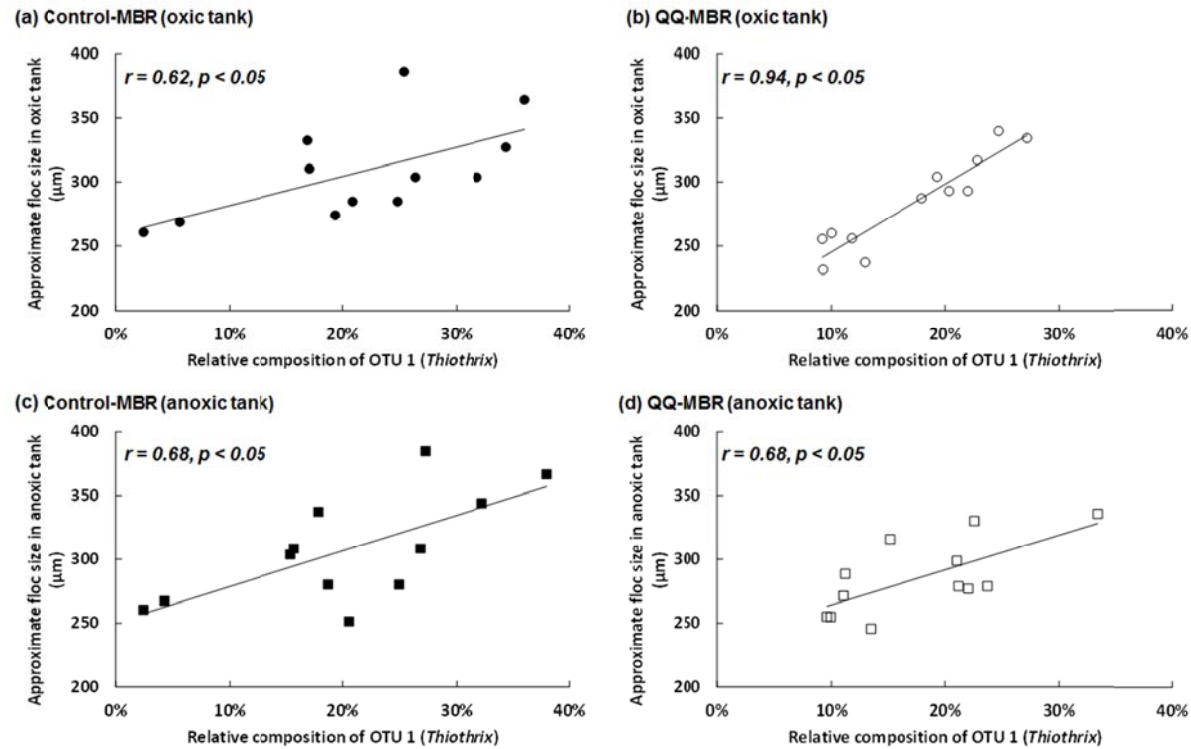


Figure IV-6. Pearson correlation coefficient between relative composition of OTU 1 (*Thiothrix*) and approximate floc size. Oxic tank in the control-MBR (a), oxic tank in the QQ-MBR (b), anoxic tank in the control-MBR (c) and anoxic tank in the QQ-MBR (d).

### **IV.3.3. Microbial network in the A/O MBR with QQ**

#### **IV.3.3.1. Network description**

A network analysis was applied for a better understanding of the complex microbial community between control- and QQ-MBR. The microbial interactions are shown in Figure IV-7 and 8. In the oxic tank, the constructed control-MBR network contains 30 nodes (30 OTUs) and 37 edges (connections among nodes), and the QQ-MBR network contains 80 nodes and 303 edges (Figure IV-7 and Table IV-5). The percentile of positive interactions in control-MBR was 49%, which was similar to that of the QQ-MBR network (53%). To characterize microbial associations, the microbial networks were analyzed using the network analyzer tool (Table 4). The average clustering coefficient is the average fraction of the pairs of nodes one link away from a node that are also linked to one another (Steele et al. 2011). The average clustering coefficient of the control-MBR network was 0.176, whereas that of the QQ-MBR network was 0.530. The density (0-1 scale) shows how densely the network is populated with edges. The density of the control-MBR network was 0.085, whereas that of the QQ-MBR network was 0.096. Thus, the control-MBR network was more compact than QQ-MBR network. The network diameter suggests the largest distance between two nodes. The control-MBR network (network diameter 5) had a larger network diameter than the QQ-MBR network (network diameter 4). The average shortest path length (characteristic path length) of the control-MBR network (2.779) was longer than that of the QQ-MBR network (2.022). Network centralization (0-1 scale) is an index of the connectivity distribution (Dong and Horvath 2007). The network centralization of the control-

MBR and QQ-MBR network was 0.463 and 0.694, respectively. The network heterogeneity suggests the tendency of a network to contain hub nodes (Kim et al. 2015). The heterogeneity of the control-MBR network was 1.285, whereas that of the QQ-MBR network was 1.674.

The microbial interactions are shown that QQ had effect on the complexities of microbial interaction in A/O MBR (Figure IV-7 and 8). The results from Figure IV-3 and Table IV-7 indicated that the QQ-MBR network was more compact, forming a clustered and more heterogeneous network than control-MBR was in the oxic tank. These results indicated that the microbial community of QQ-MBR could be sensitive to perturbation i.e., environmental change. Zhou et al. (2010) reported that the rapid communication among different members within a system (short characteristic path length) could make quick responses to environmental changes such as elevated atmospheric CO<sub>2</sub> in soil microbial communities. QQ-MBR network was more heterogeneous network than control-MBR network. Thus, it was speculated that QQ-MBR had strong tendency to contain the hub node.

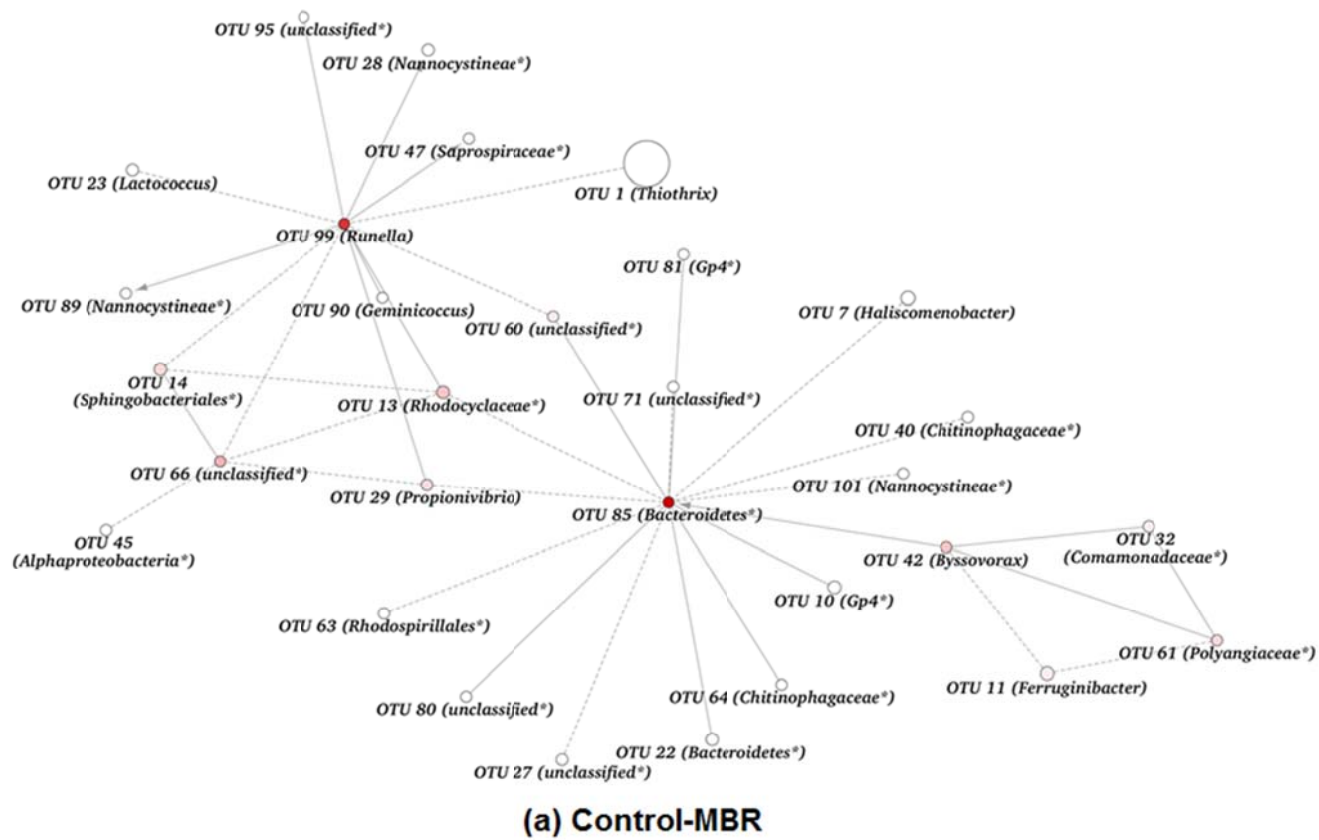


Figure IV-7. Microbial networks of activated sludge of control-MBR (a) and QQ-MBR (b) in oxic tank.

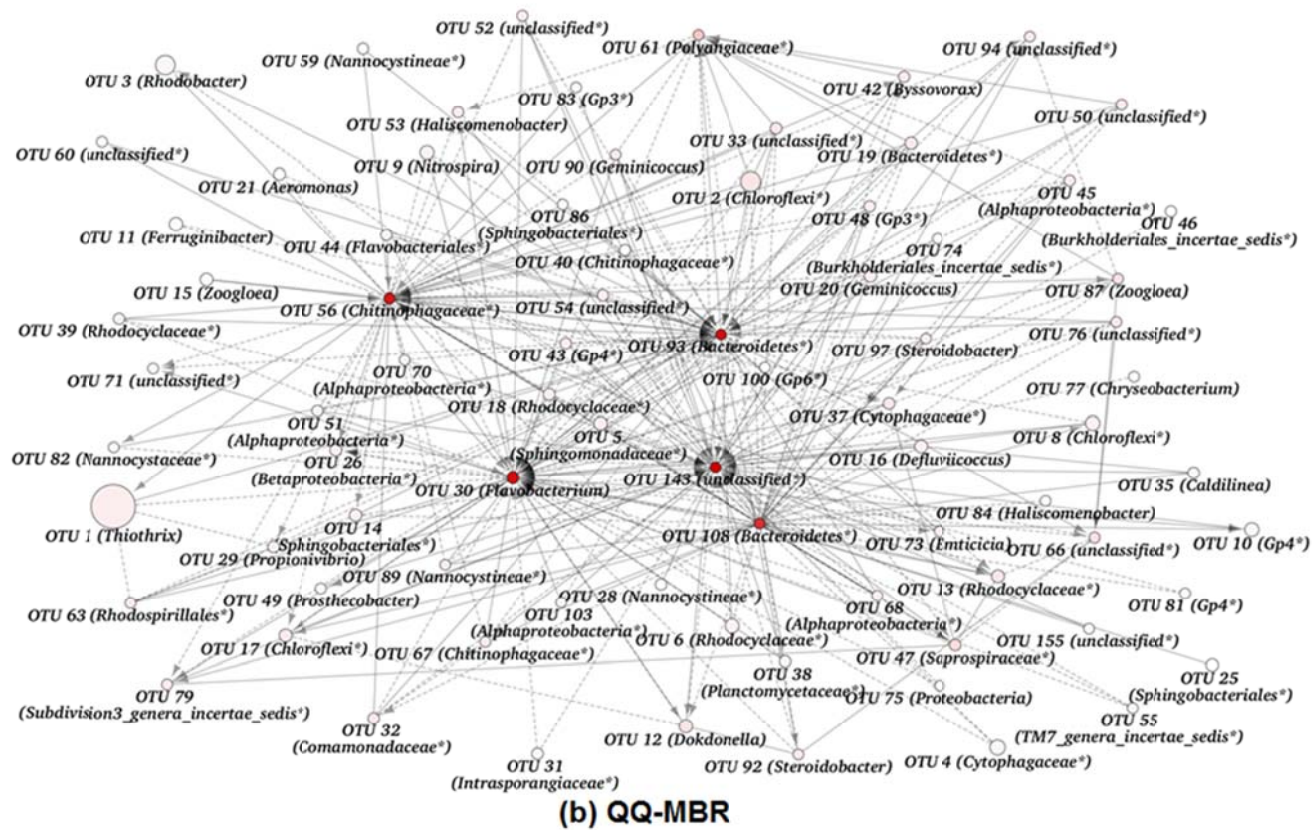


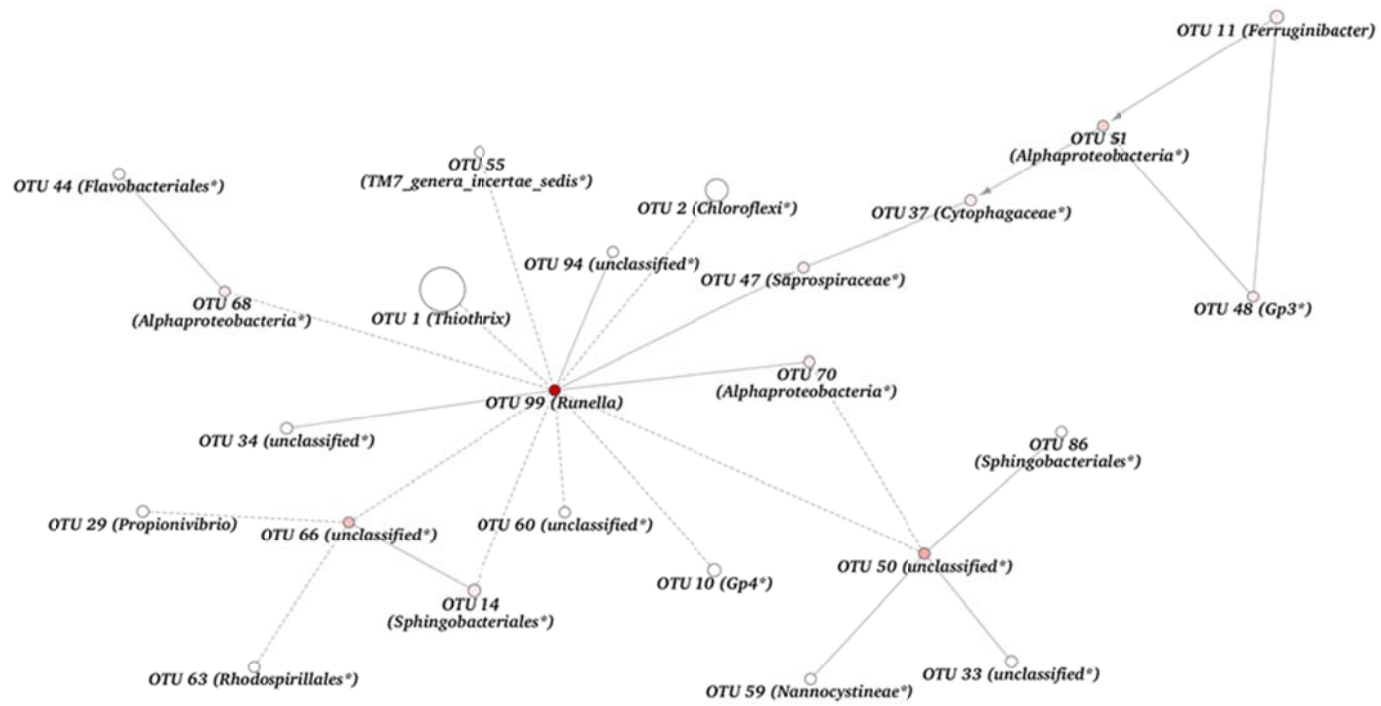
Figure IV-7. (Continued).

**Table IV-5. Characteristics of network of activated sludge.**

	Oxic tank		Anoxic tank	
	Control-MBR	QQ-MBR	Control-MBR	QQ-MBR
Number of nodes	30	80	24	72
Number of edges	37	303	26	166
Number of positive edges	18	161	14	88
Number of negative edges	19	142	12	78
Proportion of positive edges	49%	53%	54%	53%
Network diameter	5	4	6	4
Average clustering coefficient	0.176	0.530	0.171	0.389
Network centralization	0.463	0.694	0.454	0.759
Characteristic path length	2.779	2.022	2.910	2.077
Network density	0.085	0.096	0.080	0.065
Network heterogeneity	1.285	1.674	1.136	2.153

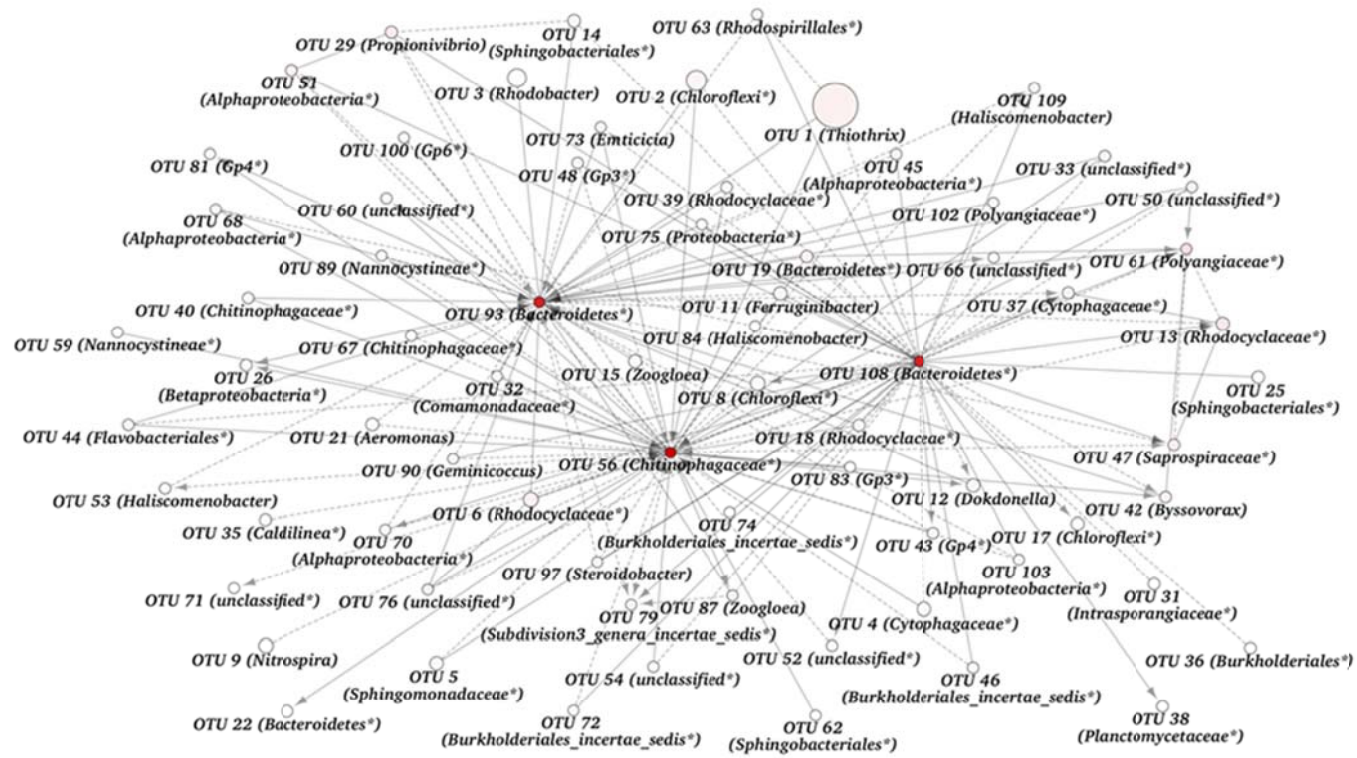
In the anoxic tank, the constructed control-MBR network contains 24 nodes and 26 edges, and the QQ-MBR network contains 72 nodes and 166 edges (Figure IV-8 and Table IV-5). The composition of positive interaction in control-MBR was 54%, which was similar to that of the QQ-MBR network (53%). The average clustering coefficient of the control-MBR network was 0.171, whereas that of the QQ-MBR network was 0.389. The density of the control-MBR network was 0.080, which was higher than that of the QQ-MBR network (0.065). Control-MBR (6) had a larger network diameter than QQ-MBR (4). The average shortest path length of the control-MBR network (2.910) was similar to that of the QQ-MBR network (2.077). The network centralization of the control-MBR and QQ-MBR network was 0.454 and 0.759, respectively. The heterogeneity of the control-MBR network was 1.136, whereas that of the QQ-MBR network was 2.153.

The results of network in the anoxic tank were similar to the oxic tank. The values of average clustering coefficient, network centralization, network heterogeneity in QQ-MBR was larger than that of control-MBR in anoxic tank except for network density (Table IV-7). Thus, it was speculated that the effect of QQ in anoxic tank is similar to that of the oxic tank due to recirculation of activated sludge in A/O MBR.



(a) Control-MBR

Figure IV-8. Microbial networks of activated sludge of control-MBR (a) and QQ-MBR (b) in anoxic tank.



(b) QQ-MBR

Figure IV-8. (Continued).

#### **IV.3.3.1. The role of OTUs with high relative abundance and network hubs in microbial network**

The OTUs with high relative abundances are listed in order of abundance in Tables IV-4. The excluded OTUs are considered to be less significantly associated in the microbial network.

In the oxic tank, 6 out of the 20 OTUs were found in the control-MBR and 18 out of 20 OTUs were found in the QQ-MBR. The OTUs with abundant relative abundances in the control-MBR network composed 27% (10/37) of the associations with microbes, whereas the OTUs with high relative abundance in QQ-MBR network composed 29% (88/303) of the associations with microbes. In the anoxic tank, 5 out of the 20 OTUs were found in the control-MBR and 19 out of 20 OTUs were found in the QQ-MBR. The OTUs with high relative abundances in the control-MBR network composed 27% (7/26) of the associations with microbes, whereas the OTUs with high relative abundance in QQ-MBR network composed 31% (51/166) of the associations with microbes. The OTUs with high relative abundance in QQ-MBR had more microbial interactions than in control-MBR. Particularly, OTU 1 (*Thiothrix*), which was the most dominant bacteria in this study, had different microbial interactions between control- and QQ-MBR. In the oxic tank, it had 1 negative interaction with microbes in the control-MBR whereas it had 2 positive interactions and 2 negative interactions with microbes in the QQ-MBR. In the anoxic tank OTU 1 (*Thiothrix*) had 1 negative interaction with microbe in control-MBR whereas it had 2 positive interactions and 2 negative interactions with microbes in QQ-MBR. The number of positive correlations of

OTU 1 (*Thiothrix*) was higher in the QQ-MBR network.

The OTUs with high relative abundance in the QQ-MBR had more microbial interactions than those in the control-MBR had. Thus, this result indicated that the microbial interactions of the OTUs with high relative abundances were increased by the effect of QQ.

In the oxic tank, the OTU 1 (*Thiothrix*), the most dominant bacteria, was negatively correlated with microbial hub node, OTU 99 (*Runella*) in the control-MBR. However, it had 1 negative correlation with hub node, OTU 30 (*Flavobacterium*) and 2 positive correlations with hub nodes, OTU 56 (*Chitinophagaceae*) and OTU 93 (*Bacteroidetes*) in the QQ-MBR. In the anoxic tank, the change of microbial interactions of OTU 1 (*Thiothrix*) was similar to the oxic tank. It was negatively correlated with the OTU 99 (*Runella*). The most abundant bacteria OTU 1 (*Thiothrix*) had negatively correlated with OTU 108 (*Bacteroidetes*) whereas it had positively correlated with OTU 56 (*Chitinophagaceae*) and OTU 93 (*Bacteroidetes*) in the QQ-MBR. Thus, the QQ had effect on the microbial interaction of the OTU 1 (*Thiothrix*). It was speculated that the decrease of OTU 1 (*Thiothrix*) composition, cause by application of QQ, led to positive correlations with hub nodes from negative correlations in the control-MBR. In addition, OTU 1 (*Thiothrix*) had negative correlation with microbial hub node in the control-MBR. Negative correlation could indicate inhibition (Kim et al. 2015). It was speculated that OTU 1 (*Thiothrix*) drove changes in the whole microbial community by inhibition of hub microbe in the control-MBR.

Nodes with more than 10 edges were considered network hub in control-MBR and Nodes with more than 30 edges were considered network hubs in QQ-MBR because the node degree (the number of edges linked) ranged from 1 to 15 in the control-MBR network and from 1 to 61 in the QQ-MBR network in the oxic tank. In the oxic tank, there was 2 microbial hub in the control-MBR network, OTU 85 (*Bacteroidetes*) and OTU 99 (*Runella*), whereas the QQ-MBR network contained 5 microbial hub nodes including OTU 143 (*unclassified*), OTU 93 (*Bacteroidetes*), OTU 30 (*Flavobacterium*), OTU 56 (*Chitinophagaceae*) and OTU 108 (*Bacteroidetes*). OTU 85 (*Bacteroidetes*) and OTU 99 (*Runella*) had 52% (14/27) of the positive associations with microbes. Although they had low relative abundance (0.32%), OTU 99 (*Runella*) was negatively associated with the most abundant bacteria species OTU 1 (*Thiothrix*) in the control-MBR. There were 5 microbial hub nodes in the QQ-MBR network: OTU 143 (*unclassified*) had 51% (31/61) of the positive associations with microbes; OTU 93 (*Bacteroidetes*) had 53% (30/57) of the positive associations with microbes; OTU 30 (*Flavobacterium*) had 54% (31/57) of the positive associations with microbes; OTU 56 (*Chitinophagaceae*) had 53% (28/55) of the positive associations with microbes; OTU 108 (*Bacteroidetes*) had 55% (27/49) of the positive associations with microbes. The most abundant bacteria OTU 1 (*Thiothrix*) was negatively correlated with OTU 30 (*Flavobacterium*) whereas it was positively correlated with OTU 56 (*Chitinophagaceae*) and OTU 93 (*Bacteroidetes*).

In the anoxic tank, there was 1 microbial hub in the control-MBR network (OTU 99 (*Runella*), whereas the QQ-MBR network contained 3 microbial hub

nodes including OTU 56 (*Chitinophagaceae*), OTU 93 (*Bacteroidetes*) and OTU 108 (*Bacteroidetes*). OTU 99 (*Runella*) had 31% (4/13) of the positive associations with microbes. Although it had low relative abundance (0.20%), it was negatively associated with first and second abundant bacteria species OTU 1 (*Thiothrix*) and OTU 2 (*Chloroflexi*) in the control-MBR. In the QQ-MBR network, OTU 56 (*Chitinophagaceae*) had 51% (16/57) of the positive associations with microbes. OTU 93 (*Bacteroidetes*) had 57% (28/49) of the positive associations with microbes. OTU 108 (*Bacteroidetes*) had 51% (25/49) of the positive associations with microbes. OTU 1 (*Thiothrix*) was negatively correlated with hub node in the control-MBR whereas it was positively correlated with microbial hubs, OTU 56 (*Chitinophagaceae*) and OTU 93 (*Bacteroidetes*), in the QQ-MBR.

The number of microbial hub nodes in the QQ-MBR network was higher than that of control-MBR network in both oxic and anoxic tank. The each hub node had similar distribution of negative and positive associations in both control-and QQ-MBR. It was speculated that QQ had not effect on the role of hub node but had effect on the complexity of microbial network because the number of microbial interactions were increased.

#### **IV.3.4. Prediction of metabolic pathway in activated sludge**

The Histogram of the LDA score showed different metabolic pathway between control-MBR and QQ-MBR (Figure IV-9). This result suggested that the metabolic pathway of RNA polymerase and Rivo flavin metabolism in QQ-MBR

was significantly different from control-MBR. RNA polymerase was related to genetic information processing and riboflavin metabolism was related to metabolism of cofactors and vitamins. Thus, it was speculated that QQ had no effect on the removal of COD and TN because it did not affect the metabolism related to carbon and nitrogen metabolism in this study.

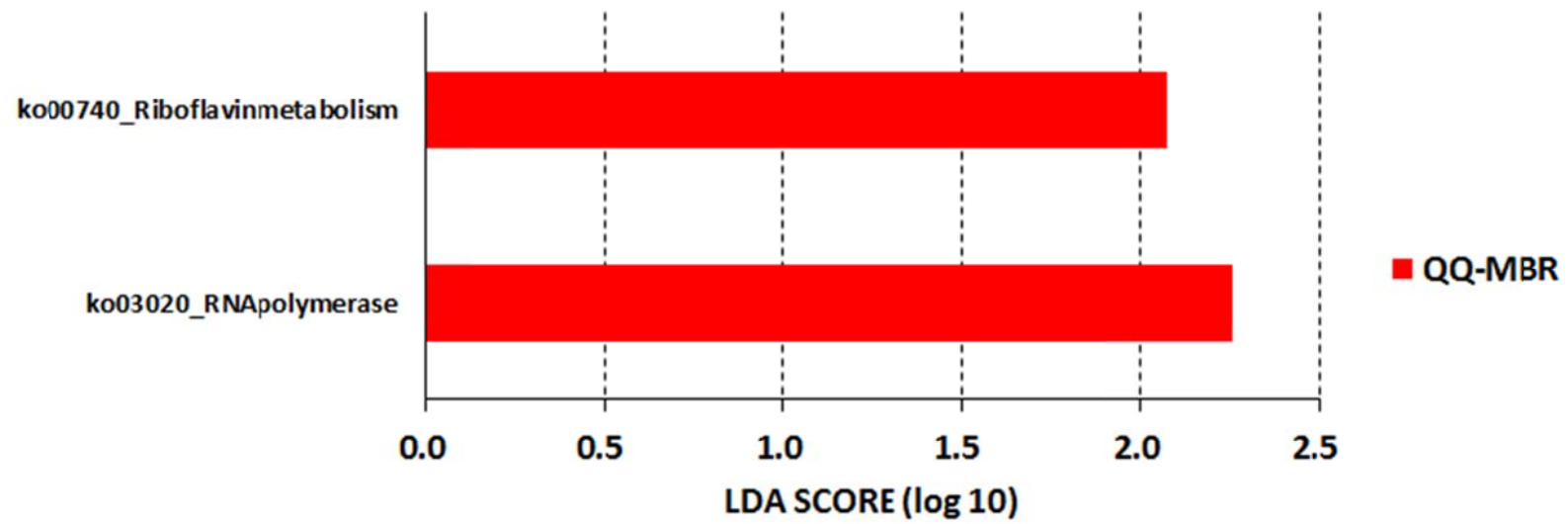


Figure IV-9. The LDA score of metabolic pathway in activated sludge.

## IV.4. Conclusions

The effect of QQ on activated sludge function and composition were investigated in A/O MBR. The evaluation of risk of application of QQ-MBR to full-scale MBR was conducted using risk assessment. The following conclusions could be drawn:

- The system performance was stable during 91days. However, the average size of floc in the control-MBR was higher than that in the QQ-MBR. These results indicated that the QQ-MBR could be applied to the real wastewater treatment without disturbing its waste removal efficiency.

- Control- and QQ-MBR networks displayed different topological characteristics in oxic tank. For instance, QQ-MBR was more compact, clustered and heterogeneous than control-MBR in oxic tank. The different microbial associations were responsible for the variation of community composition between the control- and QQ-MBR.

## Chapter V

# Survey of Microbial Community in Full-Scale MBRs for Wastewater Treatment



## V.1. Introduction

Microbial production of membrane foulants in the activated sludge as well as microbial colonization on membrane surfaces are the main causal agents for biofouling (Malaeb et al. 2013). However, the microbial ecology has not been fully elucidated to date. Specifically, there are few published survey reports about microbial systems of both biofilm and activated sludge in actual MBRs.

Because activated sludge is the sole inoculum for biofilm formation on the membrane in a MBR, the microbial community in the biofilm is likely to resemble that in the activated sludge. However, many studies have reported differences between the activated sludge and biofilm communities in lab- and pilot-scale MBRs. For instance, Piasecka et al. (2012) found that the bacterial community in activated sludge differed from that in the membrane biofilm at the initial phase in a lab-scale MBR (an 18.6-L reactor with a flat sheet membrane). Lim et al. (2012) reported that the microbial composition of a biocake that was loosely attached to the membrane differed from that of activated sludge in a lab-scale MBR (a 6-L reactor with a hollow fiber membrane). These differences were primarily observed from single-membrane bioreactors, implying a need for microbial observations from multiple MBRs to confirm whether the biofilm evolves differently from the activated sludge.

In general, environmental factors can affect the microbial community in wastewater treatment systems. Many studies have shown that various operational factors (e.g., aeration, nutrient removal processes) have important effects on the microbial community in activated sludge (Hu et al. 2012, Zhang et al. 2012 and

Zhao et al. 2014). However, only a few studies have reported the effects of environmental factors (e.g., different characteristics of membranes) on the microbial community in biofilm. For example, Lee et al. (2014) found a community difference in biofilm on polyethersulfone (PES), polytetrafluoroethylene (PTFE), and PVDF with the same pore size.

Recently, network analysis has been applied for a better understanding of the complex microbial community within the system (Fuhrman 2009, Faust and Raes 2012). Network analysis offers new insight into the structure of complex microbial communities (Barberán et al. 2012, Williams et al. 2014). For instance, Ju and Zhang (2015) found the connection between bacteria in activated sludge and environmental factors using microbial network in wastewater treatment systems.

The main objectives of this study were to determine which microbes play key roles, to elucidate the microbial complexities of biofilm and activated sludge and to determine the effects of environmental factors on microbial communities in both biofilm and activated sludge in 10 full-scale MBRs with different membrane materials, nutrient removal processes and operational factors.

## **V.2. Materials and methods**

### **V.2.1. Sampling sites and methods**

The characteristics and specific processes of 10 MBRs are shown in Table V-1 and II-4. The environmental factors (flux, flow rate, F/M ratio, size of membrane tank, aeration rate in the membrane tank, total membrane area, membrane materials, SRT, BOD, COD, TN, TP and operation mode) were provided by the operator in each MBR. The permanganate ( $\text{KMnO}_4$ ) was used for measuring COD in this study. Because this method only measures part of the organic matter (Henze 2008), most of the BOD values were greater than the COD values.  $\text{SAD}_m$  was calculated based on the aeration in the membrane tank and total membrane area. The HRT in the membrane tank was calculated based on the flow rate and size of the membrane tank. The concentration of MLSS in the membrane tank was measured in triplicate by standard methods (APHA et al. 2005). The temperature in the membrane tank was measured three times using a digital thermometer (Center technology corp., model CENTER 309, Taiwan).

The membrane module in the membrane tank was removed from the membrane tank with a crane, and the surface of the membrane with biofilm (transmembrane pressure > 20 kPa) was softly rinsed with tap water to remove debris and excess cells from the activated sludge. Sterilized gauze was used to detach the biofilm from the membrane surface, and it was kept in a sterilized conical tube (50 ml). Three sampling spots of biofilm (resulting in triplicate) in the membrane module were randomly selected within the middle part of the membrane module. Samples of activated sludge were collected from three sampling spots in

the membrane tank. Activated sludge was sampled into 50 ml of a sterilized conical tube.

### **V.2.2. DNA extraction, PCR amplification and Miseq platform sequencing**

The sample was prepared as follows for DNA extraction. A slice of gauze (1 cm x 1 cm) with biofilm was cut into small pieces. 1.5 ml of activated sludge was concentrated by centrifugation (10,000 g, 1 min, 25°C), and the pellet was re-suspended in 0.5 ml of distilled water. These samples were placed into the bead tube for DNA extraction. DNA was extracted from the precipitates using the NucleoSpin Soil kit (Macherey-Nagel GmbH, Düren, Germany). The DNA was eluted in 100 µl of the elution buffer. The eluted DNA was quantified using the ND-1000 spectrophotometer (NanoDrop Inc., Wilmington, DE, USA). To determine the microbial communities, the Illumina MiSeq platform sequencing technique of partial 16S ribosomal RNA gene was conducted. Each sequenced sample is prepared as described above.

### **V.2.3. Data analysis for bacterial community**

The sequencing data were trimmed using Mothur software. The average nucleotide length was 454 bp for the bacterial libraries. Chimeric sequences were removed using the Uchime function with the abundant sequences as a reference. All of the sequences were classified using the SILVA reference library.

**Table V-1. Characteristics of 10 different membrane bioreactors.**

MBR	Flow rate (m <sup>3</sup> /day)	Flux (LMH)	MLSS in the membrane tank (mg/L)	HRT in the membrane tank (h)	SAD <sub>m</sub> (Nm <sup>3</sup> /m <sup>2</sup> •h)	Average temperature in the membrane tank (°C)	F/M ratio (kgBOD/kgMLSS•day)	Average Influent (mg/L)				Membrane type, materials, pore size
								BOD	COD	TN	TP	
A-M	15	10.5	5093±114	44.8	0.72	14.1±0.3	0.01*	124.1	125.3	32.9	3.2	HF, PE, < 0.4 μm
B-M	9	10.8	3887±442	51.7	0.62	13.7±0.6	0.01*	119.6	127.0	28.7	2.9	HF, PE, < 0.4 μm
C-M	1200	6.5	6643±83	18.3	0.17	14.7±0.4	0.02	160.0	150.0	40.0	4.0	HF, PTFE, 0.1 μm
D-M	850	12	5520±480	13.1	0.23	13.1±0.3	0.02*	116.2	95.8	27.2	2.8	HF, PE, 0.4 μm
E-M	2300	8	7860±370	4.8	0.19	16.1±1.2	0.06	154.4	89.9	40.3	4.3	HF, PVDF, < 0.1 μm
F-M	7800	13.4	8720±1186	3.4	0.22	15.8±0.8	0.24	225.0	151.9	43.9	5.5	HF, PE, < 0.4 μm
G-M	6000	12	8413±46	5.5	0.31	18.1±0.5	0.06	268.0	155.0	80.0	5.5	FS, c-PVC, 0.4 μm
H-M	5000	7.2	10213±1473	8.8	0.28	21.7±0.6	0.06	190.0	173.0	52.4	5.2	FS, c-PVC, 0.4 μm
I-I	250	16.7	4447±114	9.12	1.7	15.6±0.4	0.06*	103.0	133.6	45.0	10.0	FS, c-PVC, 0.4 μm
J-I	25000	12.5	7606±404	2.7	0.15	22.0±0.4	0.03	200.0	140.0	35.0	7.0	HF, PE, < 0.4 μm

*Abbreviations:* F/M ratio; Food to microorganism ratio, FS; Flat sheet, HF; Hollow fiber, HRT; Hydraulic retention time, I; Industrial wastewater, M; Municipal wastewater, MLSS; Mixed liquor suspended solids, PE; Polyethylene, Polytetrafluoroethylene, PVDF; Polyvinylidene fluoride, c-PVC; Chlorinated Polyvinyl chloride, SAD<sub>m</sub>; Specific aeration demand on membrane.

An asterisk indicates that the F/M ratio was calculated based on the aeration tank.

**Table V-1. (Continued).**

MBR	Plant name & location	Membrane maker	Operation mode	Membrane tank size(m <sup>3</sup> )	SRT (day)	MBR process	Wastewater type	Sampling time (month/year)
A-M	Gangwon-A	Econity	suction 7min/relaxation 3min	28	37	KSMBR	Municipal wastewater	02/2015
B-M	Gangwon-B	Econity	suction 7min/relaxation 3min	19.4	27	KSMBR	Municipal wastewater	02/2015
C-M	Juksan, Anseong	Smitomo Electric	suction 8min relaxation 2min backwashing 1min (three times per day)	920	25	D-MBR	Municipal wastewater	03/2015
D-M	Daesin, Yeosu	Mitsubishi Rayon	suction 12min/relaxation 3min	464.4	20-25	HANT	Municipal wastewater	04/2015
E-M	Sinkwan, Gongju	Kolon	suction 9min/relaxation 1min backwashing 1min relaxation 9min (two times per day)	433	24	KIMAS	Municipal wastewater	03/2015
F-M	Munsan, Paju	Econity	suction 12min/relaxation 1min backwashing 1min relaxation 1min	1096.5	32	KSMBR	Municipal wastewater	03/2015
G-M	Keumchon, Paju	Pure-envitec	suction 10min relaxation 2min	1384.6	24-25	DF-MBR	Municipal wastewater	04/2015
H-M	Unbuk, Incheon	Pure-envitec	suction 7min relaxation 3min	1840	25-30	DF-MBR	Municipal wastewater	05/2015
I-I	Songdo incineration plant, Incheon	Pure-envitec	suction 8min relaxation 2min	95	25	A2O	Industrial wastewater	02/2015
J-I	Industrial wastewater treatment plant	Econity	suction 12min/relaxation 3min	2830	30	KSMBR	Industrial wastewater 70% Municipal wastewater 30%	04/2015

The sequencing reads were deposited into the DNA Data Bank of Japan (DDBJ) Sequence Read Archive (<http://trace.ddbj.nig.ac.jp/dra>) under accession no. DRA004059.

For the community analysis, operational taxonomic units (OTUs) were determined at 3% dissimilarity. A phylotype analysis was conducted using Mothur software. Each read was taxonomically assigned at the genus level with bootstrap values more than 80% resulting in taxonomic classification from phylum to genus. A total of 1,982,648 effective sequences were obtained after the cleaning of the raw reads. Community diversity measures (i.e., diversity, evenness and richness) were estimated by random resampling of 1,000 sequences from the original sequence libraries (18,066 ~ 52,075 sequences per sample after trimming) with 1,000 iterations. The cluster of microbial communities was visualized using the FigTree software version 1.4.2 (<http://tree.bio.ed.ac.uk>). A principal coordinate analysis (PCoA) was conducted using Mothur software. For the clustering analysis and PCoA, the Yue & Clayton similarity was calculated by random resampling of 1,000 sequences with 1,000 iterations.

#### **V.2.4. Network analysis**

A Spearman correlation-based network analysis was used to uncover the co-occurrence patterns of the biofilm's bacterial community on the membrane surface and activated sludge in the 10 full-scale MBRs. The Spearman correlation was examined using an extended local similarity analysis (eLSA software) (Xia et al. 2011). Only bacterial OTUs with an average relative abundance  $\geq 0.2\%$  were

chosen in all samples from the biofilm and activated sludge. The analysis includes the relative abundance of bacterial OTUs from each sample and 10 environmental factors, i.e., flux, MLSS in the membrane tank, HRT in the membrane tank, F/M ratio,  $SAD_m$ , average temperature in the membrane tank, BOD, COD, TN and TP. OTU was classified at the genus level, and the asterisk indicates that the OTU was assigned at the taxonomic classification level. The microbial associations were visualized from the Spearman correlation coefficient (a connection represents a strong positive Spearman's  $\rho > 0.75$  and negative Spearman's  $\rho < -0.75$ ), and their p-values were determined using Cytoscape version 3.2.1 (Shannon et al. 2003). Nonsignificant associations (edge) with  $p \geq 0.05$  were excluded. The shape of each node indicated that rectangle is environmental factor and circle is bacteria. The red color of the nodes indicates the number of connections to the nodes. Solid edges are positive associations, and dashed edges are negative associations. The network topology characteristics were calculated using the Network Analyzer tool (Assenov et al. 2008).

### **V.2.5. Statistical analysis**

A completely randomized block design (RCBD) (block, MBR; and treatment, biofilm and activated sludge) was used to analyze the variation of diversity measures (richness, diversity and evenness). The Spearman correlation between the diversity measures and 10 environmental factors was used to identify the effects of each environmental factor. In addition, the relationship between values of the principal coordinate analysis (PCoA) axis 1 and the environmental

factors also was examined. The absolute value of the Spearman correlation coefficient, which was greater than 0.5 ( $p < 0.05$ ), was considered significant in this study. The Tukey-Kramer test was used to analyze the effect of the membrane materials (PE, PTFE, PVDF and c-PVC) on the bacterial composition of biofilm (the value of PCoA axis 1 in Fig. 3 (a)). The sample size of PE, PTFE, PVDF and c-PVC was 15, 3, 3 and 9, respectively. RCBD and Spearman correlation were performed using Hmisc packages, and the Tukey-Kramer test was conducted using the DTK packages in the R environment ([www.r-project.org](http://www.r-project.org)).

### **V.2.6. Calculation of the relative proportion of quorum sensing related bacteria**

The quorum-sensing (QS) related bacteria were classified by a listing of the literature survey (Table V-2). The bacterial genera possessing complete quorum-sensing systems comprise the gene responsible for the production and reception of either *N*-acyl-homoserine lactone (AHL), autoinducing peptide (AIP), or autoinducer-2 (AI-2). The relative proportion of QS-related bacteria at the genus level was calculated using the results of the phylotype analysis.

**Table V-2. List of quorum sensing related bacteria.**

<b>Genus (signal molecule)</b>	<b>reference</b>	<b>Genus (signal molecule)</b>	<b>reference</b>	<b>Genus (signal molecule)</b>	<b>reference</b>
<i>Acidithiobacillus</i> (AHL)	C. Farah et al., <i>Appl. Environ. Microbiol.</i> (2005), 71.	<i>Erwinia</i> (AHL)	M. B. Miller et al., <i>Annu. Rev. Microbiol.</i> (2001), 55.	<i>Ralstonia</i> (AHL)	M. B. Miller et al., <i>Annu. Rev. Microbiol.</i> (2001), 55.
<i>Acidovorax</i> (AHL)	C. Tao et al., <i>Chinese Journal of Agricultural Biotechnology</i> (2009), 6.	<i>Escherichia</i> (AI-2)	Peng Zhu et al., <i>Current Medicinal Chemistry</i> (2012), 19.	<i>Rhizobium</i> (AHL)	M. B. Miller et al., <i>Annu. Rev. Microbiol.</i> (2001), 55.
<i>Acinetobacter</i> (AHL)	J D. Shrout et al., <i>ES&amp;T</i> (2012), 46.	<i>Flavobacterium</i> (AHL)	I. Wagner-Dobler et al., <i>ChemBioChem</i> (2005), 6.	<i>Rhodobacter</i> (AHL)	M. B. Miller et al., <i>Annu. Rev. Microbiol.</i> (2001), 55.
<i>Aeromonas</i> (AHL, AI-2)	J D. Shrout et al., <i>ES&amp;T</i> (2012), 46. Kozlova et al., <i>Microbial pathogenesis</i> , 45, 2008	<i>Jannaschia</i> (AHL)	V. Thiel et al., <i>ChemBioChem</i> (2009), 10.	<i>Rhodospirillum</i> (AHL)	L. Carius et al., <i>BMC Microbiology</i> (2013), 13.
<i>Agrobacterium</i> (AHL)	M. B. Miller et al., <i>Annu. Rev. Microbiol.</i> (2001), 55.	<i>Klebsiella</i> (AI-2)	D. Balestrino et al., <i>JOURNAL OF BACTERIOLOGY</i> (2005), 187.	<i>Roseobacter</i> (AHL)	L. Gram et al., <i>Appl. Environ. Microbiol.</i> (2002), 68.
<i>Arcobacter</i> (AI-2)	J D. Shrout et al., <i>ES&amp;T</i> (2012), 46.	<i>Lactobacillus</i> (AI-2)	B.L. Buck et al., <i>Journal of Applied Microbiology</i> (2009), 107.	<i>Salmonella</i> (AI-2)	Peng Zhu et al., <i>Current Medicinal Chemistry</i> (2012), 19.
<i>Bacillus</i> (AI-2)	J D. Shrout et al., <i>ES&amp;T</i> (2012), 46.	<i>Listeria</i> (AI-2)	S. C. Belval et al., <i>Appl. Environ. Microbiol.</i> (2006), 72.	<i>Serratia</i> (AHL)	M. B. Miller et al., <i>Annu. Rev. Microbiol.</i> (2001), 55.
<i>Bradyrhizobium</i> (AHL)	N. Pongsilp et al., <i>Current Microbiology</i> (2005), 51.	<i>Mesorhizobium</i> (AHL)	J. Zhu et al., <i>Journal of Applied Microbiology</i> (2003), 69.	<i>Sinorhizobium</i> (AHL)	M. TG. Holden et al., <i>Quorum Sensing, 2007 John Wiley &amp; Sons.</i>
<i>Brucella</i> (AHL)	B Taminiau et al., <i>INFECTION AND IMMUNITY</i> (2002), 70.	<i>Nitrobacter</i> (AHL)	J D. Shrout et al., <i>ES&amp;T</i> (2012), 46.	<i>Sodalis</i> (AHL)	M. H. Pontes et al., <i>PLoS ONE</i> (2008), 3.
<i>Burkholderia</i> (AHL)	A. Gotschlich et al., <i>System. Appl. Microbiol.</i> (2001), 24.	<i>Nitrosomonas</i> (AHL)	J D. Shrout et al., <i>ES&amp;T</i> (2012), 46.	<i>Sphingomonas</i> (AHL)	J D. Shrout et al., <i>ES&amp;T</i> (2012), 46.
<i>Chromobacterium</i> (AHL)	M.F. Siddiqui et al., <i>Journal of Water Process Engineering</i> (2015), 7.	<i>Nitrospira</i> (AHL)	J. Gao et al., <i>Journal of Applied Microbiology</i> (2014b), 80.	<i>Staphylococcus</i> (AIP)	M.F. Siddiqui et al., <i>Journal of Water Process Engineering</i> (2015), 7.

**Table V-2. (Continued).**

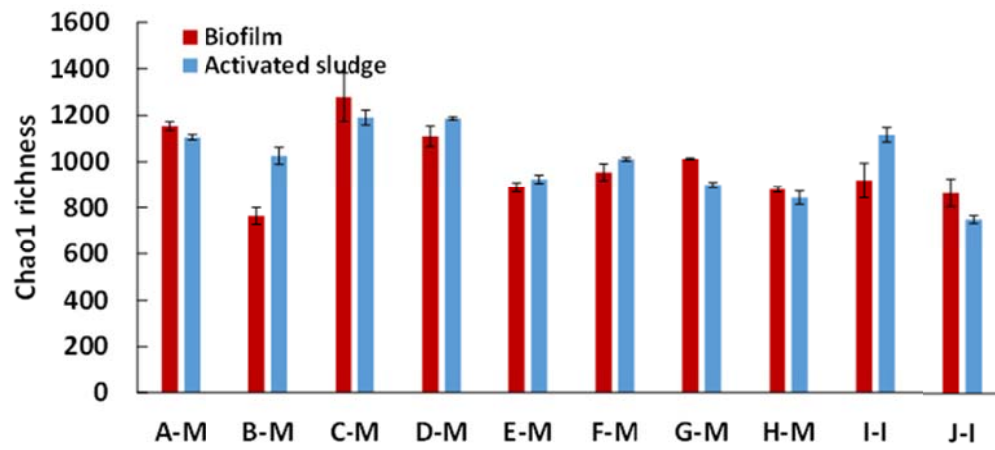
<b>Genus (signal molecule)</b>	<b>reference</b>	<b>Genus (signal molecule)</b>	<b>reference</b>	<b>Genus (signal molecule)</b>	<b>reference</b>
<i>Comamonas</i> (AHL)	J D. Shrout et al., <i>ES&amp;T</i> (2012), 46.	<i>Nocardia</i> (AIP)	J D. Shrout et al., <i>ES&amp;T</i> (2012), 46.	<i>Streptococcus</i> (AIP)	P. Suntharalingam et al., <i>TRENDS in Microbiology</i> (2005,) 13.
<i>Corynebacterium</i> (AI-2)	J D. Shrout et al., <i>ES&amp;T</i> (2012), 46.	<i>Novosphingobium</i> (AHL)	H. M. Gan et al, Journal of Bacteriology (2009), 191.	<i>Vibrio</i> (AI-2)	J D. Shrout et al., <i>ES&amp;T</i> (2012), 46.
<i>Dinoroseobacter</i> (AHL)	V. Thiel et al., <i>ChemBioChem</i> (2009), 10.	<i>Proteus</i> (AI-2)	R. Schneider et al., <i>Microbiology</i> (2002), 148.	<i>Xanthomonas</i> (DSF)	J D. Shrout et al., <i>ES&amp;T</i> (2012), 46.
<i>Enterobacter</i> (AHL)	S. Lim et al., <i>Desalination</i> (2012), 287	<i>Pseudoalteromonas</i> (AHL)	Y. Wang et al., <i>Biosci. Biotechnol. Biochem</i> (2008), 72.	<i>Yersinia</i> (AHL)	M. B. Miller et al., <i>Annu. Rev. Microbiol.</i> (2001), 55.
<i>Enterococcus</i> (AI-2)	C. Shao et al., <i>J. Proteome Res.</i> , (2012), 11.	<i>Pseudomonas</i> (AHL, PQS)	J D. Shrout et al., <i>ES&amp;T</i> (2012), 46. Spoering and Gilmore et al., <i>Curr Opin Microbiol</i> , (2006) 9		

## V.3. Results and discussion

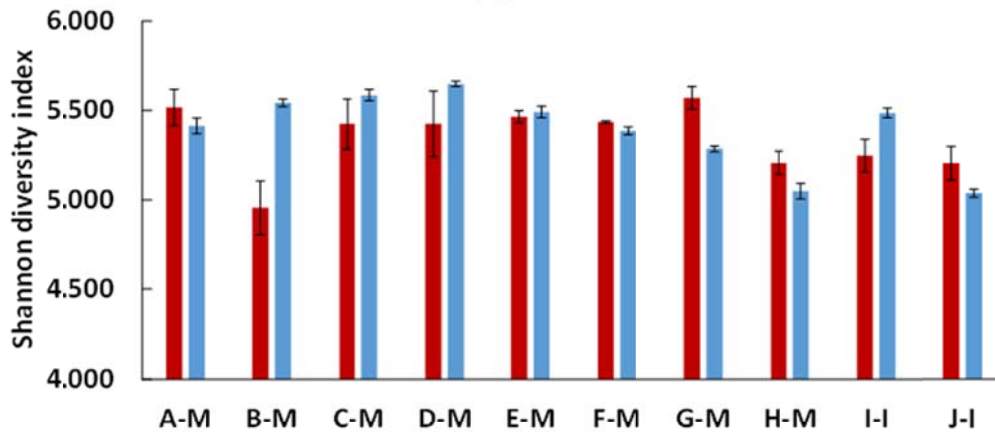
### V.3.1. Community diversity

Chao1 richness estimates, Shannon diversity indices and Shannon evenness were estimated at the sequence divergence of 3% (Figure V-1). Statistical analysis (RCBD) showed that the community diversity measures (richness, diversity and evenness) differed among MBRs (Table V-3,  $p < 0.05$ ), whereas did not differ between the biofilm and the activated sludge. This result indicated that diversity was different among the MBRs, and that the biofilm community diversity was similar to that of the activated sludge in each MBR. This result differs from previous observation on single MBR that revealed a difference of diversity between the biofilm and activated sludge (Gao et al. 2014a). It is speculated that microbial growth may not be different in the reactor and on the membrane with regards to the growth nature, i.e., both floc and biofilm result from microbial aggregates (Laspidou and Rittmann 2002, Sheng et al. 2010). In addition, the relationships between the diversity measures and the 10 environmental factors (e. g., flux, MLSS in the membrane tank, HRT in the membrane tank, F/M ratio,  $SAD_m$ , average temperature in the membrane tank, BOD, COD, TN and TP) were determined using the Spearman correlation (Table V-4). Only temperature (ranging of 13.1 to 22.0°C) was significantly correlated with the Chao 1 richness (a Spearman correlation coefficient of -0.63 with  $p < 0.05$ ), which indicated that an increase in temperature reduced the number of community members. In general, microbes can be classified as mesophiles, psychrophiles, and thermophiles by growth temperature optima (Slonczewski and Foster 2013). For instance, psychrophiles

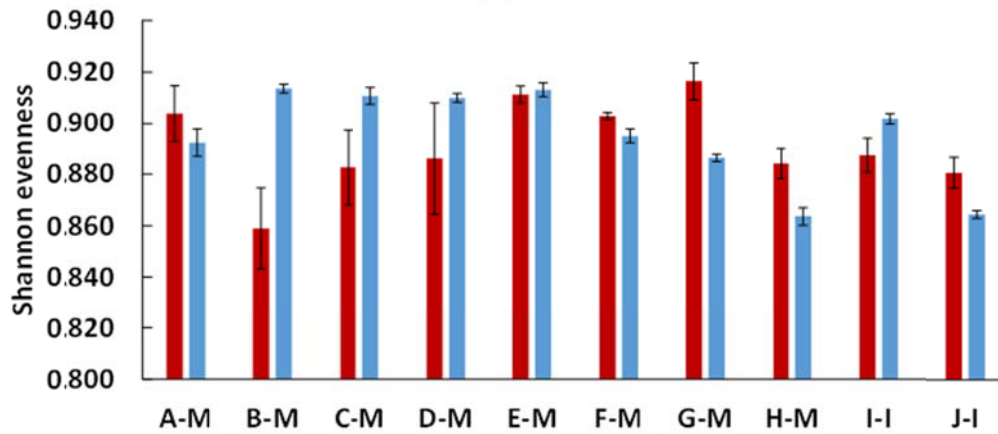
grow at a temperature range of 0 to 20°C, and their optimum growth temperature is usually approximately 15°C. The temperature transition from 13.1 to 22.0°C might reduce the community richness because psychrophiles are likely to be adversely affected over this temperature range. Levén et al. (2007) reported that different temperatures (37°C and 55°C) affected the species richness and the phylogenetic distribution of the microbial populations in a methanogenic bioreactor. Ma et al. (2013) observed that the microbial composition was changed by a temperature variation (ranging of 8.7 to 19.7°C) in a single MBR. Thus, temperature is one of the main environmental factors affecting the microbial community.



(a)



(b)



(c)

Figure V-1. Microbial community of biofilm and activated sludge richness (a), diversity (b), and evenness (c) (n=3).

**Table V-3. Statistical analysis of community diversity using completely randomized block design (block, MBR; and treatment, biofilm and activated sludge).**

	Degree of freedom	Sum of square	Mean of square	F-value	p-value
Response: Chao 1 richness					
Treatment	1	8057	8057	1.3755	0.2465
<b>Block</b>	<b>9</b>	<b>1033955</b>	<b>114884</b>	<b>19.6130</b>	<b>&lt; 0.05</b>
Residuals	49	287020	5858		
Response: Shannon diversity indices					
Treatment	1	0.03298	0.032976	1.4179	0.2395
<b>Block</b>	<b>9</b>	<b>1.21978</b>	<b>0.135531</b>	<b>5.8275</b>	<b>&lt; 0.05</b>
Residuals	49	1.13960	0.023257		
Response: Shannon evenness					
Treatment	1	0.0002004	0.00020039	0.8176	0.3703
<b>Block</b>	<b>9</b>	<b>0.0082281</b>	<b>0.00091421</b>	<b>3.7302</b>	<b>&lt; 0.05</b>
Residuals	49	0.0120093	0.00024509		

**Table V-4. Spearman correlation coefficient ( $\rho$ ) between community diversity (richness, diversity, evenness) and MBR operation factors.**

Environmental factors	Chao1 richness		Shannon diversity		Shannon evenness	
	Correlation coefficient ( $\rho$ )	p-value	Correlation coefficient ( $\rho$ )	Correlation coefficient ( $\rho$ )	p-value	Correlation coefficient ( $\rho$ )
Flux (LMH)	-0.15	0.25	-0.12	0.35	-0.09	0.51
MLSS in the membrane tank (mg/L)	-0.31	<0.05	-0.21	0.11	-0.08	0.54
HRT in the membrane tank (h)	0.47	<0.05	0.28	<0.05	0.09	0.48
F/M ratio (kgBOD/kgMLSS•day)	-0.32	<0.05	-0.17	0.19	0.03	0.82
SAD <sub>m</sub> (m <sup>3</sup> /m <sup>2</sup> •h)	0.09	0.49	0.04	0.74	0.04	0.76
<b>AVG. temperature (°C) in the membrane tank</b>	<b>-0.63</b>	<b>&lt;0.05</b>	-0.47	<0.05	-0.26	<0.05
BOD(mg/L)	-0.31	<0.05	-0.22	0.08	-0.11	0.42
COD(mg/L)	-0.23	0.08	-0.35	<0.05	-0.34	<0.05
TN(mg/L)	-0.29	<0.05	-0.21	0.11	-0.03	0.79
TP(mg/L)	-0.41	<0.05	-0.37	<0.05	-0.21	0.11

## **V.3.2. Microbial community composition in 10 MBRs**

### **V.3.2.1. The difference of bacterial composition between biofilm and activated sludge**

A clustering analysis was performed using the Yue & Clayton index which reflects the proportions of both shared and non-shared species in each community (Yue and Clayton 2005). Figure V-2 shows eleven distinct clusters. Microbial communities from each MBR were clustered together, except for B-M for which the biofilm and activated sludge communities were distinct. In the nine MBRs, biofilm and activated sludge were differently clustered. These results indicate that the bacterial community evolves differently in the membrane biofilm despite the similar community diversity. However, it was apparent that the microbial community of the membrane biofilm resembled that of the activated sludge in the MBRs.

A principal coordinate analysis (PCoA) was conducted to investigate the similarity of the bacterial communities (Figure V-3). A statistical analysis (RCBD) was performed on the values of the PCoA axis 1 to determine whether the communities were similar among the MBRs and between the biofilm and activated sludge. The results indicated that the microbial communities differed significantly among the MBRs as well as between the biofilm and activated sludge (Table V-5,  $p < 0.05$ ). This result suggests that the microbial community develops differently in biofilm, compared with the activated sludge, and it is consistent with previous studies on a single MBR. For instance, previous studies have found the microbial composition of membrane biofilm to be different from that of activated sludge

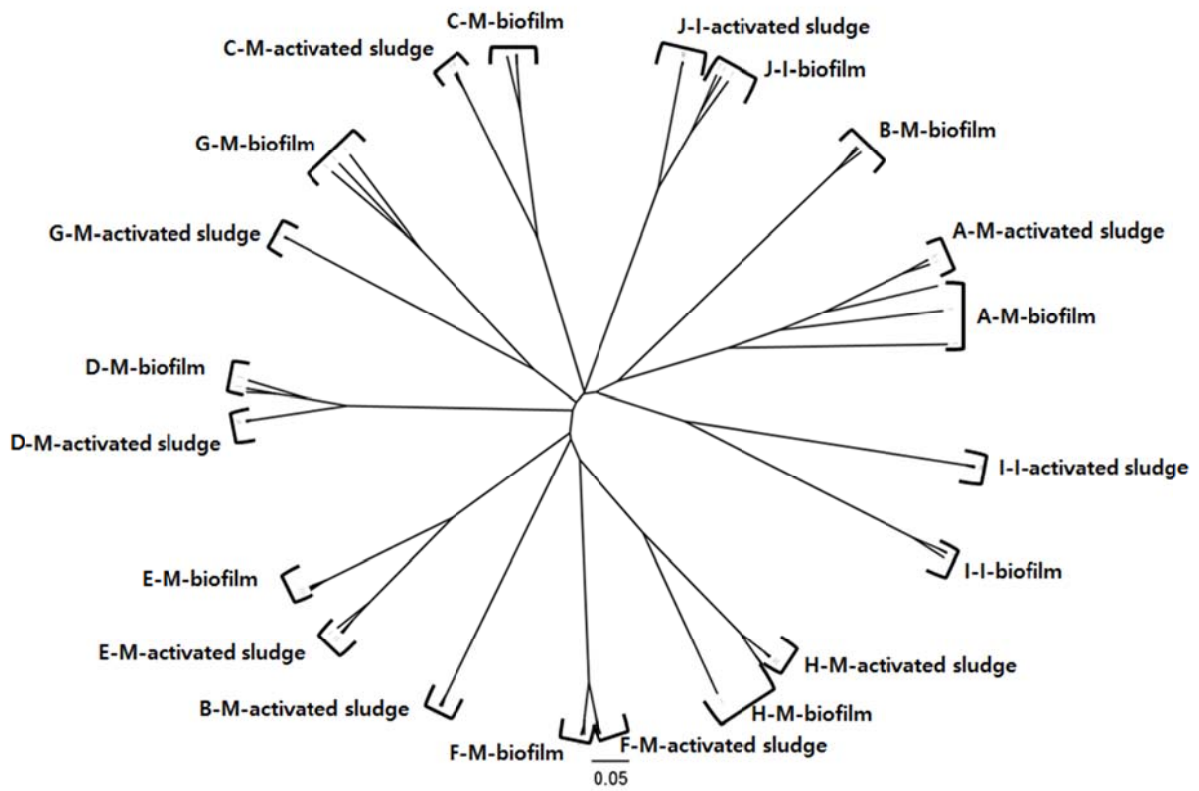


**Figure V-2. Cluster analysis of biofilm and activated sludge from MBRs. (0.05: distance of similarity).**

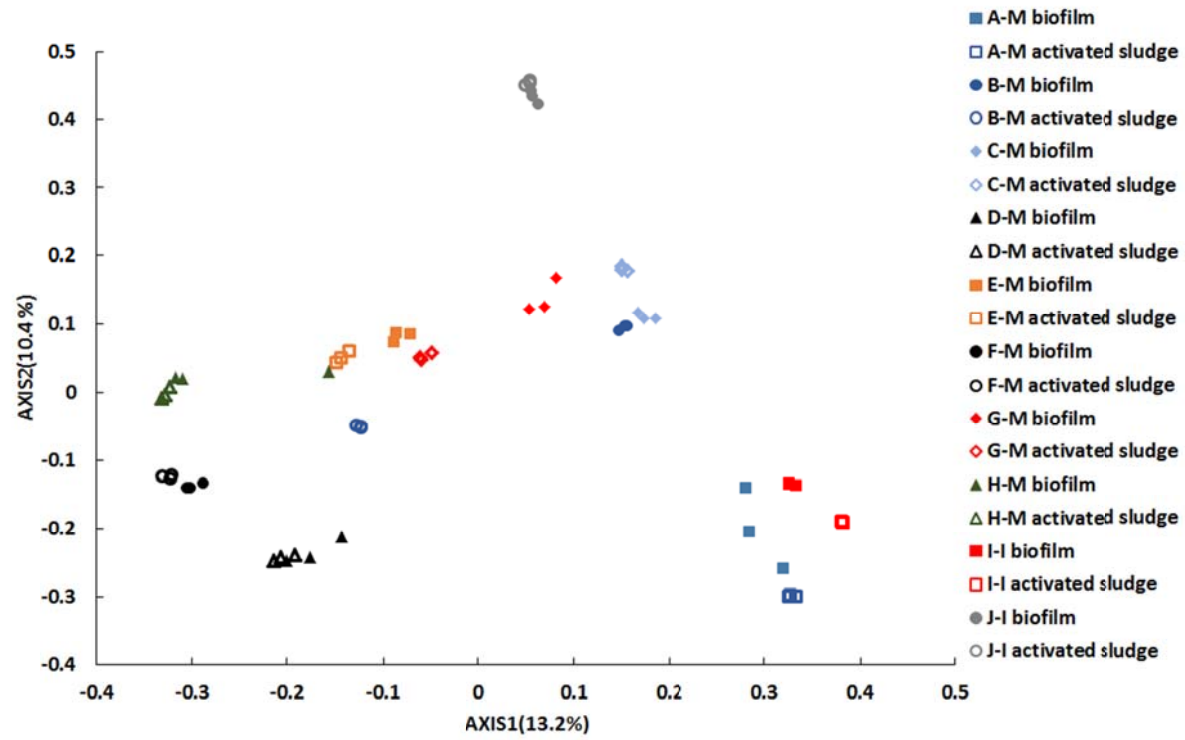


Figure V-3. The principal coordinate analysis of biofilm and activated sludge.

**Table V-5. Statistical analysis of the bacterial composition (the value of PCoA axis 1 in Fig. III-3) using completely randomized block design (block, MBR; and treatment, biofilm and activated sludge).**

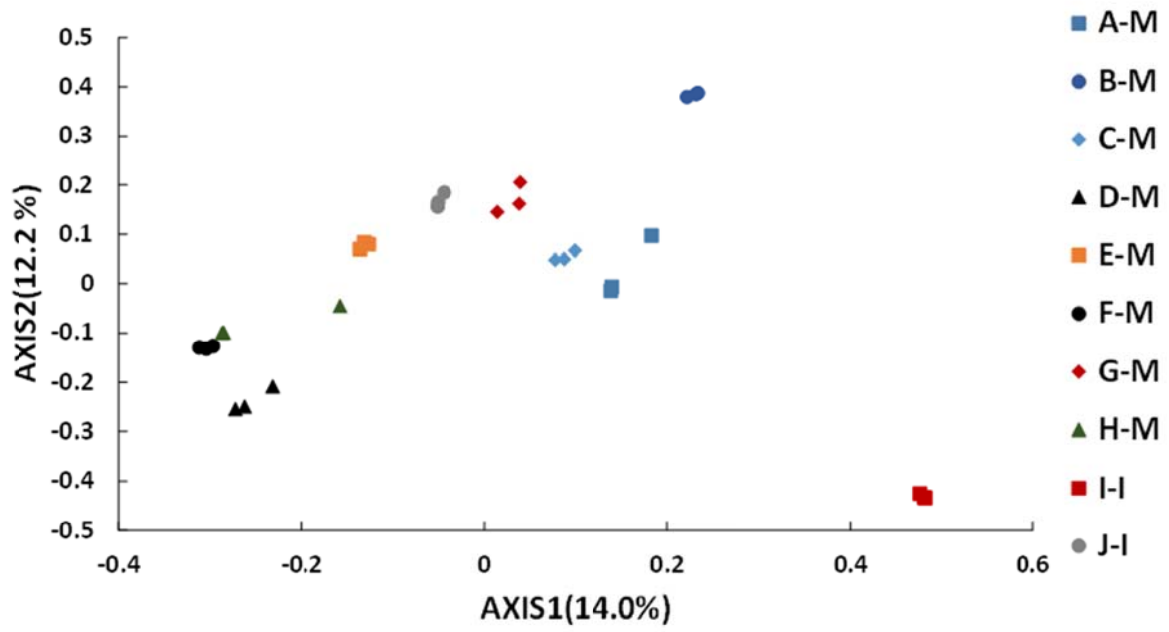
Response: The value of PCoA axis 1					
	Degree of freedom	Sum of square	Mean of square	F-value	p-value
<b>Treatment</b>	<b>1</b>	<b>0.04185</b>	<b>0.4185</b>	<b>14.833</b>	<b>&lt; 0.05</b>
<b>Block</b>	<b>9</b>	<b>2.91211</b>	<b>0.32357</b>	<b>114.699</b>	<b>&lt; 0.05</b>
Residuals	49	0.13823	0.00282		

(Miura et al. 2007a, Lim et al. 2012).

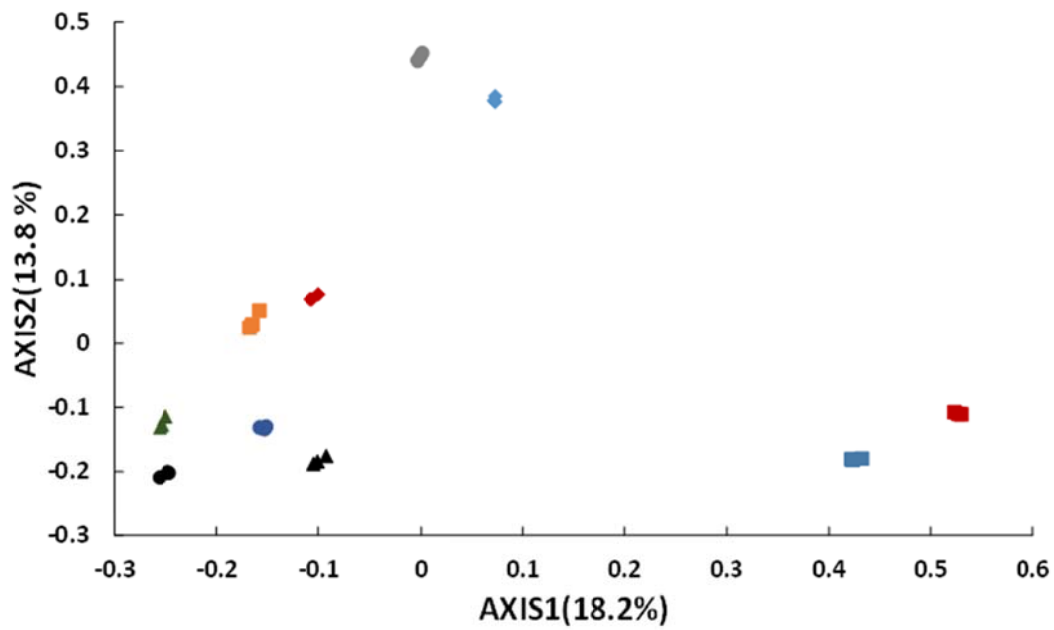
### **V.3.2.2. Effect of environmental factors on the bacterial composition in MBRs**

A PCoA was conducted on the biofilm and activated sludge communities (Figure V-4). The relationships between the bacterial communities and 11 environmental factors were investigated using the Spearman correlation (Table V-6). The MLSS in the membrane tank (3,887 ~ 10,213 mg/L), HRT in the membrane tank (2.7 ~ 51.7 h), F/M ratio (0.01 ~ 0.24 kgBOD/kgMLSS•day) and  $SAD_m$  (0.15 ~ 1.7  $Nm^3/m^2 \cdot hr$ ) were significantly correlated with the values of the biofilm PCoA axis 1. In contrast, the concentration of MLSS had an effect on both the biofilm and activated sludge communities.

In activated sludge, MLSS comprises microorganisms and non-viable organic materials (Vukovic et al. 2006). Previous studies have shown that MLSS concentrations are correlated with the abundances of specific microorganisms. For instance, Miura et al. (2007b) reported that the *Chloroflexi* was more abundant at a higher concentration of MLSS in an MBR. The MLSS determines the concentration of dissolved oxygen (DO) in the MBR due to the respiration rate; consequently, it can determine the composition of the microbial community (Meng et al. 2007b and Gao et al. 2011), which in part explains the variation. Activated sludge acts as the inoculum for the biofilm formed on the membrane and can probably interact with the biofilm in various ways. Thus, the concentration of MLSS in the membrane tank had an effect on not only the bacterial composition of



(a) Biofilm



(b) Activated sludge

Figure V-4. The principal coordinate analysis of biofilm (a) and activated sludge (b).

**Table V-6. Spearman correlation coefficient ( $\rho$ ) between PCoA axis 1 in Fig. V-4 and environmental factors.**

Environmental factors	Biofilm		Activated sludge	
	Correlation coefficient ( $\rho$ )	p-value	Correlation coefficient ( $\rho$ )	p-value
Flux (LMH)	0.04	0.82	0.19	0.32
<b>MLSS in the membrane tank (mg/L)</b>	<b>-0.79</b>	<b>&lt; 0.05</b>	<b>-0.67</b>	<b>&lt; 0.05</b>
<b>HRT in the membrane tank (h)</b>	<b>0.59</b>	<b>&lt; 0.05</b>	0.36	0.05
<b>F/M ratio (kgBOD/kgMLSS•day)</b>	<b>-0.51</b>	<b>&lt; 0.05</b>	-0.46	< 0.05
<b>SAD<sub>m</sub> (m<sup>3</sup>/m<sup>2</sup>•h)</b>	<b>0.55</b>	<b>&lt; 0.05</b>	0.27	0.15
AVG. temperature (°C) in the membrane tank	-0.32	0.08	-0.30	0.11
BOD(mg/L)	-0.49	< 0.05	-0.45	< 0.05
COD(mg/L)	-0.23	0.23	-0.28	0.13
TN(mg/L)	-0.13	0.49	-0.24	0.20
TP(mg/L)	0.02	0.91	0.10	0.61

activated sludge but also the bacterial composition of the biofilm.

A previous study reported the important role of HRT in MBRs (Meng et al. 2007a) where decreasing HRT favors the growth of filamentous bacteria which have an ability to adhere and penetrate between the membrane and membrane foulants. Thus, filamentous bacteria can contribute to the change in bacterial composition in biofilm. A Spearman correlation test was conducted to investigate the relationship between the relative abundances of the dominant filamentous bacteria in the biofilm and HRT in the membrane tank (Table V-7). *Caldilinea* (a Spearman correlation coefficient of -0.71) and *Gordonia* (-0.67) were negatively correlated with HRT in the membrane tank ( $p < 0.05$ ) but not in the other one. An increase in *Caldilinea* and *Gordonia* was coincided with a decrease in HRT in the membrane tank, suggesting that HRT in the membrane tank can favor growths of specific filamentous bacteria, resulting in a change in the bacterial community.

The F/M ratio is an important factor for controlling biomass characteristics. The previous study reported that an increase in the F/M ratio (from 0.33 to 0.52 gCOD/gVSS•day) had an effect on the microbial communities in both the biofilm and activated sludge in a single MBR (Xia et al. 2010). However, the F/M ratio could not explain the variation of bacterial composition in activated sludge, whereas it could explain the variation in the biofilm in this study. The difference between our survey and the previous study may have been caused by the different ranges in F/M ratio (0.01 to 0.24 kgBOD/kgMLSS•day) and the system operation parameters, such as MLSS, HRT, MBR process, aeration rate, SRT, and so on.

**Table V-7. The relative abundances (%) of the bacterial phylotypes of filamentous bacteria (*Caldilinea*, *Haliscomenobacter* and *Gordonia*) and the Spearman correlation coefficient ( $\rho$ ) between the relative abundance (%) of filamentous bacteria and the HRT in the membrane tank (hr).**

	<i>Caldilinea</i>	<i>Haliscomenobacter</i>	<i>Gordonia</i>	
Correlation coefficient ( $\rho$ )	<b>-0.71</b>	-0.15	<b>-0.67</b>	
p-value	<b>&lt;0.05</b>	0.42	<b>&lt;0.05</b>	
Sample name	relative abundances (%) of bacterial phylotypes			HRT in the membrane tank
A-M1	0.92	2.89	0.05	44.8
A-M2	0.58	1.67	0.02	44.8
A-M3	0.68	2.35	0.05	44.8
B-M1	0.21	0.96	0.00	51.7
B-M2	0.09	0.99	0.00	51.7
B-M3	0.08	0.72	0.00	51.7
C-M1	1.34	2.32	0.48	18.3
C-M2	1.50	2.44	0.45	18.3
C-M3	1.37	1.81	0.59	18.3
D-M1	2.60	0.43	0.29	13.1
D-M2	2.61	0.73	0.24	13.1
D-M3	2.28	0.87	0.20	13.1
E-M1	1.76	1.09	1.35	4.5
E-M2	1.53	1.11	1.18	4.5
E-M3	1.19	1.16	1.76	4.5
F-M1	4.51	0.86	0.28	3.4
F-M2	5.00	0.43	0.37	3.4
F-M3	3.88	0.91	0.39	3.4
G-M1	1.00	1.20	5.49	5.5
G-M2	1.66	0.97	5.36	5.5
G-M3	1.47	1.17	3.17	5.5
H-M1	1.02	1.56	0.42	8.8
H-M2	1.38	4.18	0.43	8.8
H-M3	1.13	3.87	0.44	8.8
I-I1	0.17	0.22	0.00	9.12
I-I2	0.10	0.09	0.00	9.12
I-I3	0.12	0.09	0.00	9.12
J-I1	3.56	4.18	5.44	2.7
J-I2	2.79	6.14	2.86	2.7
J-I3	3.42	3.94	3.28	2.7

The  $SAD_m$  can affect the bacterial composition in biofilm because the main role of  $SAD_m$  is to detach microbes and membrane foulants from the membrane surface. Thus, it is speculated that the different  $SAD_m$  in each MBR had an effect on the initial attachment of microbes on the membrane surface and changed the bacterial composition of the biofilm. For example, Miura et al. (2007a) reported that the relative abundance of *Betaproteobacteria* significantly increased and became most dominant in biofilm after the aeration rate increased from 3,500 to 5,000 L/h in a single MBR.

In addition to the operational factors, membrane materials can affect the bacterial composition of biofilm by themselves (Lee et al. 2014). The results of the Tukey-Kramer test (Table V-8) indicated that the difference in the bacterial composition of biofilm could not be fully explained by the membrane materials. Thus, membrane materials are not an important factor affecting the microbial composition in the biofilm in this study.

**Table V-8. Statistical analysis of the effect of membrane materials on the bacterial composition of biofilm using the Tukey-Kramer test (membrane, PE, PTFE, PVDF and c-PVC; and bacterial composition of biofilm, the value of PCoA axis 1 in Fig. III-4 (a)).**

The bacterial composition of PVDF was significantly different from PTFE and the bacterial composition of c-PVC was significantly different from PVDF ( $p < 0.05$ ). In contrast, the difference in the bacterial composition of PE with other materials was not significant, and the bacterial composition of c-PVC was not significantly different from PTFE.

Comparisons	The pairwise mean differences	Lower confidence interval values	Upper confidence interval values	Significance
PTFE - PE	0.1366	-0.0849	0.3581	Non-sig.
PVDF - PE	-0.0942	-0.3150	0.1266	Non-sig.
c-PVC - PE	0.1155	-0.1702	0.4013	Non-sig.
<b>PVDF – PTFE</b>	<b>-0.2308</b>	<b>-0.2553</b>	<b>-0.2062</b>	<b>Sig.</b>
c-PVC - PTFE	-0.0211	-0.2026	0.1605	Non-sig.
<b>c-PVC - PVDF</b>	<b>0.2097</b>	<b>0.0223</b>	<b>0.3971</b>	<b>Sig.</b>

### **V.3.2.3. Relative composition of QS related bacteria**

In the previous section, the environmental factors are important to control biofouling in MBRs. However, the reduction of energy consumption, the plant productivity and the effluent quality are constantly magnified as issues in MBRs. Aeration capacity, reactor size, process stability or life cycle cost are considered as an important factor for MBR design (Hai et al. 2013). Thus, the environmental factors limited the biofouling mitigation. In this study, the proportion of known quorum sensing bacterial genera ranged 1.4 to 11.6% in biofilm and 3.2 to 12.1% in activated sludge (Figure V-5). As potential quorum sensing bacteria existed in both the biofilm and activated sludge, quorum quenching is expected to be one of effective methods for mitigating biofouling in MBRs.

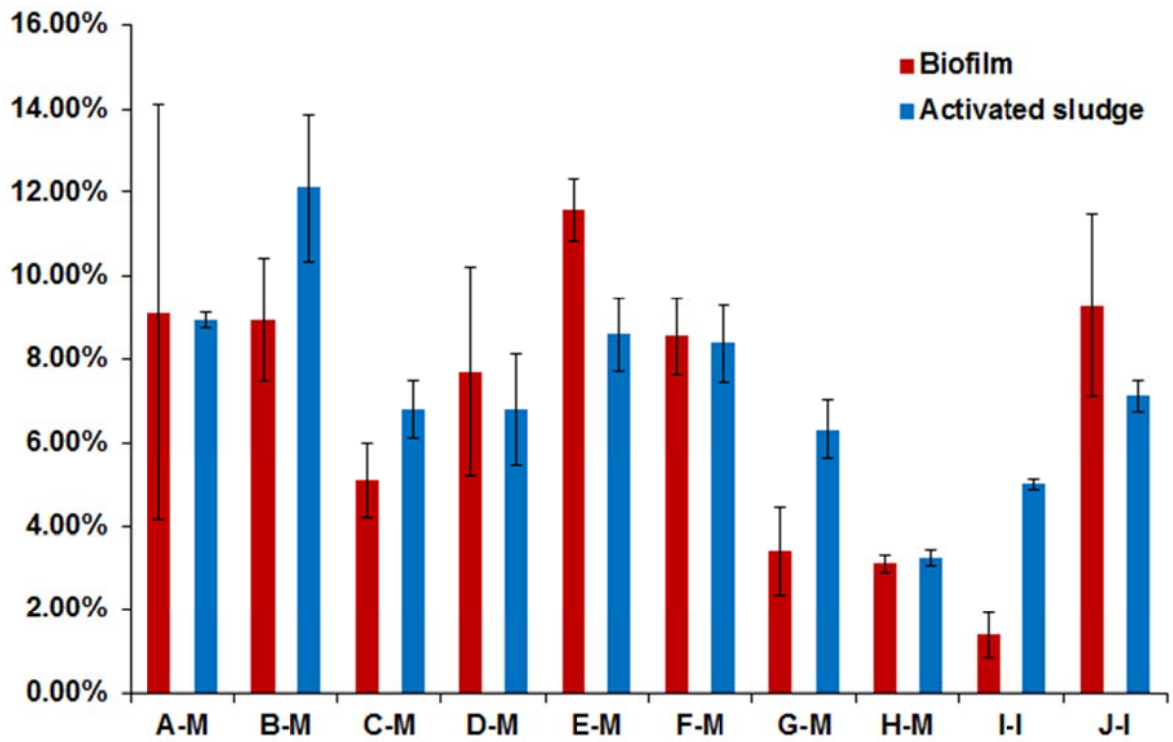


Figure V-5. Average relative abundances (%) of quorum sensing related bacteria by bacterial phlotypes in the MBR (n = 3, error bar; standard deviation).

### V3.2.4 Relative abundance of bacterial phylotypes in MBRs

A phylotype analysis was performed (Figure V-6, Table V-9 and Table V-10). The phyla *Proteobacteria* and *Bacteroidetes* were most dominant in both the biofilm and activated sludge, which is consistent with previous observations that showed *Proteobacteria* to be a dominant phylum in biofilm and activated sludge (Miura et al. 2007a, Lim et al. 2012 and Kim et al. 2013a).

The bacterial genera are listed in order of abundance in Tables V-9 and V-10. The genera *Flavobacterium*, *Dechloromonas*, *Nitrospira*, *Caldilinea* and *Haliscomenobacter* were dominant in biofilm (Table V-9), whereas *Dechloromonas*, *Flavobacterium*, *Haliscomenobacter*, *Nitrospira* and *Rhodobacter* were dominant in activated sludge (Table V-10). These bacterial genera commonly existed in the biofilm and activated sludge. Although fifteen out of the twenty genera were found in both biofilm and activated sludge, the order of genera in the biofilm differed from that in the activated sludge. This result demonstrates that although the microbial community of the biofilm was similar to that of the activated sludge, the bacterial composition of the biofilm differed from that of the activated sludge in the MBRs.

*Flavobacterium* has been isolated from the biofilms of diseased fishes, domestic drain conduits and potable dental lines (Basson et al. 2008). *Flavobacterium* was isolated from full-scale, reverse-osmosis membranes using selective culture media (Herzberg et al. 2010). Members of this genus appeared to have a strong floc-forming ability and utilize a wide variety of organic compounds, which enable them to become the predominant bacterial members in the activated

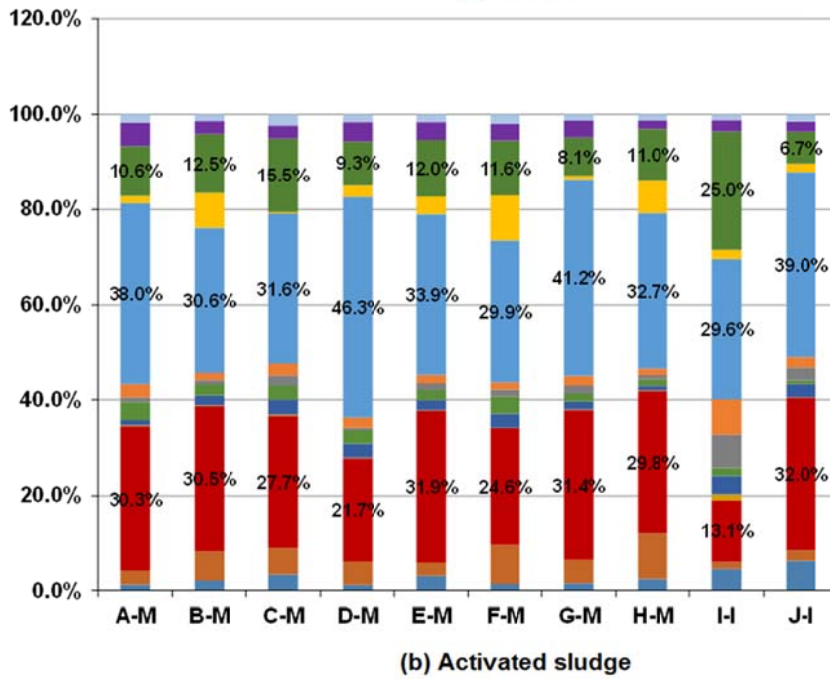
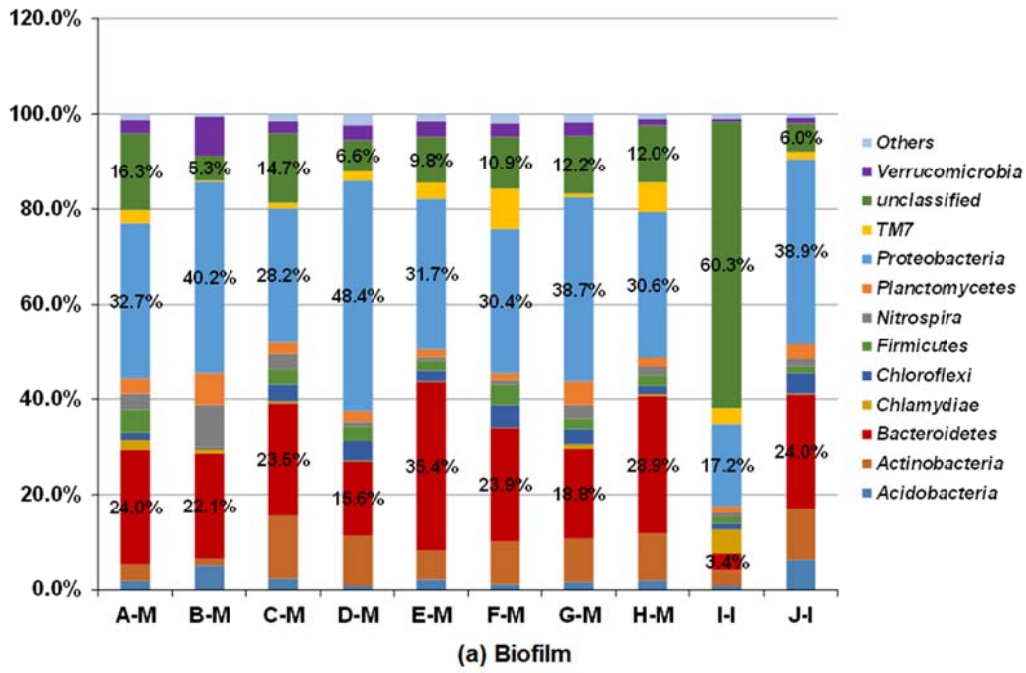


**Figure V-6.** Average relative abundances (%) of bacterial phylotypes in biofilm (a) and activated sludge (b) (n = 3). All sequences were phylogenetically classified at the phylum level. A phylum composing less than 2% of the total composition in the samples was classified as “others”.

**Table V-9. Average relative abundances (%) of the bacterial phylotypes in the biofilm (n = 3).**

Rank	genus	A-M	B-M	C-M	D-M	E-M	F-M	G-M	H-M	I-I	J-I
1	<i>Flavobacterium</i>	5.17	3.31	1.35	2.32	7.31	3.38	1.33	0.23	0.06	1.16
2	<i>Dechloromonas</i>	0.58	0.14	0.47	9.75	1.25	3.33	0.48	3.21	0.06	1.36
3	<i>Nitrospira</i>	3.46	8.75	3.24	0.93	0.76	0.94	2.90	1.67	1.00	1.65
4	<i>Caldilinea</i>	0.73	0.13	1.40	2.47	1.49	4.45	1.40	1.17	0.13	3.29
5	<i>Haliscomenobacter</i>	2.30	0.89	2.20	0.70	1.12	0.74	1.11	3.20	0.13	4.69
6	<i>Iamia</i>	0.60	0.24	9.38	2.11	0.30	0.48	0.28	0.67	0.12	0.23
7	<i>Rhodobacter</i>	0.27	2.26	0.63	1.80	1.22	1.70	0.83	1.05	0.10	1.25
8	<i>Gordonia</i>	0.04	0.00	0.50	0.24	1.42	0.35	4.64	0.43	0.00	4.00
9	<i>Trichococcus</i>	1.59	0.00	1.69	1.58	0.77	2.08	0.09	0.21	0.05	0.50
10	<i>Ferruginibacter</i>	0.54	0.24	0.30	0.33	1.58	2.70	1.57	0.83	0.01	0.09
11	<i>Dokdonella</i>	0.14	0.01	0.95	3.80	0.07	0.73	0.14	1.42	0.01	0.03
12	<i>Prostheco bacter</i>	0.17	5.71	0.46	0.53	0.54	0.81	0.15	0.52	0.06	0.10
13	<i>Novosphingobium</i>	0.23	1.71	0.48	0.78	0.39	0.88	0.09	1.03	0.04	2.23
14	<i>Mycobacterium</i>	0.23	0.05	0.06	0.52	0.52	0.19	0.61	0.74	2.38	1.80
15	<i>Planctomyces</i>	0.29	1.94	0.29	0.45	0.28	0.37	2.58	0.30	0.09	1.04
16	<i>Acinetobacter</i>	0.57	0.00	0.59	0.16	1.12	0.86	0.06	0.07	0.62	2.29
17	<i>Ilumatobacter</i>	0.06	0.13	1.43	0.29	0.40	1.29	0.68	1.25	0.11	0.19
18	<i>Rickettsia</i>	0.05	0.01	0.00	4.65	0.01	0.00	0.01	0.00	0.00	0.00
19	<i>Steroidobacter</i>	0.63	0.42	0.62	0.58	0.24	0.12	2.02	0.26	0.23	0.72
20	<i>Arcobacter</i>	0.59	0.01	0.48	0.58	0.72	1.02	0.57	0.27	0.35	0.11

**All sequences were phylogenetically classified at the genus level. Only phylotypes with a genus level observed in either library are shown.**

**Table V-10. Average relative abundances (%) of the bacterial phylotypes in the activated sludge (n = 3).**

Rank	genus	A-M	B-M	C-M	D-M	E-M	F-M	G-M	H-M	I-I	J-I
1	<i>Dechloromonas</i>	1.60	3.16	0.37	8.99	2.16	2.82	2.60	3.89	0.40	1.72
2	<i>Flavobacterium</i>	2.65	7.87	1.81	1.21	3.17	3.28	2.63	0.18	0.34	0.62
3	<i>Haliscomenobacter</i>	4.81	1.43	2.33	1.23	1.11	0.68	1.71	4.13	0.76	5.71
4	<i>Nitrospira</i>	1.01	0.89	2.11	0.58	1.42	1.45	1.66	0.92	6.91	2.72
5	<i>Rhodobacter</i>	0.40	1.75	1.04	1.38	2.09	1.85	1.45	0.81	0.54	1.02
6	<i>Ferribacterium</i>	1.02	0.55	2.48	0.36	0.73	0.01	5.35	0.63	0.00	0.00
7	<i>Caldilinea</i>	0.37	0.84	1.04	1.42	1.05	2.64	0.89	0.65	0.65	1.94
8	<i>Novosphingobium</i>	0.68	0.62	0.35	1.01	0.82	1.46	0.43	1.41	0.25	3.36
9	<i>Arcobacter</i>	1.46	0.89	1.50	1.42	1.15	0.80	0.85	0.44	0.48	0.24
10	<i>Iamia</i>	0.36	0.92	3.73	0.78	0.18	0.27	0.37	0.25	0.36	0.12
11	<i>Ferruginibacter</i>	0.25	0.91	0.63	0.43	0.86	2.72	0.84	0.99	0.02	0.09
12	<i>Dokdonella</i>	0.06	0.29	1.19	3.99	0.04	0.61	0.36	1.38	0.01	0.00
13	<i>Opitutus</i>	2.24	0.52	0.48	0.72	0.61	0.83	1.09	0.38	0.64	0.36
14	<i>Perlucidibaca</i>	4.10	0.91	0.38	0.74	0.41	0.35	0.44	0.16	0.11	0.13
15	<i>Trichococcus</i>	0.59	0.77	1.34	0.82	0.86	1.71	0.36	0.13	0.16	0.14
16	<i>Propionivibrio</i>	0.27	1.55	0.15	0.97	0.58	0.87	0.51	1.98	0.01	0.16
17	<i>Bdellovibrio</i>	0.99	0.35	0.32	0.49	0.65	0.38	0.48	0.36	1.78	0.51
18	<i>Acinetobacter</i>	0.27	0.33	0.54	0.10	0.72	0.48	0.28	0.07	2.92	0.43
19	<i>Prostheco bacter</i>	0.45	0.55	0.63	1.03	0.31	0.88	0.29	0.76	0.12	0.25
20	<i>Steroidobacter</i>	0.49	0.22	0.50	0.55	0.28	0.12	0.39	0.29	1.02	1.09

**All sequences were phylogenetically classified at the genus level. Only phylotypes with a genus level observed in either library are shown.**

sludge (Zhao et al. 2014). *Flavobacterium* dominated both the biofilm and activated sludge because they contributed to the development of the biofilm and the floc formation. *Dechloromonas* is the dominant bacteria in activated sludge. This result is consistent with previous results. For instance, Zhang et al. (2012) reported that *Dechloromonas* was one of the dominant bacteria in activated sludge, and it had the role of reducing perchlorate and accumulating phosphate in enhanced biological phosphorus removal reactors. *Caldilinea* and *Haliscomenobacter* were reported as bulking and forming bacteria in activated sludge (Guo and Zhang 2012). Sludge bulking is believed to be one of the causal agents in membrane fouling because filamentous bacteria can easily attach to the membrane surface due to the EPS production, lower zeta potential, and higher hydrophobicity of sludge flocs (Meng et al. 2006). Thus, it was speculated that *Caldilinea* and *Haliscomenobacter* were dominant in the biofilm because they have an ability to attach to the membrane surface. *Nitrospira* oxidized nitrite to nitrate in a nitrification process (Chang et al. 2011). The relative abundance of *Nitrospira* was higher in the biofilm than in the activated sludge. This result is consistent with a previous study reporting that *Nitrospira* was more enriched in the membrane biofilms in comparison with the activated sludge in a lab-scale MBR (Huang et al. 2008).

### V.3.3. Microbial network

#### V.3.3.1. Network description

A network analysis was applied to analyze the co-occurrence among microbes in the MBRs. The microbial co-occurrences are shown in Figure V-7 (*Rectangle*, environmental factors; *circle*, bacteria. The red color of the nodes indicates the number of connections to the nodes. *Solid edges* are positive associations, and *dashed edges* are negative associations ( $p < 0.05$ ). OTU was classified at the genus level, and the asterisk indicates that the OTU was assigned at the taxonomic classification level. *Node size* indicates the relative abundance of each OTU. The number in the parentheses indicates the assigned number of the OTU. A connection indicates a strong positive Spearman correlation coefficient if  $\rho > 0.75$  and negative Spearman correlation coefficient if  $\rho < -0.75$ ). The constructed biofilm network contains 61 nodes (53 OTUs and eight environmental factors) and 120 edges (connections among nodes), and the activated sludge network contains 84 nodes (75 OTUs and nine environmental factors) and 214 edges (Figure V-7). The positive interactions composed 92% of the total association in the biofilm network without environmental factors, which was 17% higher than that in the activated sludge network (75%). The difference in positive interactions with microbes between the biofilm and activated sludge may be one of the main reasons for the different bacterial composition between the biofilm and activated sludge.





The microbial networks without environmental factors were analyzed using the network analyzer tool to characterize network topology (Table V-11). The average clustering coefficient is the average fraction of the pairs of nodes one link away from a node that are also linked to one another (Steele et al. 2011). The average clustering coefficient of the activated sludge network was 0.313, which was similar to that of the biofilm network (0.314). The density (0-1 scale) shows how densely the network is populated with edges. The density of the activated sludge network was 0.064, whereas that of the biofilm network was 0.067. Thus, the activated sludge network and the biofilm network had a similar level of connected OTUs.

The network diameter suggests the largest distance between two nodes. The activated sludge network (network diameter 9) had a smaller network diameter than the biofilm network (network diameter 11). The average shortest path length (characteristic path length) of the activated sludge network (3.783) was shorter than that of the biofilm network (4.475). Thus, these structural properties indicated that the microbial community of activated sludge could be sensitive to perturbation i.e., environmental change. Zhou et al. (2010) reported that the rapid communication among different members within a system (short characteristic path length) could make quick responses to environmental changes such as elevated atmospheric CO<sub>2</sub> in soil microbial communities.

Network centralization (0-1 scale) is a simple and widely used index of the connectivity distribution (Dong and Horvath 2007). The network centralization of the activated sludge and biofilm network was 0.103 and 0.130, respectively. The

network heterogeneity suggests the tendency of a network to contain hub nodes (Kim et al. 2015b). The heterogeneity of the activated sludge network was 0.608, whereas that of the biofilm network was 0.663. These results indicated that the activated sludge network had a more evenly distributed connectivity than the biofilm network. Thus, the activated sludge network could be more robust towards hub node removal than the biofilm network. Jeong et al. (2001) reported that the deletion of a less connected node did not affect the overall topology of the network, whereas the deletion of the most connected node increased the network diameter in the protein network. In addition, Tanaka et al. (2012) reported that heterogeneous networks are extremely fragile to attacks targeted at hub nodes.

**Table V-11. Characteristics of the microbial association network without environmental factors in biofilm and activated sludge.**

	Biofilm	Activated sludge
Number of nodes	53	74
Number of edges	93	173
Number of positive edges	86	130
Number of negative edges	7	43
Average clustering coefficient	0.314	0.313
Network diameter	11	9
Average shortest path length (Characteristic path length)	4.475	3.783
Network density	0.067	0.064
Network centralization	0.130	0.103
Network heterogeneity	0.663	0.608

### **V.3.3.2. The role of OTUs with high relative abundance in microbial network**

The OTUs with high relative abundances are listed in order of abundance in Tables V-12 and V-13. These OTUs commonly existed in the biofilm and activated sludge. Fifteen out of the twenty OTUs were found in both the biofilm and activated sludge network. The excluded OTUs are considered to be less significantly associated in the microbial network. The OTUs with high relative abundances in the biofilm network composed 51% (47/93) of the associations with microbes, whereas the OTUs with high relative abundance in activated sludge network composed 43% (74/173) of the associations with microbes. Although OTUs with a high relative abundance were not fully associated with all of the microbes in the microbial network, they could play an important role in the microbial community, i.e., floc formation in activated sludge, nitrogen removal and phosphorus removal (Wagner and Loy 2002).

**Table V-12. Average relative abundances (%) of bacteria in the biofilm (n = 3).**

Rank	OTUs	Total	A-M	B-M	C-M	D-M	E-M	F-M	G-M	H-M	I-I	J-I
1	OTU 1 ( <i>Dechloromonas</i> )	2.20	0.52	0.09	0.33	9.31	1.07	3.34	0.49	3.54	0.05	0.82
2	OTU 2 ( <i>Nitrospira</i> )	1.56	2.63	7.88	1.03	0.63	0.65	0.92	1.64	1.27	0.12	1.42
3	OTU 15 ( <i>Gordonia</i> )	1.09	0.04	0.00	0.50	0.23	1.41	0.45	4.61	0.43	0.00	3.97
4	OTU 10 ( <i>Iamia</i> )	1.06	0.43	0.16	8.85	0.36	0.02	0.04	0.02	0.02	0.01	0.01
5	OTU 9 ( <i>Trichococcus</i> )	0.90	1.58	0.00	1.67	1.56	0.76	2.03	0.09	0.21	0.05	0.50
6	OTU 11 ( <i>Dokdonella</i> )	0.80	0.01	0.01	0.92	3.75	0.07	0.71	0.13	1.40	0.00	0.02
7	OTU 4 ( <i>Novosphingobium</i> )	0.77	0.21	1.45	0.54	0.76	0.67	1.04	0.15	1.16	0.04	1.89
8	OTU 5 ( <i>Rhodobacter</i> )	0.75	0.13	1.32	0.51	0.44	1.10	1.54	0.64	0.93	0.06	0.85
9	OTU 7 ( <i>Chitinophagaceae</i> )*	0.74	0.25	0.13	1.31	0.32	1.53	0.58	0.52	1.35	0.03	1.25
10	OTU 8 ( <i>Chitinophagaceae</i> )	0.74	0.36	0.00	0.34	0.01	0.04	0.04	0.12	2.23	0.02	5.30
11	OTU 3 ( <i>Intrasporangiaceae</i> )*	0.70	0.01	0.00	0.01	0.08	0.59	2.42	0.16	3.70	0.00	0.10
12	OTU 23 ( <i>Sphingomonadaceae</i> )*	0.69	0.02	2.67	0.12	0.09	2.81	0.17	0.05	0.07	0.01	0.79
13	OTU 17 ( <i>Bacteroidetes</i> )*	0.66	0.00	0.00	4.62	0.01	1.23	0.00	0.00	0.00	0.00	0.00
14	OTU 12 ( <i>TM7_genera_incertae_sedis</i> )*	0.65	0.00	0.00	0.01	0.01	1.06	2.25	0.31	1.90	0.00	0.71
15	OTU 43 ( <i>Rickettsia</i> )	0.59	0.00	0.00	0.00	4.64	0.01	0.00	0.00	0.00	0.00	0.00
16	OTU 16 ( <i>Haliscomenobacter</i> )	0.51	0.00	0.01	0.20	0.07	0.04	0.54	1.06	0.96	0.00	2.77
17	OTU 6 ( <i>Ferribacterium</i> )	0.51	0.51	0.03	2.42	0.32	0.57	0.03	0.61	0.50	0.00	0.00
18	OTU 53 ( <i>Flavobacterium</i> )	0.51	0.11	0.00	0.03	0.09	3.82	0.02	0.01	0.00	0.00	0.01
19	OTU 19 ( <i>TM7_genera_incertae_sedis</i> )*	0.51	0.00	0.00	0.05	0.00	0.98	3.23	0.04	0.00	0.00	0.00
20	OTU 20 ( <i>Gp4</i> )*	0.47	0.14	0.01	0.21	0.11	0.07	0.04	0.07	0.06	0.00	4.46

**Operational taxonomic units (OTUs) were determined at 3 % dissimilarity. OTUs were classified at the genus level, and**

**the asterisk indicates that the OTU was assigned at the taxonomic classification level.**

**Table V-13. Average relative abundances (%) of bacteria in the activated sludge (n = 3).**

Rank	OTUs	Total	A-M	B-M	C-M	D-M	E-M	F-M	G-M	H-M	I-I	J-I
1	OTU 1 ( <i>Dechloromonas</i> )	2.39	1.27	0.53	0.23	8.45	1.97	2.83	2.70	5.11	0.41	1.14
2	OTU 3 ( <i>Intrasporangiaceae</i> )*	1.43	0.00	2.78	0.00	0.17	0.91	4.68	0.48	6.04	0.00	0.08
3	OTU 6 ( <i>Ferribacterium</i> )	1.25	1.10	0.63	2.46	0.66	0.74	0.03	5.34	0.64	0.00	0.01
4	OTU 13 ( <i>Bacteroidetes</i> )*	1.19	0.00	0.00	4.10	0.00	0.27	0.01	0.51	0.17	0.00	5.48
5	OTU 4 ( <i>Novosphingobium</i> )	1.12	0.61	0.64	0.40	1.00	1.41	1.70	0.76	1.56	0.27	2.79
6	OTU 2 ( <i>Nitrospira</i> )	1.10	0.66	0.57	0.73	0.20	1.25	1.40	1.53	0.84	1.12	2.56
7	OTU 5 ( <i>Rhodobacter</i> )	1.06	0.11	1.52	0.90	0.58	1.99	1.70	1.29	0.79	0.19	1.00
8	OTU 14 ( <i>Saprospiraceae</i> )*	0.97	6.51	0.00	0.00	0.01	0.00	0.00	0.00	0.00	4.83	0.00
9	OTU 7 ( <i>Chitinophagaceae</i> )*	0.92	0.28	0.77	0.96	0.51	1.72	0.56	0.96	1.60	0.12	1.27
10	OTU 8 ( <i>Chitinophagaceae</i> )	0.92	0.15	0.00	0.57	0.01	0.04	0.04	0.07	2.68	0.18	5.66
11	OTU 12 ( <i>TM7_genera_incertae_sedis</i> )*	0.84	0.00	1.44	0.00	0.01	0.98	2.76	0.43	1.98	0.00	0.95
12	OTU 16 ( <i>Haliscomenobacter</i> )	0.81	0.00	0.34	0.15	0.21	0.05	0.57	1.32	1.06	0.00	4.52
13	OTU 11 ( <i>Dokdonella</i> )	0.76	0.02	0.29	1.17	3.91	0.04	0.57	0.34	1.35	0.00	0.00
14	OTU 26 ( <i>Bacteroidetes</i> )*	0.73	0.05	0.15	0.01	0.30	0.01	0.15	6.56	0.00	0.00	0.00
15	OTU 9 ( <i>Trichococcus</i> )	0.72	0.59	0.76	1.33	0.81	0.86	1.67	0.36	0.12	0.16	0.14
16	OTU 18 ( <i>unclassified</i> )*	0.67	0.38	0.53	0.87	0.27	1.92	0.37	0.76	0.61	0.00	0.35
17	OTU 21 ( <i>Flavobacterium</i> )	0.63	0.38	1.12	0.77	0.13	1.60	0.78	0.64	0.06	0.00	0.28
18	OTU 22 ( <i>Bacteroidetes</i> )*	0.62	0.00	0.00	0.00	0.00	1.88	0.00	1.01	2.93	0.00	0.10
19	OTU 25 ( <i>Dechloromonas</i> )	0.58	0.23	2.59	0.05	0.66	0.77	0.25	0.09	0.68	0.00	0.82
20	OTU 20 ( <i>Gp4</i> )*	0.58	0.12	0.25	0.46	0.18	0.14	0.06	0.02	0.06	0.00	4.37

**Operational taxonomic units (OTUs) were determined at 3 % dissimilarity. OTUs were classified at the genus level, and the asterisk indicates that the OTU was assigned at the taxonomic classification level.**

### V.3.3.3. Analysis of network hubs

Nodes with more than 10 edges were considered network hubs in this study because the node degree (the number of edges linked) ranged from 1 to 10 in the biofilm network and from 1 to 12 in the activated sludge. There was one microbial hub in the biofilm network (OTU 54 (*Gp4*)), whereas the activated sludge network contained five microbial hub nodes including OTU 12 (*TM7\_genera\_incertae\_sedis*), OTU 14 (*Saprospiraceae*), OTU 46 (*Flavobacterium*), OTU 69 (*Streptobacillus*) and OTU 111 (*Betaproteobacteria*). The hub nodes and their adjacent nodes are further described in Figure V-8. OTU 54 (*Gp4*) had 90% (9/10) of the positive associations with microbes. Although it had low relative abundance (0.20%), it was positively associated with high-relative-abundance bacteria species such as OTU 3 (*Intrasporangiaceae*), OTU 7 (*Chitinophagaceae*) and OTU 12 (*TM7\_genera\_incertae\_sedis*). Thus, it is speculated that OTU 54 (*Gp4*) plays a central role in the development of biofilm through the positive associations with high-relative-abundance bacteria.

In the activate sludge network, the hub nodes were positively (67%, 34/51) and negatively (33%, 17/51) associated with microbes. OTU 46 (*Flavobacterium*) was positively associated with another hub node, OTU 69 (*Streptobacillus*). It is noteworthy that although they did not have a high relative abundance, they were positively associated with microbes known to be related to the development of floc in MBRs, i.e., OTU 39 (*Caldilinea*), OTU 21 (*Flavobacterium*) and OTU 85 (*Flavobacterium*). As mentioned in a previous section, *Caldilinea*, as a filamentous bacteria, and *Flavobacterium* have a strong floc-forming ability and utilize a wide

variety of organic compounds in activated sludge. Thus, it is speculated that these two hub nodes involved the development of floc in activated sludge. Most of the negative associations (82%, 9/11) were connected with OTU 14 (*Saprospiraceae*). Because a negative correlation could indicate inhibition, it is speculated that OTU 14 (*Saprospiraceae*) disfavored the growth of nine adjacent microorganisms (nodes) for organic substrates. Moreover, it was negatively associated with another hub node, OTU 111 (*Betaproteobacteria*). OTU 14 (*Saprospiraceae*) had an effect on the adjacent nodes of OTU 111 (*Betaproteobacteria*). OTU 12 (*TM7\_genera\_insertae\_sedis*) had a high relative abundance (0.84%) and 70% (7/10) of the positive associations with microbes. It was positively associated with other high-relative-abundance bacteria such as OTU 3 (*Intrasporangiaceae*) and OTU 4 (*Novosphingobium*). OTU 12 (*TM7\_genera\_insertae\_sedis*) was supposed to contribute to a change in the microbial community of the activated sludge through the positive associations with high- and low-relative-abundance bacteria.

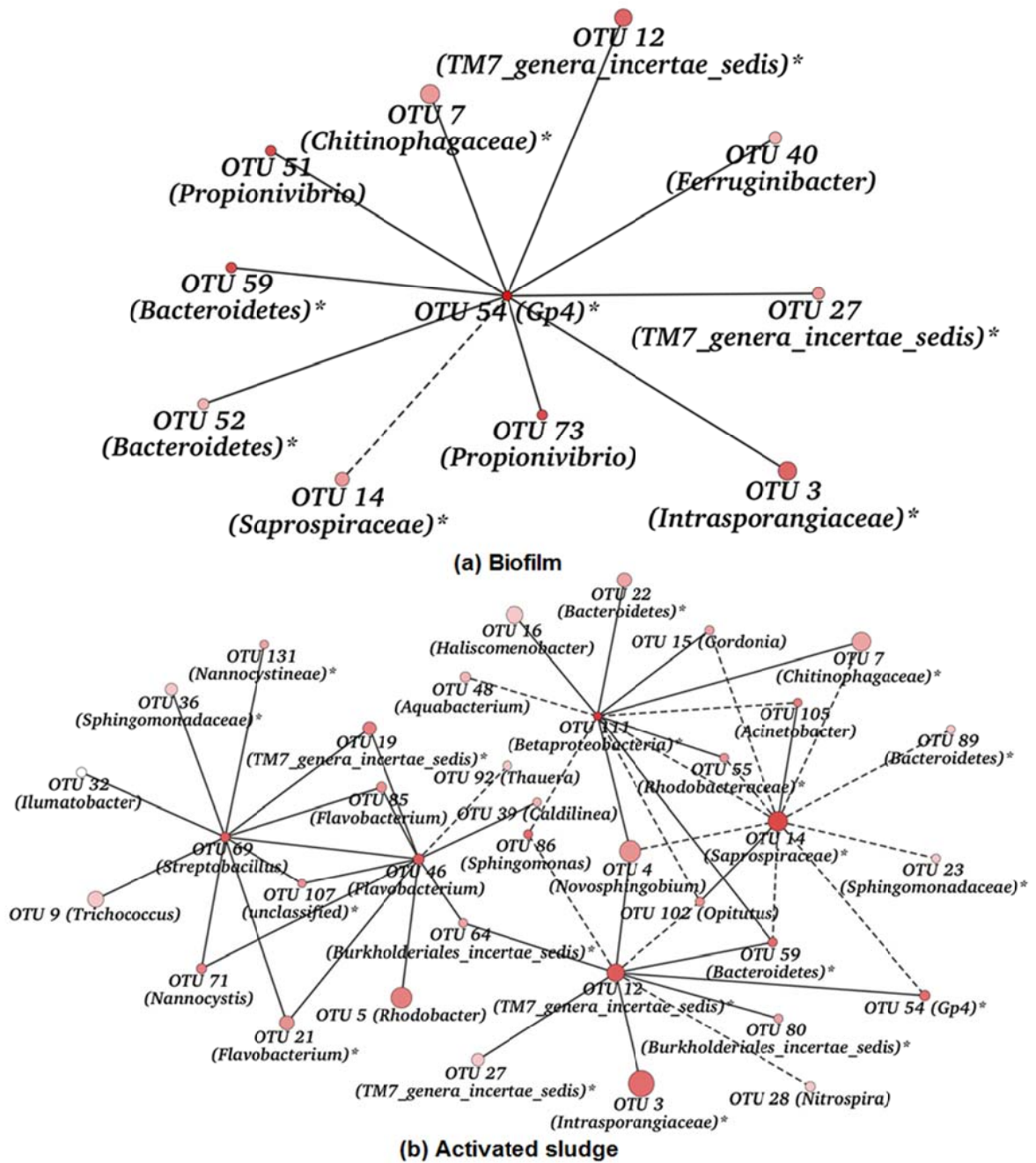


Figure V-8. The hub node networks of biofilm (a) and activated sludge (b).

#### **V.3.3.4. Effect of environmental factors on microbial network**

The sub-network was constructed by excluding the nodes that were not connected to the environmental factors (Figure V-9). The biofilm sub-network contains 27 edges with 25 nodes, and the activated sludge subnetwork contains 41 edges with 32 nodes. Figure V-9 shows that the biofilm sub-network contains eight environmental factors, and the activated sludge sub-network contains nine environmental factors interacting with microbial nodes, i.e., MLSS in the membrane tank,  $SAD_m$ , HRT in the membrane tank, the F/M ratio, BOD, TN, TP, the average temperature in the membrane tank and flux. Although both the biofilm and activated sludge had a similar number of environmental factors, the activated sludge had more microbial interactions than the biofilm network. This result supported the result of the network structure analysis which suggested that the microbial community of activated sludge reacted sensitively to environmental change. In the previous section, the MLSS in the membrane tank, HRT in the membrane tank, F/M ratio and  $SAD_m$  were correlated with the bacterial composition of the biofilm, and only MLSS was correlated with the community change in the activated sludge. However, the sub-network revealed that other environmental factors had an effect on the microbial community of both the biofilm and activated sludge because it provided more information on the microbial community of both the biofilm and activated sludge along with environmental factors than a previous analysis through microbial interactions. The MLSS and HRT in the membrane tank had many microbial interactions in both the biofilm and activated sludge network. The MLSS in the membrane tank, average temperature in

the membrane tank and TP in the activated sludge network had more microbial interactions than the biofilm network, whereas SAD<sub>m</sub> in the biofilm network had more microbial interactions than the activated sludge network.

The larger number of negative microbial associations with SAD<sub>m</sub> and HRT in the membrane tank in the biofilm network compared with that of the activated sludge network indicated that these factors disfavored the growth of particular microorganisms: OTU 7 (*Chitinophagaceae*), OTU 12 (*TM7\_genera\_incerae\_sedis*), OTU 31 (*Acinetobacter*), OTU 39 (*Caldilinea*), OTU 52 (*Bacteroidetes*), OTU 59 (*Bacteroidetes*), OTU 66 (*Aeromonas*), OTU 90 (*Intrasporangiaceae*), OTU 106 (*Solirubrobacterales*) and OTU 162 (*Chryseobacterium*). Particularly, OTU 31 (*Acinetobacter*) and OTU 66 (*Aeromonas*) were known to be related to the development of biofilm. The genus *Aeromonas* forms biofilms in a variety of environmental habitats (Lynch et al. 2002). It has been reported to be common in reverse osmosis membrane biofilm (Baker and Dudley 1998). Andersson et al. (2008) reported the biofilm formation and adherence properties of 13 bacterial strains commonly found in wastewater treatment systems studied in pure and mixed cultures using a biofilm formation assay. They found that *Acinetobacter* had a strong biofilm formation in both pure and mixed cultures. In the membrane systems, it was one of the dominant bacteria of the biofilm in a lab-scale MBR (Kim et al. 2013a). Thus, the development of a microbial community of biofilm was negatively driven by the HRT in the membrane tank and SAD<sub>m</sub>.

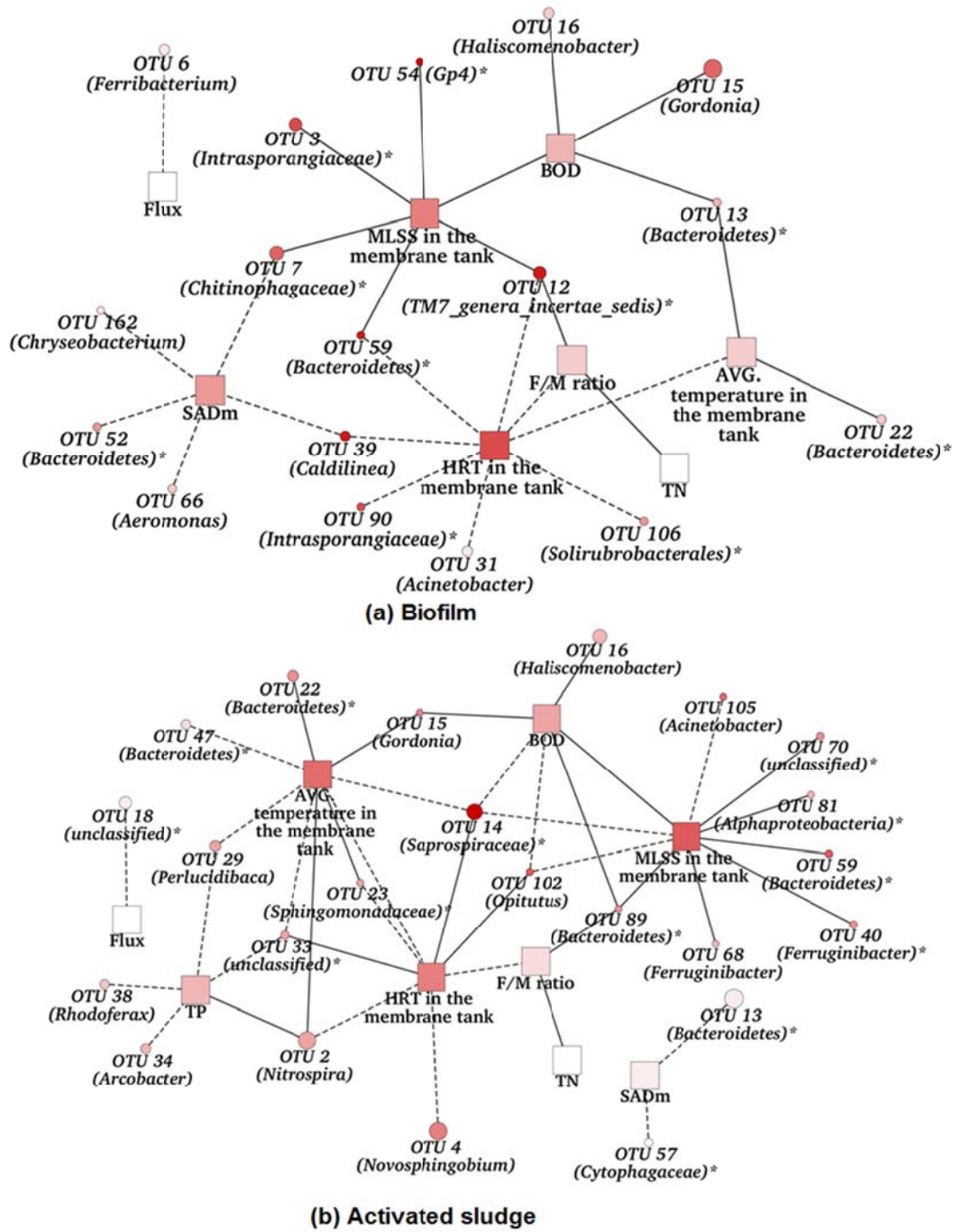


Figure V-9. The sub-network conducted to identify the microbe-environment associations in biofilm (a) and activated sludge (b).

The MLSS in the membrane tank was positively associated with BOD, and it had a major effect on the microbial interactions in both the biofilm and activated sludge in the network analysis. Although the microbial interactions with MLSS were fewer than the HRT in the membrane tank and  $SAD_m$ , MLSS was positively correlated with hub node OTU 54 (*Gp4*) in the biofilm, and it was negatively associated with hub node OTU 14 (*Saprospiraceae*) in the activated sludge. Thus, it is speculated that BOD contributes to an increase in MLSS, and it changed the bacterial composition of both the biofilm and activated sludge through associations with hub nodes and its own microbial interactions.

The larger number of microbial associations with average temperature in the membrane tank in the activated sludge network indicated a greater effect on activated sludge than on biofilm in MBRs. Particularly, OTU 2 (*Nitrospira*) was positively correlated with temperature. Previous studies have reported that low temperatures had an effect on the decrease in nitrogen removal (Chiemchaisri and Yamamoto 1994, Choi et al. 1998), and Huang et al. (2010) reported that warmer temperatures appeared to favor *Nitrospira*. The average temperature in the membrane tank was negatively associated with hub node OTU 14 (*Saprospiraceae*). Thus, it can drive changes in the microbial community through hub nodes. In addition, OTU 29 (*Perlucidibaca*) was negatively correlated with average temperature in the membrane tank. *Perlucidibaca* belongs to the *Moraxellaceae* family encompassing the genera *Psychrobacter* (Teixeira and Merquior 2014), and Hao et al. (2012) reported that *Perlucidibaca* was isolated from aeration tanks in the sewage treatment plant at water temperatures below 12°C. Thus, it is speculated

that the relative abundance of OTU 29 (*Perlucidibaca*) was disfavored by the increase in temperature because it has the characteristics of psychrophiles.

Although phosphorus is an essential nutrient for microbes, TP was negatively correlated with microbes (80%, 4/5) in the activated sludge. Thus, it is speculated that the growth of these microbes could be inhibited by the increase in phosphorus. The F/M ratio, TN and flux had a smaller impact on both the biofilm network and the activated sludge network. This result indicated that these factors did not strongly affect the microbial network in the MBRs.

## V.4. Conclusions

Microbial communities of biofilm and activated sludge were investigated from 10 different full-scale MBR plants with various environmental factors. The following conclusions could be drawn:

- Microbial community varied among the MBRs. Environmental factors such as MLSS, HRT, F/M ratio and  $SAD_m$  could explain the variation of the microbial community composition of the biofilm, whereas only MLSS could explain the compositional variation of the activated sludge.

- Bacterial community differed between the biofilm and activated sludge. However, *Flavobacterium*, *Dechloromonas*, *Nitrospira* and *Haliscomenobacter* were commonly existed in both the biofilm and activated sludge.

- The proportions of known quorum sensing bacterial genera ranged 1.39 to 11.57% in biofilm and 3.19 to 12.14% in activated sludge. As potential quorum sensing bacteria existed in both the biofilm and activated sludge, quorum quenching is expected to be one of effective methods for mitigating biofouling in MBRs.

- The biofilm and activated sludge networks displayed different topological characteristics. For instance, the sludge network was more compact and less heterogeneous. The different microbial associations were responsible for the variation of community composition between the biofilm and activated sludge.



## Chapter VI

## Conclusions



## VI. Conclusions

The effect of QQ on the microbial community was investigated in an A/O MBR. Furthermore, this study surveyed the microbial communities in 10 full-scale MBRs without QQ effect. The following conclusions could be drawn:

- The QQ had an effect on microbial community and reduced the variation of the bacterial composition in biofilm. These different characteristics of microbial community in QQ-MBR could provide useful information to mitigate biofouling in MBRs.

- The QQ had an effect on the both microbial composition and microbial interaction in activated sludge. However, the system performance was stable during 91days except for floc size. These results indicated that the QQ-MBR could be applied to the real wastewater treatment without disturbing its waste removal efficiency.

- Environmental factors such as MLSS, HRT, F/M ratio and  $SAD_m$  could change the variation of the microbial community composition of the biofilm. However, these factors had limitation to mitigate biofouling because they could have effect on the energy consumption, the plant productivity and the effluent quality in MBRs. Thus, QQ is expected to be one of effective methods for mitigating biofouling in MBRs because the potential of the presence of quorum sensing bacteria was high in both the biofilm and activated sludge.

## VI. 국문초록

고도 하·폐수처리 및 재이용이 가능한 분리막 생물 반응기(MBR)는 분리막 표면에 형성되는 생물막오염 (Biofouling)을 해결해야 하는 문제점을 안고 있다. 최근 들어 정족수감지 억제 (Qourum quenching)는 생물막오염을 제어할 수 있는 혁신적인 기술로 주목을 받고 있다. 그러나 정족수감지 억제 효과와 생물막오염 기작에 대한 생물학적 이해가 필요하지만, QQ-MBR 과 실제 full-scale MBR 에서 미생물 생태학적 정보가 여전히 부족한 상태이다. 따라서 실제 MBR 에서 성공적인 생물막오염 제어를 위해서 QQ-MBR 과 full-scale MBR 에서 미생물 군집에 대한 연구가 필요하다.

첫째, Anoxic(무산소조)/Oxic(산소조) MBR 에서 생물막 (biofilm)의 미생물 군집에 정족수감지 억제 기술이 미치는 영향에 대해서 연구하였다. 두 개의 A/O MBR 에서 control 반응기는 QQ-bead 없이 conventional MBR 과 정족수감지 억제 미생물이 고정되지 않은 vacant bead 만 넣은 vacant-MBR 로 운전했고 QQ-MBR 은 QQ-bead 를 넣고 운전했다. QQ-MBR 에서 막간차압(transmembrane pressure, TMP)이 45 kPa 에 도달할 때까지 걸리는 시간이 conventional 과 vacant-MBR 보다 거의 100~110% 지연되는 것을 확인했다. Weighted UniFrac distance metric 을 기반으로한 주좌표분석 (principal coordinate analysis)을 통해서 정족수감지 억제 효과가 미생물 군집에 영향을 주는 것을 확인했다. 그리고 대응분석 (correspondence analysis)을 이용해서 정족수감지 억제 효과가 미생물 군집 구성과 조성의 변화율에 영향을 주는 것도 확인했다.

둘째, 정족수감지 억제 기술이 활성 슬러지의 미생물 군집에 미치는 영향을 조사하였다. A/O MBR 은 91 일 동안 안정적으로 운전되어 99%의 COD 제거율과 78%의 질소 제거율을 control-MBR 과 QQ-MBR 에서 확인하였다. 그러나 평균 floc size 는 QQ-MBR control-MBR 보다 작았다. 미생물 네트워크 분석을 통해서 QQ가 미생물의 상호작용에 영향을 미치는 것을 확인했다.

마지막으로, 10 개의 full-scale MBR 에서 분리막 표면의 생물막 과 활성슬러지의 미생물 군집을 조사하였다. 전반적으로, 비율이 높은 순서로 *Flavobacterium*, *Dechloromonas* 그리고 *Nitrospira* 가 생물막에서 높은 비율을 차지했고, 활성슬러지에서는 *Dechloromonas*, *Flavobacterium* 그리고 *Haliscomenobacter*가 비율이 높았다. Quorum sensing 을 한다고 알려진 세균들의 비율을 genus level 에서 확인해본 결과, 생물막에서는 1.39 ~ 11.57%, 그리고 활성슬러지에서는 3.19~12.14 % 존재하였다. Spearman correlation 분석을 통해서 환경인자들이 미생물 군집 변화에 주는 영향을 조사했다. 분리막조의 MLSS 농도와, 분리막조에서의 폐수의 체류시간 (HRT), 유기물 부하량 (F/M ratio) 그리고 막 면적당 폭기량 ( $SAD_m$ )이 생물막의 미생물 군집 조성의 변화에 영향을 주었다. 그렇지만 활성 슬러지의 미생물 군집 조성은 분리막조의 MLSS 의 농도만이 영향을 주었다. 미생물 네트워크 분석을 통해서 생물막과 활성슬러지 미생물 군집의 미생물들의 상호 연관성을 환경인자와 같이 분석했다. 그 결과 생물막과 활성 슬러지의 네트워크가 다른 위상특성을 가지는 것을 확인했다. 이러한 결과는 생물막과 활성 슬러지의 미생물들의 서로 다른 상호 연관성이 생물막과 활성 슬러지의 미생물 조성 차이에 의한 것임을 나타낸다.

이러한 QQ-MBR 과 full-scale MBR 에서의 미생물 군집에 대한 정보는 실제 MBR 에서 생물막오염 제어를 적용할 경우에 유익하게 활용될 것으로 기대된다.

주요어: 분리막 생물 반응기, 정족수감지, 정족수감지 억제, 생물막, 활성 슬러지, 생물막오염 제어, 미생물 군집

학 번: 2011-30988

# Reference

- Abubucker S et al. (2012) Metabolic reconstruction for metagenomic data and its application to the human microbiome. *PLoS Comput Biol*, 8:e1002358
- Andersson S, Rajarao GK, Land CJ, Dalhammar G (2008) Biofilm formation and interactions of bacterial strains found in wastewater treatment systems. *FEMS Microbiol Lett*, 283:83-90
- Andreadakis AD (1993) Physical and chemical properties of activated sludge floc. *Water Res*, 27:1707-1714
- APHA, AWWA, WEF, (2005) Standard Methods for the Examination of Water and Wastewater, 21st ed. APHA, Washington, DC, USA.
- Assenov Y, Ramirez F, Schelhorn SE, Lengauer T, Albrecht M (2008) Computing topological parameters of biological networks. *Bioinformatics*, 24:282-284 doi:10.1093/bioinformatics/btm554
- Bailey JR, Bemberis I, Hubbard P, Presti JB (1971) Shipboard Sewage Treatment System. *DTIC Document*.
- Balestrino D, Haagensen JA, Rich C, Forestier C (2005) Characterization of type 2 quorum sensing in *Klebsiella pneumoniae* and relationship with biofilm formation. *Journal of bacteriology*, 187:2870-2880
- Barberán A, Bates ST, Casamayor EO, Fierer N (2012) Using network analysis to explore co-occurrence patterns in soil microbial communities. *The ISME journal*, 6:343-351
- Basson A, Flemming L, Chenia H (2008) Evaluation of adherence, hydrophobicity, aggregation, and biofilm development of *Flavobacterium johnsoniae*-like isolates. *Microbial ecology*, 55:1-14
- Baumann B (1997) Dynamics of Denitrification in *Paracoccus Denitrificans*.

- Belval SC, Gal L, Margiewes S, Garmyn D, Piveteau P, Guzzo J (2006) Assessment of the roles of LuxS, S-ribosyl homocysteine, and autoinducer 2 in cell attachment during biofilm formation by *Listeria monocytogenes* EGD-e. *Applied and environmental microbiology*, 72:2644-2650
- Bemberis I (1971) Membrane Sewage Treatment Systems: Potential for Complete Wastewater Treatment. American Society of Agricultural Engineers, Bioreactors M WEF Manual and Practice 36, 2011. ISBN 978-0-07-175366-1.
- Boyen F, Eeckhaut V, Van Immerseel F, Pasmans F, Ducatelle R, Haesebrouck F (2009) Quorum sensing in veterinary pathogens: mechanisms, clinical importance and future perspectives. *Veterinary Microbiology*, 135:187-195
- Brackman G, Defoirdt T, Miyamoto C, Bossier P, Van Calenbergh S, Nelis H, Coenye T (2008) Cinnamaldehyde and cinnamaldehyde derivatives reduce virulence in *Vibrio* spp. by decreasing the DNA-binding activity of the quorum sensing response regulator LuxR. *BMC microbiology*, 8:149
- Brigmon R, Martin H, Aldrich H (1997) Biofouling of groundwater systems by *Thiothrix* spp. *Current microbiology*, 35:169-174
- Buck B, Azcarate-Peril M, Klaenhammer T (2009) Role of autoinducer-2 on the adhesion ability of *Lactobacillus acidophilus*. *Journal of applied microbiology*, 107:269-279
- Caporaso JG et al. (2010) QIIME allows analysis of high-throughput community sequencing data. *Nature methods*, 7:335-336
- Carius L, Carius AB, McIntosh M, Grammel H (2013) Quorum sensing influences growth and photosynthetic membrane production in high-cell-density cultivations of *Rhodospirillum rubrum*. *BMC microbiology*, 13:1
- Case RJ, Labbate M, Kjelleberg S (2008) AHL-driven quorum-sensing circuits: their frequency and function among the *Proteobacteria*. *ISME JOURNAL*, 2:345
- Cassidy M, Lee H, Trevors J (1996) Environmental applications of immobilized microbial cells: a review. *Journal of Industrial Microbiology*, 16:79-101

- Chang C-Y, Tanong K, Xu J, Shon H (2011) Microbial community analysis of an aerobic nitrifying-denitrifying MBR treating ABS resin wastewater. *Bioresource technology*, 102:5337-5344
- Cheong W-S, Kim S-R, Oh H-S, Lee SH, Yeon K-M, Lee C-H, Lee J-K (2014) Design of quorum quenching microbial vessel to enhance cell viability for biofouling control in membrane bioreactor. *J Microbiol Biotechnol*, 24:97-105
- Cheong W-S et al. (2013) Isolation and identification of indigenous quorum quenching bacteria, *Pseudomonas* sp. 1A1, for biofouling control in MBR. *Industrial & Engineering Chemistry Research*, 52:10554-10560
- Chiemchaisri C, Yamamoto K (1994) Performance of membrane separation bioreactor at various temperatures for domestic wastewater treatment. *Journal of Membrane Science* 87:119-129
- Cho B, Fane A (2002) Fouling transients in nominally sub-critical flux operation of a membrane bioreactor. *Journal of membrane science*, 209:391-403
- Choi E, Rhu D, Yun Z, Lee E (1998) Temperature effects on biological nutrient removal system with weak municipal wastewater. *Water Science and Technology*, 37:219-226
- Chowdhary PK, Keshavan N, Nguyen HQ, Peterson JA, González JE, Haines DC (2007) *Bacillus megaterium* CYP102A1 oxidation of acyl homoserine lactones and acyl homoserines. *Biochemistry*, 46:14429-14437
- Deng Y, Jiang Y-H, Yang Y, He Z, Luo F, Zhou J (2012) Molecular ecological network analyses. *BMC bioinformatics*, 13:1
- Diggle SP, Griffin AS, Campbell GS, West SA (2007) Cooperation and conflict in quorum-sensing bacterial populations. *Nature*, 450:411-414
- Dong J, Horvath S (2007) Understanding network concepts in modules. *BMC systems biology*, 1:24
- Dong Y-H, Wang L-H, Xu J-L, Zhang H-B, Zhang X-F, Zhang L-H (2001) Quenching quorum-sensing-dependent bacterial infection by an N-acyl homoserine lactonase. *Nature*, 411:813-817

- Dong Y-H, Xu J-L, Li X-Z, Zhang L-H (2000) AiiA, an enzyme that inactivates the acylhomoserine lactone quorum-sensing signal and attenuates the virulence of *Erwinia carotovora*. *Proceedings of the National Academy of Sciences*, 97:3526-3531
- Drews A (2010) Membrane fouling in membrane bioreactors—characterisation, contradictions, cause and cures. *Journal of Membrane Science*, 363:1-28
- Evans J, Sheneman L, Foster J (2006) Relaxed neighbor joining: a fast distance-based phylogenetic tree construction method. *Journal of molecular evolution*, 62:785-792
- Farah C, Vera M, Morin D, Haras D, Jerez CA, Guiliani N (2005) Evidence for a functional quorum-sensing type AI-1 system in the extremophilic bacterium *Acidithiobacillus ferrooxidans*. *Applied and environmental microbiology*, 71:7033-7040
- Faust K, Raes J (2012) Microbial interactions: from networks to models. *Nature Reviews Microbiology*, 10:538-550
- Fekete A et al. (2010) Dynamic regulation of N-acyl-homoserine lactone production and degradation in *Pseudomonas putida* IsoF. *FEMS microbiology ecology*, 72:22-34
- Fetzner S (2015) Quorum quenching enzymes. *Journal of biotechnology*, 201:2-14
- Frost and Sullivan (2013) Global Membrane Bioreactor (MBR) Market. Report # M7E2-15. Frost & Sullivan, San Antonio, TX 78229-5616, USA
- Fuhrman JA (2009) Microbial community structure and its functional implications. *Nature*, 459:193-199
- Fuqua C, Winans SC (1996) Conserved cis-acting promoter elements are required for density-dependent transcription of *Agrobacterium tumefaciens* conjugal transfer genes. *Journal of Bacteriology*, 178:435-440
- Futamura O, Katoh M, Takeuchi K (1994) Organic waste water treatment by activated sludge process using integrated type membrane separation. *Desalination*, 98:17-25

- Gao D-w, Fu Y, Tao Y, Li X-x, Xing M, Gao X-h, Ren N-q (2011) Linking microbial community structure to membrane biofouling associated with varying dissolved oxygen concentrations. *Bioresource technology*, 102:5626-5633
- Gao D-W, Wen Z-D, Li B, Liang H (2014a) Microbial community structure characteristics associated membrane fouling in A/O-MBR system. *Bioresource technology*, 154:87-93
- Gao J, Ma A, Zhuang X, Zhuang G (2014b) An N-acyl homoserine lactone synthase in the ammonia-oxidizing bacterium *Nitrosospira multiformis*. *Applied and environmental microbiology*, 80:951-958
- Gonzalez A, Knight R (2012) Advancing analytical algorithms and pipelines for billions of microbial sequences. *Current opinion in biotechnology*, 23:64-71
- Gotschlich A et al. (2001) Synthesis of multiple N-acylhomoserine lactones is wide-spread among the members of the Burkholderia cepacia complex. *Systematic and Applied Microbiology*, 24:1-14
- Grady Jr CL, Daigger GT, Love NG, Filipe CD (2011) Biological wastewater treatment. CRC press.
- Gram L, Grossart H-P, Schlingloff A, Kjørboe T (2002) Possible quorum sensing in marine snow bacteria: production of acylated homoserine lactones by *Roseobacter* strains isolated from marine snow. *Applied and Environmental Microbiology*, 68:4111-4116
- Guo F, Zhang T (2012) Profiling bulking and foaming bacteria in activated sludge by high throughput sequencing. *Water Res*, 46:2772-2782
- Hai FI, Yamamoto K, Lee C-H (2013) Membrane Biological Reactors: Theory, Modeling, Design, Management and Applications to Wastewater Reuse. IWA Publishing.
- Hao Y, Jiang XG, Tian Q, Chen AY, Ma BL Isolation and identification of Nitrobacteria adapted to low temperature. *In: Advanced Materials Research*, 2012. Trans Tech Publ, pp 406-410

- Henze M (2008) Biological wastewater treatment: principles, modelling and design. IWA publishing.
- Herzberg M, Berry D, Raskin L (2010) Impact of microfiltration treatment of secondary wastewater effluent on biofouling of reverse osmosis membranes. *Water Res*, 44:167-176
- Hiraishi A, Muramatsu K, Urata K (1995) Characterization of new denitrifying *Rhodobacter* strains isolated from photosynthetic sludge for wastewater treatment. *Journal of fermentation and bioengineering*, 79:39-44
- Hu M, Wang XH, Wen XH, Xia Y (2012) Microbial community structures in different wastewater treatment plants as revealed by 454-pyrosequencing analysis. *Bioresource Technology*, 117:72-79  
doi:10.1016/j.biortech.2012.04.061
- Huang L-N, De Wever H, Diels L (2008) Diverse and distinct bacterial communities induced biofilm fouling in membrane bioreactors operated under different conditions. *Environmental science & technology*, 42:8360-8366
- Huang Z, Gedalanga PB, Asvapathanagul P, Olson BH (2010) Influence of physicochemical and operational parameters on Nitrobacter and Nitrospira communities in an aerobic activated sludge bioreactor. *Water Res*, 44:4351-4358
- Hwang B-K, Lee W-N, Park P-K, Lee C-H, Chang I-S (2007) Effect of membrane fouling reducer on cake structure and membrane permeability in membrane bioreactor. *Journal of membrane science*, 288:149-156
- Hwang B-K et al. (2008) Correlating TMP increases with microbial characteristics in the bio-cake on the membrane surface in a membrane bioreactor. *Environmental science & technology*, 42:3963-3968
- Irie Y, Parsek M (2008) Quorum sensing and microbial biofilms. In: Bacterial biofilms. Springer, pp 67-84

- Jahangir D, Oh H-S, Kim S-R, Park P-K, Lee C-H, Lee J-K (2012) Specific location of encapsulated quorum quenching bacteria for biofouling control in an external submerged membrane bioreactor. *Journal of Membrane Science*, 411:130-136
- Jekins, D. (2014) The evolution of activated sludge *Water* 21 (DEC) 37-40
- Jiang W, Xia S, Liang J, Zhang Z, Hermanowicz SW (2013) Effect of quorum quenching on the reactor performance, biofouling and biomass characteristics in membrane bioreactors. *Water Res*, 47:187-196
- Jin B, Wilén B-M, Lant P (2003) A comprehensive insight into floc characteristics and their impact on compressibility and settleability of activated sludge. *Chemical Engineering Journal*, 95:221-234
- Ju F, Zhang T (2015) Bacterial assembly and temporal dynamics in activated sludge of a full-scale municipal wastewater treatment plant. *The ISME journal*, 9:683-695
- Judd S (2008) The status of membrane bioreactor technology. *Trends in biotechnology*, 26:109-116
- Judd S (2010) *The MBR book: principles and applications of membrane bioreactors for water and wastewater treatment*. Elsevier.
- Köse-Mutlu B, Ergön-Can T, Koyuncu İ, Lee C-H (2015) Quorum quenching MBR operations for biofouling control under different operation conditions and using different immobilization media. *Desalination and Water Treatment*, 1-11
- Kappachery S, Paul D, Yoon J, Kweon JH (2010) Vanillin, a potential agent to prevent biofouling of reverse osmosis membrane. *Biofouling*, 26:667-672
- Kim H-W et al. (2013a) Microbial population dynamics and proteomics in membrane bioreactors with enzymatic quorum quenching. *Applied microbiology and biotechnology*, 97:4665-4675
- Kim J-H, Choi D-C, Yeon K-M, Kim S-R, Lee C-H (2011) Enzyme-immobilized nanofiltration membrane to mitigate biofouling based on quorum quenching. *Environmental science & technology*, 45:1601-1607

- Kim O-S et al. (2012) Introducing EzTaxon-e: a prokaryotic 16S rRNA gene sequence database with phylotypes that represent uncultured species. *International journal of systematic and evolutionary microbiology*, 62:716-721
- Kim S-R, Lee K-B, Kim J-E, Won Y-J, Yeon K-M, Lee C-H, Lim D-J (2015a) Macroencapsulation of quorum quenching bacteria by polymeric membrane layer and its application to MBR for biofouling control. *Journal of Membrane Science*, 473:109-117
- Kim S-R et al. (2013b) Biofouling control with bead-entrapped quorum quenching bacteria in membrane bioreactors: physical and biological effects. *Environmental science & technology*, 47:836-842
- Kim TG, Yun J, Cho K-S (2015b) The close relation between *Lactococcus* and *Methanosaeta* is a keystone for stable methane production from molasses wastewater in a UASB reactor. *Applied microbiology and biotechnology*, 99:8271-8283
- Kleerebezem M, Quadri LE, Kuipers OP, De Vos WM (1997) Quorum sensing by peptide pheromones and two-component signal-transduction systems in Gram-positive bacteria. *Molecular microbiology*, 24:895-904
- Klindworth A, Pruesse E, Schweer T, Peplies J, Quast C, Horn M, Glöckner FO (2012) Evaluation of general 16S ribosomal RNA gene PCR primers for classical and next-generation sequencing-based diversity studies. *Nucleic acids research*,:gks808
- Kozich JJ, Westcott SL, Baxter NT, Highlander SK, Schloss PD (2013) Development of a dual-index sequencing strategy and curation pipeline for analyzing amplicon sequence data on the MiSeq Illumina sequencing platform. *Applied and environmental microbiology*, 79:5112-5120
- Kozlova EV et al. (2008) Mutation in the S-ribosylhomocysteinase (*luxS*) gene involved in quorum sensing affects biofilm formation and virulence in a clinical isolate of *Aeromonas hydrophila*. *Microbial pathogenesis*, 45:343-354

- Lade H, Kweon J (2015) Review: Combined Effects of Curcumin and (-)-Epigallocatechin Gallate on Inhibition of N-Acylhomoserine Lactone-Mediated Biofilm Formation in Wastewater Bacteria from Membrane Bioreactor. *Journal of microbiology and biotechnology*, 25:1908-1919
- Lade H, Paul D, Kweon JH (2014) Quorum quenching mediated approaches for control of membrane biofouling. *Int J Biol Sci*, 10:550-565
- Langille MG et al. (2013) Predictive functional profiling of microbial communities using 16S rRNA marker gene sequences. *Nature biotechnology*, 31:814-821
- Lapidou CS, Rittmann BE (2002) A unified theory for extracellular polymeric substances, soluble microbial products, and active and inert biomass. *Water Res*, 36:2711-2720
- Leadbetter JR, Greenberg E (2000) Metabolism of acyl-homoserine lactone quorum-sensing signals by *Variovorax paradoxus*. *Journal of Bacteriology*, 182:6921-6926
- Lee C et al. (2008) Correlation of biofouling with the bio-cake architecture in an MBR. *Desalination*, 231:115-123
- Lee J et al. (2013) Graphene oxide nanoplatelets composite membrane with hydrophilic and antifouling properties for wastewater treatment. *Journal of Membrane Science*, 448:223-230
- Lee J, Kim J, Kang I, Cho M, Park P, Lee C (2001) Potential and limitations of alum or zeolite addition to improve the performance of a submerged membrane bioreactor. *Water Science and Technology*, 43:59-66
- Lee S-H, Hong TI, Kim B, Hong S, Park H-D (2014) Comparison of bacterial communities of biofilms formed on different membrane surfaces. *World Journal of Microbiology and Biotechnology*, 30:777-782
- Lee S et al. (2016) Crossing the Border between Laboratory and Field: Bacterial Quorum Quenching for Anti-Biofouling Strategy in an MBR. *Environmental science & technology*, 50:1788-1795

- Lee W-N, Cheong W-S, Yeon K-M, Hwang B-K, Lee C-H (2009) Correlation between local TMP distribution and bio-cake porosity on the membrane in a submerged MBR. *Journal of Membrane Science*, 332:50-55
- Lee W-N, Yeon K-M, Hwang B-K, Lee C-H, Chang I-S (2010) Effect of PAC addition on the physicochemical characteristics of bio-cake in a membrane bioreactor. *Separation Science and Technology*, 45:896-903
- Levén L, Eriksson AR, Schnürer A (2007) Effect of process temperature on bacterial and archaeal communities in two methanogenic bioreactors treating organic household waste. *FEMS microbiology ecology*, 59:683-693
- Lewandowski Z, Beyenal H (2005) Biofilms: their structure, activity, and effect on membrane filtration. *Water Science and Technology*, 51:181-192
- Li RW (2011) Metagenomics and its applications in agriculture, biomedicine, and environmental studies. Nova Science Publisher's.
- Lim S, Kim S, Yeon K-M, Sang B-I, Chun J, Lee C-H (2012) Correlation between microbial community structure and biofouling in a laboratory scale membrane bioreactor with synthetic wastewater. *Desalination*, 287:209-215
- Lozupone CA, Hamady M, Kelley ST, Knight R (2007) Quantitative and qualitative  $\beta$  diversity measures lead to different insights into factors that structure microbial communities. *Applied and environmental microbiology*, 73:1576-1585
- Lynch MJ, Swift S, Kirke DF, Keevil CW, Dodd CE, Williams P (2002) The regulation of biofilm development by quorum sensing in *Aeromonas hydrophila*. *Environ Microbiol*, 4:18-28
- Ma Z, Wen X, Zhao F, Xia Y, Huang X, Waite D, Guan J (2013) Effect of temperature variation on membrane fouling and microbial community structure in membrane bioreactor. *Bioresource technology*, 133:462-468
- Malaeb L, Le-Clech P, Vrouwenvelder JS, Ayoub GM, Saikaly PE (2013) Do biological-based strategies hold promise to biofouling control in MBRs?. *Water Res*, 47:5447-5463

- Maqbool T, Khan SJ, Waheed H, Lee C-H, Hashmi I, Iqbal H (2015) Membrane biofouling retardation and improved sludge characteristics using quorum quenching bacteria in submerged membrane bioreactor. *Journal of Membrane Science*, 483:75-83
- Matthew TG H., Stephen P D. Paul W. (2007) Quorum Sensing John Wiley & Sons  
 McKnight SL, Iglewski BH, Pesci EC (2000) The Pseudomonas quinolone signal regulates rhl quorum sensing in *Pseudomonas aeruginosa*. *Journal of Bacteriology*, 182:2702-2708
- Meng F, Shi B, Yang F, Zhang H (2007a) Effect of hydraulic retention time on membrane fouling and biomass characteristics in submerged membrane bioreactors. *Bioprocess and Biosystems Engineering*, 30:359-367
- Meng F, Zhang H, Yang F, Zhang S, Li Y, Zhang X (2006) Identification of activated sludge properties affecting membrane fouling in submerged membrane bioreactors Separation and Purification Technology 51:95-103
- Meng FG, Chae SR, Drews A, Kraume M, Shin HS, Yang FL (2009) Recent advances in membrane bioreactors (MBRs): Membrane fouling and membrane material. *Water Res*, 43:1489-1512  
 doi:10.1016/j.watres.2008.12.044
- Meng FG, Shi BQ, Yang FL, Zhang HM (2007b) New insights into membrane fouling in submerged membrane bioreactor based on rheology and hydrodynamics concepts. *Journal of Membrane Science*, 302:87-94  
 doi:10.1016/j.memsci.2007.06.030
- Miller MB, Bassler BL (2001) Quorum sensing in bacteria. *Annual Reviews in Microbiology*, 55:165-199
- Miura Y, Hiraiwa MN, Ito T, Itonaga T, Watanabe Y, Okabe S (2007a) Bacterial community structures in MBRs treating municipal wastewater: relationship between community stability and reactor performance. *Water Res*, 41:627-637
- Miura Y, Watanabe Y, Okabe S (2007b) Membrane biofouling in pilot-scale membrane bioreactors (MBRs) treating municipal wastewater: impact of biofilm formation. *Environmental science & technology*, 41:632-638

- Mulder J (2012) Basic principles of membrane technology. Springer Science & Business Media.
- Nam A, Kweon J, Ryu J, Lade H, Lee C (2015) Reduction of biofouling using vanillin as a quorum sensing inhibitory agent in membrane bioreactors for wastewater treatment. *MEMBRANE WATER TREATMENT*, 6:189-203
- Ng W-L, Bassler BL (2009) Bacterial quorum-sensing network architectures. *Annual review of genetics*, 43:197
- Nielsen PH, De Muro MA, Nielsen JL (2000) Studies on the in situ physiology of *Thiothrix* spp. present in activated sludge. *Environmental microbiology*, 2:389-398
- Nilakanta H, Drews KL, Firrell S, Foulkes MA, Jablonski KA (2014) A review of software for analyzing molecular sequences. *BMC research notes*, 7:830
- Niu C, Afre S, Gilbert E (2006) Subinhibitory concentrations of cinnamaldehyde interfere with quorum sensing. *Letters in applied microbiology*, 43:489-494
- Novick RP, Geisinger E (2008) Quorum sensing in *staphylococci*. *Annual review of genetics*, 42:541-564
- Oh H-S, Kim S-R, Cheong W-S, Lee C-H, Lee J-K (2013) Biofouling inhibition in MBR by *Rhodococcus* sp. BH4 isolated from real MBR plant. *Applied microbiology and biotechnology*, 97:10223-10231
- Oh H-S et al. (2012) Control of membrane biofouling in MBR for wastewater treatment by quorum quenching bacteria encapsulated in microporous membrane. *Environmental science & technology*, 46:4877-4884
- Park S-Y, Hwang B-J, Shin M-H, Kim J-A, Kim H-K, Lee J-K (2006) N-acylhomoserine lactonase producing *Rhodococcus* spp. with different AHL-degrading activities. *FEMS microbiology letters*, 261:102-108
- Parsek MR, Greenberg EP (2000) Acyl-homoserine lactone quorum sensing in gram-negative bacteria: a signaling mechanism involved in associations with higher organisms. *Proceedings of the National Academy of Sciences*, 97:8789-8793

- Pereira CS, Thompson JA, Xavier KB (2013) AI-2-mediated signalling in bacteria. *FEMS microbiology reviews*, 37:156-181
- Petrosino JF, Highlander S, Luna RA, Gibbs RA, Versalovic J (2009) Metagenomic pyrosequencing and microbial identification. *Clinical chemistry*, 55:856-866
- Piasecka A et al. (2012) Analysis of the microbial community structure in a membrane bioreactor during initial stages of filtration. *Biofouling*, 28:225-238
- Pongsilp N, Triplett EW, Sadowsky MJ (2005) Detection of homoserine lactone-like quorum sensing molecules in *Bradyrhizobium* strains. *Current microbiology*, 51:250-254
- Ponnusamy K, Paul D, Kim YS, Kweon JH (2010) 2 (5H)-Furanone: a prospective strategy for biofouling-control in membrane biofilm bacteria by quorum sensing inhibition. *Brazilian Journal of Microbiology*, 41:227-234
- Pontes MH, Babst M, Lochhead R, Oakeson K, Smith K, Dale C (2008) Quorum sensing primes the oxidative stress response in the insect endosymbiont, *Sodalis glossinidius*. *PLoS One*, 3:e3541
- Puskas A, Greenberg Eá, Kaplan S, Schaefer Aá (1997) A quorum-sensing system in the free-living photosynthetic bacterium *Rhodobacter sphaeroides*. *Journal of bacteriology*, 179:7530-7537
- Ramette A (2007) Multivariate analyses in microbial ecology. *FEMS Microbiology Ecology*, 62:142-160
- Reis-Filho JS (2009) Next-generation sequencing. *Breast Cancer Res*, 11:S12
- Research and Markets (2012) Membrane Bioreactor Systems Market – by Types, Configuration & Applications- Trends & Forecasts to 2017.
- Riesenfeld CS, Schloss PD, Handelsman J (2004) Metagenomics: genomic analysis of microbial communities. *Annu Rev Genet*, 38:525-552

- Roy V, Fernandes R, Tsao C-Y, Bentley WE (2010) Cross species quorum quenching using a native AI-2 processing enzyme. *ACS chemical biology*, 5:223-232
- Sainbayar A, Kim J, Jung W, Lee Y, Lee C (2001) Application of surface modified polypropylene membranes to an anaerobic membrane bioreactor. *Environmental technology*, 22:1035-1042
- Santamaria M et al. (2012) Reference databases for taxonomic assignment in metagenomics. *Briefings in bioinformatics*,:bbs036
- Santos A, Ma W, Judd SJ (2011) Membrane bioreactors: two decades of research and implementation. *Desalination*, 273:148-154
- Schloss PD et al. (2009) Introducing mothur: open-source, platform-independent, community-supported software for describing and comparing microbial communities. *Applied and environmental microbiology*, 75:7537-7541
- Scholz MB, Lo C-C, Chain PS (2012) Next generation sequencing and bioinformatic bottlenecks: the current state of metagenomic data analysis. *Current opinion in biotechnology*, 23:9-15
- Schuster M, Joseph Sexton D, Diggie SP, Peter Greenberg E (2013) Acyl-homoserine lactone quorum sensing: from evolution to application. *Annual review of microbiology*, 67:43-63
- Segata N, Izard J, Waldron L, Gevers D, Miropolsky L, Garrett WS, Huttenhower C (2011) Metagenomic biomarker discovery and explanation. *Genome biology*, 12:1
- Sha J, Pillai L, Fadl AA, Galindo CL, Erova TE, Chopra AK (2005) The type III secretion system and cytotoxic enterotoxin alter the virulence of *Aeromonas hydrophila*. *Infection and immunity*, 73:6446-6457
- Shannon P et al. (2003) Cytoscape: a software environment for integrated models of biomolecular interaction networks. *Genome research*, 13:2498-2504 doi:10.1101/gr.1239303

- Sheng G-P, Yu H-Q, Li X-Y (2010) Extracellular polymeric substances (EPS) of microbial aggregates in biological wastewater treatment systems: a review. *Biotechnology Advances*, 28:882-894
- Shrout JD, Nerenberg R (2012) Monitoring bacterial twitter: does quorum sensing determine the behavior of water and wastewater treatment biofilms?. *Environmental science & technology*, 46:1995-2005
- Siddiqui MF, Rzechowicz M, Harvey W, Zularisam A, Anthony GF (2015) Quorum sensing based membrane biofouling control for water treatment: A review. *Journal of Water Process Engineering*, 7:112-122
- Siddiqui MF, Sakinah M, Singh L, Zularisam A (2012) Targeting N-acyl-homoserine-lactones to mitigate membrane biofouling based on quorum sensing using a biofouling reducer. *Journal of biotechnology*, 161:190-197
- Singh G, Thomas PB (2012) Nutrient removal from membrane bioreactor permeate using microalgae and in a microalgae membrane photoreactor. *Bioresource technology*, 117:80-85
- Slonczewski JL, Foster JW (2013) *Microbiology: An Evolving Science: Third International Student Edition*. WW Norton & Company,
- Spoering AL, Gilmore MS (2006) Quorum sensing and DNA release in bacterial biofilms. *Curr Opin Microbiol*, 9:133-137
- Steele JA et al. (2011) Marine bacterial, archaeal and protistan association networks reveal ecological linkages. *The ISME journal*, 5:1414-1425
- Suntharalingam P, Cvitkovitch DG (2005) Quorum sensing in streptococcal biofilm formation. *Trends in microbiology*, 13:3-6
- Taminiau B et al. (2002) Identification of a quorum-sensing signal molecule in the facultative intracellular pathogen *Brucella melitensis*. *Infection and immunity*, 70:3004-3011
- Tan K, Obendorf SK (2007) Development of an antimicrobial microporous polyurethane membrane. *Journal of Membrane Science*, 289:199-209

- Tanaka G, Morino K, Aihara K (2012) Dynamical robustness in complex networks: the crucial role of low-degree nodes. *Scientific reports*, 2
- Tao C, Guo-Liang Q, Xiao-Li Y, Jun-Yi M, Bai-Shi H, Feng-Quan L (2009) Detection of a quorum sensing signal molecule of *Acidovorax avenae* subsp. *citrulli* and its regulation of pathogenicity. *Chinese Journal of Agricultural Biotechnology*, 6:49-53
- Teixeira LM, Merquior VLC (2014) The Family *Moraxellaceae*. In: The Prokaryotes. Springer, pp 443-476
- Thiel V, Kunze B, Verma P, Wagner-Döbler I, Schulz S (2009) New structural variants of homoserine lactones in bacteria. *ChemBioChem*, 10:1861-1868
- Uroz S, Chhabra SR, Camara M, Williams P, Oger P, Dessaux Y (2005) N-Acylhomoserine lactone quorum-sensing molecules are modified and degraded by *Rhodococcus erythropolis* W2 by both amidolytic and novel oxidoreductase activities. *Microbiology*, 151:3313-3322
- Uroz S et al. (2003) Novel bacteria degrading N-acylhomoserine lactones and their use as quenchers of quorum-sensing-regulated functions of plant-pathogenic bacteria. *Microbiology*, 149:1981-1989
- Uroz S, Oger PM, Chapelle E, Adeline M-T, Faure D, Dessaux Y (2008) A *Rhodococcus* qsdA-encoded enzyme defines a novel class of large-spectrum quorum-quenching lactonases. *Applied and environmental microbiology*, 74:1357-1366
- Venturi V (2006) Regulation of quorum sensing in *Pseudomonas*. *FEMS microbiology reviews*, 30:274-291
- Voelkerding KV, Dames SA, Durtschi JD (2009) Next-generation sequencing: from basic research to diagnostics. *Clinical chemistry*, 55:641-658
- Vukovic M, Briški F, Matošić M, Mijatovic I (2006) Analysis of the activated sludge process in an MBR under starvation conditions. *Chemical engineering & technology*, 29:357-363

- Wagner-Döbler I et al. (2005) Discovery of complex mixtures of novel long-chain quorum sensing signals in free-living and host-associated marine *alphaproteobacteria*. *Chembiochem*, 6:2195-2206
- Wagner M, Loy A (2002) Bacterial community composition and function in sewage treatment systems. *Current Opinion in Biotechnology*, 13:218-227
- Waters CM, Bassler BL (2005) Quorum sensing: cell-to-cell communication in bacteria. *Annu Rev Cell Dev Biol*, 21:319-346
- Weerasekara NA, Choo K-H, Lee C-H (2014) Hybridization of physical cleaning and quorum quenching to minimize membrane biofouling and energy consumption in a membrane bioreactor. *Water Res*, 67:1-10
- Williams RJ, Howe A, Hofmockel KS (2014) Demonstrating microbial co-occurrence pattern analyses within and between ecosystems. *Frontiers in microbiology*, 5
- Williams TM, Unz RF (1985) Filamentous sulfur bacteria of activated sludge: characterization of *Thiothrix*, *Beggiatoa*, and Eikelboom type 021N strains. *Applied and environmental microbiology*, 49:887-898
- Wittebolle L et al. (2009) Initial community evenness favours functionality under selective stress. *Nature*, 458:623-626
- Xia LC et al. (2011) Extended local similarity analysis (eLSA) of microbial community and other time series data with replicates. *BMC systems biology*, 5 Suppl 2:S15 doi:10.1186/1752-0509-5-S2-S15
- Xia S et al. (2010) The effect of organic loading on bacterial community composition of membrane biofilms in a submerged polyvinyl chloride membrane bioreactor. *Bioresource technology*, 101:6601-6609
- Xiong Y, Liu Y (2010) Biological control of microbial attachment: a promising alternative for mitigating membrane biofouling. *Applied microbiology and biotechnology*, 86:825-837
- Xu J (2006) Invited review: microbial ecology in the age of genomics and metagenomics: concepts, tools, and recent advances. *Molecular ecology*, 15:1713-1731

- Yamamoto K, Hiasa M, Mahmood T, Matsuo T (1989) Direct solid-liquid separation using hollow fiber membrane in an activated sludge aeration tank. *Water Science and Technology*, 21:43-54
- Yeon K-M et al. (2008) Quorum sensing: a new biofouling control paradigm in a membrane bioreactor for advanced wastewater treatment. *Environmental science & technology*, 43:380-385
- Yeon K-M, Lee C-H, Kim J (2009) Magnetic enzyme carrier for effective biofouling control in the membrane bioreactor based on enzymatic quorum quenching. *Environmental science & technology*, 43:7403-7409
- Yoon S-H et al. (2005) Effects of flux enhancing polymer on the characteristics of sludge in membrane bioreactor process. *Water Science and Technology*, 51:151-157
- Yoon S-H, Collins JH (2006) A novel flux enhancing method for membrane bioreactor (MBR) process using polymer. *Desalination*, 191:52-61
- Yu C, Wu J, Contreras AE, Li Q (2012) Control of nanofiltration membrane biofouling by *Pseudomonas aeruginosa* using D-tyrosine. *Journal of Membrane Science*, 423:487-494
- Yue JC, Clayton MK (2005) A similarity measure based on species proportions. *Communications in Statistics-Theory and Methods*, 34:2123-2131
- Zhang J, Chua HC, Zhou J, Fane A (2006) Factors affecting the membrane performance in submerged membrane bioreactors. *Journal of Membrane Science*, 284:54-66
- Zhang T, Shao MF, Ye L (2012) 454 Pyrosequencing reveals bacterial diversity of activated sludge from 14 sewage treatment plants. *Isme Journal*, 6:1137-1147 doi:10.1038/ismej.2011.188
- Zhao DY, Huang R, Zeng J, Yu ZB, Liu P, Cheng SP, Wu QLL (2014) Pyrosequencing analysis of bacterial community and assembly in activated sludge samples from different geographic regions in China. *Applied Microbiology and Biotechnology*, 98:9119-9128 doi:10.1007/s00253-014-5920-3

- Zhou J, Deng Y, Luo F, He Z, Tu Q, Zhi X (2010) Functional molecular ecological networks. *MBio*, 1:e00169-00110
- Zhu J, Chai Y, Zhong Z, Li S, Winans SC (2003) Agrobacterium bioassay strain for ultrasensitive detection of N-acylhomoserine lactone-type quorum-sensing molecules: detection of autoinducers in *Mesorhizobium huakuii*. *Applied and Environmental Microbiology*, 69:6949-6953
- Zhu P, Li M (2012) Recent progresses on AI-2 bacterial quorum sensing inhibitors. *Current medicinal chemistry*, 19:174-186
- Zodrow KR, Schiffman JD, Elimelech M (2012) Biodegradable polymer (PLGA) coatings featuring cinnamaldehyde and carvacrol mitigate biofilm formation. *Langmuir*, 28:13993-13999
- Zodrow KR, Tousley ME, Elimelech M (2014) Mitigating biofouling on thin-film composite polyamide membranes using a controlled-release platform. *Journal of Membrane Science*, 453:84-91